

A Thesis Submitted for the Degree of PhD at the University of Warwick

Permanent WRAP URL:

<http://wrap.warwick.ac.uk/165228>

Copyright and reuse:

This thesis is made available online and is protected by original copyright.

Please scroll down to view the document itself.

Please refer to the repository record for this item for information to help you to cite it.

Our policy information is available from the repository home page.

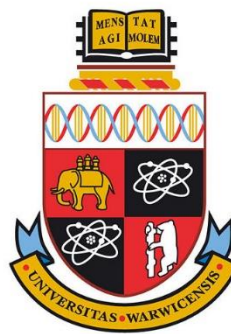
For more information, please contact the WRAP Team at: wrap@warwick.ac.uk

An electrophysiological evaluation of novel cognitive enhancers

by

Signe Springe BSc (Hons), MReS

*A thesis written in partial fulfillment of the criteria set for the degree of
Doctor of Philosophy*



Warwick Medical School 2020

Funded by Neurosolutions Ltd.

Table of contents

List of figures.....	vi
List of tables	xii
Acknowledgements	xiv
Declaration	xv
Summary.....	xvi
Abbreviations	xviii
 Chapter 1: General introduction	 1
1.1 Types of Learning and Memory.....	2
1.2 Neurological disorders of Learning and Memory	2
1.3 Alzheimer's Disease: A Major Public Health concern.....	3
1.3.1 Alzheimer's Disease: Diagnostic guidelines	3
1.3.2 Neuropathology of Alzheimer's Disease: Macroscopic Characteristics	4
1.3.3 Amyloid β plaques.....	6
1.3.4 Neurofibrillary tangles and neuropil threads	9
1.4 Other neurodegenerative disorders associated with dementia	11
1.5 Obesity and disturbances in Learning and Memory	11
1.6 Insulin resistance	12
1.7 The Hippocampus: Role in Learning and memory.....	13
1.8 The Hippocampus: Anatomy and structural organisation.....	14
1.9 An overview of Long-term potentiation of synaptic transmission in learning and memory	18
1.9.1 Induction of LTP	20
1.9.2 Maintenance of LTP	24
1.9.3 NMDA receptors	25
1.9.4 AMPA receptors.....	27
1.9.5 Metabotropic Glutamate receptors	28
1.9.6 Nicotinic cholinergic receptors.....	30
1.9.7 Adenosine.....	32
1.9.7.1 A ₁ receptor.....	32
1.9.7.2 A _{2A} receptor.....	34
1.9.7.3 A _{2B} receptor	35
1.9.7.4 A ₃ receptor.....	35

1.9.8	Glia	35
1.9.9	LTP and Neurodegeneration.....	38
1.9.10	LTP and Metabolism	39
1.10	High fat diet, Obesity, and synaptic plasticity	42
1.11	Treatment of Alzheimer's disease.....	45
1.12	Current outlook in AD therapy.....	46
1.13	Summary and Hypotheses	48
 Chapter 2: Materials and methods.....		49
2.1	Electrophysiology: Slice preparation.....	49
2.2	Electrophysiological Recording and Data Analysis	50
2.3	Solutions, Drugs, and drug application protocols	57
2.4	Data and Statistical analysis.....	59
2.5	Whole-cell patch-clamp electrophysiology.....	60
 Chapter 3: The effects of extracellular glucose on LTP in the hippocampus and the role of adenosine		62
3.1	Introduction	62
3.2	The importance of the blood-brain barrier	63
3.3	Glucose transport into the brain.....	65
3.4	Glucose presence in the brain.....	66
3.5	Glucose metabolism in the brain.....	67
3.6	Glucose-sensing mechanisms in the brain.....	68
3.7	The effects of extracellular glucose on LTP.....	69
3.8	Adenosine.....	71
3.9	Adenosine production and metabolism in the CNS: Intracellular....	71
3.10	Adenosine production and metabolism in the CNS: Extracellular...	72
3.11	Adenosine receptors.....	73
3.12	ARs as therapeutic targets.....	76
3.13	Hypothesis and aims of research.....	76
3.14	Results: The effects of adenosine antagonists on LTP <i>in vitro</i>.....	78
3.14.1	The effects of extracellular glucose on LTP in rat CA1 <i>in vitro</i>	79
3.14.2	The effects of the A ₁ receptor antagonist DPCPX on LTP induced in CA1 in the presence of 10 and 2 mM extracellular glucose.....	83

3.14.3	The effects of the A _{2A} receptor antagonist KW-6002 on LTP induced in CA1 in the presence of 10, 5 and 2mM extracellular glucose.....	91
3.14.4	The effects of the A _{2B} receptor antagonist PSB603 on LTP induced in CA1 in the presence of 10mM extracellular D-glucose.....	103
3.14.5	The effects of the A ₃ receptor antagonist MRS1523 on LTP induced in CA1 in the presence of 10mM extracellular glucose.....	106
3.14.6	The effects of the non-selective adenosine receptor antagonist CGS15943 on LTP induced in CA1 in the presence of 10 and 5mM extracellular glucose.....	109
3.14.7	Results: A summary of the effects of adenosine receptor antagonists on the LTP in the presence of aCSF containing 10mM of glucose..	117
3.14.8	Results: A summary of the effects of adenosine receptor antagonists on the LTP in the presence of aCSF containing 5 mM of glucose..	121
3.14.9	Results: A summary of the effects of adenosine receptor antagonists on the LTP in the presence of aCSF containing 2 mM of glucose...	124
3.15	Conclusions and Discussion.....	126
3.15.1	The effects of extracellular glucose on LTP in rat hippocampus	128
3.15.2	Conclusions: Effect of the A ₁ receptor antagonist DPCPX on LTP induced in CA1 in the presence of 10 a 2 mM extracellulat glucose	130
3.15.3	Effects of the A _{2A} receptor antagonist KW-6002 on LTP induced in CA1 in the presence of 10, 5 and 2 mM extracellular glucose.....	131
3.15.4	Effects of the A _{2B} receptor antagonist PSB603 on LTP induced in CA1 in the presence of 10 mM extracellular glucose	133
3.15.5	Effects of the A ₃ receptor antagonist MRS1523 on LTP induced in CA1 in the presence of 10 mM extracellular glucose	134
3.15.6	Effects of the non-selective adenosine receptor antagonist CGS15943 on LTP induced in CA1 in the presence of 10 and 5 mM extracellular glucose.....	135
3.16	Future Experiments	136
 Chapter 4: An electrophysiological evaluation of novel, α7nAChR-targeting compounds.....		
4.1	Introduction	137
4.2	α7nACh - the target of interest	138

4.2.1	$\alpha 7$ nAChR agonists	139
4.2.2	$\alpha 7$ nAChR positive allosteric modulators (PAMs)	140
4.3	Results: The Effects of Encenicline (EVP-614) on LTP in the hippocampus <i>in vitro</i>	141
4.4	Results: The Effects of BNC375 and L-436 on LTP in the hippocampus <i>in vitro</i>	150
4.4.1	The effects of $\alpha 7$ nAChR-targeting compounds in the hippocampi of WT mice	150
4.4.2	The effects of $\alpha 7$ nAChR-targeting compounds in the hippocampi of Aca $\alpha 7$ - mice	151
4.4.3	The effects of $\alpha 7$ nAChR-targeting compounds in the hippocampi of SD rats	152
4.5	Conclusions and Discussion.....	162
 Chapter 5: The pursuit of the mechanism of action of SD118, a novel SV2A-		
	targetting compound	170
5.1	Introduction	170
5.2	Racetams and cognition	171
5.3	Levetiracetam: The New Generation AED	171
5.3.1	Levetiracetam: Mechanism of action	172
5.4	Results	175
5.4.1	Effects of SD118 on Paired-pulse Ratio.....	176
5.4.2	Frequency-dependent effects of SD118 on excitatory synaptic transmission.....	180
5.4.2.1	Frequency-dependent effects of SD118 on excitatory synaptic transmission: 1Hz.....	180
5.4.2.2	Frequency-dependent effects of SD118 on excitatory synaptic transmission: 2Hz.....	188
5.4.2.3	Frequency-dependent effects of SD118 on excitatory synaptic transmission: 5Hz.....	194
5.4.2.4	Frequency-dependent effects of SD118 on excitatory synaptic transmission: 10Hz	202
5.4.2.5	Frequency-dependent effects of SD118 on excitatory synaptic transmission: 20Hz	209
5.5	Discussion.....	217

List of Figures

Figure 1.1: An overview of the taxonomy of memory systems and brain structures associated with them.

Figure 1.2: Coronal sections of formalin-fixed tissue slices taken at the level of the anterior hippocampus of a person without dementia (A) and a patient with severe AD ((B) and (C)).

Figure 1.3: A commonly used schematic diagram for visualising if the processing of the amyloid precursor protein (APP).

Figure 1.4: Photomicrographs of A β plaques.

Figure 1.5: Photomicrographs depicting neurofibrillary tangles and neuropil threads.

Figure 1.6: The anatomical arrangement of the dorsal hippocampus, including the principal layers and areas.

Figure 1.7: A diagram of the trisynaptic circuit of the hippocampus.

Figure 1.8: A schematic representation of the vital aspects of the LTP experiments performed by Bliss & Lomo (1973).

Figure 1.9: A diagram of the postsynaptic mechanism of LTP.

Figure 1.10: A diagram of the structure and binding sites of the NMDAR.

Figure 1.11: A schematic representation of the three mGluR groups.

Figure 1.12: A simplified diagram of glucose metabolism.

Figure 2.1: A simplified diagram of a modified Brain Slice chamber system.

Figure 2.2: A schematic representation of the hippocampal trisynaptic circuit and electrode placement.

Figure 2.3: A schematic representation of the hippocampal trisynaptic circuit and electrode placement.

Figure 2.4: A schematic representation of the stimulation protocols utilized in our studies and their corresponding chapters.

Figure 2.5: An example of typical fEPSP traces before (a) and after (b) high frequency stimulation

Figure 2.6: An example of a typical scatter plot representing mean normalised fEPSP amplitude before and after high frequency (HFS) or theta burst stimulation (TBS) WT mice

Figure 3.1: The effects of extracellular glucose concentration on LTP in the CA1 area of the hippocampus

Figure 3.2: The effects of extracellular glucose concentration on LTP in the CA1 area of the hippocampus

Figure 3.3: The effect of A₁ receptor antagonist DPCPX on LTP in the CA1 area of the hippocampus, in the presence of 10 mM extracellular D-glucose

Figure 3.4: The effect of A₁ receptor antagonist DPCPX on LTP in the CA1 area of the hippocampus, in the presence of 10 mM extracellular D-glucose.

Figure 3.5: The effects of adenosine antagonists on LTP in the CA1 area of the hippocampus in 2 mM glucose-containing aCSF

Figure 3.6: The effects of adenosine A₁R antagonist 1 μ M DPCPX on LTP in the CA1 area of the hippocampus in experiments utilizing 2 mM glucose-containing aCSF

Figure 3.7: The effects of A₁ adenosine receptor antagonists on LTP in the CA1 area of the hippocampus.

Figure 3.8: The effects of A₁ adenosine receptor antagonists (1 μ M DPCPX) on LTP in the CA1 area of the hippocampus in experiments utilizing 10 and 2 mM-glucose-containing aCSF, respectively

Figure 3.9: The effects of the adenosine A_{2A} receptor antagonist KW-6002 on LTP in the CA1 area of the hippocampus in 10 mM extracellular D-glucose

Figure 3.10: The effects of the A_{2A}R antagonists on LTP in the CA1 area of the hippocampus in 10mM extracellular D-glucose

Figure 3.11: The effects of the A_{2A}R antagonists on LTP in the CA1 area of the hippocampus in 5mM extracellular D-glucose

Figure 3.12: The effects of adenosine A_{2A}R antagonist (50 nM KW-6002) on LTP in the CA1 area of the hippocampus in experiments utilizing 5 mM glucose-containing aCSF

Figure 3.13: The effects of the adenosine A_{2A} receptor antagonist KW-6002 on LTP in the CA1 area of the hippocampus in 2 mM glucose aCSF

Figure 3.14: The effects of adenosine A_{2A}R antagonists (50 nM KW-6002) on LTP in the CA1 area of the hippocampus in experiments utilizing 2 mM-glucose-containing aCSF

Figure 3.15: The effects of the A_{2A}R adenosine antagonist (KW-6002) on LTP in the CA1 area of the hippocampus

Figure 3.16: The effects of the A_{2A}R adenosine antagonists (50 nM KW-6002) on LTP in the CA1 area of the hippocampus in experiments utilizing 10, 5 and 2 mM aCSF

Figure 3.17: The effects of the adenosine A_{2B} receptor antagonist PSB603 on LTP in the CA1 area of the hippocampus in 10 mM extracellular glucose

Figure 3.18: The effects of the adenosine A_{2B} receptor antagonist PSB603 on LTP in the CA1 area of the hippocampus in 10 mM extracellular glucose

Figure 3.19: The effects of the adenosine A₃ receptor antagonist MRS1523 on LTP in the CA1 area of the hippocampus in 10 mM extracellular glucose

Figure 3.20: The effects of the adenosine A₃ receptor antagonist MRS1523 on LTP in the CA1 area of the hippocampus in 10 mM extracellular glucose

Figure 3.21: The effects of the non-selective adenosine receptor antagonist CGS15943 on LTP in the CA1 area of the hippocampus in 10 mM extracellular glucose

Figure 3.22: The effects of the non-selective adenosine receptor antagonist CGS15943 on LTP in the CA1 area of the hippocampus in 10 mM extracellular glucose

Figure 3.23: The effects of the non-selective adenosine receptor antagonist CGS15943 on LTP in the CA1 area of the hippocampus in 5 mM extracellular glucose

Figure 3.24: The effects of adenosine antagonist 100nM CGS15943 on LTP in the CA1 area of the hippocampus in experiments utilizing 5 mM glucose-containing aCSF

Figure 3.25: The effects of the non-selective adenosine receptor antagonist on LTP in the CA1 area of the hippocampus

Figure 3.26: The effect of the non-selective adenosine antagonist (100 nM CGS15943) on LTP in the CA1 area of the hippocampus in experiments utilizing 10 and 5 mM glucose-containing aCSF

Figure 3.27: The effects of adenosine receptor antagonists on LTP in the CA1 area of the hippocampus in the presence of 10 mM extracellular glucose

Figure 3.28: The effects of adenosine receptor antagonists on LTP in the CA1 area of the hippocampus in the presence of 10 mM extracellular glucose

Figure 3.29: The effects of adenosine receptor antagonists on LTP in the CA1 area of the hippocampus in the presence of 5 mM extracellular glucose

Figure 3.30: The effects of adenosine receptor antagonists (100 nM CGS15943 and 50 nM KW-6002) on LTP in the CA1 area of the hippocampus in experiments utilizing 5 mM glucose-containing aCSF

Figure 3.31: The effects of adenosine receptor antagonists on LTP in the CA1 area of the hippocampus in 2 mM glucose aCSF

Figure 3.32: The effects of adenosine receptor antagonists (1 μ M DPCPX and 50 nM KW-6002) on LTP in the CA1 area of the hippocampus in experiments utilizing 2 mM glucose-containing aCSF

Figure 3.33: The equation for determining the net flux of glucose for tissue slices at an air-aCSF interface experimental configuration

Figure 4.1: The Effects of 1 nM EVP-6214 on LTP in the CA1 region of the hippocampus

Figure 4.2: The Effect of 1.78 nM EVP-6214 on LTP in the CA1 region of the hippocampus

Figure 4.3: The Effect of 3.16 nM EVP-6214 on LTP in the CA1 region of the hippocampus

Figure 4.4: The Effect of 5.62 nM EVP-6214 on LTP in the CA1 region of the hippocampus

Figure 4.5: The Effect of 10 nM EVP-6214 on LTP in the CA1 region of the hippocampus

Figure 4.6: The effects of increasing concentrations of EVP-6124 on LTP in the CA1 region of the hippocampus

Figure 4.7: EVP-6124 induced a concentration-dependent enhancement of LTP in the CA1 region of the hippocampus

Figure 4.8: The effects of compounds L-436 and BNC375 on LTP in the CA1 region of the hippocampus of WT mice

Figure 4.9: The effects of $\alpha 7$ nAChR-targeting compounds on LTP in the CA1 region of the hippocampus

Figure 4.10: The effects of L-436 on LTP in the CA1 region of the hippocampus of $\text{Acr}\alpha 7$ - mice

Figure 4.11: Summary of the effect of L-436, an $\alpha 7$ nAChR-targeting compound on LTP in the CA1 region of the hippocampus of $\text{Acr}\alpha 7$ - mice

Figure 4.12: Summary bar chart comparing the effect of the nAChR-targeting compound L-436 on LTP in the CA1 region of the hippocampus of WT and $\text{Acr}\alpha 7$ - mice

Figure 4.13: The effects of increasing concentrations of L-436 on LTP in the CA1 region of the hippocampus of SD rats

Figure 4.14: The effects of the $\alpha 7$ nAChR antagonist MLA on LTP in the CA1 region of the hippocampus of SD rats

Figure 4.15: The effects of MLA on L-436-induced enhancement of LTP in the hippocampus of SD rats

Figure 4.16: Summary bar chart showing the effects of increasing concentrations of the $\alpha 7$ nAChR-targeting compound L-436 on LTP and the effects of the $\alpha 7$ nAChR antagonist MLA on L-436-induced effects

Figure 5.1: A schematic representation of the proposed mechanisms of action of Levetiracetam (LEV) in the excitatory synapse, with SV2A regarded as the main target (solid arrow).

Figure 5.2: An example of a typical paired-pulse experiment subject to 50-msec ISIs

Figure 5.3: An example of a typical paired-pulse experiment subject to 100-msec ISIs

Figure 5.4: An example of a Paired-pulse experiment, showing stability in amplitude (mV) throughout the course of the experiment

Figure 5.5: A summary of the frequency-dependent effects of SD118, novel putative cognition-enhancing compound on excitatory synaptic transmission

Figure 5.6: Summary data of the effects of SD118 on EPSCs evoked at low frequency (with 1 Hz high frequency).

Figure 5.7: EPSCs during application of SD118

Figure 5.8: EPSCs throughout SD118 trials

Figure 5.9: Summary data of the effects of SD118 on EPSCs evoked at 1 Hz.

Figure 5.10: The effects of SD118 on EPSCs evoked at low frequency (with 2 Hz high frequency)

Figure 5.11: Summary data of the effects of SD118 on EPSCs evoked at low frequency (with 2 Hz high frequency)

Figure 5.12: EPSCs during stimulation trials

Figure 5.13: Summary data of the effects of SD118 on EPSCs evoked at 2 Hz

Figure 5.14: Summary of the effects of SD118 on EPSCs evoked at low frequency (with 5 Hz high frequency)

Figure 5.15: EPSCs during stimulation trials

Figure 5.16: The effects of SD118 on EPSCs evoked at low frequency (with 5 Hz high frequency)

Figure 5.17: A summary of the frequency-dependent effects of SD118 on excitatory synaptic transmission at 5 Hz trials

Figure 5.18: Summary data of the effects of SD118 on EPSCs evoked at 5 Hz

Figure 5.19: Summary data of the effects of SD118 on EPSC amplitudes evoked at 5 Hz

Figure 5.20: Summary data of the effects of SD118 on EPSCs evoked at low frequency (with 10 Hz high frequency)

Figure 5.21: Summary data of the effects of SD118 on EPSCs evoked at 0.1 Hz (with 10 Hz high frequency stimulation)

Figure 5.22: An example of the effects of SD118 on EPSCs evoked at 10 Hz (3 trials)

Figure 5.23: Summary data of the effects of SD118 on EPSCs evoked at 10 Hz

Figure 5.24: Summary data of the effects of SD118 on EPSCs evoked at 10 Hz with data pooled from all trials

Figure 5.25: A summary of the frequency-dependent effects of SD118 on excitatory synaptic transmission

Figure 5.26: The reversal of the SD118 effect

Figure 5.27: The reversal of the SD118 effect on EPSC amplitudes

Figure 5.28: Summary data of the effects of SD118 on EPSCs evoked at 0.1 Hz (with 20 Hz high frequency trains)

Figure 5.29: An example of the effects of SD118 on EPSCs evoked at 20 Hz (3 trials)

Figure 5.30: Summary data of the effects of SD118 on EPSCs evoked at 20 Hz with data pooled from all cells and all trials

Figure 5.31: A. Summary overview data of the effects of SD118 on EPSCs evoked at a frequency of 0.1 Hz (in series with high frequency trains of stimuli at 1, 2, 5, 10 and 20Hz)

List of Tables

Table 1.1: Summary of receptors/signalling molecules and mechanisms and their role in neuronal plasticity.

Table 2.1: Composition of aCSF

Table 2.2: Drugs utilized in our studies.

Table 2.3: Adenosine antagonists utilized in our studies.

Table 3.1: Adenosine receptors in the brain.

Table 3.2: Mean magnitude of LTP measured 50-60 minutes after a 5xTBS stimulation in rat hippocampal slices prepared with aCSF containing 10, 5 or 2 mM glucose and treated with vehicle.

Table 3.3: Mean fEPSP amplitudes measured 50-60 minutes after a 5xTBS stimulation in rat hippocampal slices prepared with aCSF containing 10 mM D-glucose and treated with vehicle or 1 μ M DPCPX.

Table 3.4: Mean fEPSP amplitudes measured 50-60 minutes after a 5xTBS stimulation in rat hippocampal slices prepared with aCSF containing 2 mM D-glucose and treated with vehicle or 1 μ M DPCPX

Table 3.5: Mean fEPSP amplitudes measured 50-60 minutes after a 5xTBS stimulation in rat hippocampal slices prepared with aCSF containing 10 or 2 mM glucose and treated with adenosine antagonist DPCPX.

Table 3.6: Mean fEPSP amplitudes measured 50-60 minutes after a 5xTBS stimulation in rat hippocampal slices prepared with aCSF containing 10mM D-glucose and treated with vehicle or 50 nM KW-6002

Table 3.7: Mean fEPSP amplitudes measured 50-60 minutes after a 5xTBS stimulation in rat hippocampal slices prepared with aCSF containing 5 mM D-glucose and treated with vehicle or 50 nM KW-6002

Table 3.8: Mean fEPSP amplitudes measured 50-60 minutes after a 5xTBS stimulation in rat hippocampal slices prepared with aCSF containing 2 mM D-glucose and treated with vehicle or 50 nM KW-6002

Table 3.9: Mean fEPSP amplitudes measured 50-60 minutes after a 5xTBS stimulation in rat hippocampal slices prepared with aCSF containing 10, 5 or 2 mM glucose and treated with adenosine antagonist KW-6002

Table 3.10: Mean fEPSP amplitudes measured 50-60 minutes after a 5xTBS stimulation in rat hippocampal slices prepared with aCSF containing 10 mM D-glucose and treated with vehicle or 100 nM PSB603

Table 3.11: Mean fEPSP amplitudes measured 50-60 minutes after a 5xTBS stimulation in rat hippocampal slices prepared with aCSF containing 10 mM D-glucose and treated with vehicle or 300 nM MRS1523

Table 3.12: Mean fEPSP amplitudes measured 50-60 minutes after a 5xTBS stimulation in rat hippocampal slices prepared with aCSF containing 10 mM D-glucose and treated with vehicle or 100 nM CGS15943

Table 3.13: Mean fEPSP amplitudes measured 50-60 minutes after a 5xTBS stimulation in rat hippocampal slices prepared with aCSF containing 5 mM glucose and treated with adenosine antagonist CGS15943

Table 3.14: Mean fEPSP amplitudes measured 50-60 minutes after a 5xTBS stimulation in rat hippocampal slices prepared with aCSF containing 10 or 5 mM glucose and treated with adenosine antagonist CGS15943

Table 3.15: Mean fEPSP amplitudes measured 50-60 minutes after a 5xTBS stimulation in rat hippocampal slices prepared with aCSF containing 10 mM glucose and treated with vehicle or adenosine antagonists

Table 3.16: Mean fEPSP amplitudes measured 50-60 minutes after a 5xTBS stimulation in rat hippocampal slices prepared with aCSF containing 5 mM glucose and treated with vehicle or adenosine antagonist

Table 3.17: Mean fEPSP amplitudes measured 50-60 minutes after a 5xTBS stimulation in rat hippocampal slices prepared with aCSF containing 2 mM glucose and treated with vehicle or adenosine antagonist

Table 4.1: Summary table showing the mean magnitude of LTP measured 50-60 minutes after a 10xTBS stimulation in WT mice hippocampal slices treated with vehicle (aCSF + 0.1% DMSO) or test compounds.

Table 4.2: Summary table showing the mean magnitude of LTP measured 50-60 minutes after a 10xTBS stimulation in $\text{Ac}\alpha 7^-$ mice hippocampal slices treated with vehicle or test compounds.

Table 4.3: Comparison of the mean fEPSP amplitudes measured 50-60 minutes after a TBS in hippocampal slices treated with L-436, an $\alpha 7$ nAChR-targeting compound within this study.

Table 4.4: Summary table showing the effects of increasing concentrations of the $\alpha 7$ nAChR-targeting compound L-436 on LTP and the effects of the $\alpha 7$ nAChR antagonist MLA on L-436-induced effects.

Acknowledgements

I would like to thank Neurosolutions Ltd., for financial support and resources provided over the course of my PhD. I would also like to express my gratitude to my supervisor Professor David Spanswick for his assistance, guidance, and dedication to science. I would also like to express my gratitude to Dr. Andrew Whyment for the supervision and direction provided in the initial stages of my doctoral training program.

I would also like to use this opportunity to thank my family, my partner and my friends for their patience, kindness, and support.

Declaration

I hereby declare that this thesis has been composed solely by myself and that it has not been accepted in any previous application for a degree. Apart from the Whole-cell electrophysiology data (Chapter 5), which was shared by Professor Spanswick, all work has been done by myself and all sources used have been specifically acknowledged by means of a reference.

Summary

The collection of studies presented in this thesis evaluates novel therapeutics and assesses their potential as cognitive enhancers. The study also examines the impact of ambient glucose levels on a widely used cellular model for learning and memory. Finally, the work described here explores a possible mechanism of action of an experimental nootropic compound. Taken together, this thesis aims to address the prevailing public health threat of cognitive decline by expanding the existing knowledge on nootropics and on the effects of glucose on learning and memory.

1. The validity of a L-436, a novel and potentially beneficial positive allosteric modulator (PAM) of $\alpha 7$ nAChRs, developed by Merck, was assessed via the application of the extracellular recording electrophysiology technique. The effectiveness of L-436 was compared with known modulators of these receptors: a partial agonist, EVP-6124 and a PAM BNC-375. The key findings from this study are that L-436 induced a concentration-dependent enhancement of LTP in both mouse and rat hippocampal slices. This effect was not present in mice lacking $\alpha 7$ nAChRs (Acr $\alpha 7$ - mice) unlike their wild-type littermates. In rat hippocampal slices, the maximum effect of L-456 on LTP, observed around a concentration of 10 μ M, was inhibited in the presence of the selective $\alpha 7$ nAChR antagonist MLA. Consequently, these data suggest that L-436 enhances LTP via a direct effect on $\alpha 7$ nAChRs. Therefore, the effects of L-436 on LTP are similar those of established partial agonists of $\alpha 7$ nAChRs such as EVP-6124, GTS-21, S 24795 and SSR180711.
2. The second study evaluated the effects of three different ambient D-glucose concentrations (10, 5 and 2 mM) on theta-burst-induced LTP, in the presence of either vehicle or a selection of adenosine receptor-targeting antagonists with the aim to elucidate the role of adenosine receptors in LTP. It was also of interest to investigate the influence of extracellular D-glucose on LTP due to the well-known disparity between extracellular glucose concentration *in vitro*, as opposed to *in vivo* conditions. Data presented here suggest little effect of extracellular glucose on LTP and does not support the idea that ambient

extracellular glucose levels impact LTP via a glial-adenosine-dependent mechanism as is observed in hypothalamus.

- 3.** The aim of the third study was to provide an insight into the mechanism of action SD118, novel putative cognition-enhancing compound developed by SyndesI, using Levetiracetam as the scaffold structure. By using whole-cell patch clamp recording techniques in hippocampal slices SD118 was shown to enhance excitatory glutamatergic synaptic transmission in the hippocampus in a frequency-dependent manner. Excitatory synaptic responses were little affected at low frequencies of stimulation (0.1 to 2 Hz) but were potentiated at higher frequencies (10 and 20 Hz). Therefore, SD118 shares the frequency-dependent effect on excitatory synaptic transmission with Levetiracetam, albeit with different outcomes. Unlike Levetiracetam, SD118 enhances synaptic transmission and could therefore be beneficial for cognitive enhancement.

Abbreviations

aCSF	artificial cerebrospinal fluid
A β	amyloid beta
ACh	acetylcholine
AD	Alzheimer's Disease
ADP	adenosine diphosphate
AICD	APP intracellular domain
AMPA	α -amino-3-hydroxy-5-methyl-4-isoxazolepropionic acid receptor
APP	amyloid precursor protein
ATP	adenosine triphosphate
BAPTA	1,2-bis(o-aminophenoxy)ethane-N,N,N',N'-tetraacetic acid)
BBB	blood brain barrier
BDNF	brain-derived neurotrophic factor
BMI	body mass index
cAMP	cyclic adenosine monophosphate
CNS	central nervous system
CREB	cAMP response element-binding protein
CSF	cerebrospinal fluid
D ₂ R	dopamine receptor D ₂
DG	dentate gyrus
E-LTP	early long-term potentiation
ERK	extracellular signal-regulated kinase
GABA	γ -aminobutyric acid
GLUTs	Glucose transporters
HFD	high-fat diet
HK	hexokinase
I-LTP	initial long-term potentiation
IU	international unit
LTD	long-term depression
LTP	long-term potentiation
MAP	microtubule-associated protein
MRI	magnetic resonance imaging
nAChR	nicotinic acetylcholine receptor
NFT	neurofibrillary tangle

NMDA	<i>N</i> -Methyl-D-aspartic acid
NT	neurotransmitter
PLC	Phospholipase C
PKA	Protein kinase A
PPP	Pentose phosphate pathway
sA β	soluble amyloid beta
STP	short-term potentiation
TBS	theta burst stimulus
T2D	type II diabetes
VDCCs	voltage-gated calcium channels

Chapter 1: General Introduction

1.1 Types of Learning and Memory

Learning and memory are two key cognitive functions that provide organisms with the ability to adapt their behaviour in response to changing environments. Memories are categorized into two broad groups: nondeclarative and declarative (Fig.1.1). Non-declarative memories can be recalled without conscious awareness. These memories include skills and habits (e.g., driving a car, playing the piano, etc.), priming (i.e., exposure to a stimulus influences the response to a subsequent stimulus), simple classical conditioning (e.g., Pavlovian conditioning), and nonassociative learning, such as habituation and sensitization. In contrast, declarative memories are memories that can be consciously recalled, such as events, experiences, and facts (Eichenbaum 1997, Squire 2004). Declarative memories are further classified into either episodic memory, which include the recall of events or specific experiences, or semantic memory, which is the recollection of general facts and knowledge (Eichenbaum 1997). It is important to note that although both declarative and nondeclarative memory systems are commonly associated with specific brain regions, the processes underlying these memory systems are likely to interact therefore involving partially overlapping domains.

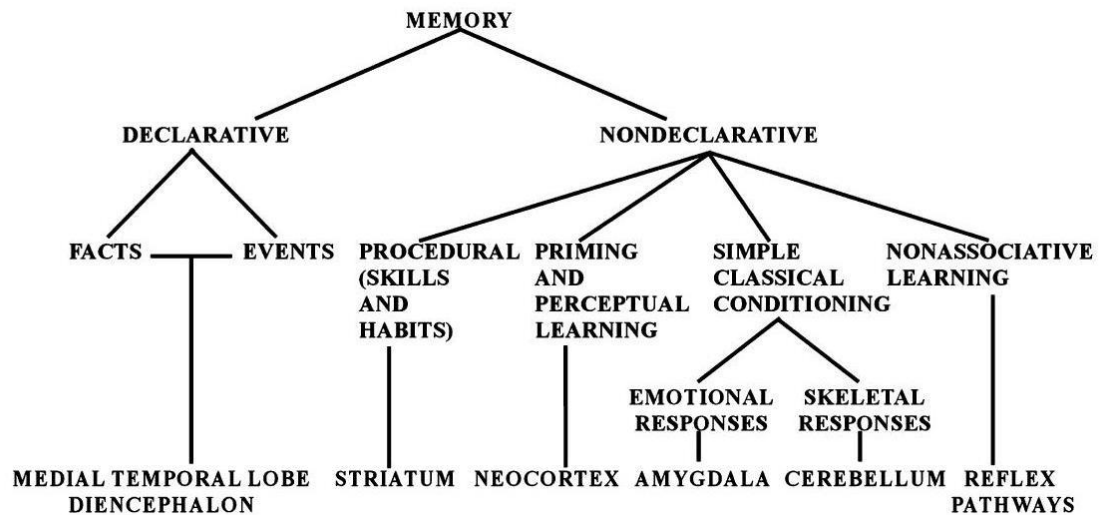


Figure 1.1 An overview of the taxonomy of memory systems and brain structures associated with them (Squire *et al.*, 2004).

1.2 Neurological disorders and learning and memory

Memory dysfunction can be caused by a wide range of neuropathologies that affect the neural networks underlying these memory systems in the human brain. The process of ageing is frequently accompanied by some degree of cognitive impairment (e.g., forgetfulness) that with appropriate management does not severely affect one's quality of life. However, minor cognitive disturbances can escalate further to mild-cognitive impairment, that in turn can lead to extensive cognitive deficits, resulting in a form of dementia. Dementia is defined as a gradual and irreversible loss of cognitive functions, encompassing loss and deterioration of processes such as memory, information processing, understanding and judgement. In recent years links between obesity and development of dementia have been recognised, highlighting poor diet and obesity as potential risk factors for dementia (Kiliaan *et al*, 2014).

1.3 Alzheimer's Disease: A major public health concern

To date, the most common cause for dementia is Alzheimer's disease (AD). In the UK alone, an estimated 850,000 individuals suffer from a form of dementia, AD being the major contributor to this statistic. The healthcare costs associated with dementia currently total £26.3bn and the worldwide estimate for this cost has reached US\$818bn (World Alzheimer report, 2015). In addition, a worrying statistic has been reported by Alzheimer's Research UK (2018) showing that only a third of respondents think it is possible to reduce their risk of developing dementia; conversely over 80% of respondents believe in reducing the likelihood of developing diabetes. It is apparent that dementia and the diseases it encompasses pose a major socio-economic burden that is predicted to worsen in the future. At present, there is no cure for AD and the available treatment options are of limited efficacy. Whilst further research of the mechanisms underlying AD onset and progression is urgently required, raising public awareness about dementia-associated lifestyle factors is equally as important.

1.3.1 Alzheimer's Disease: Diagnostic guidelines

Alzheimer's disease is characterized by a gradual and advancing decline in memory and executive functions, progressing to an inability to perform basic daily activities, and ultimately resulting in death. The onset and advancement of AD among patients is highly unpredictable, therefore increasing the challenge of finding appropriate treatments. In addition, reaching a definite diagnosis confirming Alzheimer's disease is a complex and not wholly reliable process. According to clinical guidelines, in addition to the "core criteria" for AD, such as evidence of cognitive decline and ruled out vascular, traumatic, or medical causes of cognitive impairment, several tiers of probability for confidence in a diagnosis of AD have been developed, i.e., "*proven AD*", "*probable AD*" and "*possible AD*". *Proven AD* is confirmed by the presence of AD-associated neuropathology criteria at autopsy after death

or after biopsy. However, it should be noted that a brain biopsy is usually considered as an investigational process of last resort for patients exhibiting neurological decline of undetermined etiology or atypical presentations due to the recent advances in the less invasive imaging and CSF analysis techniques (Schott *et al.*, 2010; Magaki *et al.*, 2015; Hansson *et al.*, 2019). *Probable* AD refers to a history of progressive worsening of amnesic dementia and lack of aphasia, cardiovascular disease, dementia with Lewy bodies or frontotemporal dementia. Lastly, *possible* AD refers to the presence of the “core” cognitive impairments in addition to some evidence of other medical conditions that could account for the cognitive disturbances.

It is of note that motor-skill learning appears to be spared or at least substantially less affected in patients with AD. First documented by Eslinger and Damasio (1986) this disassociation in learning supports the theory of two learning systems – “declarative” and “non-declarative”. Furthermore, this supports the view that AD affects memory likely via changes in the hippocampal function.

1.3.2 Neuropathology of Alzheimer’s Disease: Macroscopic Characteristics

It is widely accepted that AD-associated cognitive deficits are complemented by major macroscopic and microscopic changes of the brain. Post-mortem examinations of brain specimens obtained from AD patients reveal a considerable degree of cerebro-cortical atrophy (Fig.1.2). which mainly affects the medial temporal lobes but somewhat spares the primary motor, sensory and visual cortices. This manner of cortical thinning makes the lateral and third ventricles appear dilated. In addition, cerebral gyri narrow, whereas sulci – widen. This specific pattern of atrophy can be detected by MRI as early as a decade before the onset of cognitive decline and hence could be useful marker (Dickerson *et al.*, 2011). Such structural changes, however, have been observed in brain scans from aged but cognitively intact individuals.

Therefore, cortical thinning it is not a guaranteed sign of future cognitive decline. Nevertheless, a greater proportional brain tissue loss has been correlated with a more rapid cognitive decline in older patients (Double, 1996).

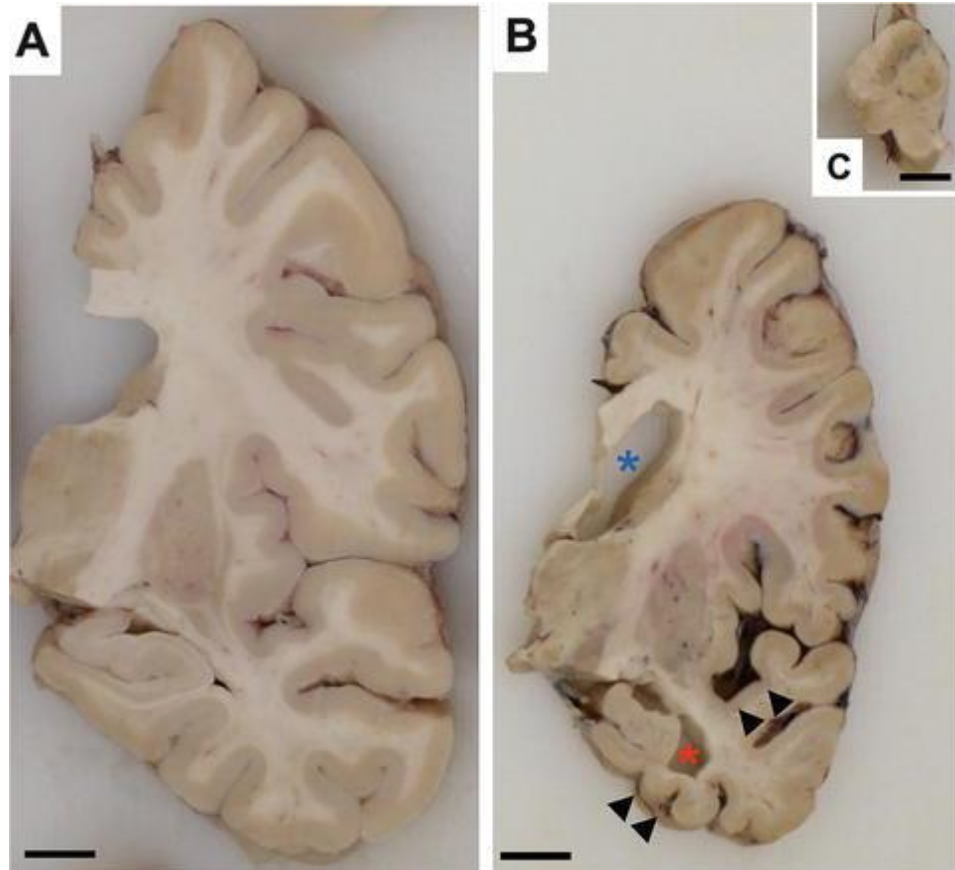


Figure 1.2. Coronal sections of formalin-fixed tissue slices taken at the level of the anterior hippocampus of a person without dementia (A) and a patient with severe AD ((B) and (C)).

There is a considerable enlargement of the lateral ventricle (blue asterisk), substantial atrophy of the medial temporal lobe (red asterisk), as well as thinning of the gyri and widening of the sulci (arrowheads). A section of the midbrain shows the presence of pigmentation (C). Both scale bars are 1 cm. Photographs by Dr. Christopher Morris and the Newcastle Brain Tissue Resource (Attems *et al.*, 2018).

1.3.3 Amyloid β plaques

In addition to the macroscopic changes, histological examinations of AD-affected brains reveal additional abnormalities. The presence of senile (Amyloid- β) plaques is widely recognized as one of the hallmarks of Alzheimer's disease. The A β plaques are extracellular, insoluble accumulations of small (40 or 42 amino acids long) amyloid- β peptides (A β 40, A β 42), which are the by-products of abnormal processing of the amyloid precursor protein (APP) (Fig. 1.3.).

There are two morphologically distinct types of A β plaques – diffuse and dense-core (or focal). Diffuse A β plaques are frequently found in the brains of cognitively intact elderly individuals, whereas dense-core plaques are mainly found in patients affected by AD. The presence of dense-core plaques is associated with further damage to the neuropil, including dystrophic neurites, synaptic loss, neuron loss and activation of both astrocytes and microglia (Knowles *et al.*, 1999; Urbanc *et al.*, 2002; Vehmas *et al.*, 2003). However, the true pathological significance of the presence of A β plaques and their influence on the severity or progression rate of Alzheimer's disease, remains controversial (Thal, *et al.*, 2002; Giannakopoulos, *et al.*, 2003).

Both in vitro and in vivo studies have shown that the amyloid peptide in its soluble form is produced by normal, healthy cells (Haas *et al.*, 1992). However soluble A β (sA β) appears to be a major contributor towards the pathogenesis of AD, since there is a strong correlation between sA β levels and the severity of AD-associated neuropathological changes (Shankar *et al.*, 2008). Studies have indicated that sA β promotes synaptic failure and impairment of cognitive functions, and dysregulation of specific neuronal miRNAs, which are likely to further contribute to the pathogenesis seen in AD (Müller *et al.*, 2013; Boissonneault *et al.*, 2009). In addition, Li *et al.*, (2014) showed that the sA β -induced miRNA dysregulation was reversed by NMDA receptor antagonists, suggesting a NMDAR-dependent mechanism for altered miRNA expression.

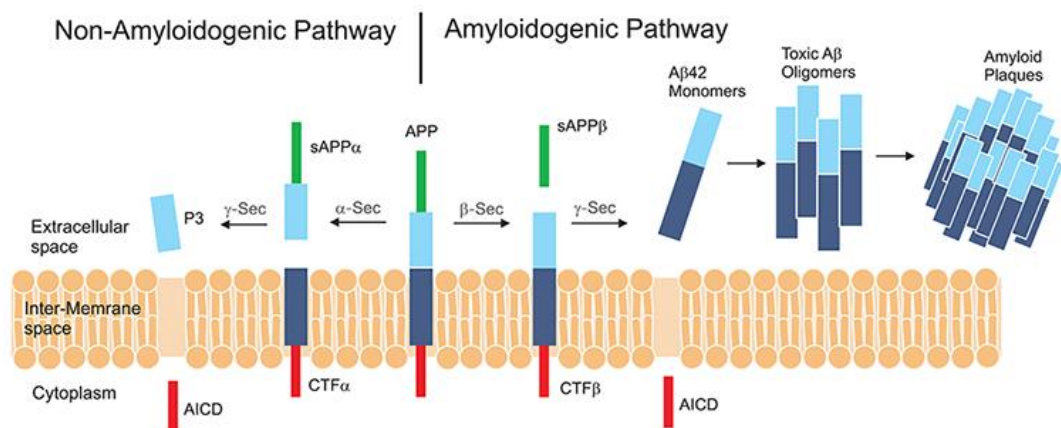


Figure 1.3. A commonly used schematic diagram for visualising the processing of the amyloid precursor protein (APP).

Briefly, it shows two processing pathways and their end products. The non-amyloidogenic pathway is initiated by α -secretase releasing soluble APP (sAPP α) into the intracellular space. The resulting CTF- α fragment is cleaved by γ -secretase in the intermembrane space resulting in both the APP intracellular domain (AICD) and p3 peptide fragments that are both non-plaque-forming elements. The cleavage of APP of β -secretase and subsequently by γ -secretase results in the production of an amyloid plaque. The pathogenic (amyloidogenic pathway) initiated by β -secretase and resulted in sAPP- β release externally. The remaining CTF- β fragment is cleaved by γ -secretase and releases A β_{38-42} amino acid amyloid monomers. The externally released A β fragment forms toxic oligomers and are eventually arranged in amyloid plaques – a hallmark of AD pathology (Bachurin *et al.*, 2017).

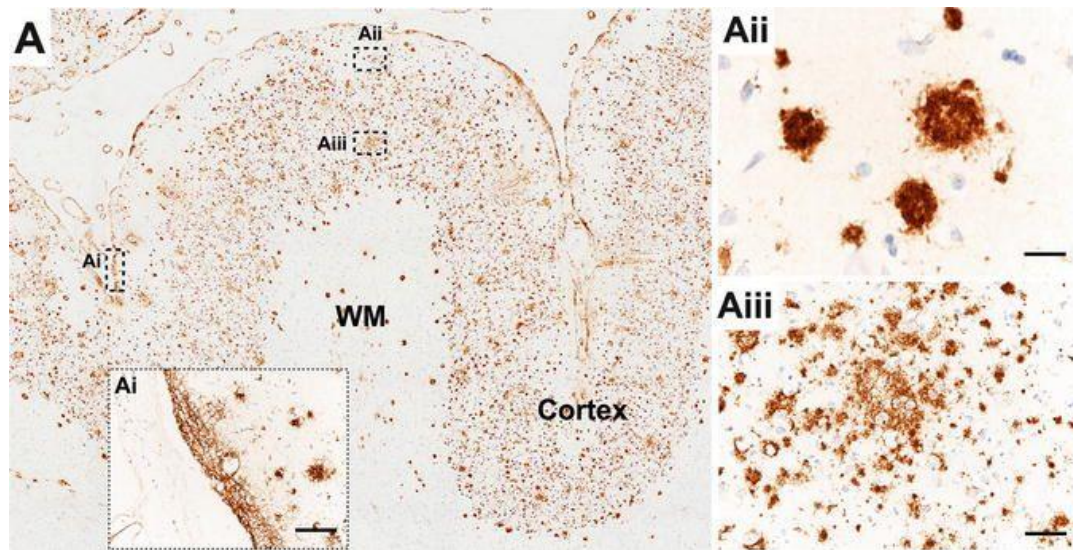


Figure 1.4. Photomicrographs of A β plaques.

(A) Distribution of A β immunoreactivity in the prefrontal cortex of an Alzheimer's disease patient. (Ai) Subpial A β load; (Aii) dense-core A β accumulations; (Aiii) diffuse A β deposits. WM, white matter; A β , amyloid beta. Immunohistochemistry was performed with antibody against amyloid precursor protein, 4G8. Scale bars: Ai and Aiii, 50 μ m; Aii, 20 μ m (Attems *et al.*, 2018).

1.3.4 Neurofibrillary tangles and neuropil threads

Neurofibrillary tangles (NFTs) and neuropil threads (NTs) are also considered as hallmarks of AD (Fig. 1.4). These filaments are made up of hyperphosphorylated microtubule-associated protein (MAP) *tau* (HP-T): a microtubule-stabilizing protein that is found in both axons and dendrites. In case of pathological conditions, MAP *tau* undergoes phosphorylation and subsequent disintegration of microtubules and accumulation of insoluble *tau* filaments or fibrils. In addition, NFTs and NTs are thought to contribute towards neurodegeneration by disrupting microtubule networks, leading to cytoskeletal destabilization and synaptic withdrawal (Billingsley & Kincaid, 1997; Ballatore *et al.*, 2007). In the early stages of AD, NFTs and NTs are primarily found in the trans-entorhinal and entorhinal cortices, from where they gradually spread into the hippocampus and isocortex (Braak and Braak, 1991).

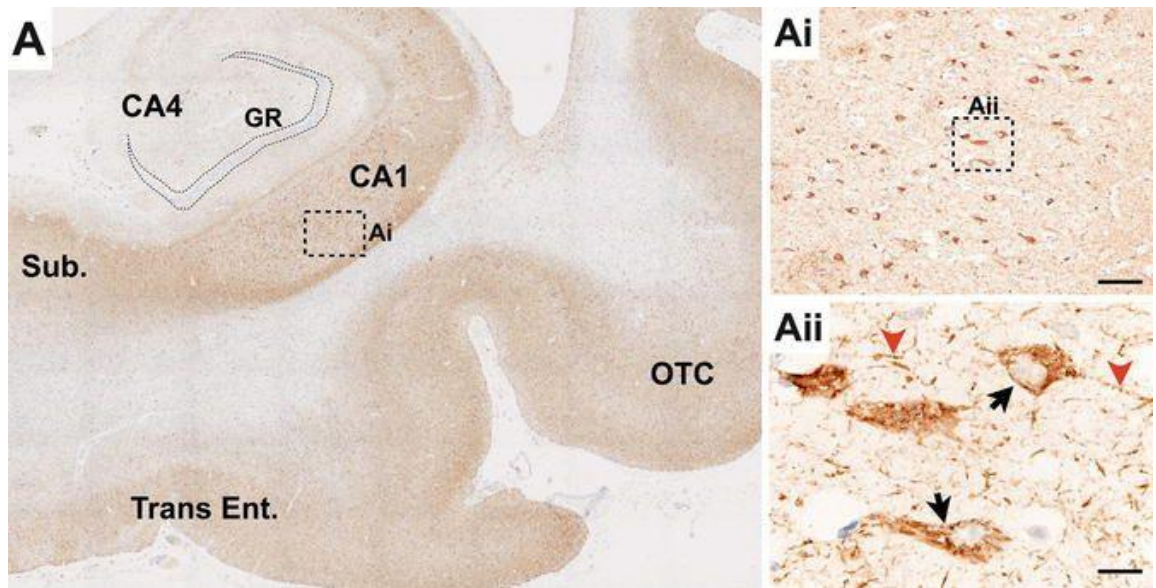


Figure 1.5. Photomicrographs depicting neurofibrillary tangles and neuropil threads.

(A) Distribution of *tau* immunoreactivity in the hippocampus, subiculum, transentorhinal, and occipital-temporal cortex of an Alzheimer's disease patient. (Ai) Neurofibrillary tangles and neuropil threads in the CA1 area of the hippocampus. (Aii) Neurofibrillary tangles present within the neuronal soma (black arrow); immunoreactive neuropil thread in the neuronal process (red arrowhead). CA1 and CA4, hippocampal cornu ammonis regions 1 and 4; GR, granule cell layer of the dentate gyrus; Sub, subiculum; Trans Ent, transentorhinal cortex; OTC, occipital-temporal cortex. Immunohistochemistry with antibody against hyperphosphorylated *tau*, AT8. Scale bars: Ai, 50 μ m; Aii, 10 μ m (Attems *et al.*, 2018).

1.4 Other neurodegenerative disorders associated with dementia

AD is not the only neurodegenerative condition with dementia as its major component. Other diseases, such as vascular dementia, frontotemporal dementia, dementia with Lewy bodies, Korsakoff's syndrome (an alcohol-related pathology), and HIV-associated cognitive impairment also exhibit varying degrees of dementia. In addition, traumatic brain injury is a risk factor for developing dementia. Moreover, many of the AD-associated neuropathological features, e.g., neural loss, senile plaques or NFTs are also present in some of the disorders mentioned above. This overlap in pathologies is creating a challenging environment for the diagnosis and potential treatment of those affected.

1.5 Obesity and disturbances in learning and memory

Over the past few decades, a substantial rise in the prevalence of obesity has been observed. Obesity is usually quantified via the use of the body mass index (BMI) calculation: $\text{Body weight (Kg)}/\text{height (m)}^2$ (Gray and Fujioka, 1991). A BMI score of >25 is classified as overweight, whereas >30 as obese. In England, 29% of all adults are classified as obese and hospital admissions where obesity was a factor have risen to 711,000, which is an increase by 15% compared to data gathered in 2016/2017 (NHS, 2019). In addition, obesity is strongly linked with a range of co-morbidities, including osteoarthritis, hypertension, coronary heart disease, non-alcoholic fatty liver disease, type II diabetes (T2D) and cancer. Therefore, we are dealing with a major health and socioeconomic burden that is only expected to worsen.

Besides the obesity-associated secondary diseases, there is mounting evidence implicating excess body fat and calorie-dense diet as potential contributors towards cognitive impairment. Various studies have linked elevated intake of saturated fats and carbohydrates to increased incidence of AD (Pasinetti *et al.*, 2008) and milder forms of cognitive disturbances (Morris

et al., 2004). In animals, the use of Western-style diet (WS-diet), even if for a brief period, results in selective impairment on tests involving hippocampal-dependent memory and learning (Beilharz *et al.*, 2014). Similar findings have recently been reported from human trials (Stevenson *et al.*, 2020). In addition, selective hippocampal damage in rodents and pathologies that are largely confined to the hippocampus in humans are associated with increased energy intake (Davidson *et al.*, 2009). Thus, we can conclude that dietary factors are associated with the emergence of hippocampal pathology and that hippocampal pathology in turn is correlated with an increase in food intake and body weight gain.

1.6 Insulin resistance

A proposed common factor for connecting hippocampal impairment and excessive food intake is glucoregulation. An increased intake of saturated fats and refined carbohydrates can lead to metabolic syndrome, characterized by insulin resistance and glucose intolerance (Hu *et al.*, 2001). Insulin resistance is a common symptom of obesity and is characterized by poor glycemic control resulting from continued extreme elevations in, and decreased concentrations of, peripheral insulin (Martyn *et al.*, 2008). In elderly, healthy individuals who do not have T2D, a reduction in insulin sensitivity is associated with impaired cognitive performance, while cognitive function is improved in individuals with T2D following treatments with glucoregulatory compounds (Ryan *et al.*, 2006). Likewise, a delay in verbal memory has been reported by studies on persons with insulin resistance and poor glycemic control and similar deficits have been found in individuals with damage to the hippocampus (Greenwood *et al.*, 2003).

1.7 The hippocampus: role in learning and memory

The hippocampus is one of the most studied structures of the brain and its significance for learning and memory is indisputable. This was first highlighted by an early study based on the clinical case of patient H.M., a man who became an amnesiac after his medial temporal lobe was removed to lessen his epileptic seizures (Scoville and Milner, 1957; Corkin, 1997). Although most of his cognitive abilities, including working memory and perceptual and motor learning were intact, H.M. was found to be lacking in declarative memory. In addition to this deficit in learning ability, H.M. also suffered from retrograde amnesia. Collectively, these observations suggested that learning and subsequent consolidation of newly acquired information required the involvement of the hippocampal system. Hippocampal dysfunction, damage or surgical removal can lead to loss of memory and problems with establishing new memories. As AD progresses, the hippocampus is one of the first brain areas to be affected coinciding with confusion and loss of memory.

The mechanisms underlying the consolidation of declarative memories remains a highly debated subject. One view is that the hippocampus plays a time-limited role in memory consolidation; it is primarily active during initial stages of memory acquisition and these memories later become independent of the hippocampus as they are moved to parts of the neocortex for long-term storage. On the other hand, it is possible that the hippocampus plays an active role in both memory acquisition and their recall. (Eichenbaum, 1997).

1.8 The hippocampus: anatomy and structural organisation.

The hippocampus is a paired structure, with mirror-image halves found in each brain hemisphere. In humans and other primates, the hippocampus is found in the medial temporal lobe, whereas in mice and rats it is located between the thalamus and the cerebral cortex. Along with amygdala, thalamus, hypothalamus, basal ganglia, and cingulate gyrus, the hippocampus forms a substantial part of the limbic system. The hippocampus itself consists of the hippocampus proper (or cornu Ammonis - CA) and the fascia dentata (or dentate gyrus - DG), with one lamina folded around the other Amaral & Lavenex, 2007).

The hippocampus proper is divided into three regions: CA1, CA2, and CA3. Anatomically, the CA1 arises from the subiculum, a structure located between the hippocampus proper and entorhinal cortex. The CA1-3 areas consist of clearly defined layers: the *stratum oriens*, *stratum pyramidale*, *stratum lucidum*, *stratum radiatum*, *stratum lacunosum*, and *stratum moleculare*, with the latter two layers frequently grouped together as *stratum lacunosum – moleculare*. On the other hand, the DG contains only three layers: molecular (*stratum moleculare*), granular cell (*stratum granulosum*) and polymorphic layer (Fig. 1.5.). The hippocampus receives inputs (afferents) from the entorhinal cortex, which in turn, receives inputs from the cingulate, temporal, orbital, and olfactory cortices, and amygdala. Outputs (efferents) from the hippocampus go from the subiculum to the entorhinal cortex and amygdala or via the fornix to an array of anterior brain structures.

The hippocampus receives most of its inputs via the perforant pathway. Perforant path axons form excitatory synaptic connections with the dendrites of granule cells, which then project to the dendrites of CA3 pyramidal cells via the mossy fiber pathway. CA3 pyramidal cells then synapse with CA1 pyramidal cells via Schaffer collaterals and to CA1 cells in the contralateral hippocampus via commissural connections (Fig.1.6). This connectivity phenomenon is known as the tri-synaptic loop of the

hippocampus, and it has a central role in most electrophysiological studies of the potential mechanisms underlying learning and memory.

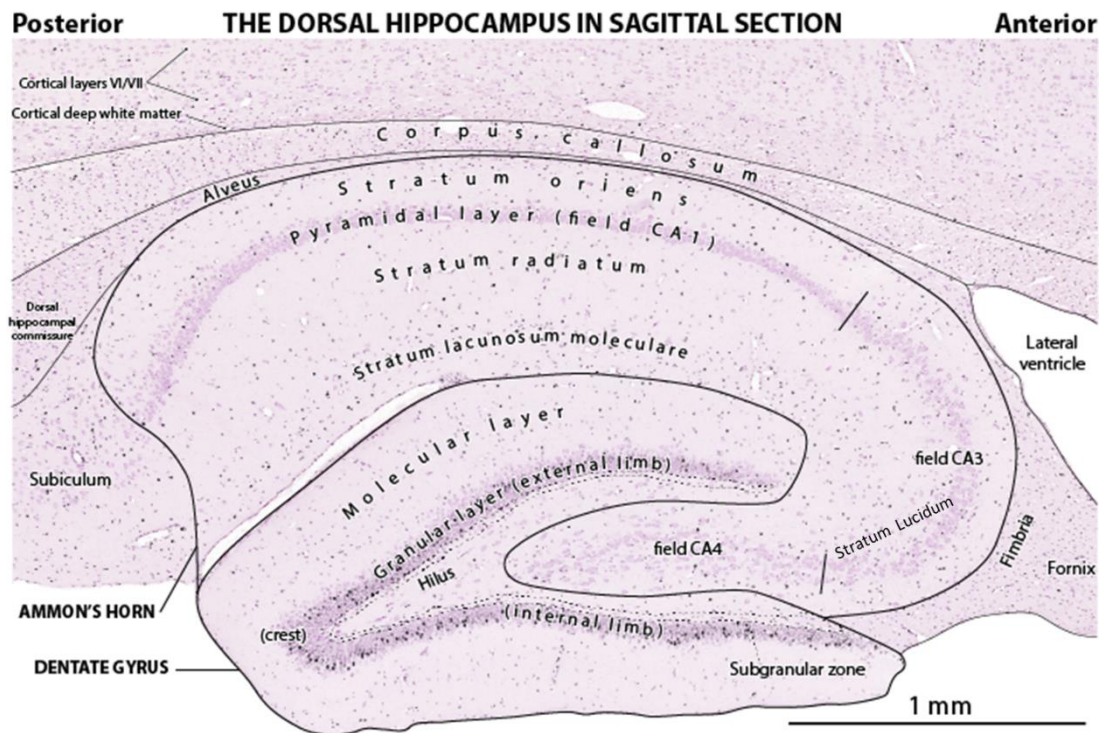


Figure 1.6. The anatomical arrangement of the rat dorsal hippocampus, including the principal layers and areas.

The alveus consists of axons of the hippocampal and subicular neurones. **The Stratum oriens** mainly contains basket cells. **The Pyramidal layer** contains pyramidal neurons (the main output neurons of the hippocampus), as well as interneurons and stellate neurons. **The Stratum lucidum** is only found in the CA3 area and it is occupied by the mossy fiber axons originating from the dentate gyrus. **The stratum radiatum** contains apical dendrites from pyramidal neurons and interneurons. **The stratum lacunosum moleculare** consists of apical dendrites from Schaffer collaterals, commissural fibres and interneurons. **The molecular layer** is where most performant path fibres form synapses with the granule cells of dentate gyrus. (Altman and Bayer, Braindevelopmentmaps.org).

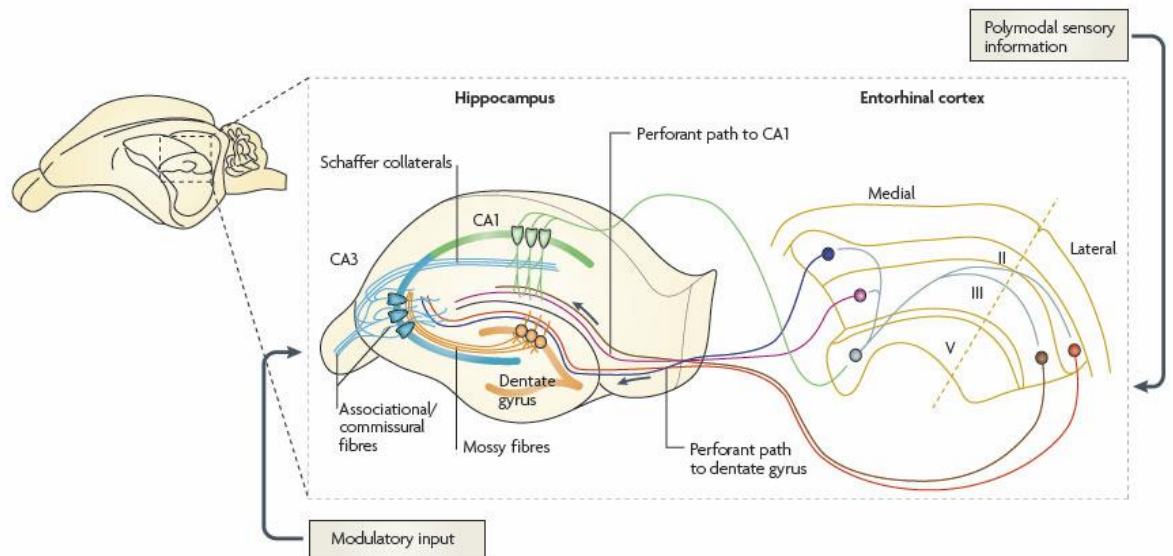


Figure 1.7. A diagram of the tri-synaptic circuit of the mouse hippocampus.

Perforant path provides the major input to the hippocampus. The axons encompassed in the perforant path originate from layers II and III of the entorhinal cortex (red and brown lines, respectively). Additional axons join the perforant path from layers IV and V. Axons originating from layers IV and V project to the granule cells of the dentate gyrus (yellow), pyramidal neurons of the CA3 (blue). The mossy fibres are the axons of DG granule cells. They travel from the dentate gyrus to CA3 pyramidal cells, forming their major input (light brown). Axons from layers III and V project to pyramidal neurons of the CA1 and the subiculum (green) (the temporoammonic pathway) (Neves *et al*, 2008).

1.9 An overview of long-term potentiation of synaptic transmission in learning and memory

The ability of synapses to change their activity behaviours in response to stimuli is known as synaptic plasticity. First hypothesized by Hebb in 1949 (Sejnowski, 1999), until activity-dependent changes in synaptic strength was first demonstrated by Bliss and Lomo in 1973. They reported a long-lasting increase in the post-synaptic response after applying electrical stimuli to the perforant pathway in the hippocampal formation. This enhancement of synaptic activity has since been referred to as long-term potentiation (LTP). In contrast, subsequent studies revealed a sustained reduction in synaptic response, induced in an activity-dependent manner by different electrical stimuli, and was named long-term depression (LTD) of synaptic transmission. The discovery of both LTP and LTD were significant not only because these electrophysiological phenomena supported the theoretical Hebbian model of plasticity, but also because they were initially found in the hippocampal formation – an area known for its involvement in aspects of learning and memory (Fig. 1.7).

Extensive research into the mechanisms underlying LTP suggest at least three different stages: an initial or short-term potentiation (I-LTP/STP), early LTP (E-LTP), and late LTP (L-LTP; Frey *et al.*, 1993; Sweatt, 2003). I-LTP, is the earliest stage of LTP and is a continued response from NMDA receptor-dependent synaptic plasticity. I-LTP lasts about 30–60 minutes and does not require protein kinase involvement (Roberson *et al.*, 1996). Due to its decremental potentiation, I-LTP used to be regarded as an unstable phase of the LTP, however it has been shown that it is a relevant and mechanistically separate to LTP (Park *et al.*, 2014). E-LTP lasts 2–3 hours and is mediated by kinases, such as calcium/calmodulin-dependent protein kinase II (CaMKII) and protein kinase C (PKC), whereas L-LTP lasts 5–6 hours and involves protein synthesis and changes in gene expression (Frey *et al.*, 1993; Kelleher *et al.*, 2004).

Overall, LTP possesses numerous electrophysiological characteristics that make it an attractive as a learning and memory candidate mechanism, for example - state dependence, i.e., the extent of depolarization of the postsynaptic cell determines LTP will take place. Input specificity is another important factor as it means that LTP will be restricted to only activated synapses, instead of all the synapses within a given area, ensuring that particular sets of inputs are selectively enhanced. Likewise, associativity is a crucial property of LTP, i.e., should a stimulation of a pathway be too weak to trigger LTP on its own, but a strong activation of a neighbouring pathway onto the same cell occurs at the same time, both synaptic pathways undergo LTP. This factor is important as it aids in linking networks and prevents degradation of information.

fast induction, long-term maintenance with capacity for long-term persistence, increased persistence with spread out induction protocols, input specificity, associativity (between both presynaptic inputs, as well as pre- and postsynaptic cells), management by neuromodulators, and abundant expression at synapses throughout the nervous system (e.g., Löwel & Singer, 1992; Abraham *et al.*, 2002).

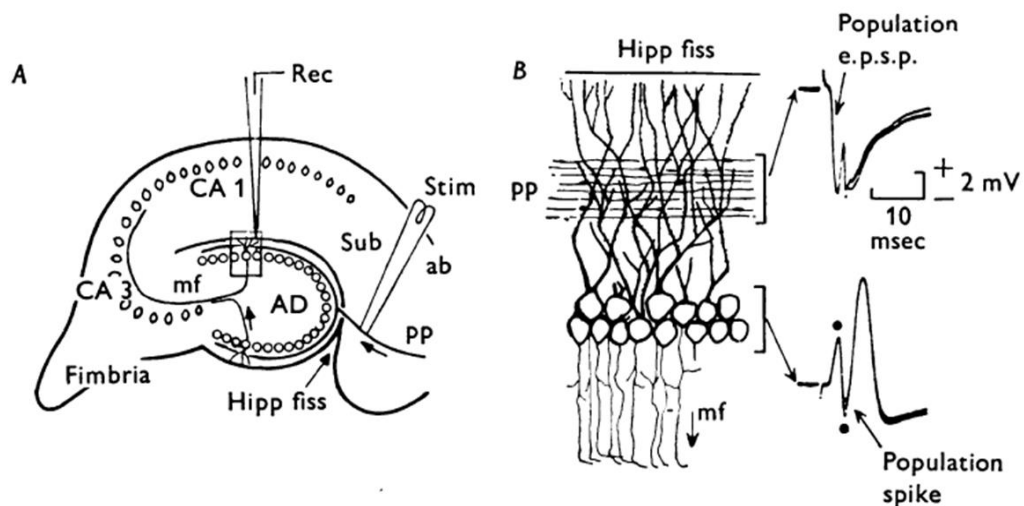


Figure 1.8. A schematic representation of the vital aspects of the LTP experiments performed by Bliss & Lomo (1973).

(A) The sagittal section of the hippocampus showing the placements of the stimulating and recording electrodes. (B) A magnified area of the dentate gyrus (AD) (rectangle from fig.(A) showing apical dendrites of the granule cells with perforant path fibres. The field electrophysiological postsynaptic potential (fEPSP) evoked in the synaptic layer (upper trace) and the population spike evoked in the cell body layer (lower trace).

1.9.1 Induction of LTP

The early electrophysiological studies of the induction of LTP involved the application of a brief (1 s) burst of high-frequency electrical stimuli (100 Hz). However, under normal conditions neurons do not fire at a rate of 100 Hz and as a result, several other stimulation paradigms were established. For example, the “theta-burst” (TBS) stimulation paradigm was created based on the finding that in normal, freely moving rodents the hippocampal pyramidal neurons fire action potentials at a frequency of approximately 5 Hz, creating what is known as “theta rhythm,” a sinusoidal oscillation of the hippocampal electroencephalography, which is critical feature for mnemonic processing (Bland, 1986; Lynch *et al.*, 1988). Therefore,

the use of this frequency could provide more physiologically relevant conclusions.

LTP is not solely confined to the hippocampal formation, rather it has been recorded from other brain areas, such as cerebral cortex, amygdala, hypothalamus and cerebellum. According to Malenka & Bear (2004), LTP is likely to be present in all excitatory synapses throughout the brain. Different forms of LTP can be found throughout the brain, most notably: *N*-methyl-D-aspartate (NMDA) receptor-dependent and NMDA receptor-independent long-term potentiation (Grover and Teyler, 1992; Cavus & Teyler, 1996). For example, LTP recorded from the CA3-CA1 hippocampal synapses employing high-frequency stimulation or TBS is NMDA receptor-dependent (Collingridge *et al.*, 1983; Harris *et al.*, 1984; Morris *et al.*, 1986), whereas a NMDA-independent LTP can be induced at the same synapse by using a 200-Hz stimulation protocol (Grover, 1998). In addition, LTP at mossy fiber-CA3 synapses is induced by NMDA receptors (Harris & Kotman, 1986; Rebola *et al.*, 2008). It should be noted that the focus of our research project remains on the NMDA receptor-dependent form of LTP at Schaffer-collateral/commissural synapses in area CA1 of rat hippocampus. An important reason for favouring an NMDAR-dependent forms of LTP is that it is input- or synapse-specific, i.e., only synapses that actively contribute to the induction process will undergo plasticity. This is because NMDARs on the synapses must be activated by synaptically released glutamate during the induction protocol.

The fast, excitatory synaptic transmission is mainly mediated via the release of L-glutamate, the most abundant excitatory neurotransmitter, from presynaptic glutamatergic neurons. This neurotransmitter quickly diffuses across the synaptic cleft where it binds to its postsynaptic receptors: α -amino-3-hydroxy-5-methyl-4-isoxazolepropionic acid receptors (AMPA) and NMDA receptors (NMDARs). Both AMPARs and NMDARs are ionotropic receptors that are permeable to Na^+ and K^+ ions, with NMDARs also being permeable to Ca^{2+} . Activation of calcium-permeable AMPARs (CP-AMPA),

a distinct receptor group that lack the GluA2 subunit) leads to an influx of Na^+ into the postsynaptic neuron and a moderate efflux of K^+ , resulting in the net depolarization of the postsynaptic cell. AMPARs mediate low-frequency synaptic transmission with little contribution from NMDARs, which under resting or low-frequency conditions are subject to a voltage-dependent block by magnesium ions (Mg^{2+}). However, in case of repetitive stimulation, continued AMPAR-mediated depolarization can be sufficient to remove the Mg^{2+} block of NMDARs, leading to the activation of NMDARs and leading to Ca^{2+} influx into postsynaptic dendritic spines: a key step for the induction of LTP (Fig.1.8). This requirement for synchronized pre- and post-synaptic activity is what confirms this synapse as Hebbian. In addition, the necessity for intracellular Ca^{2+} elevation has been proven by a lack of LTP with the application of Ca^{2+} chelators such as EGTA or BAPTA (Lynch *et al.*, 1983; Mulkey & Malenka, 1992), whereas LTP is induced if the postsynaptic cell has received calcium ion loading (Malenka *et al.*, 1988).

Activation of NMDARs and consequent increase in Ca^{2+} concentration leads to the activation of calcium/calmodulin-dependent kinase II (CaMKII), which is present at high concentrations in dendritic spines and are required for LTP (Lisman *et al.*, 2002). This leads to the phosphorylation of various proteins, including additional AMPARs. The phosphorylation of AMPARs can lead to an increase in AMPAR channel conductance (Benke *et al.*, 1998), a postsynaptic occurrence that contributes to the early phase of LTP. Furthermore, increased CaMKII activity leads to insertion of additional AMPARs into the postsynaptic membrane (Ehlers, 2000; Davies *et al.*, 2008; 1989) and this increased availability of functional postsynaptic AMPARs is also a contributing factor to LTP.

While CaMKII is well acknowledged as the major trigger for LTP, the full signaling cascades underlying the induction and maintenance of LTP are extremely complex. Several additional protein kinases, e.g., cAMP-dependent protein kinase (PKA) and protein kinase C (PKC), have been

identified as contributing factors to the processes underlying LTP (Malenka & Nicoll, 1999).

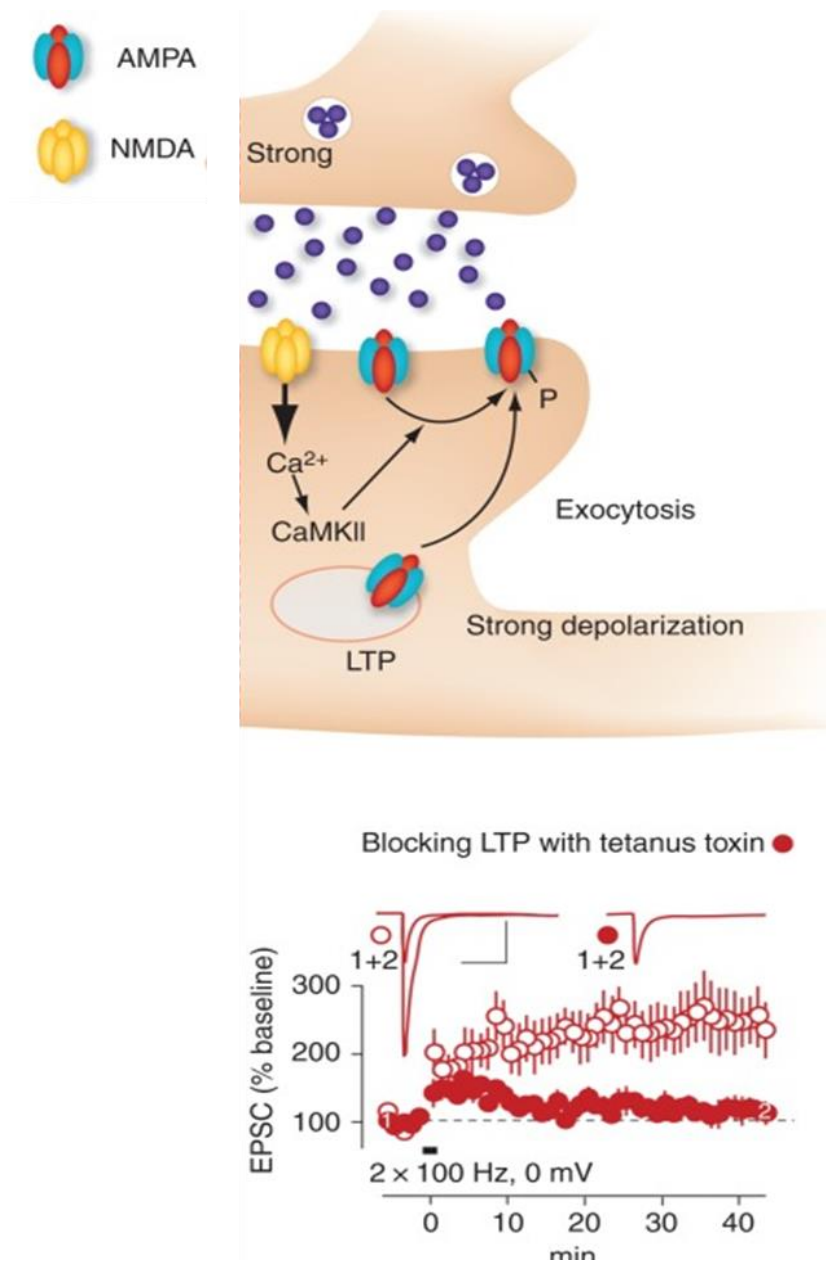


Figure 1.9. A diagram of the postsynaptic mechanism of LTP. LTP is triggered by strong depolarization, leading to CaMKII activation, receptor phosphorylation and AMPAR exocytosis. (Below) AMPAR Exocytosis and LTP is blocked by Tetanus toxin (control experiment – white circles, tetanus toxin – red circles). (Lüscher, 2012). The collective evidence suggests that NMDARs are required to initiate the LTP of AMPAR-mediated synaptic transmission.

1.9.2 Maintenance of LTP

In order to maintain long term potentiation for long periods of time, significant changes must take place within the postsynaptic density (PSD) area. Because most synaptic proteins have lifespans of some hours to a few days (Ehlers, 2003), it is likely to conclude that not all LTP events will result in long-lasting memories. Therefore, additional mechanisms that preserve the potentiated synapses must exist.

AMPA receptors are docked in the PSD by scaffolding proteins connecting them to cytoskeletal components such as actin. Insertion of additional AMPA receptors is therefore likely to affect the ultrastructure of the synapse, i.e., the spines associated with synapses that undergo LTP will enlarge (Matsuzaki *et al.* 2004). In addition to the physical enlargement of the existing spines, new dendritic spines arise from the neural shaft within minutes of the induction of LTP, therefore increasing the overall dendritic spine density (Toni *et al.* 1999).

The maintenance of LTP-induced change in synaptic magnitude is dependent upon protein synthesis. Signaling molecules, such as extracellular signal-regulated kinase (ERK) initiate protein synthesis either locally in the dendrites or via nuclear transcription (Sacktor 2008). Both local dendritic and nuclear transcription and somatic translation processes synthesize the proteins required for the maintenance of functional and structural flexibility following the onset of LTP. These mechanisms are likely instrumental for LTP to direct the selective stabilization of synaptic inputs that are of coincident activity, whereas nonactivated inputs may be replaced by new spines. One of the earliest-acting genes is the activity-regulated cytoskeleton-associated protein (*Arc*) which has been implicated in directing the translation of dendritic mRNA, which in turn is required for actin polymerization and steady expansion of dendritic spines during LTP (Bramham *et al.* 2010).

1.9.3 NMDA receptors

As mentioned above, NMDARs have an established role in triggering LTP. These receptors are structurally complex and possess multiple separate binding sites for glutamate, glycine, Mg^{2+} , Zn^{2+} and various polyamines. NMDARs belong to the ionotropic glutamate receptor subtype and they are made up of three separate subunit families: GluN1, GluN2 and GluN3. A functional NMDAR is a heteromeric complex typically combined of two glycine-binding GluN1 subunits and two glutamate-binding GluN2 subunits (Salussolia *et al.*, 2011). Depending on the subunit composition, the NMDA receptors will have varying pharmacological and biophysical properties. Thus, NMDARs in different parts of the brain can have diverse roles and functional properties (Fig.1.9).

NMDARs are highly permeable to Ca^{2+} . However, at resting membrane potentials (~ -65 to -75 mV), external magnesium (Mg^{2+}) ions flow into the NMDAR pore, but unlike the Ca^{2+} ions, they bind tightly and prevent any other ion permeation (Novak *et al.*, 1984). Extracellularly Mg^{2+} ions are present at millimolar concentrations, whereas intracellular Mg^{2+} concentrations are in the micromolar range, yielding a net inward driving force for Mg^{2+} ions at negative membrane potentials. A strong depolarization is needed to remove the Mg^{2+} ions from the pore, thereby allowing the flow of Ca^{2+} into the postsynaptic cell. Thus, for NMDARs to be activated both the concurrent binding of glutamate and glycine to their respective binding sites and sufficient depolarization are required to remove the Mg^{2+} block.

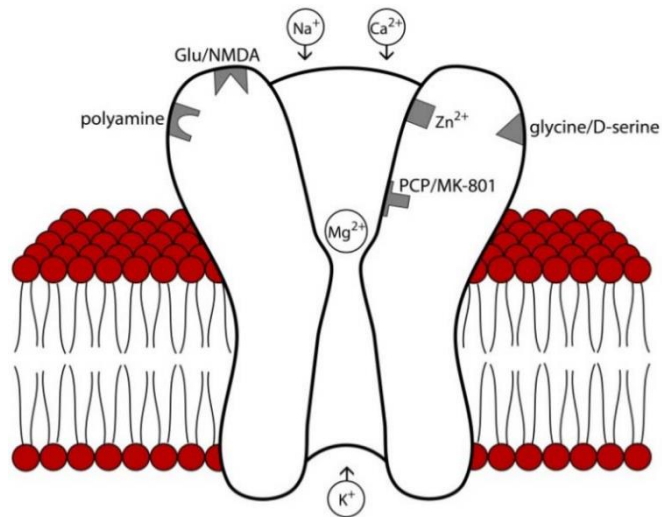


Figure 1.10. A diagram of the structure and binding sites of the NMDAR.

At rest, the receptor is blocked by Mg^{2+} which is removed upon depolarization of the membrane. Extracellular domains of the NMDA receptor host binding sites for glutamate, the endogenous co-agonists D-serine and glycine, and endogenous modulators such as polyamines, Zn^{2+} , and protons. The co-agonists and modulators may affect the functional properties of this ligand gated ion channel and therefore likely influence LTP. NMDA antagonists such as phencyclidine (PCP) and MK-801 bind to deeper areas of the channel pore (Tomek *et al*, 2013).

1.9.4 AMPA receptors

The α -amino-3-hydroxy-5-methyl-4-isoxazolepropionic acid receptors (AMPA receptors) belong to a class of ionotropic transmembrane receptors for glutamate that facilitate fast synaptic transmission in the central nervous system (CNS). Functional AMPARs are hetero-tetramers composed of four types of subunits (GluA1-4). In addition, changes in the receptor subunit composition determine the functional receptor properties. For example, an AMPAR's permeability to Ca^{2+} depends upon the presence of the GluA2 subunit within the tetramer. More specifically, the ability of the GluA2 subunits to allow for the AMPARs to become Ca^{2+} -permeable is determined by RNA editing of the GluA2 mRNA via post-transcriptional alteration of a codon encoding glutamine (Q) to a codon encoding arginine (R). Therefore, AMPARs are not Ca^{2+} -permeable if the edited GluA2 (R) subunit is part of the receptor, whereas the AMPARs are permeable to Ca^{2+} if they contain an unedited GluA2 (Q) or no GluA2 subunit at all (Hollman & Heinemann, 1994; Mayer & Armstrong, 2004). These receptors are also recognised as substantial modulators towards synaptic plasticity (Song & Huganir, 2002).

1.9.5 Metabotropic Glutamate receptors

The neurotransmitter glutamate exerts its modulatory actions via metabotropic glutamate receptors (mGluRs). Eight different mGluRs have been identified (mGluR₁ – mGluR₈), which depending on their structure and activity are further divided into three groups – I, II, and III (Fig.1.10). All mGluR receptor groups are widely expressed throughout the central nervous system, including neocortex, hippocampus, basal ganglia, thalamus/hypothalamus, cerebellum, and spinal cord (Martin *et al.*, 1992; Shigemoto *et al.*, 1993; Romano *et al.*, 1995; Berthele *et al.*, 1999).

Group-I mGluRs are primarily found postsynaptically, whereas Group II/III mGluRs are mainly found in presynaptic locations. Group III receptors are highly expressed in glial cells. The group-III receptors are likely responsible for the mediation of presynaptic depression of glutamatergic synaptic potentials, probably via inhibition of voltage-gated Ca²⁺ entry and regulation of glutamate release. Antagonism of Group I mGluRs results in substantial impairment in both the induction and maintenance of LTP (Manahan-Vaughan & Braunewell, 2005).

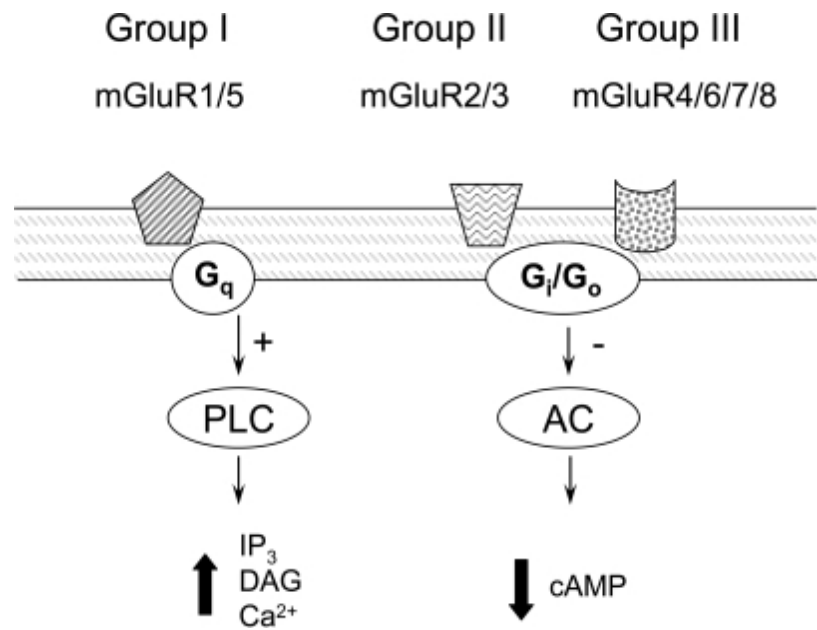


Figure 1.11. A schematic representation of the three mGluR groups. Group I consists of mGluRs1 and 5, Group II consists of mGluRs2 & 3, and Group III – mGluRs4, 5, 7, and 8. Intracellular signalling pathways of different mGluRs. Group I are coupled to PLC through activation of a G_q type G-protein and subsequent production of inositol triphosphate (IP₃), release of calcium from intracellular stores and production of diacylglycerol (DAG), activate protein kinase C. Group II/III are negatively coupled to adenylyl cyclase (AC) via G-protein of the G_i/G_o type, resulting in a decrease in cyclic AMP (cAMP) production (Hovelsø *et al*, 2012).

1.9.6 Nicotinic cholinergic receptors

The nicotinic acetylcholine receptors (nAChRs) are a super-family of ligand-gated, pentameric ion channels that are activated by the neurotransmitter acetylcholine (ACh). Presently, 16 different nAChR subunits ($\alpha 1-7$, $\alpha 9-10$, $\beta 1-4$, δ , ϵ , γ) have been identified in humans. These subunits form a variety of homopentameric and heteropentameric receptors with varied structural and pharmacological characteristics (Millar & Gotti, 2009).

The $\alpha 7$ nAChR is composed of five identical $\alpha 7$ subunits and contains five acetylcholine binding sites (Drisdell & Green, 2000). The $\alpha 7$ receptor subunit has a high conductance for Ca^{2+} ions (Berg & Conroy, 2002), low affinity to ACh (Clarke, 1992) and a high affinity for α -bungarotoxin (Marks & Collins, 1982; Rangwala *et al.*, 1997). This receptor is widely distributed throughout the brain and is present in both neural and non-neural cells and its presence, activity or lack thereof is associated with feeding behaviours, ageing, Alzheimer's disease and trauma (Mcfadden *et al.*, 2014; Court *et al.*, 1997; Okada *et al.*, 2013; Hoffmeister *et al.*, 2011).

In neurons, the activation of $\alpha 7$ nAChRs results in an increase in intracellular Ca^{2+} either directly through voltage-gated channels or indirectly - from intracellular sources (Dajas-Bailador *et al.*, 2002). The intracellular increase in Ca^{2+} concentration then regulates the release of glutamate and GABA (Maggi *et al.*, 2001; Radcliffe & Dani, 1998). In addition, Ca^{2+} influx and subsequent Ca^{2+} release from internal stores promotes the activation of CaMKII/IV and ERK/MAPK signaling cascades and the perpetuated phosphorylation of CREB, resulting in changes in gene expression (Hu *et al.*, 2002). This CREB-dependent gene transcription plays a further role in long-term memory formation (Bourtchouladze *et al.* 2003). Supporting evidence shows that mutant mice models lacking the CREB function have impaired memory formation and L-LTP, whereas mutant mice displaying a gain in the CREB function showed increased memory formation and a lowered threshold of L-LTP, overall indicating that CREB is an important factor in the positive

regulation of memory formation and LTP (Bourtchouladze *et al.* 1994; Kida, 2012). This connection between nAChRs and LTP strongly suggests that the nicotinic receptors are directly involved in the synaptic plasticity of the hippocampus. In hippocampal astrocytes $\alpha 7$ nAChRs appear to be involved in Ca^{2+} release from intracellular stores. However, the $\alpha 7$ nAChRs are expressed in much lower densities in glia than in hippocampal interneurons (Shen & Yakel, 2012).

1.9.7 Adenosine

Adenosine is a ribonucleoside that consists of adenine and D-Ribose and that is produced from the metabolism of adenosine triphosphate (ATP). In addition to playing a substantial role in cellular metabolism, adenosine and its derivatives have wide-ranging physiological effects upon arousal and sleep, cognition and learning and memory. In the central nervous system (CNS), adenosine operates as a neuromodulator by contributing to processes such as neurotransmitter release (Sebastio & Ribeiro, 2000), synaptic plasticity (de Mendonca & Ribeiro, 2001) and neuroprotection in ischemic, hypoxic and oxidative stress events (Fredholm *et al.*, 2011).

In the CNS, adenosine exerts its effects via G-protein coupled receptors (GPCRs) known as A₁, A_{2A}, A_{2B}, and A₃ (Fredholm *et al.*, 1994). The four ARs have different affinities for adenosine, distribution throughout tissues, and signaling pathways. It is generally accepted that activation of the A₁ and A₃ receptors elicit inhibitory effects, whereas the A_{2A} and A_{2B} receptors facilitate excitatory outcomes upon CNS cells (Klinger *et al.*, 2002).

1.9.7.1 The A₁ receptor

The A₁ receptor can be found in the cerebellum, cortex, hippocampus, spinal cord, and glia (Chen *et al.*, 2013). Due to its widespread presence in the CNS, the A₁AR is considered to be a major component in a wide range of physiological events, including analgesia, sleep regulation, sedation, inhibition of neurotransmitter release and reduction of neuronal excitability (Varani *et al.*, 2017; Stenberg *et al.*, 2003; Gessi *et al.*, 2011; Sawynok, 2016; Vincenzi *et al.*, 2016a, b). The mechanism underlying these effects is the activation of A₁AR and subsequent inhibition of adenylyl cyclase (AC) via the activation of G-proteins (G_i/G_o), resulting in increased activity of phospholipase-C (PLC). In neurons, activation of A₁ARs can also lead to activation of K⁺ channels and

inhibition of Q/P-, and N-type Ca^{2+} channels (Haas & Greene, 1984; Gundlfinger *et al.*, 2007).

The use of adenosine A_1 receptor agonists diminishes LTP in the hippocampus. Endogenous adenosine wields a tonic inhibitory effect on LTP since A_1 receptor antagonists consistently facilitate LTP (de Mendonça & Ribeiro, 1994). Application of adenosine $\text{A}_{2\text{A}}$ receptor agonists can enhance LTP (Almeida *et al.*, 2003). However, the role of endogenous adenosine mediated via $\text{A}_{2\text{a}}$ receptors towards the modulation of synaptic plasticity is still the subject to investigation (Sebastião & Ribeiro, 2009). The A_3 receptors may interfere with several modulatory systems in the hippocampus. The A_3 receptor agonists desensitize A_1 receptor-mediated responses (Dunwiddie *et al.*, 1997).

The effects of adenosine on synaptic plasticity should be relevant for the enhancement of intellectual performance and compounds acting via adenosine receptors might prove helpful in the treatment of memory disorders (de Mendonça & Ribeiro, 2001).

1.9.7.2 The A_{2A} receptor

The A_{2A} receptor is present in the striatum, especially in the GABAergic striatopallidal neurons, cholinergic interneurons, and corticostriatal glutamatergic terminals. In addition, the A_{2A} receptor can be found in the cerebral cortex, hippocampus, olfactory tubercle, and glial cells.

Activation of A_{2A} receptors increases AC activity via coupling to G_{s/olf} proteins leading to an increase in cyclic-AMP (cAMP) levels, resulting in the activation of protein kinase A (PKA), which in turn regulates cAMP responsive element binding protein (CREB). Subsequent phosphorylation of CREB activates c-fos and other genes such as preproenkephalin (Ferré, 2008). Interestingly, A_{2A}Rs can form heteromers with dopamine D₂ receptor (D₂R), which show robust functional antagonistic interaction, which in turn appears to be important for striatal functioning under both baseline and pathological conditions (Beggato *et al.*, 2014; Prasad *et al.*, 2021).

1.9.7.3 The A_{2B} receptor

The A_{2B} receptor is expressed at low levels on both neuronal and glial cells but compared to other AR subtypes, its role in the CNS is less established. The A_{2B} receptors have a low affinity for adenosine compared with other ARs (>10 μ M vs. 0.1-1 μ M) (Klinger *et al.*, 2002). Upon activation, A_{2B} receptors can couple to both G_s and G_q proteins, with G_s signaling leading to activation of the cAMP pathway, or G_q involvement resulting in PLC and PKC activation (Dunwiddie & Masino, 2001).

1.9.7.4 The A₃ receptor

Low levels of A₃ receptor expression have been detected in the cortex, thalamus, hypothalamus and hippocampus (Borea *et al.*, 2015). Like the A₁R, the A₃R couples to G_i proteins, resulting in decreased cAMP levels and reduced PKA activity (Dunwiddie & Masino, 2001). However, A₃ARs can also activate PLC and increase Ca²⁺ concentration if G_q proteins or G $\beta\gamma$ subunits are involved. Unlike A₁ARs, A₃ARs undergo fast, agonist-dependant desensitization (Palmer *et al.*, 1996).

1.9.8 Glia

The neural mechanisms underlying LTP have been investigated in extensive detail but increasing evidence suggests that glial cells have a substantial role in this process as well. Several studies have shown that glia participate more actively in neural circuit function than previously thought (Araque & Navarrete, 2010).

The Hebbian-like long-term potentiation that we have focused on so far, relies on *N*-methyl-D- NMDARs, and it has been shown that glia, such as astrocytes can adjust the activation of NMDARs via Ca²⁺-dependent release of the NMDAR co-agonist D-serine (Henneberger *et al.*, 2010). Astrocytic endfeet, containing both NMDARs and AMPARs surround synaptic clefts, therefore modulating/regulating synaptic plasticity (Verkhratsky & Kirchhoff,

2007). However, increases in Ca^{2+} concentration in astrocytes can also release other signaling molecules, most notably glutamate, ATP and tumour necrosis factor- α , while neurons themselves can synthesize and supply D-serine. (Zorec *et al.*, 2012; Rosenberg *et al.*, 2010). Furthermore, astrocytic loading with exogenous Ca^{2+} buffers do not suppress LTP obtained from the Schaffer collaterals, and the physiological significance of experiments in cell cultures or strong exogenous stimuli applied to astrocytes has been discussed. Therefore, the involvement of glia in LTP induction remains to be elaborated. A variety of additional neuroactive molecules affect neuronal plasticity and LTP (table 1.1) (Ota *et al.*, 2013).

Table 1.1: Summary of receptors/signaling molecules and mechanisms and their role in neuronal plasticity (adapted from Ota *et al.*, 2013).

Molecule	Receptor (s)	Mechanism of action in plasticity/memory formation
Acetylcholine	Muscarinic AchRs	Causes an increase in [Ca ²⁺] activating mGluRs
Adenosine	A1 Receptors	Inhibition of cAMP-dependent transcription
ATP	P2Y Receptors	Enhances concentration of AMPA receptors
Cytokines		
1. TNF	1. CXCR4	1. Glutamate release AMPAR insertion
2. CCL2	2. NMDA Receptors	2. Inhibition of NMDAR activity
3. Interleukin-1	3. IL1 Receptors	3. Unknown
D-serine	NMDA Receptors	Co-agonist of receptors
Ephrin		
1. Ephrin-A	1. EphrinA Receptors	1. Promotes retraction of dendritic spines
2. Ephrin-B	2. EphrinB Receptors	2. Regulates D-serine release
Glutamate	AMPA Receptors NMDA Receptors mGlu Receptors	Increased EPSP Upregulation of AMPARs
Lactate	MCT2	Provides additional metabolic energy for growth/plasticity
Nicotine	nACh Receptors	Releases Ca ²⁺ Promotes the release of D-serine

1.9.9 LTP and neurodegeneration

Although ageing-associated neuronal loss does affect most brain structures, it is not considered to be the primary cause for the various cognitive deficits that arise with advancing age. Instead, these cognitive deficits could be brought about via age-related changes in synaptic plasticity. Support for this theory comes from studies proving that the threshold for induction of LTP increases in older animals with higher stimulus frequencies or repeated induction stimuli being required to achieve the levels of potentiation comparable to their younger counterparts. Maintenance of LTP is also affected, i.e., the potentiation decays faster in hippocampi from aged animal brains. Conversely, the threshold for induction of LTD is reduced in aged animals (Norris *et al.*, 1996; Kamal *et al.*, 2000). Thus, the age-related decline in synaptic transmission may reflect a shift in the LTP/LTD balance, with insufficient LTP induction and maintenance and excessive synaptic depression (Foster *et al.*, 2001; Foster & Kumar, 2007).

With advancing age, changes in the mode of Ca^{2+} entry into neurones is an additional factor that may contribute to the shift in LTP/LTD balance, i.e., influx of Ca^{2+} via NMDARs is being reduced whereas Ca^{2+} influx via L-type voltage-gated calcium channels (VDCCs) is enhanced. The proposed underlying mechanisms for this imbalance include NMDAR hypofunction and redox sensitivity, while changes in phosphorylation of the L-type Ca^{2+} channels might contribute towards the increase in Ca^{2+} influx via L-type VDCCs (Kumar *et al.*, 2019; Bodhinathan *et al.*, 2010; Potier *et al.*, 2000; Norris *et al.*, 2002). L-type VDCCs are vital for NMDAR-independent induction of LTP (Morgan & Teyler, 1999), yet they also affect the NMDAR-dependent LTP via enhancing the afterhypolarization and subsequently diminishing the activation of NMDARs, thereby contributing towards the impairment of synaptic plasticity seen in aged rats (Landfield & Pitler, 1984). Aged neurons show other dysfunctional characteristics of Ca^{2+} homeostasis, such as increased release of Ca^{2+} from the endoplasmic reticulum (ER) (Gant *et al.*, 2006), reduced export of Ca^{2+} via the plasma membrane ATPase (Gao *et*

al, 1998), reduced cellular Ca^{2+} buffering (Murchinson & Griffith, 1999) and decreased mitochondrial Ca^{2+} sink capacity (Xiong *et al*, 2002). These events result in an overall increase in intracellular Ca^{2+} that in turn increases the threshold frequency for induction of LTP (Ris & Godaux, 2007). In summary, these changes in intracellular Ca^{2+} levels and localisation could underlie age-associated deficits in learning and memory. Indeed, application of the cell permeable Ca^{2+} chelator BAPTA, improves decreased presynaptic cytosolic and mitochondrial Ca^{2+} dynamics in hippocampal CA1 synapses of aged rats (Tonkikh & Carlen, 2009), and enhances spatial learning (Tonkikh *et al*, 2006). Changes in Ca^{2+} homeostasis have been linked to neuronal degeneration in both normal ageing and neurodegenerative conditions such as AD. Therefore, an increase in intracellular Ca^{2+} is thought to contribute towards increased neuronal vulnerability to further insults, including factors associated with AD.

1.9.10 LTP and metabolism

The main source of energy for the brain arises from glucose. The metabolism of glucose generates adenosine triphosphate (ATP) which fuels physiological brain functioning and is a crucial component for cellular upkeep and neurotransmitter generation. Thus, tight regulation of glucose metabolism is critical for normal brain physiology and disturbances in glucose metabolism in the brain underlies various pathological conditions, affecting both the brain itself, as well as the rest of the organism.

Glucose enters cells via glucose transporters (GLUTs) and is phosphorylated by hexokinase (HK) to produce glucose-6-phosphate. Glucose 6-phosphate is then processed via several metabolic pathways, for example, glycolysis, which leads to lactate production or mitochondrial metabolism. The pentose phosphate pathway (PPP) is another mode of metabolism, as is glycolysis, although the latter is present in astrocytes only (Fig. 1.11). Eventually, glucose is almost entirely oxidized to CO_2 and water in the brain. However, different glucose-metabolism routes result in a variety of metabolic

intermediates that can subsequently be oxidized by brain cells for energy production (e.g., lactate, pyruvate, glutamate, or acetate) (Zielke *et al.*, 2009). It is thought that both oxidative and non-oxidative (e.g., glycolysis) processes are required in order to meet increased metabolic demand during brain activity.

Hormones are critical for glucose homeostasis and they activate different signal transduction cascades in the brain. For example, insulin and insulin-like growth factor (IGF-I) activate the phosphatidylinositol trisphosphate kinase (PI3K)/Akt and Ras/MAPK-ERK pathways, thus affecting gene expression, with major consequences for neural stem cell proliferation and neuronal activity (Blazquez *et al.*, 2014). In addition, animal studies support the involvement of insulin in learning and memory, e.g., Zucker fa/fa rats (a leptin receptor mutation-dependent rat model for obesity) display impaired insulin sensitivity, which correlates with poor performance in the Morris Water Maze (MWM) (Kamal *et al.*, 2013). In agreement with this finding, heterozygous knockout (KO) mice for insulin receptor show lower performance in the novel object recognition test (Nisticó *et al.*, 2012). Furthermore, Zucker fa/fa rats show loss of insulin sensitivity and a subsequent reduction in LTP at CA3–CA1 synapses, whereas LTD is unaffected. In addition, the heterozygous KO mouse model show a normal LTP induction that does not become consolidated, resulting in an impairment of long-term synaptic plasticity (Nisticó *et al.*, 2012).

Other studies show that insulin facilitates LTP by lowering the stimulus frequency required for LTP – a result due to the activation of PI3K pathway and subsequent upregulated NMDAR exocytosis. Therefore, insulin appears to be an influential mediator of LTP and learning and memory (Van der Heide *et al.*, 2005). Thus, insulin resistance associated with obesity-induced T2D may be a mechanism contributing to impaired cognitive function in the metabolic syndrome.

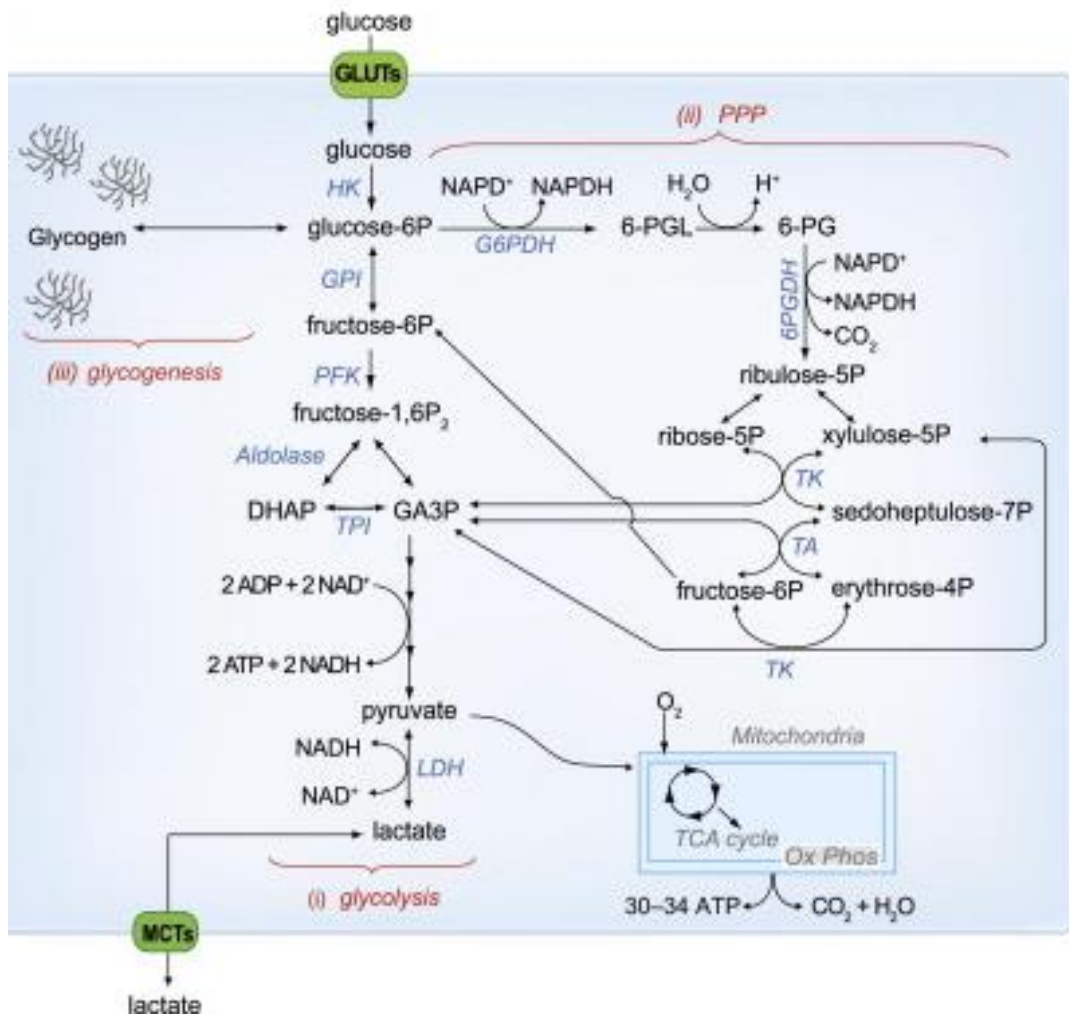


Figure 1.12. A simplified diagram of glucose metabolism.

Glucose enters cells via glucose transporters (**GLUTs**) and is phosphorylated by hexokinase (**HK**), resulting in glucose-6-phosphate (**glucose-6P**). Glucose-6P can be further processed via three main metabolic pathways. First, it can be metabolized via glycolysis (i), resulting in two molecules of pyruvate, and producing **ATP** and **NADH**. Mitochondria can then utilize pyruvate via the tricarboxylic acid (**TCA**) cycle and oxidative phosphorylation (**Ox Phos**), producing **ATP** and **CO₂** while using oxygen. Pyruvate can otherwise be reduced to lactate by lactate dehydrogenase (**LDH**). The lactate can then be released in the extracellular space through monocarboxylate transporters (**MCTs**) where it can be taken up by neurons via MCTs in parallel with glucose. The complete oxidation of glucose yields larger amounts of energy in the form of ATP in the mitochondria (30–34 ATP) than that resulting from glycolysis (2 ATP). Alternatively, glucose-6P can be consumed via the pentose phosphate pathway (**PPP**) (ii), resulting in the production of reducing equivalent (NADPH). Note that the PPP and glycolysis are linked at the level of glyceraldehyde-

3-phosphate (**GA3P**) and fructose-6-phosphate(fructose-6P). Glucose-6P can also be used by astrocytes to store glucosyl units as glycogen (iii). Unlike neurons, astrocytes can store glycogen. (Bélanger *et al.*, 2011).

1.10 High fat diet, obesity, and synaptic plasticity

Previously we have outlined some of the main reasons why obesity and high-fat diet (HFD) have been implicated as risk-factors for dementia and related deficits in learning and memory. Several mechanisms contributing to this phenomenon have been proposed, including insulin resistance, developmental disturbances, altered membrane functioning, oxidative stress, inflammation, and altered vascularization (Stranahan *et al.*, 2008).

A study by Stranahan *et al* (2008) investigated diet-induced insulin resistance by feeding rats a HFD, supplemented with high fructose corn syrup. The alterations to energy and lipid metabolism included elevated fasting glucose, cholesterol, and triglyceride levels that were like those described in cases of clinical diabetes. Compared to control animals, rats subject to this diet for an extended period (8 months) showed decreased performance on spatial learning tasks. In addition, the HFD/corn syrup-fed animals had diminished hippocampal dendritic spine density and LTP at Schaffer collateral CA1 synapses and decreased hippocampal brain-derived neurotrophic factor (BDNF) levels.

These findings could be significant as according to Craft *et al* (2009) and Schioth *et al* (2012) insulin resistance could be a contributing factor for the progression of AD. Indeed, an early pilot study utilizing intranasal insulin as a potential therapy in patients with mild-cognitive impairment showed promising results (Craft *et al.*, 2012), as did a subsequent four-month long study which compared the effects of 20 IUs twice daily of a long-acting insulin analog detemir to 20 IUs of regular insulin twice daily in 36 patients. Regular insulin, but not detemir, improved memory compared with placebo, and was

associated with preserved brain volume in several regions on MRI (Craft *et al.*, 2017). Interestingly, a prior study by Claxton *et al.* (2015) indicated that detemir improved memory in ApoE4 carriers. Considering that ApoE4 has been identified as a major genetic risk factor for late-onset AD (Apostolova *et al.*, 2018), targeting this facet of AD-associated pathology would be extremely beneficial. Nevertheless, the effects of detemir were not as long-lived as hoped and the use of regular insulin remains a more favourable choice for current clinical studies, where it continues to show promise as a potential treatment option for mild cognitive impairment and Alzheimer's disease (Muñoz-Jiménez *et al.*, 2020; Kellar *et al.*, 2021).

Pro-inflammatory cytokines such as IL-1, IL-6, and TNF- α are responsible for initiating an inflammatory response to many stimuli, both peripherally and in the brain. Primarily, these cytokines are able to cross the blood brain barrier (BBB). Pro-inflammatory cytokines can also be produced by cells within the brain parenchyma, e.g., by microglial cells, astrocytes, and endothelial cells of the BBB (Parnet *et al.*, 2002). IL-1 and IL-6 receptors are abundant in the hippocampus, therefore suggesting a possible involvement in learning and memory circuitry. Indeed, a systemic or intraventricular IL-1 β injection gives rise to spatial memory impairments in rats (Gemma and Bickford, 2007) and an indirect IL-1 blockade, significantly improves memory in aged rats, suggesting that IL-1 could be involved in impaired performance on memory tasks with aging (Gemma *et al.*, 2004). Specifically, IL-1 has been shown to inhibit NMDAR-mediated and non-NMDA-mediated synaptic potentiation, LTP, and glutamate release in the hippocampus (Murray & Lynch, 1998), providing a physiological explanation for inflammation-induced memory impairment in rodent models. Furthermore, IL-1 has been shown to affect learning and memory, BDNF expression, neurogenesis, and microglial activation (Barrientos *et al.*, 2004).

Studies subjecting aged rats to HFD (e.g., Pistell *et al.*, 2010) reported increases in body mass, impaired cognition, increased brain inflammation, and decreased BDNF levels. Similarly, Lewis *et al.* (2010) showed that the high

cholesterol diet led to an increase in interleukin (IL)-4, IL-6, IL-12p70, IL-13 and this diet-induced change in cytokine expression in the hippocampus was age dependent. In addition, HFD results in hippocampal morphological changes such as an increased load of activated microglia. Therefore, inflammation could be regarded as an inevitable accompanying factor of HFD, cognitive problems and ageing.

1.11 Treatment of Alzheimer's disease

For many decades, a substantial part of the scientific community has endeavoured to search for an effective treatment for Alzheimer's disease. Unfortunately, these efforts have resulted in modest successes. Over the years, it has become clear that at present, there is no cure for AD and continual research on this condition suggests that finding a treatment that could slow the progression of AD is a more realistic goal.

In line with the current understanding of the the pathogenic mechanisms underlying Alzheimer's disease, the formation of A β plaques remains a focal point in the progression of this disease while the formation of NFTs under certain conditions could be a secondary response to an injury (Nelson *et al.*, 2012). Therefore, the search for an effective AD treatment has been based upon utilizing the following knowledge:

- Formation of A β peptides and their subsequent plaques will be suppressed upon the inhibition of α , β and γ secretases (e.g., McLeod *et al.*, 2015)
- Inhibition of *tau* protein kinases will reduce the tau phosphorylation, thereby reducing the formation of NFTs (e.g., Yoshiyama *et al.*, 2013).
- Employing chemical agents that can remove or dissolve A β plaques and NFTs (e.g., Decourt *et al.*, 2021; Sonawane *et al.*, 2020).
- Another major theory explaining the cognitive deficits seen in AD assigns a substantial role to the decrease in acetylcholine neurotransmitter presence due to a reduced synthesis and release of ACh brought upon by the death of neuronal cells. Therefore, raising the ACh levels or preventing its catabolism could improve the cognitive

functions of AD sufferers (e.g., Davies & Maloney; Bertrand & Wallace, 2020).

- Growing evidence supports a likely association between cognitive decline seen in AD and conditions such as diabetes mellitus and cardiovascular diseases. Therefore, an appropriate management of these conditions could aid in reducing the risk for developing AD (e.g., Akter *et al.*, 2011; Stampfer, 2006).

1.12 Current outlook in AD therapy

At present, the existing treatments and both past and future clinical trials are largely centered around the pathological pathways mentioned previously. The drugs that have been given FDA approval are donepezil, rivastigmine, galantamine, memantine (Melnikova, 2007) and Namzaric® (a combination of donepezil and extended release memantine) (Actavis & Adamas Pharmaceuticals, 2015). Despite mounting evidence casting doubts over its efficacy in AD patients, a new addition to these five treatments is the recently approved aducanumab (Aduhelm), an amyloid beta-directed monoclonal antibody (Alexander & Karlawish, 2021).

Acetylcholinesterase inhibitors (AChEIs) such as donepezil, rivastigmine and galantamine and the NMDAR antagonist memantine do not arrest the progression of AD, although they provide some relief to the symptoms of AD and appear to reduce mortality among dementia sufferers (Alcolea-Palafox *et al.*, 2014; Folch *et al.*, 2018; Hapca *et al.*, 2018). Therefore, considering the financial and personal strain that this condition continues to bring upon communities all over the world, the rush to find more suitable treatment options is understandable.

The high rate of failure in AD drug development with 99% of trials showing no drug-placebo difference, has been a major concern (Cummings *et al.*, 2019). Multiple contributing factors for this undesirable outcome have been suggested, ranging from poor clinical trial design (Fogel, 2018), difficulty in determining the starting point of the AD pathophysiology and thus finding an appropriate starting point for the treatment (Huang *et al.*, 2020), to name a few. In addition, we should consider the collection of cultural, economic, and regulatory factors that form the so-called “Valley of Death” which prevents new drug candidates from being promoted to clinical trials or approved for use (Beach, 2013). Indeed, a fair number of preclinical studies have often shown great promise and offered temporary hope to AD patients with few positive developments following the initial findings. For example, illustrating this situation is a study following academic drug discovery projects between the years 1995 and 2015 at 36 academic institutions in the United States indicated that at the preclinical stage there was a 23% success rate among the 65 projects focusing on the diseases of the nervous system with only 1 project reaching the final approval stage (Takebe *et al.*, 2018).

A practical strategy towards improving the AD drug development process would be to repurpose the already FDA-approved compounds as some have shown to exhibit AD-relevant effects (Parsons *et al.*, 2019). An additional reason in favour of investigating the benefits of drug repurposing lies within the evidence of lack of reversal of cognitive decline in amyloid-targeting drug trials; for example, patients with AD in whose brains A β plaques were virtually cleared by anti-amyloid immunotherapy did not show cognitive improvements (Selkoe & Hardy, 2016). This indicates that instead of focusing the therapeutic approach onto the obvious pathogenic feature which is considered to be a major hallmark of AD, it might be of importance to address the multitude of other pathophysiologies associated with this disease and target neuroprotection, anti-inflammation and metabolic aspects.

1.13 Summary and hypotheses

Considerable evidence has been accumulated, indicating that the ageing population and lifestyle factors, such as calorie-dense diet contribute to the development of impairments in learning and memory. Since most studies have failed at both clearing AD-associated neuropathologies, i.e., A β plaques and *tau* tangles, and restoring the baseline levels of cognitive capacity in either animal models or human subjects, we propose focusing on the possibility of enhancing one's cognitive capacity via the use of cognitive enhancers. These compounds affect receptors that in turn have an influence on LTP. We will also explore the role of adenosine antagonists on LTP in control animals.

Chapter 2: Materials and Methods

2.1 Electrophysiology: Slice preparation

Hippocampal slice preparations were obtained from male Sprague Dawley (SD) rats (Charles River UK or Harlan UK) between six and nine weeks of age, as well as from male wild type mice (C57BL/6J) and homozygous for the $\alpha 7$ nicotinic acetylcholine receptor null allele mice (Acra7-), supplied by Merck. All animals were housed on a 12/12 hour light/dark cycle. All brain tissue slices were obtained during the light phase of this cycle. A subset of WT rats was subject to a 24h fast prior to tissue harvesting. All other rodents were provided with food and water *ad libitum*.

The animals were terminally anaesthetized with isoflurane and following confirmation of permanent cessation of the circulation, subsequently decapitated according to a Schedule One protocol. All procedures were conducted in agreement with the Animals (Scientific Procedures) Act, 1986 (U.K. Government Home Office), incorporating European Directive 2010/63/EU on the protection of animals used for scientific purposes. The brain was rapidly removed from the intracranial space and placed in freshly prepared, cold (2°C - 4°C), oxygenated (95% O_2 , 5% CO_2) artificial cerebrospinal fluid (aCSF). The composition of aCSF, shown in Table 2.1 with a pH of 7.4 and an osmolarity of 309-315 mOsm kg^{-1} . For experiments where 5 mM or 2 mM glucose-containing aCSF was used instead of 10 mM glucose-containing aCSF, glucose was substituted in equimolar quantities by D-mannitol to maintain osmolarity. The brains were trimmed and mounted on a specimen holder that was then securely placed in a tissue slicer (Leica VT1000S, Leica Microsystems GmbH, Wetzlar, Germany). Throughout the slicing process, the brain tissue was surrounded by chilled aCSF. Coronal slices containing the hippocampus were cut at a thickness of 400 μm and

subsequently stored in oxygenated aCSF at room temperature for at least 1 hour prior to electrophysiological recordings. After the recovery period, individual slices were transferred to a modified Haas submersion chamber (Fig.2.1) and continuously perfused with oxygenated, warm (30°C) aCSF at a flow rate of approximately 2ml.min⁻¹.

2.2 Electrophysiological Recording and Data Analysis

A concentric bipolar electrode (FHC, Bowdoin, ME, USA) was placed within the Schaffer collateral pathway where stimulation was applied (1-30 V, 0.1 ms pulse width, 0.033 Hz; DS2A,DS3 Constant Voltage/Constant current isolated stimulator, Digimeter LTD) and the evoked extracellular field excitatory postsynaptic potentials (fEPSPs) recorded from the stratum radiatum of the cornu ammonis 1 (CA1) region of the hippocampus (see Figure 2.2) with a glass capillary microelectrode (GF150TF-10; Harvard Apparatus) filled with 2 M NaCl (resistance 2-6 MΩ).

Stimulation parameters were set to produce a fEPSP of approximately 30-50% of the maximum amplitude. A stable baseline period (control) was recorded for 10 minutes using Axon software (pClamp), followed by administration of test compound or adenosine antagonist, or DMSO control for 15, 20 or 30 minutes. The brain slices were then subjected to a high frequency stimulation paradigm. The paradigms selected were either a theta-burst stimulation protocol (TBS) of 10 mini-trains: 4 pulses, 100 Hz, 200 msec apart (10xTBS), or 5 mini-trains: 4 pulses, 100Hz, 200msec apart (5xTBS), or a high-frequency stimulation: 1sec, 100 Hz train (HFS) (Fig. 2.4). Test compound was applied for a further 5 minutes. In accordance with Neurosolutions Ltd Standard operating procedures, experiments with unstable baselines were discarded, as were those not showing clear initial/early or late phases of LTP induction because such lack of hallmarks within an LTP experiment is often caused by technical issues, e.g., unhealthy brain tissue, inadequate oxygenation or improper electrode placement, to name a few. In

successful experiments fEPSPs were monitored for 60 minutes after LTP induction (see Figs. 2.5. and 2.6).

Alternatively, the stimulation electrode was placed along the mossy fiber pathway from the dentate gyrus to CA3 with the recording electrode – positioned in CA3 (Fig. 2.3). A selection of paired-pulse (PP) stimulation protocols were utilized, i.e., (50, 100, 250ms inter-pulse intervals, 0.1Hz).

It should be noted that at strong stimulus intensities fEPSPs recordings may be contaminated by an action potential, i.e., population spike which may not always be visible in the fEPSP traces. Therefore, using the fEPSP peak potential as a measurement of choice is often replaced by measuring the slope of the fEPSP instead.

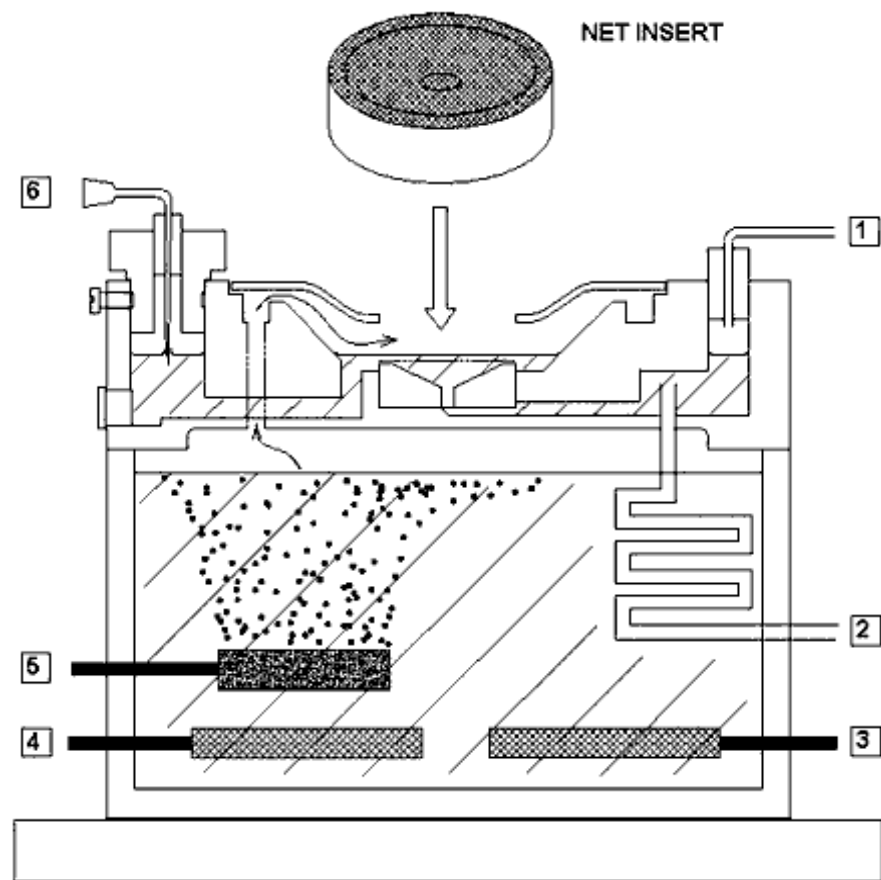


Figure 2.1 A simplified diagram of a modified brain slice chamber system.

(1) **Bubble trap** - prevents bubbles from the perfusion solution, from entering under the net insert. (2) **Heat exchanger element** – allows the incoming perfusion solution to reach the required temperature before it arrives the net insert holding the brain slice. (3 & 4) **Heating elements** – apply heat to the distilled water within the chamber. (5) **Oxygen/Carbon dioxide gas bubbler** – provides humid conditions for the brain tissue. (6) **Exit for perfusion fluid via suction line** – a replaceable hypodermic needle is used to adjust fluid height (Scientific Systems Design Inc. Science Products GmBh, 2020).

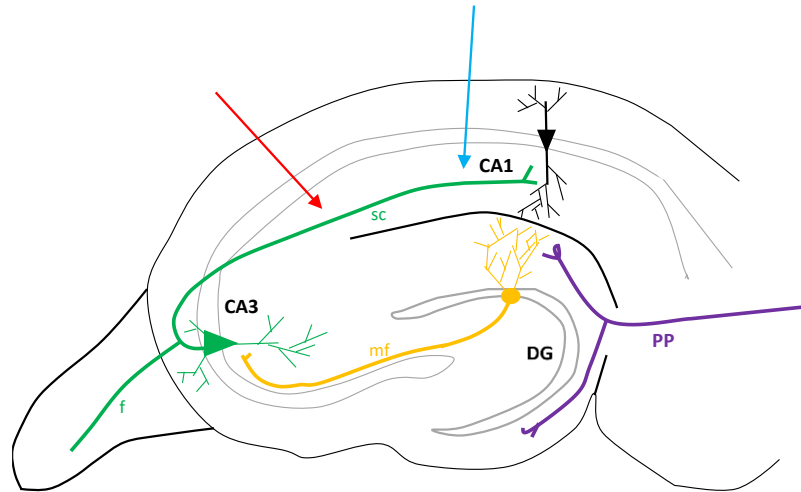


Figure 2.2 A schematic representation of the hippocampal trisynaptic circuit and electrode placement.

fEPSPs were recorded from the stratum radiatum of the CA1 region of the hippocampus (blue arrow) in response to stimulation of the Schaffer collateral (sc) - commissural fibre pathway (red arrow).

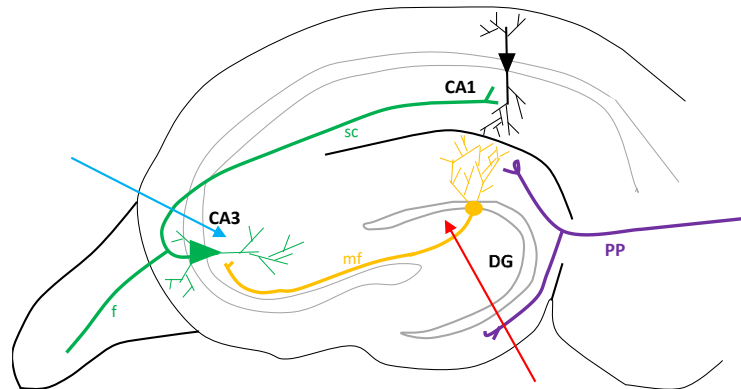
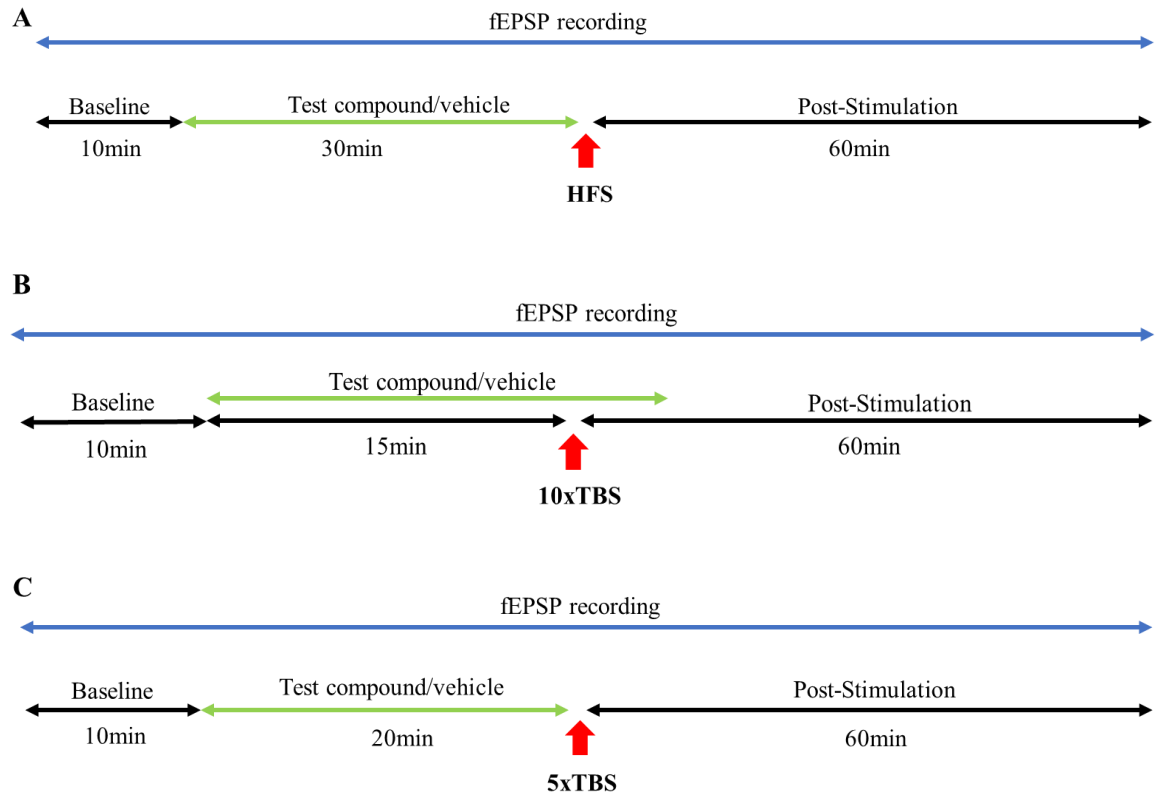


Figure 2.3 A schematic representation of the hippocampal trisynaptic circuit and electrode placement.

fEPSPs were recorded from the CA3 (blue arrow) in response to paired-pulse stimulation applied to the mossy fiber (mf) pathway.



Stimulation Protocol	Chapter
A	3
B	3
C	4

Figure 2.4 A schematic representation of the stimulation protocols utilized in our studies and their corresponding chapters.

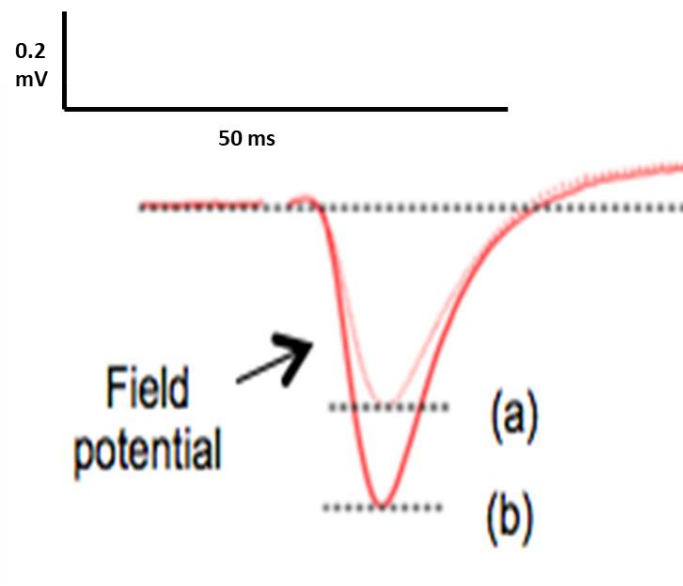


Figure 2.5 An example of typical fEPSP traces before (a) and after (b) high frequency stimulation.

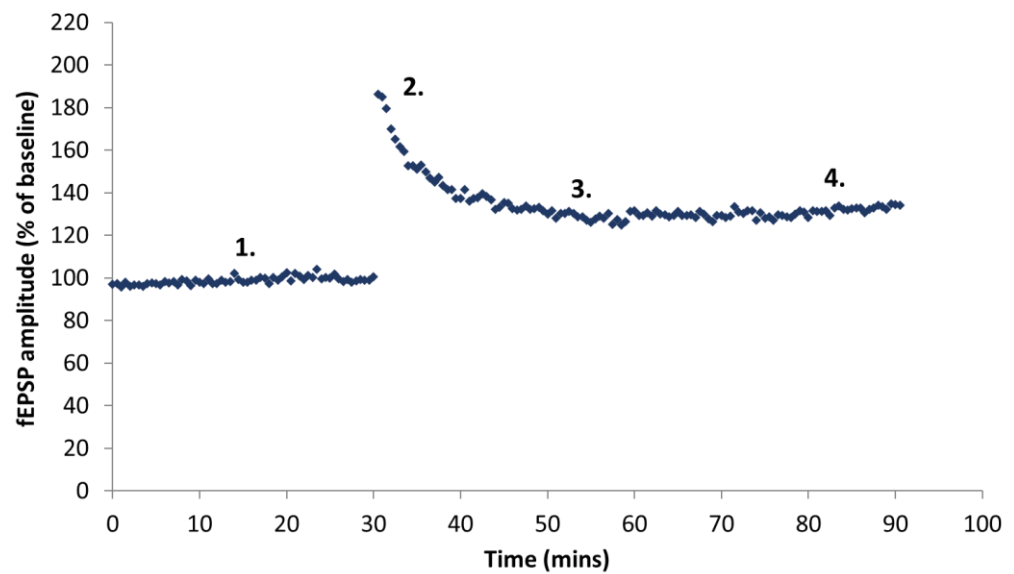


Figure 2.6 An example of a typical scatter plot representing mean normalised fEPSP amplitude before and after high frequency (HFS) or theta burst stimulation (TBS).

The image is showing a baseline (1.) and phases of LTP: initial (I-LTP) (2.), early (E-LTP) (3.) and late (L-LTP) (4.). The initial/early phases of LTP are characterised by an initial transient increase in synaptic efficiency, which appears as a marked increase in the amplitude of the field EPSP immediately following high frequency stimulation. As these phases settle and diminish, another phase becomes established (L-LTP) which appears as an increase in synaptic efficiency compared to baseline control.

2.3 Solutions, drugs, and drug application protocols

L-436, methyllycaconitine (MLA), BNC375, L-250, L-614 and L-592 were supplied in powder form by Merck. KN-93 and D-AP5 were supplied by Abcam UK. Levetiracetam and Syndesi compound were provided by Syndesi. CGS15943, DPCPX, Istradefylline and PSB603 were obtained from Tocris, and MRS1523-from Sigma (Tables 2.2 and 2.3). Final concentrations of drugs were selected based on previous experiments performed by Prof. Spanswick's research group. All compounds were stored at -20°C and prepared fresh on the day of use. All compounds were applied to the brain tissue from 50 ml syringes arranged in series with the main perfusion line from the aCSF reservoir via three-way valves.

Table 2.1 Composition of aCSF solutions utilized in our studies

	<u>10 mM glucose- containing aCSF (in mM)</u>	<u>5mM glucose- containing aCSF (in mM)</u>	<u>2 mM glucose- containing aCSF (in mM)</u>
NaCl	127	127	127
KH₂PO₄	1.2	1.2	1.2
KCl	1.9	1.9	1.9
NaHCO₃	26.0	26.0	26.0
Glucose	10	5.0	2.0
D-Mannitol	0	5.0	8.0
CaCl₂	2.4	2.4	2.4
MgCl₂	1.3	1.3	1.3

Table 2.2 Drugs utilized in our studies.

Drug	Function	Solvent	Supplier
L-436	$\alpha 7$ nACh receptor antagonist	DMSO	Merck
Methyllycaconitine (MLA)	$\alpha 7$ nACh receptor antagonist ($K_i = 1.4$ nM). Interacts with $\alpha 4\beta 2$ & $\alpha 6\beta 2$ receptors at > 40 nM.	ddH ₂ O	Merck
BNC375	$\alpha 7$ nACh receptor antagonist	DMSO	Merck
L-250	CaM kinase II inhibitor	DMSO	Merck
L-614	CaM kinase II inhibitor	DMSO	Merck
L-592	CaM kinase II inhibitor	DMSO	Merck
KN-93	CaM kinase II inhibitor ($IC_{50}=0.37$ μ M), direct extracellular open channel blocker of voltage-gated K^+ channels ($IC_{50}=307$ nM for $K_{V1.5}$).	ddH ₂ O	Abcam UK
D-APV	NMDA glutamate site antagonist	ddH ₂ O	Abcam UK
<i>Syndesi</i>	Mechanism unknown	ddH ₂ O	Syndesi
Levetiracetam	Racetam anticonvulsant Exact mechanism unknown	ddH ₂ O	Syndesi

Table 2.3 Adenosine antagonists utilized in our studies.

Adenosine antagonist	Target (in rat)	Solvent	Concentration applied	Supplier
CGS15943	A ₁ , A _{2A} , A _{2B} , A ₃ (K _i = 6.4, 3.3, 16 and 51 nM respectively).	DMSO	100 nM [Stock] 0.5 mM	Tocris
DPCPX	A ₁ R antagonist (K _i = 0.5 nM)	DMSO	1 µM [Stock] 1 mM	Tocris
Istradefylline (KW6002)	A _{2A} antagonist (K _i = 2.2 nM)	DMSO	50 nM [Stock] 0.2 mM	Tocris
PSB603	A _{2B} antagonist (K _i = 0.355 nM)	DMSO	100 Nm [Stock] 0.5 mM	Tocris
MRS1523	A ₃ antagonist (K _i = 113 nM)	DMSO	300 nM [Stock] 0.5 mM	Sigma

2.4 Data and Statistical Analysis

Data was filtered and digitized as appropriate and stored on a PC running pClamp data acquisition software for later off-line analysis using Clampfit software. All data in this study are presented as means \pm S.E.M. Effects of test compounds on baseline fEPSP amplitudes are normalised to the initial 10 minutes of recording before application of test compound or vehicle. Effects of compounds upon the magnitude of LTP are normalised to the 10 minutes or recording immediately prior to TBS. Significant differences between groups were calculated using Student's unpaired t-test or One-way ANOVA to compare group mean normalised values. Probability values of less than 0.05 were considered to indicate statistical significance.

2.5 Whole-cell patch-clamp electrophysiology

As described previously, male Sprague Dawley rats (8-12 weeks old) were housed in a temperature-controlled room on a 12-hour light/12-hour dark cycle with food and water available *ad libitum*. All experiments were performed in accordance with the UK Animals (Scientific Procedures) Act 1986 incorporating European Directive 2010/63/EU on the protection of animals used for scientific purposes.

On the day of experiment, animals were terminally anaesthetized using isoflurane and the brain harvested. Brain slices containing the striatum (thickness 400 μm) were cut using a vibrating blade microtome (Leica VT1000S) in ice-cold aCSF. Slices were subsequently maintained in aCSF at room temperature (21–23°C). For recording, slices were transferred to a custom-built recording chamber continuously perfused with aCSF at a rate of 3–5 $\text{ml}\cdot\text{min}^{-1}$. aCSF had the following composition (in mM): 127 NaCl; 1.9 KCl; 1.2 KH_2PO_4 ; 2.4 CaCl_2 ; 1.2 MgCl_2 ; 26 NaHCO_3 ; 10 D-glucose, equilibrated with 95% O_2 -5% CO_2 .

Whole-cell patch-clamp recordings were obtained from neurons in the striatum at room temperature (20°C) using a Multiclamp 700B or Axopatch 1D amplifier employing the ‘blind’ version of the patch-clamp technique. Patch pipettes were pulled from thin-walled borosilicate glass and had resistances of 5–8 $\text{M}\Omega$ when filled with intracellular solution of the following composition (in mM): K Glu , 140; EGTA-Na, 1; HEPES, 10; Na_2ATP , 4; GTP, 0.3; QX-314 4; pH was adjusted to 7.3. SD118 was aliquoted at a stock concentration of 30 mM in DMSO and stored at -4 °C until use and diluted in aCSF prior to use.

A bipolar stimulating electrode was placed in the stratum radiatum to stimulate Schaffer collateral-mediated inputs. AMPA receptor-mediated EPSPs and EPSCs in CA1 neurones were evoked at a frequency of 0.1 Hz (low-frequency) interspersed with periods of high frequency stimulation 1, 2,

5, 10 and 20 Hz (see Chapter 5 for details of stimulation protocols) in aCSF that contained the NMDA receptor antagonist D-AP5 (20 μ M), the GABA_A receptor antagonist GABA_zine (10 μ M) and the GABA_B receptor antagonist CGP55485 (400 nM), in order to pharmacologically isolate AMPAR-mediated activity. For voltage-clamp experiments, neurones were clamped at a holding potential of -70 mV.

Data were acquired on a PC running pClamp data acquisition software, filtered, and digitally stored for later off-line analysis. Statistical comparisons were made using paired Student's t-test as detailed on individual slides with $P < 0.05$ taken to indicate statistical significance.

Chapter 3: The effects of extracellular glucose on LTP in the hippocampus and the role of adenosine

3.1 Introduction

For decades glucose has been regarded as the obligatory source of energy for the mammalian brain. In the adult brain, neurons have the highest rate of energy consumption, therefore requiring a reliable and continuous supply of the substrates necessary for cells to generate the cellular fuel; ATP, is provided via the blood. Although in humans, the brain constitutes for ~2% of the body weight, it consumes ~20-25% of the total body glucose consumption rate, therefore making it the main consumer of glucose (Rolfe & Brown, 1997; Raichle *et al.*, 2006). This elevated demand for glucose is justified upon considering the broad range of physiological brain functions, such as neuronal and non-neuronal cellular maintenance and neurotransmitter production, all of which depend on the availability of ATP, generated by the metabolism of glucose. More specifically, the foremost energy demands of the brain are linked with processes encompassed within neuronal signalling, e.g., resting potentials, action potentials, glutamate cycling, postsynaptic receptors, calcium homeostasis accounting for ~70% of the calculated energy expenditure (Yu *et al.*, 2018). The remaining 30% are consumed by nonsignaling activities, such as actin cytoskeleton remodelling, axonal transport, etc. In addition, excitatory neurons require ~80%-85% of the calculated ATP use, while inhibitory neurons and glia consume ~15%-20% (Yu *et al.*, 2018). Consequently, the regionally heterogeneous metabolic rates of grey matter are considerably higher than those in white matter, as white matter has a higher portion of non-signalling energy demands than grey matter (Sokoloff *et al.*, 1977). Therefore, tight regulation of glucose metabolism is crucial for brain physiology and disturbances in glucose delivery or

metabolism in the brain gives rise to various disorders, affecting both the brain function itself, as well as the whole organism.

3.2 The importance of the blood-brain barrier

The dependence of the brain on glucose as its chief source of energy originates due to the presence of the blood-brain barrier (BBB), a highly selective, semipermeable membrane that prevents a non-selective entry of solutes from the blood into the brain. Although glucose cannot be substituted for another energy source, it can be supplemented in cases of strenuous physical activity when blood lactate levels are increased, or during extended periods of starvation when blood concentration of ketone bodies is elevated and BBB monocarboxylic acid transporters (MCTs) are augmented (Nielsen *et al.*, 2009; Lutas & Yellen, 2013).

The BBB is a highly specialised cellular system that consists of a basal membrane, pericytes and astrocytic end-feet all of which provide support to the endothelial cells of cerebral capillaries (Fig 3.1). The endothelial cells found in the brain differ from the endothelial cells found in other organs in three ways; first, the fenestrations are absent; second, vesicular transport is sparse; third, continuous tight junctions are found between the cerebral endothelial cells. Due to TJs, the flux of hydrophilic molecules across the BBB is limited, whereas small lipophilic molecules such as O₂ and CO₂ can diffuse freely across this barrier into the brain (Grieb *et al.*, 1985). Nutrients such as glucose and amino acids enter the brain via transporters, while larger molecules such as insulin and leptin are taken up via receptor-mediated endocytosis (Partridge *et al.*, 1985).

Some brain areas, known as circumventricular organs (CVOs), lack the BBB and therefore are exposed to a wider range of molecules than the BBB-protected brain areas. The CVOs are small midline structures located

around the third and fourth ventricles and they play important roles in brain homeostasis.

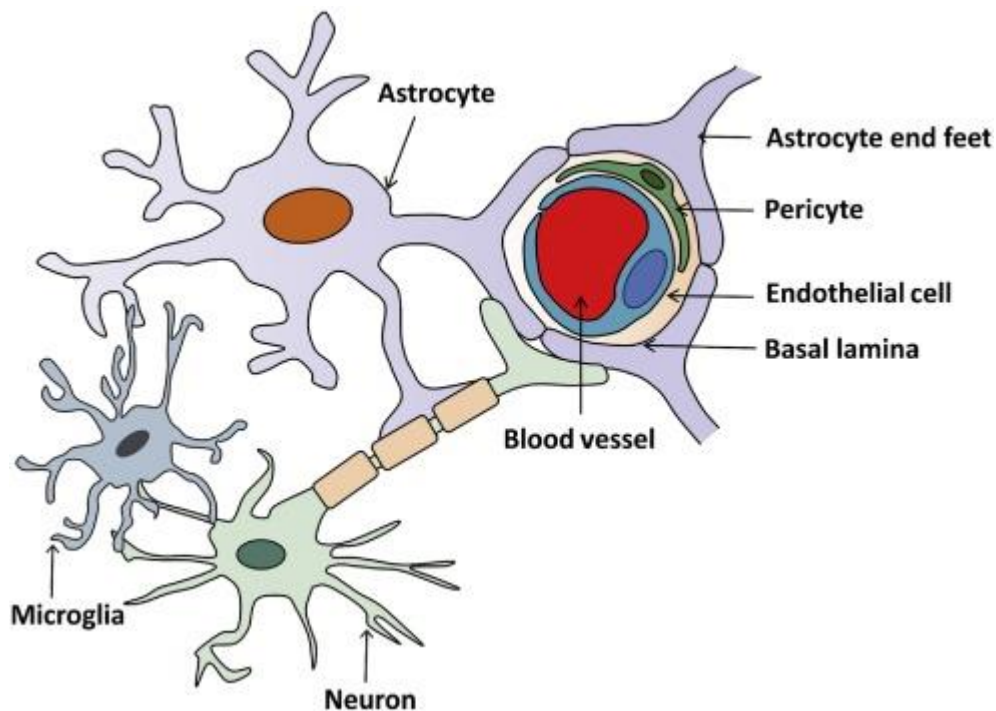


Figure 3.1 A schematic illustration of the BBB which is comprised of a monolayer

The BBB comprises a monolayer of endothelial cells joined together by tight junctions and the underlying basal lamina. The integrity of the BBB is further supported by pericytes and the astrocyte end-feet. The BBB, together with microglia and neurons, forms the neurovascular unit (Nishanth & Schlüter, 2019).

3.3 Glucose transport into the brain

The blood-to-brain concentration gradient drives the facilitated transport of glucose across the endothelial cells via GLUT-1 glucose transporters into the extracellular space of the brain (Drewes., 1998). GLUT-1 also facilitates glucose uptake from the extracellular space into astrocytes, oligodendrocytes and microglia, while GLUT-3, which has a higher rate of glucose transport than GLUT-1, mediates neuronal glucose uptake (Simpson *et al.*, 2007). It is important to note that the capacity of glucose transport

exceeds demand, and that the higher rate of transport via GLUT-3 guarantees sufficient supply of glucose under varying glucose utilization rates and neuronal activity levels (Dienel, 2012). Although most glucose from the extracellular fluid is taken up by neurons, some enters astrocytic end-feet and diffuses down its concentration gradient to other gap junction-coupled astrocytes, where this glucose can be released into the extracellular solution at sites which are further away from the capillaries (Harris *et al.*, 2012; Gandhi *et al.*, 2009).

Interestingly, alternatives to the focus on glucose in the brain have been proposed, e.g., the astrocyte-neuron lactate shuttle which represents the generation of lactate by astrocytes, the export of said lactate to neurones and its subsequent conversion to pyruvate, followed by its use in ATP production (Pellerin & Magistretti, 1994). Initially considered as a necessary process for ATP generation during periods of limited glucose availability, this mechanism has been found to have some involvement in LTP and memory, thereby highlighting the complexity of brain energy metabolism (Suzuki *et al.*, 2011).

3.4 Glucose presence in the brain

In both animals and humans, the steady-state brain-to-plasma glucose concentration ratio overall is 0.2-0.3 (Dienel *et al.*, 1991; Gruetter *et al.*, 1998). In a normal rat brain, the brain glucose levels range from 2-3 $\mu\text{mol/g}$, with the overall brain glucose concentration exceeding 1mmol/l, provided that the arterial plasma glucose level exceeds 5 mmol/l. Furthermore, detailed investigations of basal glucose levels in anaesthetised preparations indicate that CSF glucose levels vary depending on the brain region, for example, 3.3 mmol/l in the cortex, 2.6 mmol/l in the hippocampus and 2.4 mmol/l in the ventromedial area of the hypothalamus (Ronne-Engstrom *et al.*, 1995; Hu & Wilson, 1997; Silver & Ercinska, 1994). Once transported intracellularly, the glucose is catalysed by hexokinases which have a K_m for glucose at $\sim 0.05\text{mmol/l}$ (Wilson, 2003). Therefore, should intracellular glucose concentration exceed

0.5 mmol/l, hexokinase will reach a saturation level of ~90%. If the intracellular glucose concentration decreases, hexokinase becomes unsaturated and its rate of glucose catalysis falls. However, if there is an increase in steady-state plasma and brain glucose concentrations that exceed the normoglycaemic range and reach hyperglycaemic levels, local rates of brain glucose utilization in rat brains will not be altered (Schuier *et al.*, 1990). Thus, cerebral metabolic rates of glucose are controlled by the demand for energy, rather than the supply of it, except when the energy supply is low during hypoglycaemia.

3.5 Glucose metabolism in the brain

Once intracellular glucose is phosphorylated by HKI glucose-6-phosphate (Glc-6-P) is formed, which is a “branch-point” metabolite that not only governs the HKI activity by feedback inhibition, but also has various downstream metabolic fates. For example, Glc-6-P can be processed via the glycolytic pathway, generating pyruvate, which can subsequently be used in the mitochondria by oxidative metabolism via the tricarboxylic (TCA) cycle, leading to the production of ATP. Alternatively, Glc-6-P can enter the pentose phosphate shunt pathway (PPP), generating NADPH, which is then used for management of oxidative stress and nucleic acid synthesis.

In astrocytes Glc-6-P is a precursor for glycogen, the only energy reserve of the brain. Under normal conditions, glycogen turnover takes place when the glucose levels are normal, serving as a local energy buffer for astrocytes.

3.6 Glucose-sensing mechanisms in the brain

In order to comply with the ever-changing metabolic demands of the brain and integrate the exogenous availability of nutrient supplies, specialized neuronal networks have evolved, linking peripheral regulation of glucose and central glucose sensing. One such area of interest is the subpopulation of nuclei encompassed within the hypothalamus, which lie in the vicinity of fenestrated capillaries, ependymal cells, and tanycyte cells. Therefore, these nuclei are exposed to and are likely to monitor and integrate the multitude of glucose signals simultaneously from blood, brain and CSF. For example, neurons of the hypothalamic arcuate nucleus (ARC) respond to a wide range of glucose concentrations (from 0.5 to 10mmol/l), while the glucosensing neurons of ventromedial hypothalamic nucleus (VMN) respond to a much finer range in glucose concentration (from 0.1 to 2.5mmol/l) (Hanna *et al.*, 2020).

Two groups of glucosensing neurons have been identified: glucose-excited (GE) and glucose-inhibited (GI), respectively. The best described mechanism of action of the GE neurons predicts the involvement of the high-affinity glucose transporters (GLUT3) as the main transporter (Manolescu *et al.*, 2007). Subsequently, the intracellular glucose undergoes phosphorylation by HKIs, ultimately leading to an increase in the ATP:ADP ratio. ATP then binds to and inactivates the ATP-sensitive K^+ channels (K_{ATP}), leading to depolarization of the cell membrane, followed by influx of extracellular calcium via voltage-dependent calcium channels and resulting in an increase in action potential frequency. Astrocytic release of adenosine inhibits the firing rate of GE AgRP neurons, resulting in an inhibition of food intake and modifying the overall response to metabolic hormones such as ghrelin (Yang *et al.*, 2015). In addition, glial cells contribute towards the glucose-sensing mechanism as well.

Considering the normoglycaemic range and the resulting physiologically-relevant brain glucose levels, it is important to explore whether these factors are significant in experiments performed on brain tissue

in vitro. However, most *in vitro* brain electrophysiology studies involve the use of aCSF with a glucose content of at least 10 mM which is a substantial departure from the naturally occurring steady-state brain glucose levels. Since the purpose of *in vitro* studies is to investigate and explain phenomena that also take place in living, intact organisms, e.g., the mechanisms underlying learning and memory, the experimental conditions for *in vitro* studies should be as close as possible to the conditions seen *in vivo*.

3.7 The effects of extracellular glucose on LTP

According to numerous observations, an increase in the availability of glucose enhances learning and memory (Gold, 1986; Kopf & Baratti, 1996; McNay & Gold, 2001). Since the best candidate mechanism for learning and memory remains long-term potentiation (LTP), it is of importance to pinpoint the role of glucose in this process.

Maintenance of LTP depends upon a series of intracellular events, such as DNA transcription, RNA translation and signalling via the mammalian Target of Rapamycin (mTOR) pathway. Findings by Potter *et al.*, (2010) showed that AMP-activated protein kinase (AMPK) couples energy metabolism to LTP expression via association with the mTOR pathway. Likewise, direct injection of glucose into the rat hippocampus both improved long-term memory and was associated by a downregulated AMPK activity and an upregulated mTor cascade (Dash *et al.*, 2006).

Since it has been established that glucose and its metabolism are irreplaceable essentials for ensuring a sufficient functioning of the brain, it is of importance to explore the pathological causes for disturbances in this complex support system and the subsequent impact on the physiological processes in the brain. One such clinically significant condition is diabetes mellitus (DM), which encompasses a host of insults to the CNS in both type-1

and -2 diabetic patients as well as in experimental animal models (Malone, 2016).

The diabetes-associated hyperglycaemia and reactive carbonyl species (RCS) compromise the integrity of BBB, leading to numerous cerebrovascular complications. In addition, many experimental studies show that hyperglycaemia appears to reduce the glucose transport across the BBB due to downregulation of glucose transporter proteins, indicative of the measures taken by brain from preventing excessive intake of glucose (Duelli *et al.*, 2000; Hou *et al.*, 2007; Pardridge *et al.*, 1990). However, this view remains inconclusive due to additional evidence from both human and animal studies showing no significant changes in the BBB glucose transporter protein expression in D2M (Simpson *et al.*, 1999; Seaquist *et al.*, 2005). Nevertheless, the role of BBB in preserving the brain homeostasis is well established, therefore identifying a metabolism-associated vulnerability in this system would point towards a potential solution to obesity-induced cognitive impairment.

A likely point of such interest is the endothelial adenosine receptor A_{2A}. Yamamoto *et al* (2019) reported that in diabetic mice endothelial A_{2A} receptors promoted BBB permeability and that the same mouse model exhibited a lower hippocampal LTP, compared to the control animals. This reduction in LTP was ameliorated upon systemic administration of an A_{2A} receptor antagonist (SCH58261), while application of this compound directly to the brain slice *in vitro* did not yield a similar result. These findings indicate that systemic reinstatement of the BBB via the use of an AR antagonist might contribute towards a rescue of synaptic plasticity in mice with diet-induced insulin resistance. Furthermore, the recovery of BBB integrity is part of an upstream mechanism for improvements in synaptic plasticity and memory.

3.8 Adenosine

Adenosine is an endogenous and widely distributed molecule which participates in numerous physiological events, particularly in excitable tissues such as the heart and brain. Some of the better-known actions of adenosine include the reduction of activity of the excitable tissues, such as slowing of heart rate; or increase in the distribution of metabolic substrates via induction of vasodilation. Hence, adenosine plays a substantial role in coupling the rate of energy expenditure to the energy supply. However, this type of singular effect of adenosine does not account for many of its other actions, for example its role as an intercellular messenger. This becomes particularly apparent in the brain, which expresses high levels of adenosine receptors, and where adenosine has been shown to exert its influence upon both normal and pathophysiological processes, such as arousal, sleep, analgesia, neuroprotection, and epilepsy, in addition to mediating the effects of alcohol and chronic drug use (Dunwiddie & Masino, 2001).

3.9 Adenosine production and metabolism in the CNS: Intracellular

In the CNS, adenosine is produced by both neural and glial cells in situ in the extracellular space, and in turn, it can modulate the activity of nearby cells acting in an autocrine or paracrine manner.

Intracellular adenosine serves as an intermediate substrate for the synthesis of nucleic acids and adenosine trisphosphate (ATP). It is produced from 5'-adenosine monophosphate (AMP) by 5'-nucleotidase and can be turned back into AMP by adenosine kinase. Adenosine can also be derived from S-adenosylhomocysteine (SAH), a homocysteine precursor, by the activity of SAH hydrolase. The metabolism of intracellular adenosine is carried out by adenosine deaminase (ADA) or adenosine kinase, creating inosine or AMP, respectively. Inosine produced via deamination can exit the

cell or can be further degraded into hypoxanthine, xanthine and eventually – uric acid. Low levels of intracellular adenosine can also be released into the extracellular space via equilibrative nucleoside transporters (ENTs) (King *et al.*, 2006). This release of intracellular adenosine is augmented in cases of such insults as ischemia, hypoxia and seizures.

3.10 Adenosine production and metabolism in the CNS: Extracellular

The presence of adenosine in the CNS under basal conditions is understood to provide the inhibitory tone of neurotransmission and neuroprotection, which can be substantially impaired should the system be subject to stress. Under baseline physiological conditions, the concentration of adenosine both extra- and intracellularly remains low due to a multitude of mechanisms. For example, the maintenance of extracellular adenosine levels relies upon a balance of production and removal. Some of the proposed mechanisms for adenosine origin and release include ATP metabolism, release via gap junction hemi-channels, uptake from the cell cytoplasm or even by direct release of adenosine (Jo & Schlichter, 1999; Pearson *et al.*, 2005; Gu *et al.*, 1995; Wall & Dale, 2007). In addition, maintenance of low levels of intracellular adenosine might be the result of the adenosine-phosphorylating action of adenosine kinase (Boison, 2006).

However, in response to metabolic stress the adenosine levels increase significantly. This level of adenosine varies depending on the brain area, as well as the experimental methods involved in determining it, nevertheless the physiological base level of extracellular adenosine is normally maintained at 50-200 nM (Latini & Pedata, 2001).

There are two main mechanisms which allow adenosine to reach the extracellular spaces in the brain, i.e., adenosine release from cells via transporters and dephosphorylation of adenine nucleotides by ectonucleotidases. Conversion of adenine nucleotides such as ATP or ADP is

a rapid process, which takes less than a second (Dunwiddie *et al.*, 1997). Inactivation of extracellular adenosine is primarily controlled by its uptake across the cell membranes of either neural or non-neural cells and subsequent phosphorylation to AMP by adenosine kinase (AK) or deamination to inosine by adenosine deaminase (ADA). The balance between intracellular and extracellular adenosine as well as the multitude of factors affecting it ultimately determines the bioavailability of extracellular adenosine at receptor sites.

3.11 Adenosine receptors

All the known ARs are G-protein-coupled receptors, composed of seven transmembrane domains and are linked to various transduction mechanisms (see Table 1 for summary). The A₁ receptor is especially abundant in the brain and is coupled to activation of K⁺ channels and inhibition of Ca²⁺ channels (Trussell & Jackson, 1985; Macdonald *et al.*, 1986), both of which result in inhibition of neuronal activity. The A_{2A} receptors is highly expressed throughout some regions of the brain and is primarily linked to the activation of adenylyl cyclase as its mode of transduction.

In the CNS adenosine has a pervasive and generally inhibitory effect upon neuronal activity. Due to the readily available adenosine in the extracellular space in brain tissue, tonic activation of A₁ and A_{2A} receptors result in inhibitory effects. Since this tonic inhibition is removed by AR antagonists such as caffeine, therefore accounting for the excitatory action of these agents, at least in rodents (Marston *et al.*, 1998). The A_{2B} receptor also possesses an adenylyl cyclase-activating mechanism. Due to the relatively low quantities of this AR within the brain, it has been challenging to link this receptor to definite physiological or behavioural outputs (Feoktistov & Biahhioni, 1997). However, upon the creation of a A_{2B} receptor KO mouse it transpired that while these animals showed no anatomical abnormalities, they exhibited increased levels of pro-inflammatory cytokines (Yang *et al.*, 2006). Furthermore, the activation of this low-affinity adenosine receptor promotes

the uptake of glucose in neurons and astrocytes (Lemos *et al.*, 2015). The characteristics of the A₃ receptor are also somewhat elusive, yet they have been reported to uncouple A₁ and mGluRs via a protein kinase C-dependent mechanism, therefore its function may be involved in modulating the activity of other receptors (Dunwiddie *et al.*, 1997; Macek *et al.*, 1998).

Interestingly, the other ARs also exhibit the ability to influence other types of G-protein-coupled receptors. For example, synergistic exchanges have been documented between low concentrations of A₁R and GABA_B agonists on GIRKs (G-protein-coupled inwardly-rectifying K⁺ channels), which implies that a tonic, low level of occupation of A₁Rs might adjust the strength of GABA_B synapses (Sodickson & Bean, 1998). Additional evidence, primarily from studies on the striatum, have shown direct interactions between A_{2A}Rs and D1Rs, and between A₁ and D2 receptors (Fuxe *et al.*, 1998).

Table 3.1 Adenosine receptors in the brain

GIRKs – G-protein-dependent activation of inwardly rectifying K⁺ channels; PLC – phospholipase-C

Receptor	Adenosine Affinity	G-protein	Transduction mechanisms	Physiological actions in the brain	Distribution in the brain
A ₁	~70 nM	G _i and G _o	Inhibits adenylyl cyclase Activates GIRKs Inhibits Ca ²⁺ channels Activates PLC	Inhibits synaptic transmission Hyperpolarizes neurons	Widespread
A _{2A}	~150 nM	G _s	Activates adenylyl cyclase Inhibits Ca ²⁺ channels	Facilitates neurotransmitter release Inhibits neurotransmitter release	Striatum, olfactory tubercle, nucleus accumbens
A _{2B}	~5100 nM	G _s	Activates adenylyl cyclase Activates PLC	Increases cAMP in brain slices Modulation of Ca ²⁺ channel function (?)	Widespread, but at low levels
A ₃	~6500 nM	G _{i3} , G _q	Inhibits adenylyl cyclase Activates PLC Increases intracellular Ca ²⁺	Uncouples A ₁ , mGluRs	Widespread

3.12 ARs as therapeutic targets

The potential of ARs as therapeutic targets has been highlighted by numerous sources (Jacobson & Gao, 2006; Pacher *et al.*, 2008; Fredholm, 2010). Due to technological advances in medicinal chemistry and introduction of radioligands for adenosine receptors, both agonists and antagonists with high affinity and selectivity for the human variants for the four ARs have been generated (Fredholm *et al.*, 2001). In addition, both agonist and antagonist ligands containing positron-emitting radio-isotopes have been utilized to examine the *in vivo* occupancy of ARs in humans (Muller & Jacobson, 2011). Hence, a lack of selective ligands cannot be regarded as a limiting factor for research and development on AR-targeting compounds, as has been the case for several other GPCRs. A much bigger concern is the broad distribution of ARs and therefore, achieving tissue-selectivity remains a challenge.

Considering the overall influence of adenosine on glucose signalling and LTP, it is of relevance to investigate this neuromodulator and its receptors further.

3.13 Hypothesis and aims of research

Preliminary research undertaken by Prof. Spanswick's group at Monash University revealed a critical role of glial-derived adenosine in mediating glucose-sensing in neurones in energy status-sensing neural networks in the hypothalamus. In these neural circuits, raising extracellular glucose from fasted levels (1-2 mM) to fed levels (5 mM) induced excitation of pro-opiomelanocortin (POMC) neurones via release of adenosine from glia and activation of A₁ receptors. In other POMC neurones, raising glucose-induced inhibition via activation of A_{2a} receptors. Ambient glucose levels were signalled via tonic activation of A₁ and A₃ receptors leading to the suggestion that ambient glucose levels are signalled via adenosine receptors. This led to the suggestion that neural circuit function generally may be regulated by tonic

activity of a glucose-adenosine-dependent signalling pathway (Spanswick; unpublished observations). This led to the suggestion that hippocampal function may operate in a similar manner and cognitive, learning and memory deficits observed in the obese may reflect dysfunction of this glucose-glial adenosine signalling matrix. Preliminary experiments performed by Prof. Spanswick's group at Warwick University indicated an optimum level of ambient extracellular glucose of approximately 5mM, lower and higher levels yielding significantly lower LTP. The aim of the current study was to extend these preliminary observations.

The specific aims of this project were:

1. To determine the effects of physiologically relevant levels of extracellular glucose on LTP in the hippocampus.
2. To determine the role of adenosine receptors in mediating the effects of extracellular glucose on LTP.

3.14 Results: The effects of adenosine antagonists on LTP *in vitro*

Extracellular field excitatory postsynaptic potentials (fEPSP) were recorded in the CA1 region of the hippocampus of adult male Sprague- Dawley rats (aged 6-8 weeks, 120-250g), evoked in response to electrical stimulation of the Schaffer-collateral pathway. The effects of three concentrations of extracellular glucose were tested: 2 mM, 5 mM, and 10 mM. In every step of the brain tissue preparation and experimental procedures aCSF glucose concentration to be tested was maintained consistent throughout. For experiments with either 2 or 5 mM glucose, D-mannitol (8 and 5 mM, respectively) was added to the aCSF, to correct for changes in osmolarity. A 10-minute baseline was recorded, followed by a 20-minute application of vehicle (0.1% DMSO) or an adenosine receptor antagonist.

The following receptor antagonists were tested on LTP induced in 10 mM D-glucose: the non-selective A₁, A_{2A}, A_{2B} and A₃ receptor antagonist CGS15943 (100 nM); the selective A₁ receptor antagonist DPCPX (1 µM); the selective A_{2A} receptor antagonist KW-6002 (50 nM); the selective A_{2B} receptor antagonist PSB603 (100 nM); the selective A₃ receptor antagonist MRS1523 (300 nM). For experiments with 5 mM or 2 mM glucose-consisting aCSF adenosine receptor antagonists tested were: N: vehicle = 6; 100 nM CGS15943 = 3; 50 nM KW-6002 = 5, and N: vehicle = 4; 1 µM DPCPX = 2; 50 nM KW-6002 = 2, respectively.

3.14.1. The effects of extracellular glucose on LTP in rat CA1 hippocampus *in vitro*

Physiological glucose levels at the level of the brain closely mirror those of the plasma amounting to around 2-3 mM under normal basal conditions although this can vary depending on energy status (e.g. fed versus fasted), age, brain region and under pathophysiological conditions (see van den Top *et al.*, 2017). In the hippocampus, basal levels of glucose in CSF are indicated around 2.6 mM (Hu & Wilson, 1997). Here the effects of 3 concentrations of glucose were tested on LTP evoked in response to a theta burst stimulation (see Figs 3.1. & 3.2.). In the presence of 2 mM extracellular D-glucose the magnitude of LTP amounted to $131.6 \pm 4\%$ (mean \pm SEM; $n = 4$) of control pre-LTP (100%) baseline levels. In 5 mM extracellular D-glucose the magnitude of LTP increased to $141.8 \pm 5.2\%$ of control pre-LTP levels (mean \pm SEM; $n = 6$). However, this effect did not reach statistical significance, possibly reflecting the low n numbers in this study. Like 5 mM extracellular glucose, the magnitude of LTP recorded in the presence of 10 mM extracellular glucose amounted to $143.9 \pm 4.4\%$ (mean \pm SEM; $n = 8$). Thus, there appeared no statistically significant effect of extracellular glucose concentration on the magnitude of LTP although there was a trend to reduced LTP in the presence of 2 mM D-glucose compared to 5 and 10 mM D-glucose ($p > 0.05$, One-way ANOVA, for 2 versus 10 mM D-glucose, 2 versus 5 mM glucose and 5 versus 10 mM glucose; see Table 3.2.).

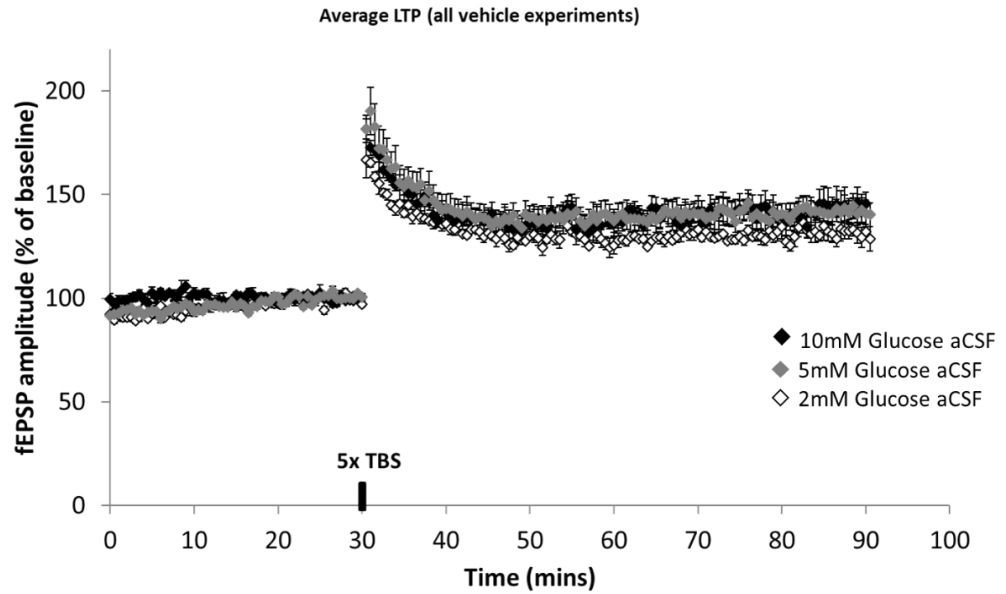


Figure 3.1. The effects of extracellular glucose concentration on LTP in the CA1 area of the hippocampus.

Composite scatter plot representing mean normalised fEPSP amplitudes before and after 5xTBS induction in rat hippocampal slices treated with varying concentrations of D-glucose, i.e., 10 mM glucose aCSF (black diamonds) ($n = 8$), 5 mM glucose aCSF (grey diamonds) ($n = 6$), or 2 mM glucose aCSF (white diamonds) ($n = 4$). Data are expressed as a percentage of the average of fEPSP amplitudes recorded during the 10-minute period before the application of 5xTBS protocol. Error bars represent standard error of the mean (SEM).

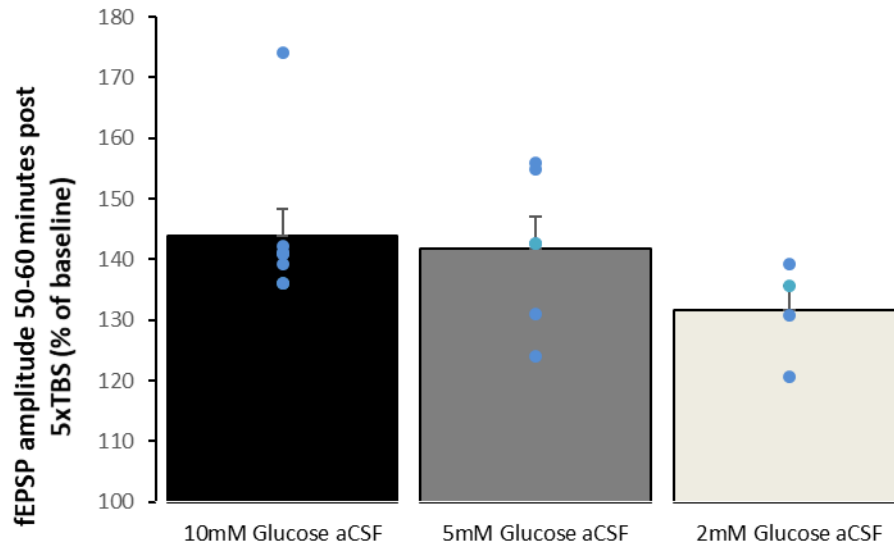


Figure 3.2. The effects of extracellular glucose concentration on LTP in the CA1 area of the hippocampus.

Bar chart summarizing the effects of different extracellular glucose concentrations on LTP. The level of LTP was measured 50-60 minutes after 5xTBS induction paradigm from rat hippocampal slices treated with vehicle. The magnitude of LTP was measured as the average of the evoked fEPSPs recorded during the last 10 minutes expressed as a percentage of the average baseline fEPSP amplitude recorded in the 10-minute period immediately prior to induction of LTP. Application of the vehicle control in experiments subject to the conditions of 2 mM ($n = 4$) or 5 mM glucose-containing aCSF ($n = 6$) did not result in significant changes in the magnitude of LTP induced 50-60 mins post-induction., vehicle application in experiments utilizing aCSF containing 10 mM glucose ($n = 8$) (statistical results summarized in Table 3.2, One-way ANOVA).

Table 3.2. Mean magnitude of LTP measured 50-60 minutes after a 5xTBS stimulation in rat hippocampal slices prepared with aCSF containing 10, 5 or 2 mM glucose and treated with vehicle (aCSF + 0.1% DMSO) (One way-ANOVA, NS, non-significant).

Treatment	Mean	SEM	n	<i>P</i> vs 10 mM Glucose aCSF
Vehicle: 10 mM Glucose aCSF	143.9	4.4	8	
Vehicle: 5 mM Glucose aCSF	141.8	5.2	6	NS
Vehicle: 2 mM Glucose aCSF	131.6	4.0	4	NS

3.14.2 Effects of the A₁ receptor antagonist DPCPX on LTP induced in CA1 in the presence of 10 and 2 mM extracellular glucose

In the following set of experiments the effects of an A₁ selective adenosine receptor antagonist (1 μ M DPCPX) on LTP were examined, in the presence of either 10 mM or 2 mM extracellular D-glucose. LTP was measured as an increase in amplitude of the fEPSP relative to vehicle controls. In experiments utilizing 10 mM extracellular glucose, LTP in CA1 induced in response to 5xTBS, in the presence 0.1% DMSO (vehicle control) amounted to an increase in the fEPSP of $143.9 \pm 4.4\%$ (mean \pm SEM), compared to pre-stimulation baseline levels (n = 8). In response to the application 5xTBS in the presence of 1 μ M DPCPX (n = 7), the fEPSP amplitude rose to $136.2 \pm 3.9\%$ (mean \pm SEM) when compared with the level of fEPSP before the stimulation (see Fig. 3.3. & 3.4.). This reduction in LTP in the A₁ receptor antagonist was not significantly different to that observed in the vehicle control group (all groups: $p > 0.05$, unpaired student's t-test, see table 3.3.).

In the presence of 2 mM extracellular D-glucose, the LTP induced in response to 5xTBS, accompanied by 0.1% DMSO application (vehicle control), resulted in an increase in the amplitude of fEPSP of $131.6 \pm 4.0\%$ (mean \pm SEM), compared to pre-stimulation fEPSP amplitude (n = 4). In response to 5xTBS in the presence of 1 μ M DPCPX the fEPSP amplitude rose to $149.1 \pm 5.2\%$ (mean \pm SEM), compared to pre-5xTBS fEPSP amplitude (n = 2) (see Fig. 3.5. & 3.6.). Due to the low experiment count, the significance of this effect could not be determined. This effect was significantly different to the control group (table 3.4.). This increase in amplitude was also compared to the value obtained from the set of experiments testing DPCPX in the presence of 10 mM extracellular glucose (see Figs. 3.7. & 3.8.). However, no significant difference could be detected at this time (see table 3.5.)

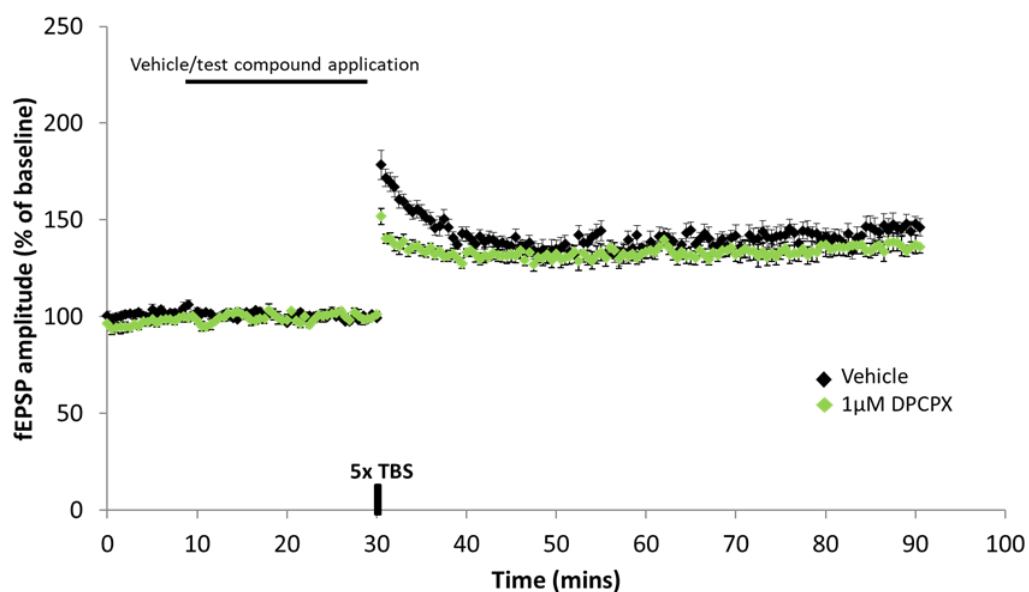


Figure 3.3 The effect of the A₁ receptor antagonist DPCPX on LTP in the CA1 area of the hippocampus, in the presence of 10 mM extracellular D-glucose.

Composite scatter plot representing mean normalised fEPSP amplitudes before and after 5xTBS induction in rat hippocampal slices pre-treated for 20 minutes with either vehicle or the A₁ receptor antagonist DPCPX. Data are expressed as a percentage of the average of fEPSP amplitudes recorded during the 10-minute period before the application of 5xTBS protocol. Following a 10-minute stable baseline recording period (no compound treatment), vehicle (black diamonds) or 1 μM DPCPX (green diamonds), was applied for 20 minutes (black bar). Theta-burst (5xTBS; indicated by the bar on the timeline), induced LTP. Error bars represent standard error of the mean (SEM). N: vehicle = 8; DPCPX = 7

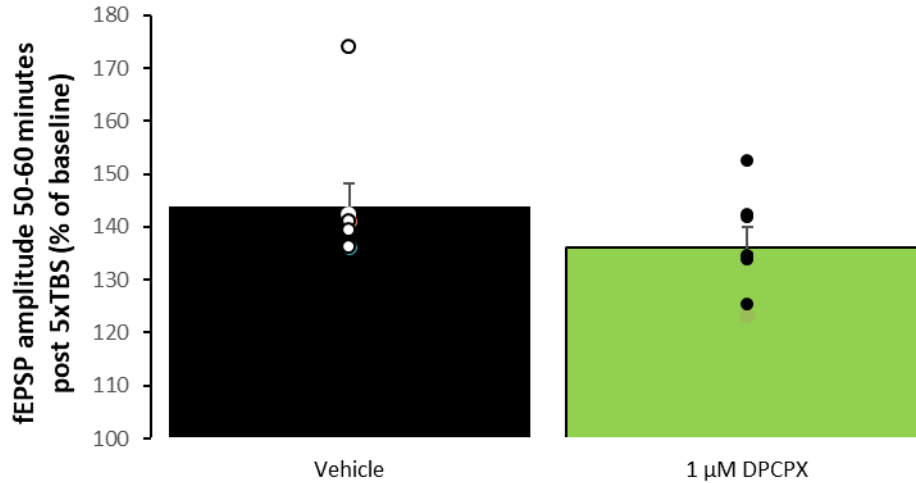


Figure 3.4 The effect of the A₁ receptor antagonist DPCPX on LTP in the CA1 area of the hippocampus, in the presence of 10 mM extracellular D-glucose.

Bar chart summarizing the effects of the adenosine antagonist DPCPX on LTP. The level of LTP was measured 50-60 minutes after 5xTBS induction paradigm from rat hippocampal slices treated with either vehicle, or the adenosine A₁ receptor antagonist DPCPXs. The magnitude of LTP was measured as the average of the evoked fEPSPs recorded during the last 50-60 minutes expressed as a percentage of the average baseline fEPSP amplitude recorded in the 10-minute period immediately prior to induction of LTP. Application of DPCPX did not result in significant changes in fEPSP amplitude, compared to vehicle (statistical results summarized in Table 4.3, unpaired Student's t-test). (N: vehicle = 8; DPCPX = 7).

Table 3.3 Mean fEPSP amplitudes measured 50-60 minutes after a 5xTBS stimulation in rat hippocampal slices prepared with aCSF containing 10 mM D-glucose and treated with vehicle (aCSF + 0.1% DMSO) or 1 μ M DPCPX, (unpaired Student's t-test, NS, non-significant).

Treatment	Mean	SEM	n	P vs Vehicle
Vehicle	143.9	4.4	8	
1 μ M DPCPX	136.2	3.9	7	NS

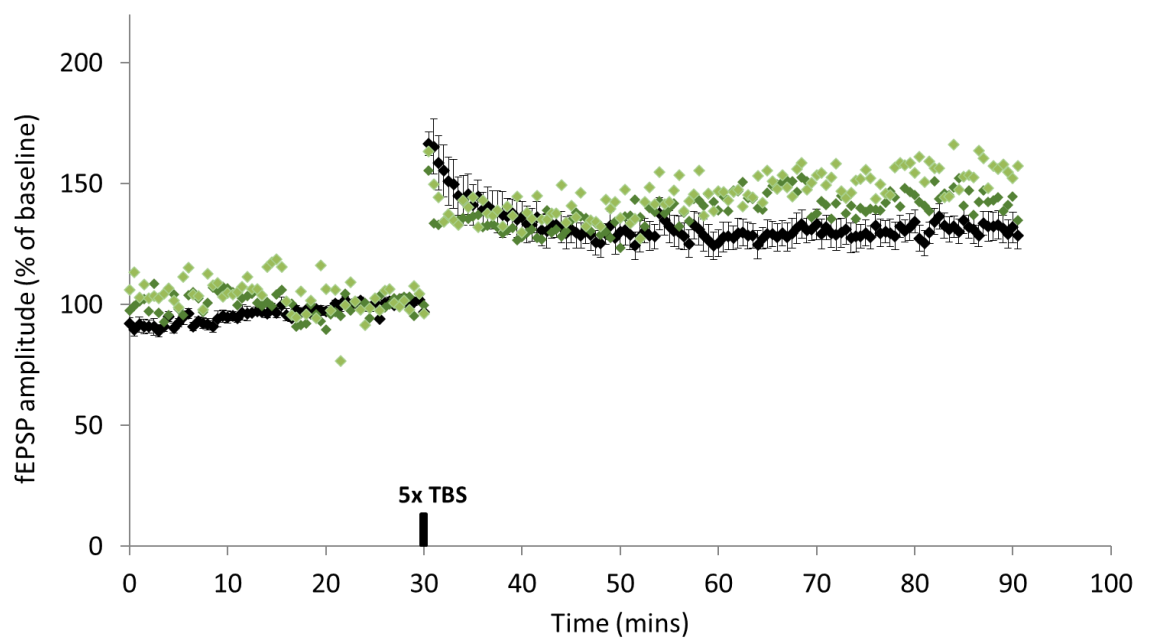


Figure 3.5 The effects of adenosine A₁ receptor antagonist DPCPX on LTP in the CA1 area of the hippocampus in 2 mM glucose-containing aCSF.

Composite scatter plot representing mean normalised fEPSP amplitudes before and after 5xTBS induction in rat hippocampal slices pre-treated for 20 minutes with either vehicle A₁ receptor antagonist, 1 μ M DPCPX. Data are expressed as a percentage of the average of fEPSP amplitudes recorded during the 10-minute period before the application of 5xTBS protocol. Following a 10-minute stable baseline recording period (no compound treatment), vehicle (black diamonds) or 1 μ M DPCPX (green diamonds) was applied for 20 minutes (black bar). Due to 1 μ M DPCPX $n = 2$, both experiments were plotted. Theta-burst (5xTBS; indicated by the bar on the timeline), induced LTP.

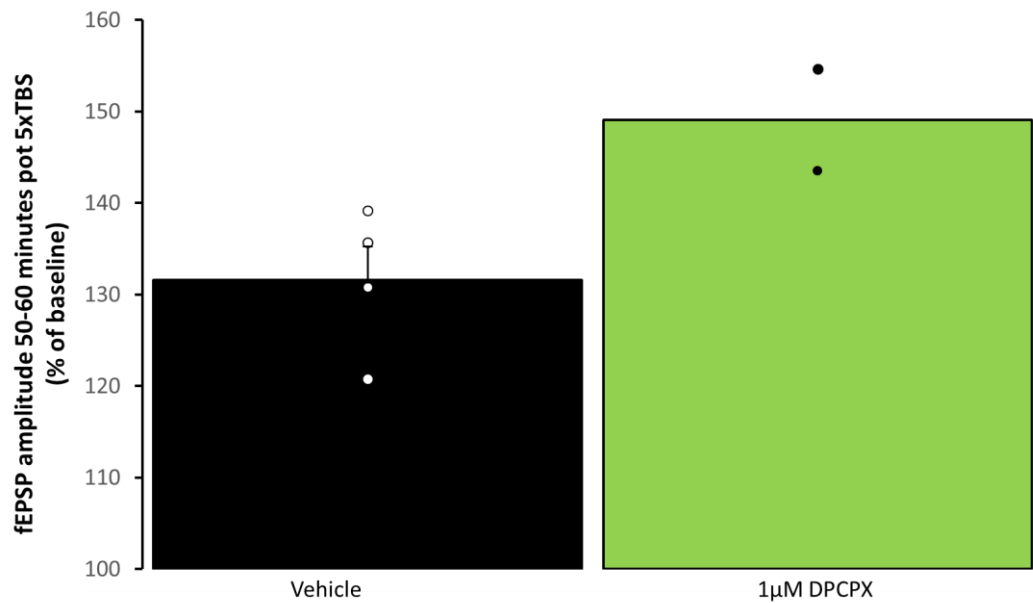


Figure 3.6 The effects of A₁ adenosine antagonist 1 μM DPCPX on LTP in the CA1 area of the hippocampus in experiments utilizing 2 mM glucose-containing aCSF

Bar chart summarizing the effects of 1 μM DPCPX on LTP. The level of LTP was measured 50-60 minutes after 5xTBS induction paradigm from rat hippocampal slices treated with either vehicle, or A₁ adenosine receptor antagonists, 1 μM DPCPX. The magnitude of LTP was measured as the average of the evoked fEPSPs recorded during the last 50-60 minutes expressed as a percentage of the average baseline fEPSP amplitude recorded in the 10-minute period immediately prior to induction of LTP. Application of 1 μM DPCPX resulted in an increase in fEPSP amplitude, compared to vehicle.

Table 3.4. Mean fEPSP amplitudes measured 50-60 minutes after a 5xTBS stimulation in rat hippocampal slices prepared with aCSF containing 2 mM D-glucose and treated with vehicle (aCSF + 0.1% DMSO) or 1 μ M DPCPX

Treatment	Mean	SEM	n	<i>P</i> vs Vehicle
Vehicle	131.6	4	4	
1 μ M DPCPX	149.1	5.5	2	NA

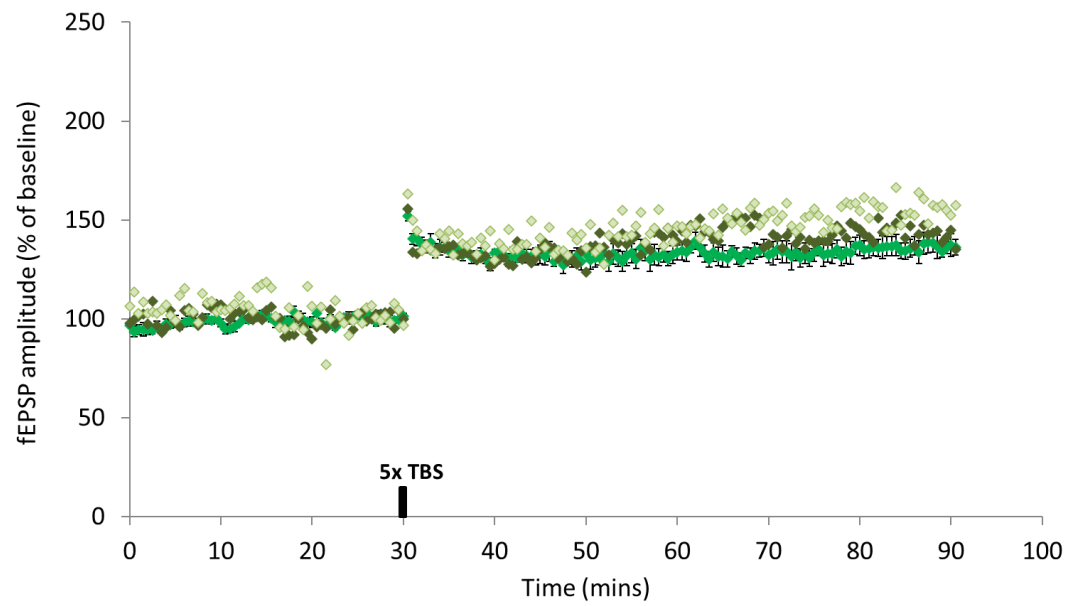


Figure 3.7. The effects of A₁ adenosine receptor antagonist DPCPX on LTP in the CA1 area of the hippocampus.

Composite scatter plot representing mean normalised fEPSP amplitudes before and after 5xTBS induction in rat hippocampal slices pre-treated for 20 minutes with 1 μ M DPCPX in experiments using 10 mM glucose aCSF (green diamonds) ($n = 7$), or 2 mM glucose aCSF (2 individual recordings: light and dark green diamonds, respectively) ($n = 2$). Data are expressed as a percentage of the average of fEPSP amplitudes recorded during the 10-minute period before the application of 5xTBS protocol.

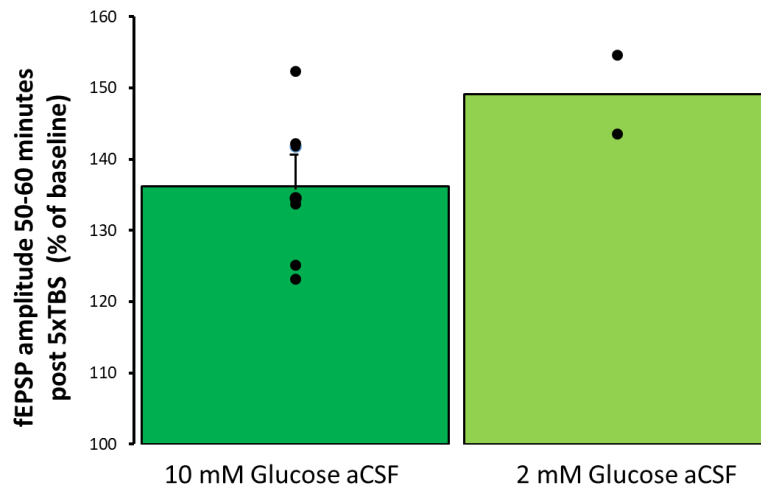


Figure 3.8. The effects of the A₁ receptor (1 μ M DPCPX) on LTP in the CA1 area of the hippocampus in experiments utilizing 10 and 2mM-glucose-containing aCSF, respectively.

Bar chart summarizing the effects of different adenosine antagonists on LTP. The level of LTP was measured 50-60 minutes after 5xTBS induction paradigm from rat hippocampal slices treated with the adenosine antagonist DPCPX. The magnitude of LTP was measured as the average of the evoked fEPSPs recorded during the last 50-60 minutes expressed as a percentage of the average baseline fEPSP amplitude recorded in the 10-minute period immediately prior to induction of LTP. Application of the adenosine antagonist DPCPX, at a concentration of 1 μ M in experiments subject to the conditions of 2 mM glucose-containing aCSF (n = 2) did not result in significant changes in fEPSP amplitudes, compared to the same antagonist applied in experiments utilizing aCSF containing 10 mM glucose (n = 7).

Table 3.5. Mean fEPSP amplitudes measured 50-60 minutes after a 5xTBS stimulation in rat hippocampal slices prepared with aCSF containing 10 or 2 mM glucose and treated with adenosine antagonist DPCPX (NS, non-significant).

Treatment	Mean	SEM	N	P vs Vehicle
10 mM Glucose aCSF & 1 μ M DPCPX	136.2	3.9	7	
2 mM Glucose aCSF & 1 μ M DPCPX	149.1	5.5	2	NS

3.14.3 The effects of the A_{2A} receptor antagonist KW-6002 on LTP induced in CA1 in the presence of 10, 5 and 2mM extracellular glucose

LTP was measured as an increase in amplitude of the fEPSP relative to vehicle controls. In experiments utilizing 10mM extracellular D-glucose, LTP induced in response to 5xTBS in the presence of 0.1% DMSO (vehicle control) amounted to an increase in the fEPSP of $143.9 \pm 4.4\%$ (mean \pm SEM), compared to pre-stimulation baseline levels (n = 8). A fEPSP increase of $132.6 \pm 4\%$ (mean \pm SEM), compared to the pre-5xTBS amplitude of fEPSP was observed in the group of experiments using 50 nM KW-6002 (n = 5), see Figures 3.9. & 3.10. This reduction in LTP in the presence of the A_{2A} receptor antagonist was not significantly different to that observed in the vehicle control group (p>0.05, unpaired Student's t-test, see Table 3.6.).

In the experiments performed in 5 mM D-glucose aCSF, the vehicle controls (0.1% DMSO) yielded an increase in the amplitude of fEPSP of $141.8 \pm 5.2\%$ (mean \pm SEM), compared to pre-stimulation baseline levels (n = 6). In the presence of 50 nM KW-6002 (n = 5), the LTP was represented by an increase in fEPSP amplitude of $132.9 \pm 3.6\%$ (mean \pm SEM), compared to pre-5xTBS fEPSP amplitude (Fig. 3.11. & 3.12). No significant effect was detected (p>0.05, unpaired Student's t-test, see table 3.7.).

In the presence of 2mM extracellular D-glucose, the vehicle control (0.1% DMSO) LTP fEPSP was $131.6 \pm 4\%$ (mean \pm SEM), compared to pre-stimulation fEPSP amplitude ($n = 4$). The application of 50 nM KW-6002 led to an increase in fEPSP amplitude of $122 \pm 3.5\%$ (mean \pm SEM), compared to the fEPSP amplitude before the 5xTBS application (see Fig. 3.13. & 3.14.). This reduction in LTP was not significantly different to the results collected from the vehicle control group ($p > 0.05$, unpaired Student's t-test, see table 3.8.).

Lastly, the fEPSP amplitudes obtained from experiments using 5- and 2 mM extracellular D-glucose and the adenosine receptor antagonist, were compared to the increase in fEPSP amplitude seen upon the application of KW-6002 in the presence of 10 mM D-glucose (see fig. 3.15. & 3.16.). However, no significant differences were detected upon comparing the influence of KW-6002 in the presence of 5 or 2 mM and the effect of KW-6002 in the presence of 10 mM D-glucose ($p > 0.05$, unpaired student's t-test, see Table 3.9.).

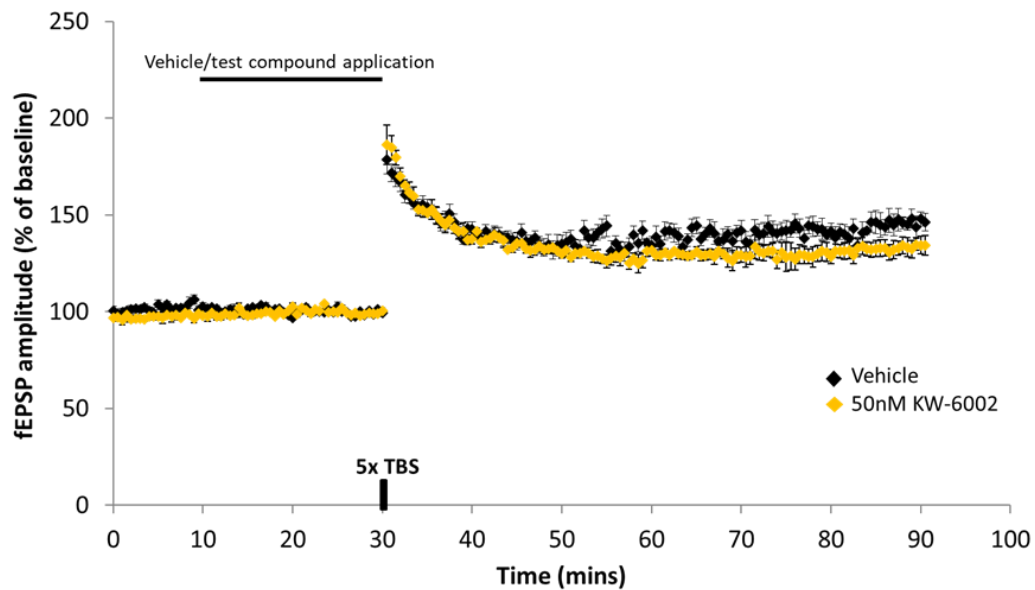


Figure 3.9. The effects of the adenosine A_{2A} receptor antagonist KW-6002 on LTP in the CA1 area of the hippocampus in 10mM extracellular D-glucose.

Composite scatter plot representing mean normalised fEPSP amplitudes before and after 5xTBS induction in rat hippocampal slices pre-treated for 20 minutes with either vehicle or test compound. Data are expressed as a percentage of the average of fEPSP amplitudes recorded during the 10-minute period before the application of 5xTBS protocol. Following a 10-minute stable baseline recording period (no compound treatment), vehicle (black diamonds) or 50 nM KW-6002 (yellow diamonds) was applied for 20 minutes (black bar). Theta-burst (5xTBS; indicated by the bar on the timeline), induced LTP. Error bars represent standard error of the mean (SEM). N: vehicle = 8; KW-6002 = 5

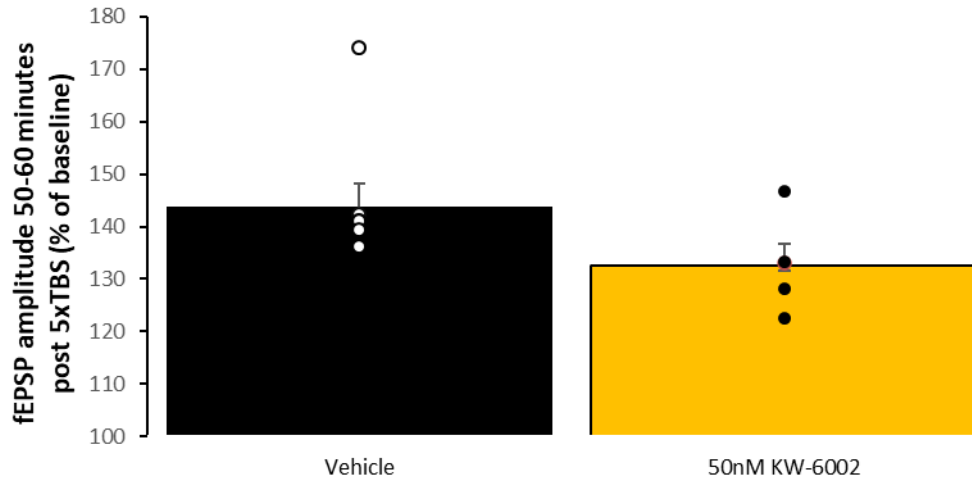


Figure 3.10. The effects of the $A_{2A}R$ antagonists on LTP in the CA1 area of the hippocampus in 10mM extracellular D-glucose.

Bar chart summarizing the effects of different adenosine antagonists on LTP. The level of LTP was measured 50-60 minutes after 5xTBS induction paradigm from rat hippocampal slices treated with either vehicle, or adenosine receptor antagonists. The magnitude of LTP was measured as the average of the evoked fEPSPs recorded during the last 50-60 minutes expressed as a percentage of the average baseline fEPSP amplitude recorded in the 10-minute period immediately prior to induction of LTP. Application of the adenosine antagonists did not result in significant changes in fEPSP amplitudes, compared to vehicle (statistical results summarized in Table 3.6, unpaired Student's t-test). (N: vehicle = 8; KW-6002 = 5).

Table 3.6. Mean fEPSP amplitudes measured 50-60 minutes after a 5xTBS stimulation in rat hippocampal slices prepared with aCSF containing 10 mM D-glucose and treated with vehicle (aCSF + 0.1% DMSO) or 50 nM KW-6002, (unpaired Student's t-test, NS, non-significant).

Treatment	Mean	SEM	n	P vs Vehicle
Vehicle	143.9	4.4	8	
50 nM KW-6002	132.6	4	5	NS

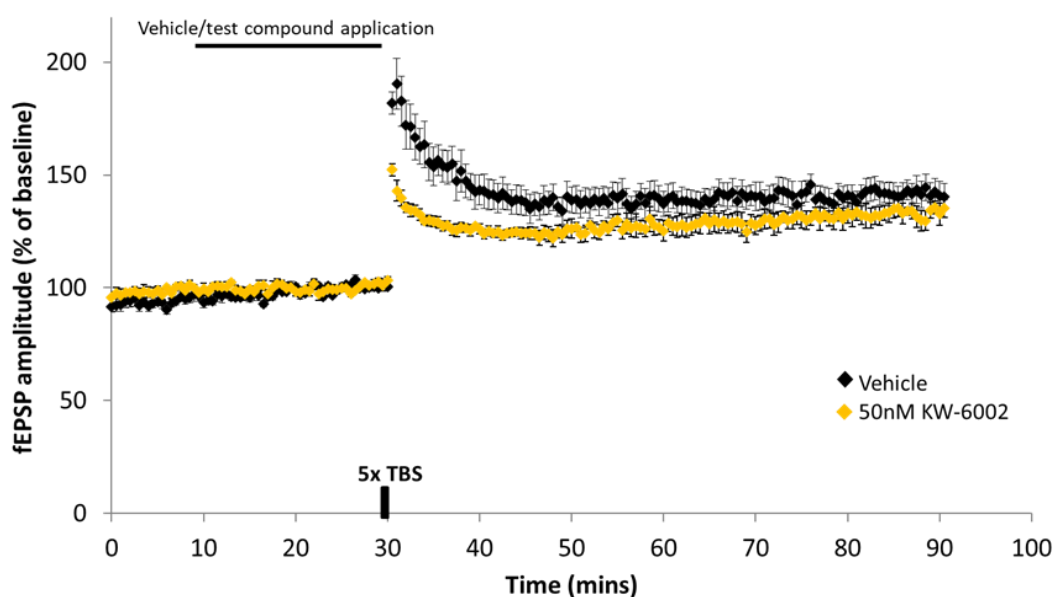


Figure 3.11. The effects of the $A_{2A}R$ antagonists on LTP in the CA1 area of the hippocampus in 5mM extracellular D-glucose.

Composite scatter plot representing mean normalised fEPSP amplitudes before and after 5xTBS induction in rat hippocampal slices pre-treated for 20 minutes with either vehicle or test compound. Data are expressed as a percentage of the average of fEPSP amplitudes recorded during the 10-minute period before the application of 5xTBS protocol. Following a 10-minute stable baseline recording period (no compound treatment), vehicle (black diamonds) or 50 nM KW-6002 (yellow diamonds) was applied for 20 minutes (black bar). Theta-burst (5xTBS; indicated by the bar on the timeline), induced LTP. Error bars represent standard error of the mean (SEM). N: vehicle = 6; KW-6002 = 5

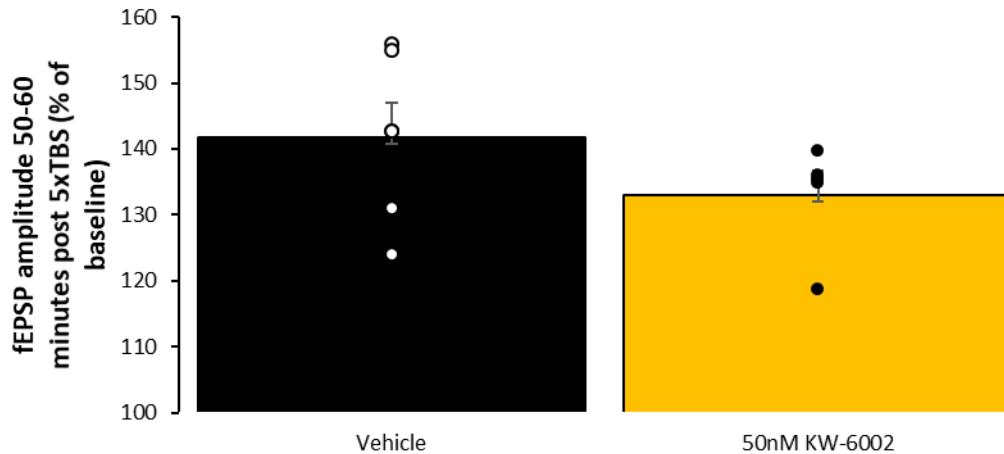


Figure 3.12. The effects of the $A_{2A}R$ antagonist (50 nM KW-6002) on LTP in the CA1 area of the hippocampus in experiments utilizing 5mM glucose-containing aCSF.

Bar chart summarizing the effects of 50 nM KW-6002 on LTP. The level of LTP was measured 50-60 minutes after 5xTBS induction paradigm from rat hippocampal slices treated with either vehicle, or 50 nM KW-6002. The magnitude of LTP was measured as the average of the evoked fEPSPs recorded during the last 50-60 minutes expressed as a percentage of the average baseline fEPSP amplitude recorded in the 10-minute period immediately prior to induction of LTP. Application of the adenosine antagonist 50 nM KW-6002 did not result in significant changes in fEPSP amplitudes, compared to vehicle (statistical results summarized in Table 4.7, unpaired Student's t-test). Error bars represent standard error of the mean (SEM) (N: vehicle = 6; KW-6002 = 5).

Table 3.7. Mean fEPSP amplitudes measured 50-60 minutes after a 5xTBS stimulation in rat hippocampal slices prepared with aCSF containing 5mM D-glucose and treated with vehicle (aCSF + 0.1% DMSO) or 50 nM KW-6002, (unpaired Student's t-test, NS, non-significant).

Treatment	Mean	SEM	n	P vs Vehicle
Vehicle	141.8	5.2	6	
50 nM KW-6002	132.9	3.6	5	NS

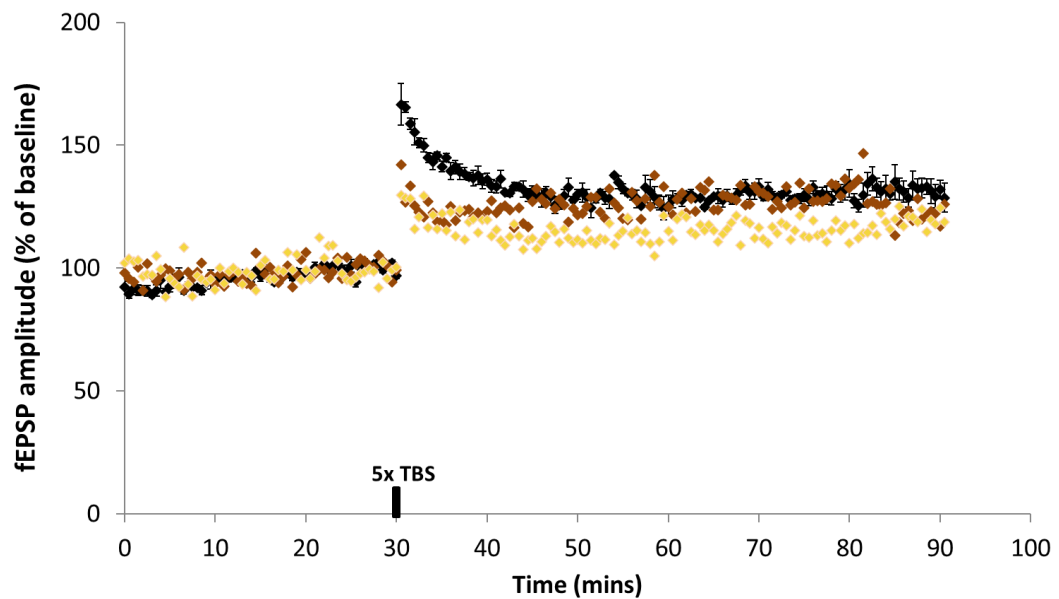


Figure 3.13. The effects of the adenosine A_{2A} receptor antagonist KW-6002 on LTP in the CA1 area of the hippocampus in 2mM glucose aCSF.

Composite scatter plot representing mean normalised fEPSP amplitudes before and after 5xTBS induction in rat hippocampal slices pre-treated for 20 minutes with either vehicle or test compound. Data are expressed as a percentage of the average of fEPSP amplitudes recorded during the 10-minute period before the application of 5xTBS protocol. Following a 10-minute stable baseline recording period (no compound treatment), vehicle (black diamonds) or 50 nM KW-6002 (yellow and brown diamonds) was applied for 20 minutes. Theta-burst (5xTBS; indicated by the bar on the timeline), induced LTP. Error bars represent standard error of the mean (SEM) (N: vehicle = 6; KW-6002 = 2).

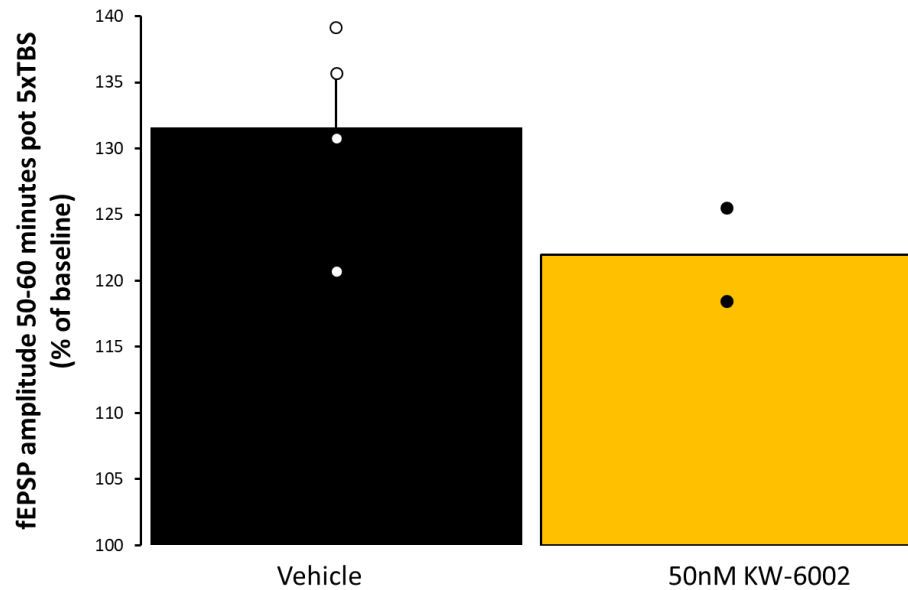


Figure 3.14. The effects of the $A_{2A}R$ adenosine antagonists (50 nM KW-6002) on LTP in the CA1 area of the hippocampus in experiments utilizing 2mM-glucose-containing aCSF.

Bar chart summarizing the effects of different adenosine antagonists on LTP. The level of LTP was measured 50-60 minutes after 5xTBS induction paradigm from rat hippocampal slices treated with either vehicle, or an adenosine receptor antagonist. The magnitude of LTP was measured as the average of the evoked fEPSPs recorded during the last 50-60 minutes expressed as a percentage of the average baseline fEPSP amplitude recorded in the 10-minute period immediately prior to induction of LTP. Application of the adenosine antagonist did not result in significant changes in fEPSP amplitudes, compared to vehicle (N: vehicle = 4; KW-6002 = 2).

Table 3.8. Mean fEPSP amplitudes measured 50-60 minutes after a 5xTBS stimulation in rat hippocampal slices prepared with aCSF containing 2 mM D-glucose and treated with vehicle (aCSF + 0.1% DMSO) or 50 nM KW-6002, (NS, non-significant).

Treatment	Mean	SEM	n	<i>P</i> vs Vehicle
Vehicle	131.6	4	4	
50 nM KW-6002	122	3.5	2	NS

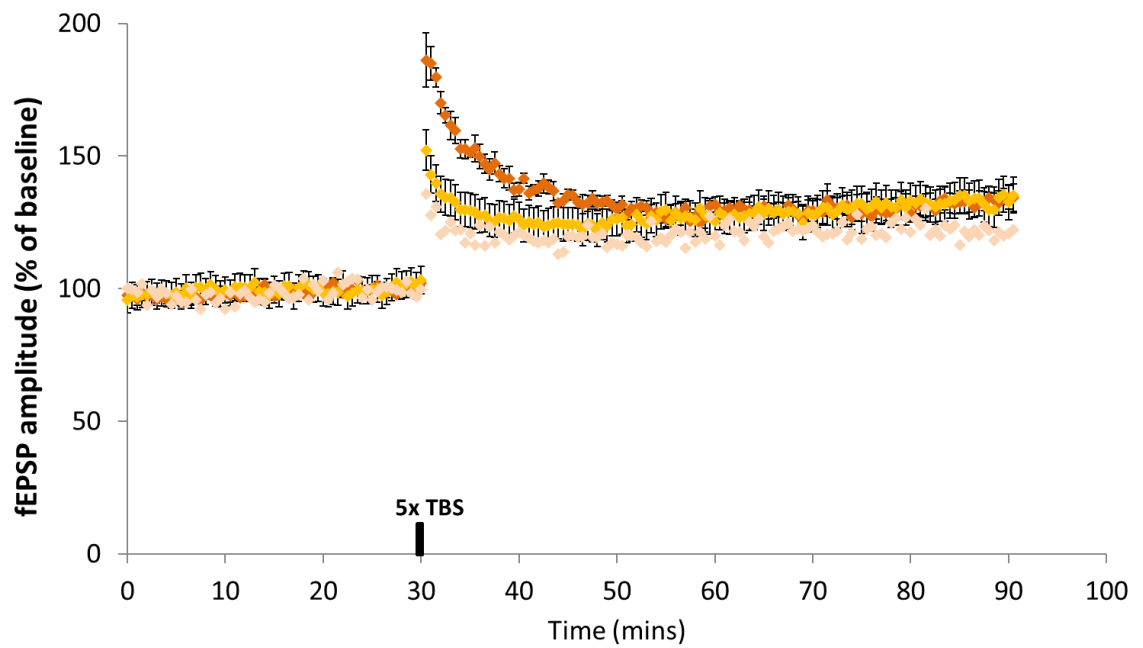


Figure 3.15. The effects of the $A_{2A}R$ adenosine antagonist (KW-6002) on LTP in the CA1 area of the hippocampus.

Composite scatter plot representing mean normalised fEPSP amplitudes before and after 5xTBS induction in rat hippocampal slices pre-treated for 20 minutes with 50 nM KW-6002 in experiments using 10mM glucose aCSF (dark orange diamonds) ($n = 7$), 5mM glucose aCSF (yellow diamonds) ($n = 5$), or 2mM glucose aCSF (light orange diamonds) ($n = 2$). Data are expressed as a percentage of the average of fEPSP amplitudes recorded during the 10-minute period before the application of 5xTBS protocol.

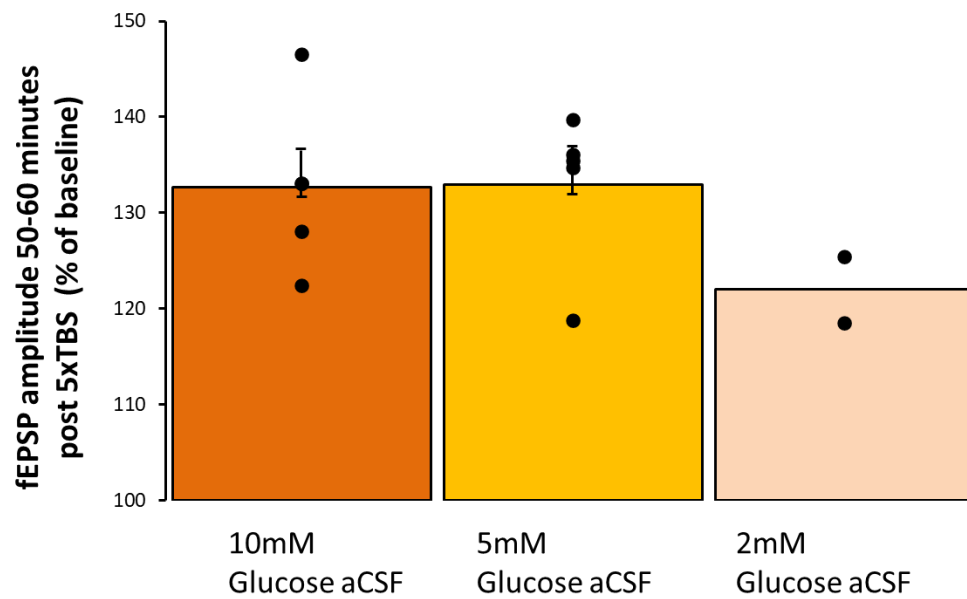


Figure 3.16. The effects of $A_{2A}R$ antagonists (50 nM KW-6002) on LTP in the CA1 area of the hippocampus in experiments utilizing 10, 5 and 2mM aCSF.

Bar chart summarizing the effects of different adenosine antagonists on LTP. The level of LTP was measured 50-60 minutes after 5xTBS induction paradigm from rat hippocampal slices treated with adenosine receptor antagonists. The magnitude of LTP was measured as the average of the evoked fEPSPs recorded during the last 50-60 minutes expressed as a percentage of the average baseline fEPSP amplitude recorded in the 10-minute period immediately prior to induction of LTP. Application of the adenosine antagonist KW-6002 in experiments subject to the conditions of 2 mM ($n = 2$) or 5mM glucose-containing aCSF ($n = 5$) did not result in significant changes in fEPSP amplitudes, compared to the same antagonist applied in experiments utilizing aCSF containing 10 mM glucose ($n = 5$) due to a low experiment count.

Table 3.9. Mean fEPSP amplitudes measured 50-60 minutes after a 5xTBS stimulation in rat hippocampal slices prepared with aCSF containing 10, 5 or 2mM glucose and treated with adenosine antagonist KW-6002 (NS, non-significant).

Treatment	Mean	SEM	n	<i>P</i> vs Vehicle
10 mM Glucose aCSF & 50 nM KW-6002	132.6	4	5	
5 mM Glucose aCSF & 50 nM KW-6002	132.9	3.6	5	NS
2 mM Glucose aCSF & 50 nM KW-6002	122	3.5	2	NS

3.14.4 The effects of the A_{2B} receptor antagonist PSB603 on LTP induced in CA1 in the presence of 10mM extracellular D-glucose

LTP was measured as an increase in amplitude of the fEPSP relative to vehicle controls. LTP in CA1 induced in response to 5xTBS in the presence of 0.1% DMSO (vehicle control) amounted to an increase in the fEPSP of $143.9 \pm 4.4\%$ (mean \pm SEM), compared to pre-stimulation baseline levels (100%; n = 8). LTP induced in the presence of PSB603 at a concentration of 100 nM was associated with an increase in the fEPSP to $138.9 \pm 4.1\%$ (mean \pm SEM), compared to baseline levels pre-5xTBS (n = 5) (see figs. 3.17. & 3.18). The effect of PSB603 on the fEPSP amplitude was not significant when compared to the vehicle ($p > 0.05$, unpaired student's t-test, see table 3.10.).

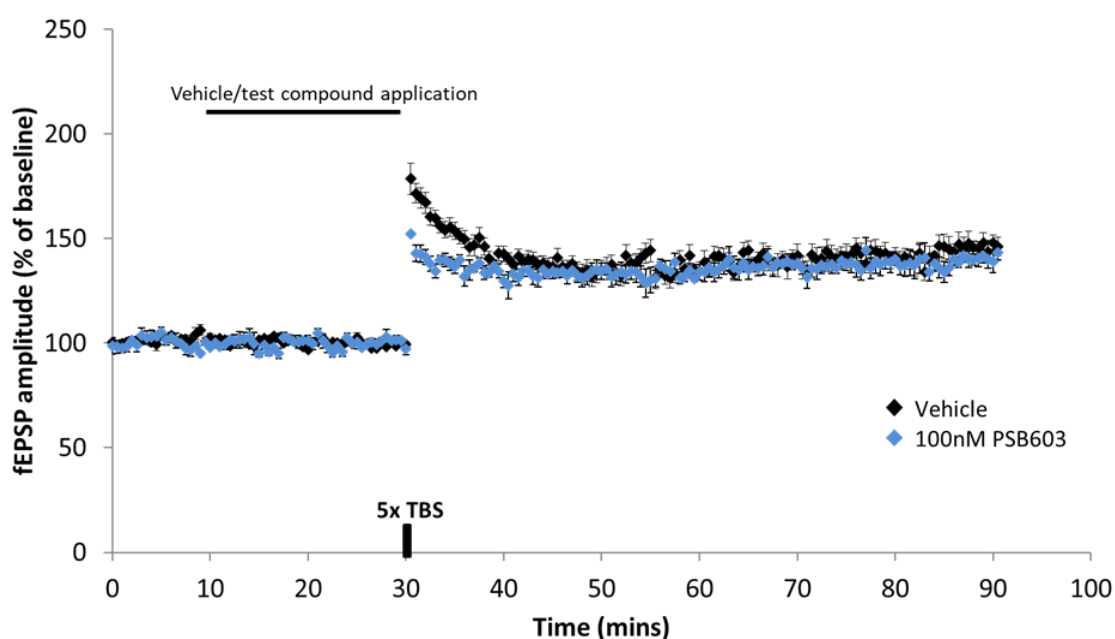


Figure 3.17. The effects of the adenosine A_{2B} receptor antagonist PSB603 on LTP in the CA1 area of the hippocampus in 10mM extracellular glucose

Composite scatter plot representing mean normalised fEPSP amplitudes before and after 5xTBS induction in rat hippocampal slices pre-treated for 20 minutes with either vehicle or test compound. Data are expressed as a percentage of the average of fEPSP amplitudes recorded during the 10-minute period before the application of 5xTBS protocol. Following a 10-minute stable baseline recording period (no compound treatment), vehicle (black diamonds) or 100 nM PSB603 (blue diamonds) was applied for 20 minutes (black bar). Theta-burst (5xTBS; indicated by the bar on the timeline), induced LTP. Error bars represent standard error of the mean (SEM). N: vehicle = 8; PSB603 = 5

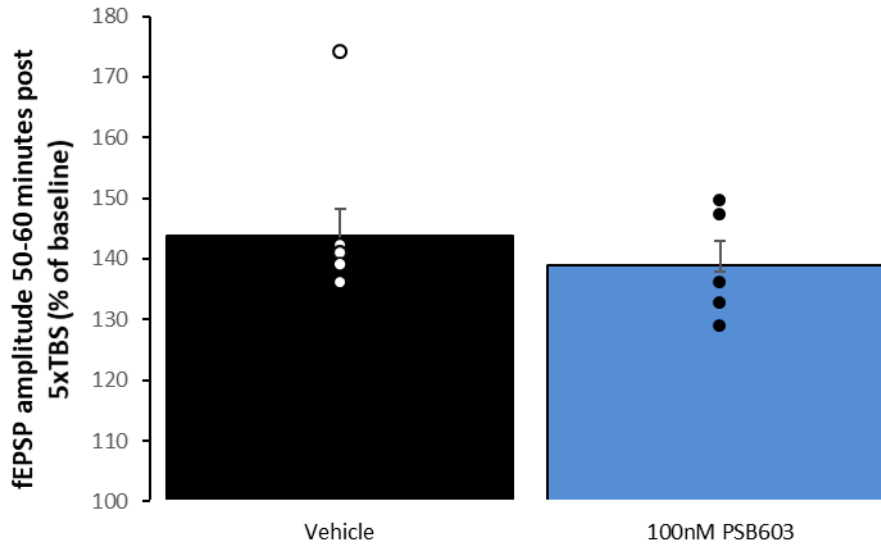


Figure 3.18. The effects of the adenosine A_{2B} receptor antagonist PSB603 on LTP in the CA1 area of the hippocampus in 10mM extracellular glucose.

Bar chart summarizing the effects of different adenosine antagonists on LTP. The level of LTP was measured 50-60 minutes after 5xTBS induction paradigm from rat hippocampal slices treated with either vehicle, or A_{2B} receptor antagonist PSB603. The magnitude of LTP was measured as the average of the evoked fEPSPs recorded during the last 50-60 minutes expressed as a percentage of the average baseline fEPSP amplitude recorded in the 10-minute period immediately prior to induction of LTP. Application of the adenosine antagonists did not result in significant changes in fEPSP amplitudes, compared to vehicle (statistical results summarized in Table 3.10., unpaired Student's t-test). (N: vehicle = 8; PSB603 = 5).

Table 3.10. Mean fEPSP amplitudes measured 50-60 minutes after a 5xTBS stimulation in rat hippocampal slices prepared with aCSF containing 10mM D-glucose and treated with vehicle (aCSF + 0.1% DMSO) or 100 nM PSB603, (unpaired Student's t-test, NS, non-significant).

Treatment	Mean	SEM	n	P vs Vehicle
Vehicle	143.9	4.4	8	
100 nM PSB603	138.9	4.1	5	NS

3.14.5 The effects of the A₃ receptor antagonist MRS1523 on LTP induced in CA1 in the presence of 10mM extracellular glucose

LTP was measured as an increase in amplitude of the fEPSP relative to vehicle controls. LTP in CA1 induced in response to 5xTBS in the presence of 0.1% DMSO (vehicle control) amounted to an increase in the fEPSP of $143.9 \pm 4.4\%$ (mean \pm SEM), compared to pre-stimulation baseline levels (n = 8). Lastly, the effect of 300 nM MRS1523 (n = 5) was recorded as an increase of $134.4 \pm 4.4\%$ (mean \pm SEM) in fEPSP amplitude when compared with the corresponding baseline level (Fig.3.19 & 3.20). None of the effects reported were significantly different to that observed in the vehicle control group (all groups: $p > 0.05$, unpaired Student's t-test, see table 3.11.).

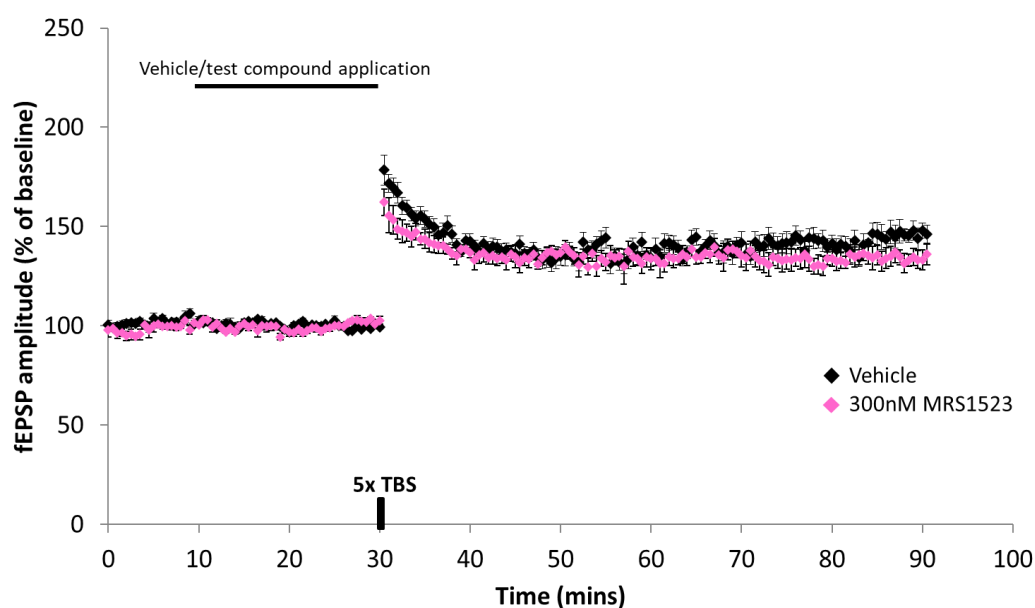


Figure 3.19. The effects of the adenosine A_3 receptor antagonist MRS1523 on LTP in the CA1 area of the hippocampus in 10mM extracellular glucose

Composite scatter plot representing mean normalised fEPSP amplitudes before and after 5xTBS induction in rat hippocampal slices pre-treated for 20 minutes with either vehicle or the test compound. Data are expressed as a percentage of the average of fEPSP amplitudes recorded during the 10-minute period before the application of 5xTBS protocol. Following a 10-minute stable baseline recording period (no compound treatment), vehicle (black diamonds) or 300 nM MRS1523 (pink diamonds) was applied for 20 minutes (black bar). Theta-burst (5xTBS; indicated by the bar on the timeline), induced LTP. Error bars represent standard error of the mean (SEM). N: vehicle = 8; MRS1523 = 5

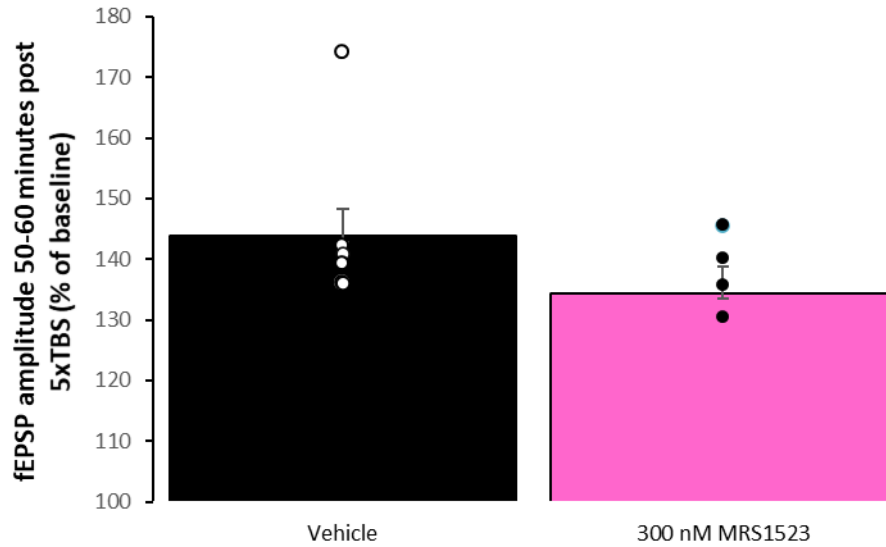


Figure 3.20. The effects of the adenosine A_3 receptor antagonist MRS1523 on LTP in the CA1 area of the hippocampus in 10mM extracellular glucose

Bar chart summarizing the effects of different adenosine antagonists on LTP. The level of LTP was measured 50-60 minutes after 5xTBS induction paradigm from rat hippocampal slices treated with either vehicle, or the A_3 receptor antagonist MRS1523. The magnitude of LTP was measured as the average of the evoked fEPSPs recorded during the last 50-60 minutes expressed as a percentage of the average baseline fEPSP amplitude recorded in the 10-minute period immediately prior to induction of LTP. Application of the adenosine antagonists did not result in significant changes in fEPSP amplitudes, compared to vehicle (statistical results summarized in Table 3.11., unpaired Student's t-test). (N: vehicle = 8; MRS1523 = 5).

Table 3.11. Mean fEPSP amplitudes measured 50-60 minutes after a 5xTBS stimulation in rat hippocampal slices prepared with aCSF containing 10mM D-glucose and treated with vehicle (aCSF + 0.1% DMSO) or 300 nM MRS1523, (unpaired Student's t-test, NS, non-significant).

Treatment	Mean	SEM	n	<i>P</i> vs Vehicle
Vehicle	143.9	4.4	8	
300 nM MRS1523	134.4	4.4	5	NS

3.14.6 The effects of the non-selective adenosine receptor antagonist CGS15943 on LTP induced in CA1 in the presence of 10 and 5mM extracellular glucose

LTP was measured as an increase in amplitude of the fEPSP relative to vehicle controls in the presence of aCSF containing either 10 or 5mM D-glucose. In experiments with 10mM D-glucose, LTP in CA1 induced in response to 5xTBS in the presence of 0.1% DMSO (vehicle control) amounted to an increase in the fEPSP of $143.9 \pm 4.4\%$ (mean \pm SEM), compared to pre-stimulation baseline levels ($n = 8$) (see figs 3.21 & 3.22). Compared to the baseline levels prior the 5xTBS stimulation, an increase in the fEPSP of $135.4 \pm 8.2\%$ (mean \pm SEM) was detected in the presence of the AR antagonist CGS15943, at a concentration of 100 nM ($n = 5$). The effect reported was not significantly different to that observed in the vehicle control group ($p > 0.05$, unpaired student's t-test, see table 3.12.).

In experiments utilizing 5 mM D-glucose, the vehicle control (0.1% DMSO) group showed an increase in the amplitude of fEPSP of $141.8 \pm 5.2\%$ (mean \pm SEM), compared to pre-stimulation baseline levels ($n = 6$). Application of 5xTBS in the presence of 100 nM CGS15943 ($n = 3$) resulted in an increase in fEPSP amplitude to $139.9 \pm 7.8\%$ (mean \pm SEM), compared with the fEPSP amplitude at baseline level. The effects of 100 nM CGS15943 was not significantly different to the increase in fEPSP amplitude observed in the vehicle control group (all groups: $p > 0.05$, unpaired student's t-test, see Figs. 3.23 & 3.24, table 3.13).

In addition, no statistically significant outcome was seen upon comparing the effect of 100 nM CGS15943 on LTP (See Fig. 3.25 & 3.26) in experiments using 5 mM D-glucose aCSF ($n = 3$), to that seen in the presence of 10 mM D-glucose ($p > 0.05$, unpaired student's t-test, see table 3.14.).

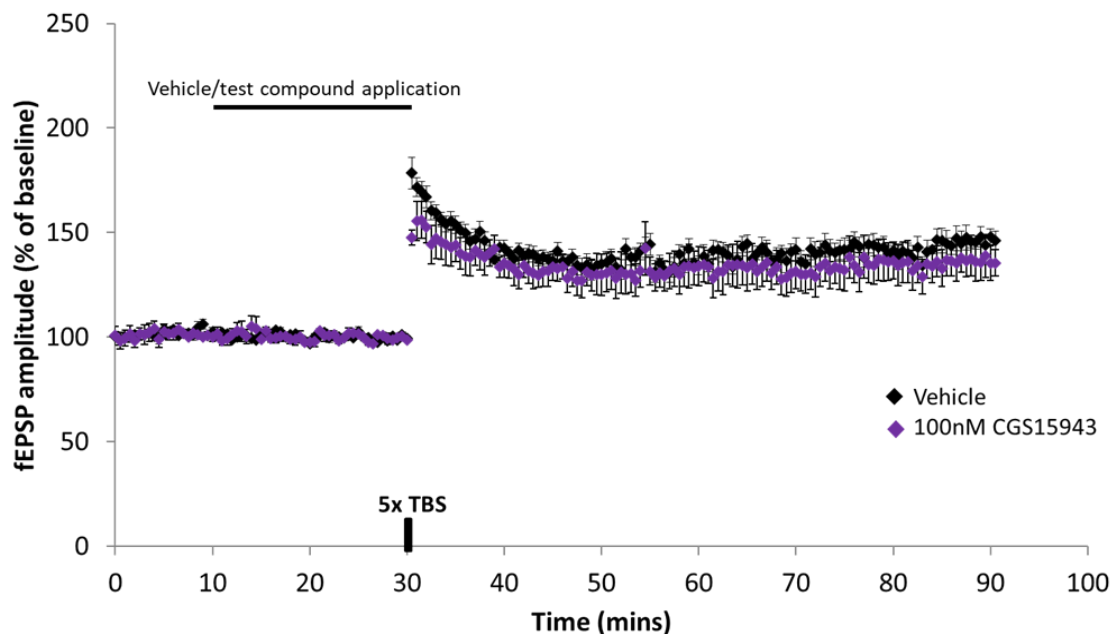


Figure 3.21. T The effects of the non-selective adenosine receptor antagonist CGS15943 on LTP in the CA1 area of the hippocampus in 10 mM extracellular glucose

Composite scatter plot representing mean normalised fEPSP amplitudes before and after 5xTBS induction in rat hippocampal slices pre-treated for 20 minutes with either vehicle or test compound. Data are expressed as a percentage of the average of fEPSP amplitudes recorded during the 10-minute period before the application of 5xTBS protocol. Following a 10-minute stable baseline recording period (no compound treatment), vehicle (black diamonds) or 100 nM CGS15943 (purple diamonds), was applied for 20 minutes (black bar). Theta-burst (5xTBS; indicated by the bar on the timeline), induced LTP. Error bars represent standard error of the mean (SEM). N: vehicle = 8; CGS15943 = 5

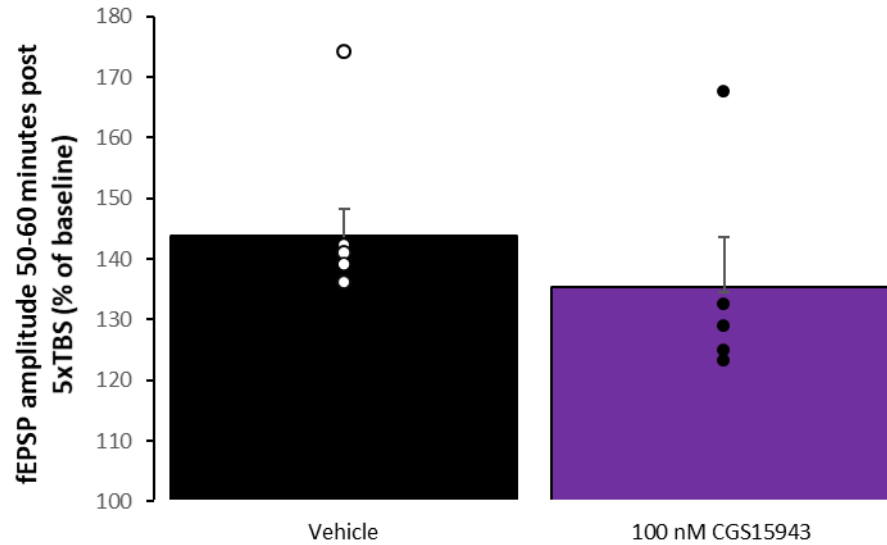


Figure 3.22. The effects of the non-selective adenosine receptor antagonist CGS15943 on LTP in the CA1 area of the hippocampus in 10mM extracellular glucose

Bar chart summarizing the effects of the non-selective adenosine receptor antagonist CGS15943 on LTP. The level of LTP was measured 50-60 minutes after 5xTBS induction paradigm from rat hippocampal slices treated with either vehicle, or non-selective adenosine receptor antagonist CGS15943. The magnitude of LTP was measured as the average of the evoked fEPSPs recorded during the last 50-60 minutes expressed as a percentage of the average baseline fEPSP amplitude recorded in the 10-minute period immediately prior to induction of LTP. Application of CGS15943 did not result in significant changes in fEPSP amplitudes, compared to vehicle (statistical results summarized in Table 3.12, unpaired Student's t-test). (N: vehicle = 8; CGS15943 = 5).

Table 3.12. Mean fEPSP amplitudes measured 50-60 minutes after a 5xTBS stimulation in rat hippocampal slices prepared with aCSF containing 10mM D-glucose and treated with vehicle (aCSF + 0.1% DMSO) or 100 nM CGS15943, (unpaired Student's t-test, NS, non-significant).

Treatment	Mean	SEM	n	P vs Vehicle
Vehicle	143.9	4.4	8	
100 nM CGS15943	135.4	8.2	5	NS

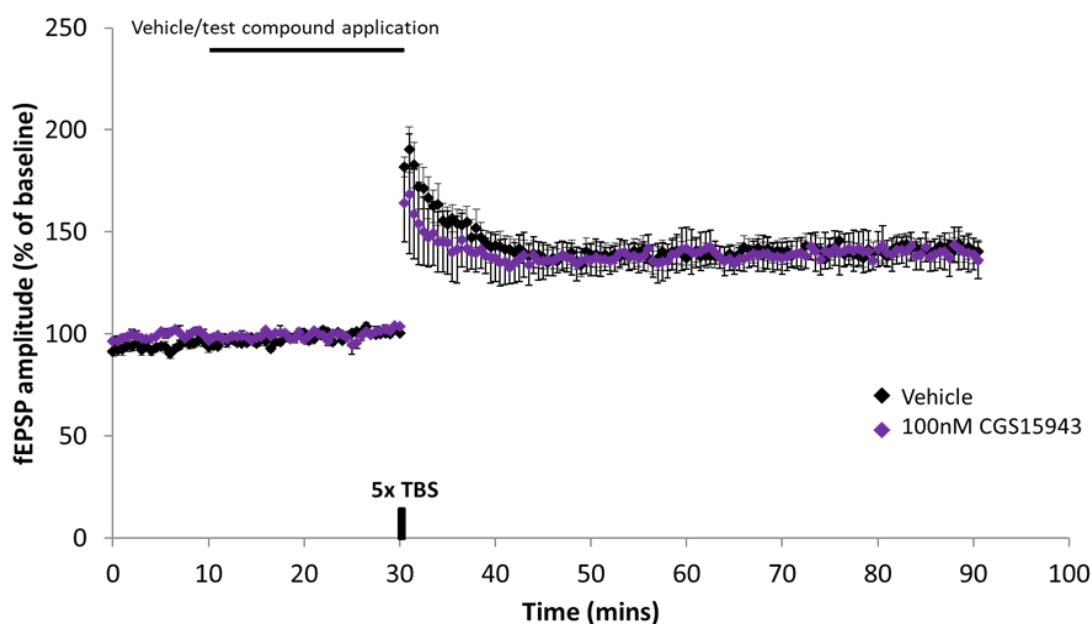


Figure 3.23. The effects of the non-selective adenosine receptor antagonist CGS15943 on LTP in the CA1 area of the hippocampus in 5 mM extracellular glucose

Composite scatter plot representing mean normalised fEPSP amplitudes before and after 5xTBS induction in rat hippocampal slices pre-treated for 20 minutes with either vehicle or test compound. Data are expressed as a percentage of the average of fEPSP amplitudes recorded during the 10-minute period before the application of 5xTBS protocol. Following a 10-minute stable baseline recording period (no compound treatment), vehicle (black diamonds) or 100 nM CGS15943 (purple diamonds) was applied for 20 minutes (black bar). Theta-burst (5xTBS; indicated by the bar on the timeline), induced LTP. Error bars represent standard error of the mean (SEM). N: vehicle = 6; CGS15943 = 3

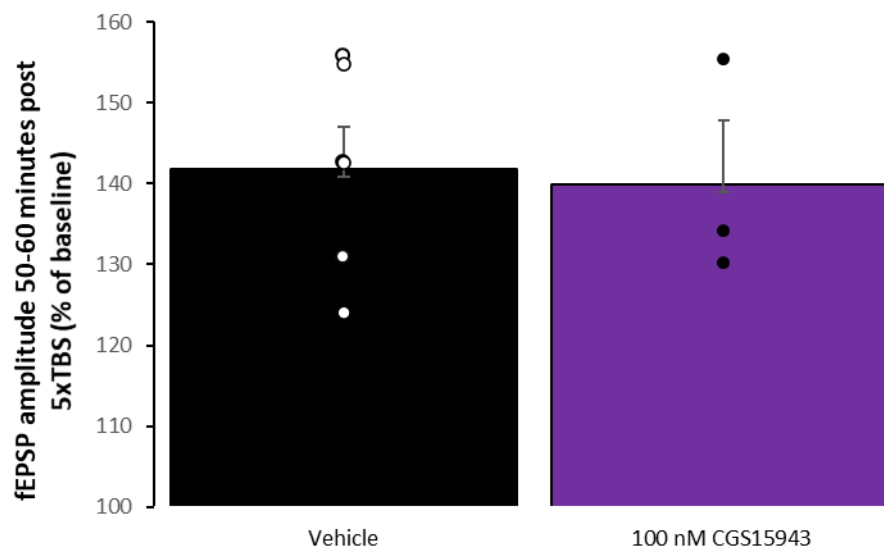


Figure 3.24. The effects of non-selective adenosine antagonist 100 nM CGS15943 on LTP in the CA1 area of the hippocampus in experiments utilizing 5mM glucose-containing aCSF

Bar chart summarizing the effects of different adenosine antagonists on LTP. The level of LTP was measured 50-60 minutes after 5xTBS induction paradigm from rat hippocampal slices treated with either vehicle, or adenosine receptor antagonists. The magnitude of LTP was measured as the average of the evoked fEPSPs recorded during the last 50-60 minutes expressed as a percentage of the average baseline fEPSP amplitude recorded in the 10-minute period immediately prior to induction of LTP. Application of the adenosine antagonists did not result in significant changes in fEPSP amplitudes, compared to vehicle (statistical results summarized in Table 3.13., unpaired Student's t-test). (N: vehicle = 6; CGS15943 = 3).

Table 3.13. Mean fEPSP amplitudes measured 50-60 minutes after a 5xTBS stimulation in rat hippocampal slices prepared with aCSF containing 5mM D-glucose and treated with vehicle (aCSF + 0.1% DMSO) or 100 nM CGS15943, (unpaired Student's t-test, NS, non-significant).

Treatment	Mean	SEM	n	P vs Vehicle
Vehicle	141.8	5.2	6	
100 nM CGS15943	139.9	7.8	3	NS

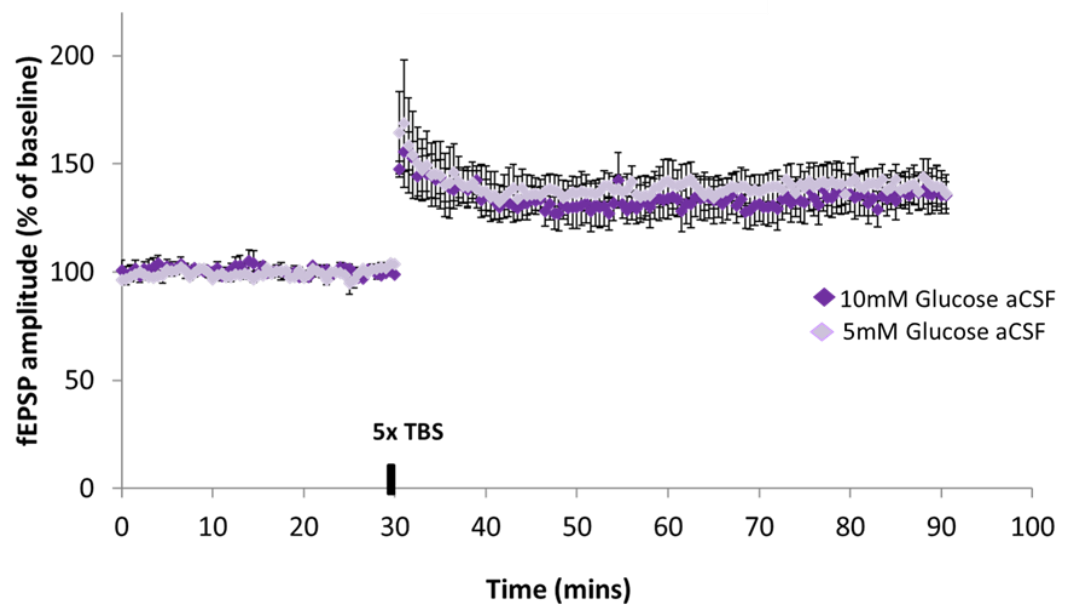


Figure 3.25. The effects of the non-selective adenosine antagonist CGS15943 on LTP in the CA1 area of the hippocampus

Composite scatter plot representing mean normalised fEPSP amplitudes before and after 5xTBS induction in rat hippocampal slices pre-treated for 20 minutes with 100 nM CGS15943 in experiments using 10mM glucose aCSF (dark purple diamonds) ($n = 5$), or 5 mM glucose aCSF (light purple diamonds) ($n = 3$). Data are expressed as a percentage of the average of fEPSP amplitudes recorded during the 10-minute period before the application of 5xTBS protocol. Error bars represent standard error of the mean (SEM).

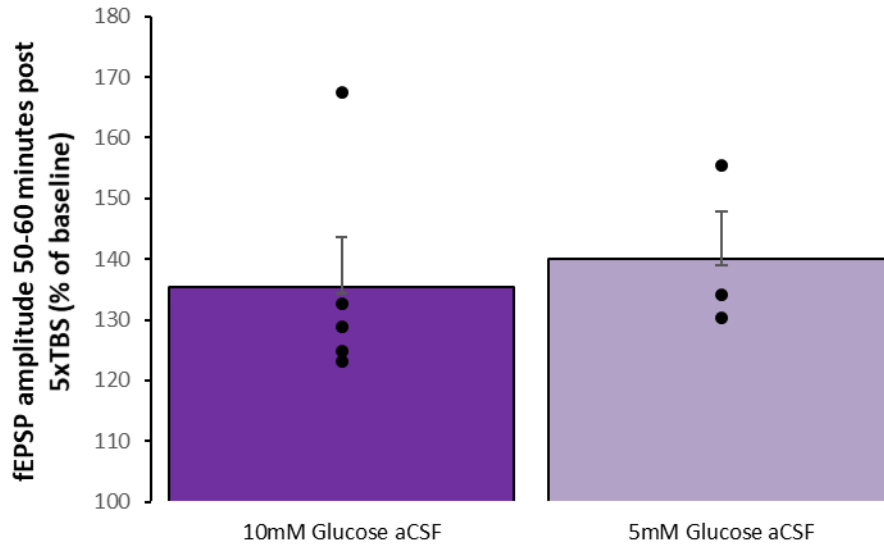


Figure 3.26. The effect of the non-selective adenosine receptor antagonist 100 nM CGS15943 on LTP in the CA1 area of the hippocampus in experiments utilizing 10 and 5mM glucose-containing aCSF

Bar chart summarizing the effects of different adenosine antagonists on LTP. The level of LTP was measured 50-60 minutes after 5xTBS induction paradigm from rat hippocampal slices treated with adenosine receptor antagonists. The magnitude of LTP was measured as the average of the evoked fEPSPs recorded during the last 50-60 minutes expressed as a percentage of the average baseline fEPSP amplitude recorded in the 10-minute period immediately prior to induction of LTP.

Application of the adenosine antagonist in experiments subject to the conditions of 5 mM glucose-containing aCSF (n = 3) did not result in significant changes in fEPSP amplitudes, compared to the same antagonist applied in experiments utilizing aCSF containing 10mM glucose (n = 5), (statistical results summarized in Table 3.14., unpaired Student's t-test).

Table 3.14. Mean fEPSP amplitudes measured 50-60 minutes after a 5xTBS stimulation in rat hippocampal slices prepared with aCSF containing 10 or 5mM glucose and treated with adenosine antagonist CGS15943 (unpaired Student's t-test, NS, non-significant).

Treatment	Mean	SEM	n	P vs Vehicle
10 mM Glucose aCSF & 100 nM CGS15943	138.9	4.1	5	
5 mM Glucose aCSF & 100 nM CGS15943	139.9	7.8	3	NS

3.14.7 Results: A summary of the effects of adenosine receptor antagonists on the LTP in the presence of aCSF containing 10mM of glucose

LTP was measured as an increase in amplitude of the fEPSP relative to vehicle controls. LTP in CA1 induced in response to 5xTBS in the presence of 0.1% DMSO (vehicle control) amounted to an increase in the fEPSP of $143.9 \pm 4.4\%$ (mean \pm SEM), compared to pre-stimulation baseline levels ($n = 8$). LTP induced in the presence of PSB603 at a concentration of 100 nM was associated with an increase in the fEPSP to $138.9 \pm 4.1\%$ (mean \pm SEM), compared to baseline levels pre-5xTBS ($n = 5$). Compared to the baseline levels prior the 5xTBS stimulation, an increase in the fEPSP of $135.4 \pm 8.2\%$ (mean \pm SEM) was detected in the presence of the non-selective AR antagonist CGS15943, at a concentration of 100 nM ($n = 5$). In response to the application of 1 μ M DPCPX ($n = 7$), the fEPSP amplitude rose to $136.2 \pm 3.9\%$ (mean \pm SEM) when compared with the level of fEPSP before the stimulation. An fEPSP increase of $132.6 \pm 4\%$ (mean \pm SEM), compared to the pre-5xTBS amplitude of fEPSP was observed in the group of experiments using 50 nM KW-6002 ($n = 5$). Lastly, the effect of 300 nM MRS1523 ($n = 5$) was recorded as an increase of $134.4 \pm 4.4\%$ (mean \pm SEM) in fEPSP amplitude when compared with the corresponding baseline level (Fig.3.27. & 3.28.). None of the effects reported were significantly different to that observed in the vehicle control group (all groups: $p > 0.05$, unpaired student's t-test, see table 3.15.).

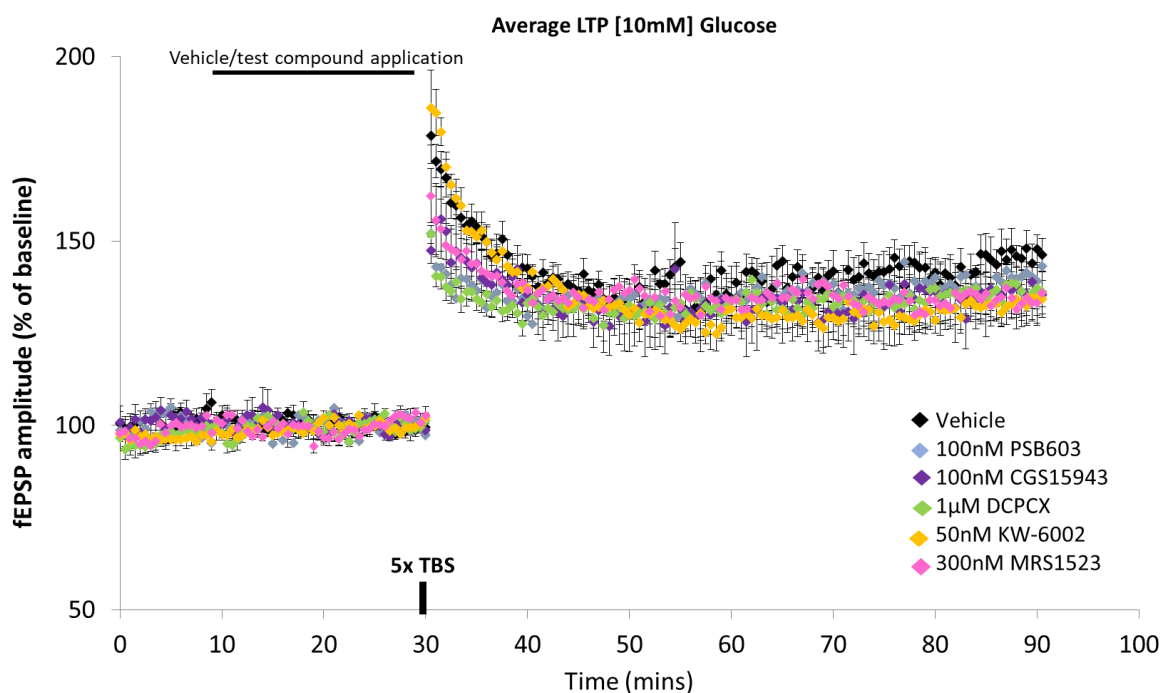


Figure 3.27. The effects of adenosine receptor antagonists on LTP in the CA1 area of the hippocampus in the presence of 10mM extracellular glucose

Composite scatter plot representing mean normalised fEPSP amplitudes before and after 5xTBS induction in rat hippocampal slices pre-treated for 20 minutes with either vehicle or test compound. Data are expressed as a percentage of the average of fEPSP amplitudes recorded during the 10-minute period before the application of 5xTBS protocol. Following a 10-minute stable baseline recording period (no compound treatment), vehicle (black diamonds), 100 nM PSB603 (blue diamonds), 100 nM CGS15943 (purple diamonds), 1 μ M DPCPX (green diamonds), 50 nM KW-6002 (yellow diamonds) or 300 nM MRS1523 (pink diamonds) was applied for 20 minutes (black bar). Theta-burst (5xTBS; indicated by the bar on the timeline), induced LTP. Error bars represent standard error of the mean (SEM). N: vehicle = 8; PSB603 = 5; CGS15943 = 5; DPCPX = 7; KW-6002 = 5; MRS1523 = 5

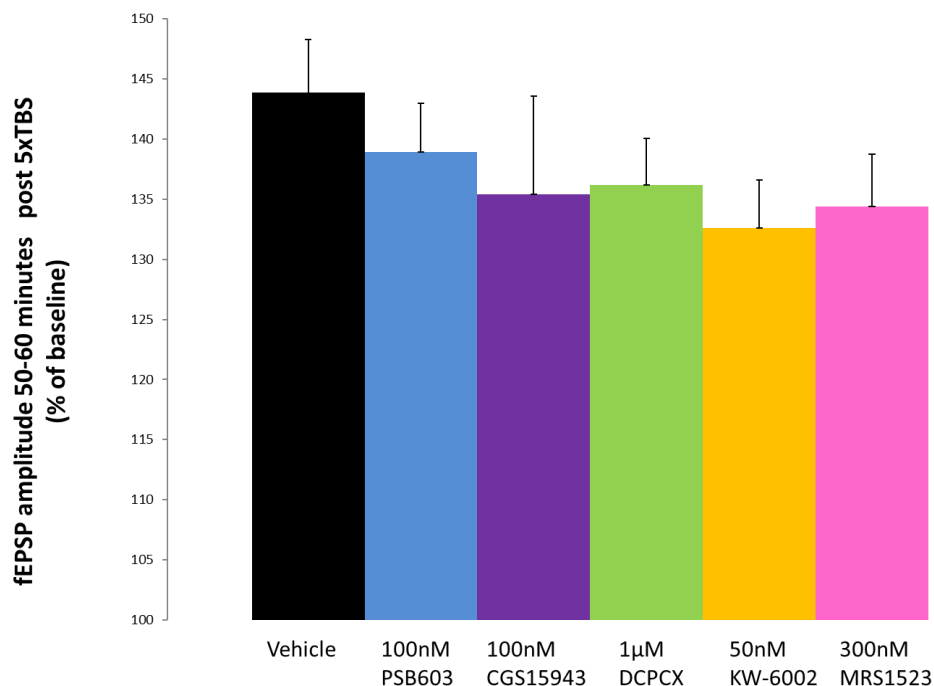


Figure 3.28. The effects of adenosine receptor antagonists on LTP in the CA1 area of the hippocampus in the presence of 10mM extracellular glucose

Bar chart summarizing the effects of different adenosine antagonists on LTP. The level of LTP was measured 50-60 minutes after 5xTBS induction paradigm from rat hippocampal slices treated with either vehicle, or adenosine receptor antagonists. The magnitude of LTP was measured as the average of the evoked fEPSPs recorded during the last 50-60 minutes expressed as a percentage of the average baseline fEPSP amplitude recorded in the 10-minute period immediately prior to induction of LTP. Application of the adenosine antagonists did not result in significant changes in fEPSP amplitudes, compared to vehicle (statistical results summarized in Table 3.15., unpaired Student's t-test). (N: vehicle = 8; PSB603 = 5; CGS15943 = 5; DPCPX = 7; KW-6002 = 5; MRS1523 = 5).

Table 3.15. Mean fEPSP amplitudes measured 50-60 minutes after a 5xTBS stimulation in rat hippocampal slices prepared with aCSF containing 10 mM glucose and treated with vehicle or adenosine antagonists, (One-way ANOVA, NS, non-significant).

Treatment	Mean	SEM	n	<i>P</i> vs Vehicle
Vehicle	143.9	4.2	8	
100 nM PSB603	138.9	5.3	5	NS
100 nM CGS15943	135.4	5.3	5	NS
1 μ M DPCPX	136.2	4.5	7	NS
50 nM KW-6002	132.6	5.3	5	NS
300 nM MRS1523	134.4	5.3	5	NS

3.14.8 Results: A summary of the effects of adenosine receptor antagonists on the LTP in the presence of aCSF containing 5 mM of glucose

In the following set of experiments, LTP was measured as an increase in amplitude of the fEPSP relative to vehicle controls. LTP in CA1 induced in response to 5xTBS in the presence of 0.1% DMSO (vehicle control) resulted in an increase in the amplitude of fEPSP of $141.8 \pm 5.2\%$ (mean \pm SEM), compared to pre-stimulation baseline levels ($n = 6$). Application of 100 nM CGS15943 ($n = 3$) showed an increase in fEPSP amplitude of $139.9 \pm 7.8\%$ (mean \pm SEM), compared with the fEPSP amplitude at baseline level. In the presence of 50 nM KW-6002 ($n = 5$), the LTP was represented by an increase in fEPSP amplitude of $132.9 \pm 3.6\%$ (mean \pm SEM), compared to pre-5xTBS fEPSP amplitude (Fig.3.29. & 3.30.). The effects of 100 nM CGS15943 or 50 nM KW-6002 were not significantly different to the increase in fEPSP amplitude observed in the vehicle control group (all groups: $p > 0.05$, unpaired student's t-test, see table 3.16.).

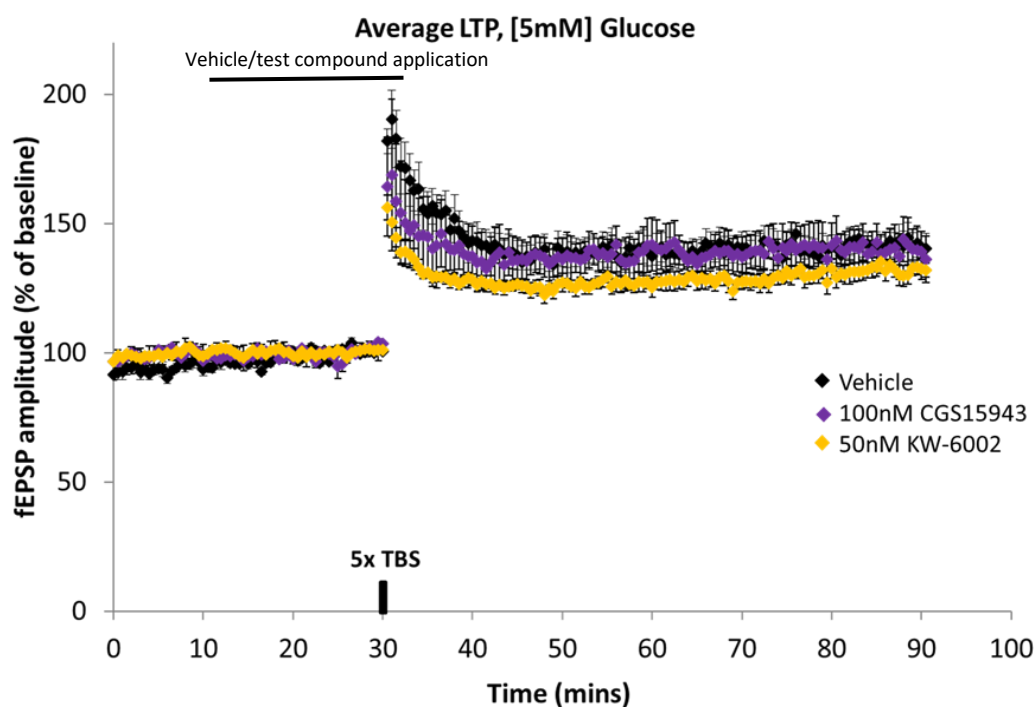


Figure 3.29. The effects of adenosine receptor antagonists on LTP in the CA1 area of the hippocampus in the presence of 5 mM extracellular glucose

Composite scatter plot representing mean normalised fEPSP amplitudes before and after 5xTBS induction in rat hippocampal slices pre-treated for 20 minutes with either vehicle or test compound. Data are expressed as a percentage of the average of fEPSP amplitudes recorded during the 10-minute period before the application of 5xTBS protocol. Following a 10-minute stable baseline recording period (no compound treatment), vehicle (black diamonds), 100 nM CGS15943 (purple diamonds) or 50 nM KW-6002 (yellow diamonds) was applied for 20 minutes (black bar). Theta-burst (5xTBS; indicated by the bar on the timeline), induced LTP. Error bars represent standard error of the mean (SEM). N: vehicle = 6; CGS15943 = 3; KW-6002 = 5

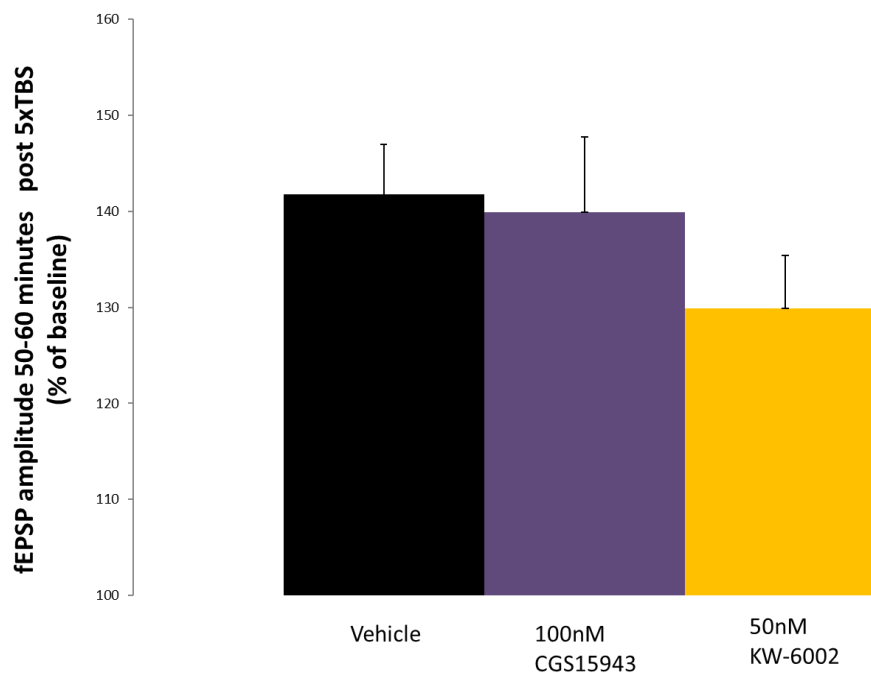


Figure 3.30. The effects of adenosine receptor antagonists (100 nM CGS15943 and 50 nM KW-6002) on LTP in the CA1 area of the hippocampus in experiments utilizing 5 mM glucose-containing aCSF

Bar chart summarizing the effects of different adenosine antagonists on LTP. The level of LTP was measured 50-60 minutes after 5xTBS induction paradigm from rat hippocampal slices treated with either vehicle, or adenosine receptor antagonists. The magnitude of LTP was measured as the average of the evoked fEPSPs recorded during the last 50-60 minutes expressed as a percentage of the average baseline fEPSP amplitude recorded in the 10-minute period immediately prior to induction of LTP. Application of the adenosine antagonists did not result in significant changes in fEPSP amplitudes, compared to vehicle (statistical results summarized in Table 3.16., unpaired Student's t-test). (N: vehicle = 6; CGS15943 =3; KW-6002 = 5).

Table 3.16. Mean fEPSP amplitudes measured 50-60 minutes after a 5xTBS stimulation in rat hippocampal slices prepared with aCSF containing 5 mM glucose and treated with vehicle or adenosine antagonist, (unpaired Student's t-test, NS, non-significant).

Treatment	Mean	SEM	n	P vs Vehicle
Vehicle	141.8	5.2	6	
100 nM CGS15943	139.9	7.8	3	NS
50 nM KW-6002	132.9	3.6	5	NS

3.14.9 Results: A summary of the effects of adenosine receptor antagonists on the LTP in the presence of aCSF containing 2 mM of glucose

LTP in CA1 induced in response to 5xTBS in the presence of 0.1% DMSO (vehicle control) resulted in an increase in the amplitude of fEPSP of $131.6 \pm 4\%$ (mean \pm SEM), compared to pre-stimulation fEPSP amplitude (n = 4). In response to 1 μ M DPCPX the fEPSP amplitude rose to $149.1 \pm 5.2\%$ (mean \pm SEM), compared to pre-5xTBS fEPSP amplitude (n = 2) (see Fig. 3.31. & 3.32.). This effect appeared larger when compared to the control group (see table 3.17.). The application of 50 nM KW-6002 led to an increase in fEPSP amplitude of $122 \pm 3.5\%$ (mean \pm SEM), compared to the fEPSP amplitude before the 5xTBS application, however it cannot be determined if this effect is significantly different to the results collected from the vehicle control group (see table 3.17.).

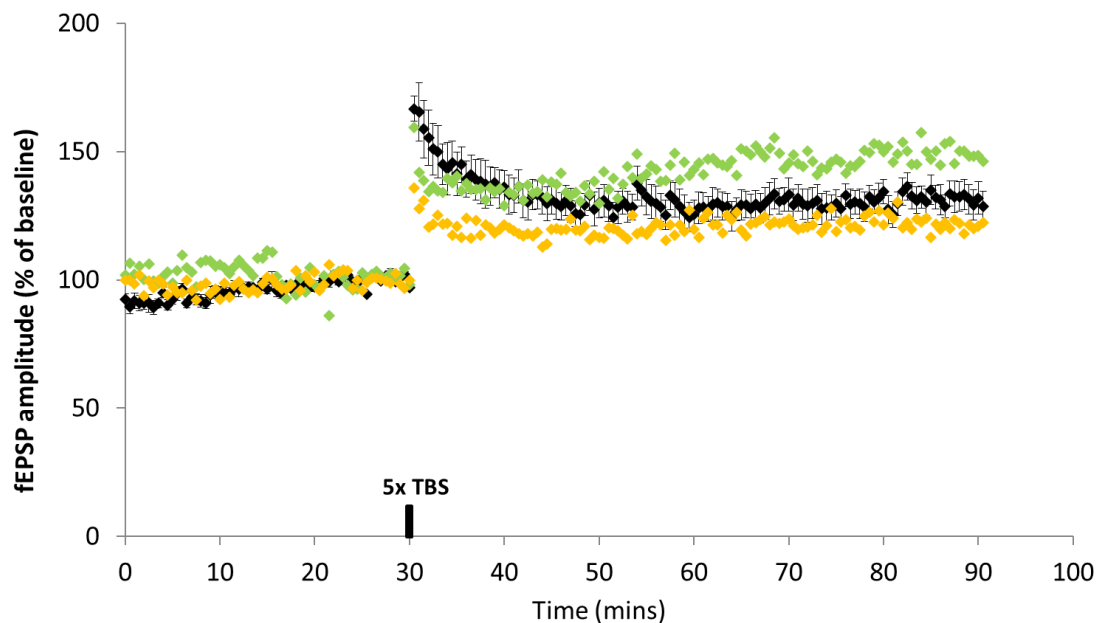


Figure 3.31. The effects of adenosine receptor antagonists on LTP in the CA1 area of the hippocampus in 2 mM glucose aCSF

Composite scatter plot representing mean normalised fEPSP amplitudes before and after 5xTBS induction in rat hippocampal slices pre-treated for 20 minutes with either vehicle or test compound. Data are expressed as a percentage of the average of fEPSP amplitudes recorded during the 10-minute period before the application of 5xTBS protocol. Following a 10-minute stable baseline recording period (no compound treatment), vehicle (black diamonds), 1 μ M DPCPX (green diamonds), or 50 nM KW-6002 (yellow diamonds) was applied for 20 minutes (black bar). Theta-burst (5xTBS; indicated by the bar on the timeline), induced LTP. N: vehicle = 6; DPCPX = 2; KW-6002 = 2

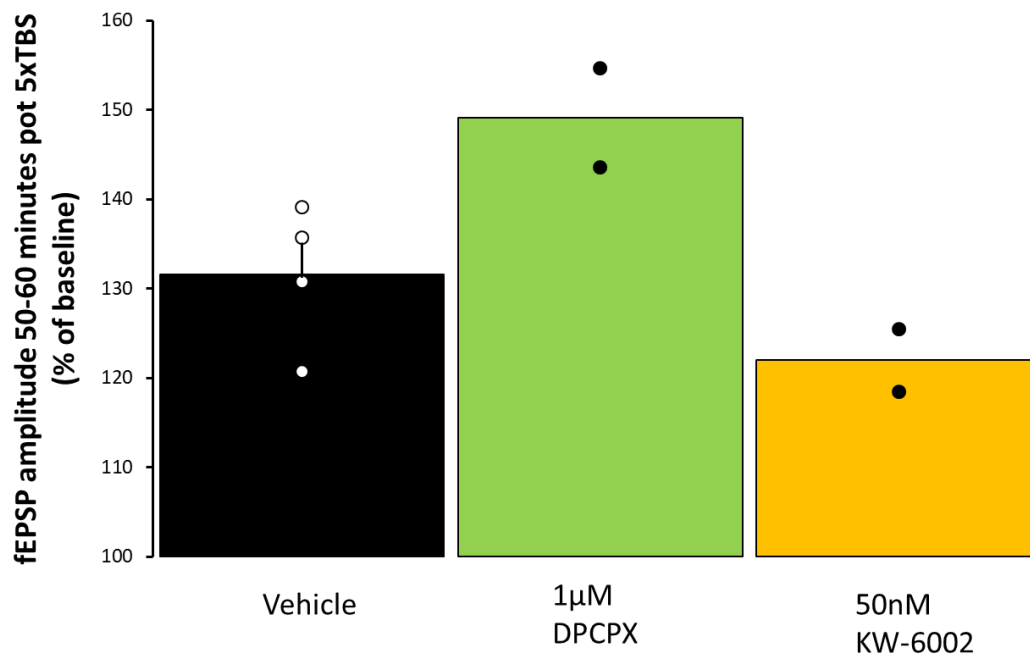


Figure 3.32. The effects of adenosine receptor antagonists (1 μ M DPCPX and 50 nM KW-6002) on LTP in the CA1 area of the hippocampus in experiments utilizing 2 mM glucose-containing aCSF

Bar chart summarizing the effects of different adenosine antagonists on LTP. The level of LTP was measured 50-60 minutes after 5xTBS induction paradigm from rat hippocampal slices treated with either vehicle, or adenosine receptor antagonists. The magnitude of LTP was measured as the average of the evoked fEPSPs recorded during the last 50-60 minutes expressed as a percentage of the average baseline fEPSP amplitude recorded in the 10-minute period immediately prior to induction of LTP. Application of 1 μ M DPCPX resulted in a significant change in fEPSP amplitude, compared to vehicle (N: vehicle = 4; DPCPX = 2; KW-6002 = 2).

Table 3.17. Mean fEPSP amplitudes measured 50-60 minutes after a 5xTBS stimulation in rat hippocampal slices prepared with aCSF containing 2 mM glucose and treated with vehicle or adenosine antagonist, (NS, non-significant).

Treatment	Mean	SEM	n	P vs Vehicle
Vehicle	131.6	4	4	
1 μ M DPCPX	149.1	5.5	2	NS
50 nM KW-6002	122	3.5	2	NS

3.15 Conclusions

In this project we have evaluated the effects of various D-glucose concentrations (10, 5 and 2mM) on 5xTBS-induced LTP, in the presence of either vehicle (0.1% DMSO) or a selection of adenosine receptor-targeting antagonists (the non-selective A₁, A_{2A}, A_{2B} and A₃ receptor antagonist CGS15943 (100 nM); the selective A₁ receptor antagonist DPCPX (1 μ M); the selective A_{2A} receptor antagonist KW-6002 (50 nM); the selective A_{2B} receptor antagonist PSB603 (100 nM); the selective A₃ receptor antagonist MRS1523 (300 nM)).

3.15.1 The effects of extracellular glucose on LTP in rat hippocampus

According to extensive research identifying the physiologically relevant range of glucose in the brain, the widely accepted use of aCSF containing 10 mM D-glucose for *in vitro* brain slice electrophysiology experiments is not entirely comparable to the conditions the brains are exposed to *in vivo*. Therefore, a reduction in D-glucose levels in aCSF solutions might provide a more physiologically relevant result. Our findings show that with lower D-glucose levels, the amplitude of LTP decrease as well. Although the reduction in LTP seen in experiments utilizing 2 or 5 mM D-glucose aCSF was not significant once compared to the LTP from the 10 mM experiments, more experiments are required to substantiate this, given the low n numbers recorded here for 2 mM glucose. Nevertheless, it can be concluded that increased concentration of extracellular glucose appears to enhance LTP. Although these results do not exactly correspond with the findings of Moriguchi *et al* (2011) who reported an up to a two-fold increase in LTP in the presence of 10 mM extracellular glucose, as opposed to LTP collected from experiments utilizing 3.5 mM extracellular glucose.

To elaborate upon the influence of extracellular glucose concentration on fEPSP amplitudes, some of the technical aspects utilized in these *in vitro* experiments, should be discussed. Specifically, the use of an interface chamber and brain slices. This type of experimental setup provides an almost unrestricted supply of glucose directly to the surface of the brain tissue, leading to a larger diffusion gradient between the surface of the slice and its interior, compared to brain *in vivo*. According to Tekkok *et al* (2002), this gradient can be modelled, giving an estimate of the interior glucose concentration within the brain slice. By adapting this equation (Figure 3.33., Tekkok *et al.*, 2002) to the experimental conditions of this study, the interior glucose concentration at a depth of 200 μm can be approximated for different ambient aCSF glucose concentrations: 10 mM glucose in aCSF decreases to 7.34 mM; 5 mM to 2.34 mM; and 2 mM aCSF glucose would amount to 0 mM, assuming that the rate

of glucose utilization remains constant. Although the depths of the stimulating and recording electrodes in most fEPSP experiments are usually a somewhat arbitrary measure, it appears that in cases where glucose concentration is of interest it might be of importance to consider the varying levels of glucose throughout the tissue.

$$A \quad [G]_e = [G]_s - \frac{(a/2D^*)(2x-l-x^2)}{l}$$

$$B \quad [G]_e = [G]_s - 0.19(9x-x^2)$$

Figure 3.33. The equation for determining the net flux of glucose for tissue slices at an air-aCSF interface experimental configuration

(A) and its simplified form for slice thickness of 450 μM (B).

Obtaining the steady-state extracellular concentration of glucose ($[G]_e$) at a given depth (x) requires the glucose concentration at the surface of the slice ($[G]_s$), the rate of glucose utilization (a), the effective diffusion quotient (D^*), and the slice thickness (l). The rate of glucose utilization has been estimated to be about $5 \text{ nmol g}^{-1} \text{ s}^{-1}$. The diffusion coefficient (D) of glucose in agar is $3.3 \times 10^{-6} \text{ cm}^2 \text{ s}^{-1}$ (Lund-Andersen and Kjeldsen, 1976); taking a value of 1.6 for the tortuosity factor (λ) (i.e., the relationship between effective resistance to macroscopic flow and the particular resistance of the medium encompassing the microscopic flow), leading to $D^* = D/\lambda^2 = 1.3 \times 10^{-6} \text{ cm}^2 \text{ s}^{-1}$ (adapted from Tekkok *et al.*, 2002).

Another factor to consider is the presence of mannitol in brain slice preparations using 5 mM and 2 mM D-glucose. Mannitol is commonly used in emergency medical cases involving traumatic brain injury as an osmotherapeutic agent where it exerts its neuroprotective effect via increasing the osmotic pressure in the CSF. *In vitro*, the use of mannitol is justified as additional neuroprotective support, especially when investigating ischemic

edema. However, mannitol itself has been shown to have an inhibitory effect upon fEPSP magnitude (Nakijama *et al.*, 2004). Therefore, the reduction in LTP seen in the presence of 5 and 2 mM D-glucose could be explained not only due to lack of glucose but also due to presence of mannitol, collectively impeding synaptic transmission.

Although *in vitro* slice electrophysiology has been considered a reliable investigatory technique for several decades, the present collective knowledge regarding glucose, its uses within the brain, the low ATP levels in brain slice preparations, and imperfect oxygenation of the brain tissue due to the removal of the BBB and further mechanical damage to both vascular supply and brain tissue due to slicing, has raised questions whether this laboratory method can offer a true explanation for the physiological events responsible for learning and memory (Capron *et al.*, 2006; Slanzi *et al.*, 2020). On the other hand, while the search for the perfect experimental technique continues, slice electrophysiology could represent a window into investigating brain injury.

3.15.2 Conclusions: Effects of the A₁ receptor antagonist DPCPX on LTP induced in CA1 in the presence of 10 and 2mM extracellular glucose

The application of the selective A₁ receptor antagonist DPCPX on the hippocampal slice preparation in the presence of 10mM extracellular D-glucose did not result in a significant change in LTP once compared with the vehicle, whereas some difference in the fEPSP amplitude was observed upon application of DPCPX in the presence of 2mM D-glucose. The latter result is somewhat anticipated since antagonism of the A₁R is known to increase neuronal activity, although it should be noted that based on n=2 it is not appropriate to draw a definite conclusion in favour of this observation. According to literature, application of DCPCX facilitates the induction of LTP as well as enhances its magnitude, at least in young adult rats (Costenla *et al.*,

2011). Since there is an influence of intracellular ATP on extracellular adenosine and neuronal excitability, i.e., in cases of sufficient intracellular ATP (Zur Nedden *et al.*, 2011, 2014; Hall & Frenguelli, 2018), reducing extracellular glucose induces release of adenosine and activation of adenosine A₁ receptors (Kawamura *et al.*, 2010).

In addition, it can be argued that lowering extracellular glucose levels mimics aspects of ketogenic diet *in vitro*, i.e., should normal or elevated intracellular levels of ATP be accompanied by a reduced extracellular glucose concentration, the pannexin-1 channels will open and release intracellular ATP into extracellular space. This ATP will rapidly undergo conversion into adenosine, subsequently activating the A₁Rs, leading to opening of K_{ATP} channels and eventually – hyperpolarization and reduced excitability (Kawamura *et al.*, 2010). This factor could explain the DPCPX-related increase in LTP seen in the presence of 2 mM but not 10 mM D-glucose aCSF.

3.15.3 Effects of the A_{2A} receptor antagonist KW-6002 on LTP induced in CA1 in the presence of 10, 5 and 2 mM extracellular glucose

In 2019, the selective A_{2A} receptor antagonist KW-6002, or Istradefylline (Nourianz) was approved by the FDA as an add-on therapy to levodopa/carbidopa treatment in adults with Parkinson's disease. The success of this compound highlights the significance of A_{2A} antagonism via the amelioration of motor response, accompanied by the rescue of dopamine and its metabolites, and glutamate, and GABA levels in the striatum, resulting in the observed beneficial outcomes for cognition (Uchida *et al.*, 2014).

Furthermore, the involvement of the A_{2A} adenosine receptor in LTP facilitation has been well established. As follows, the use of A_{2A}R antagonists result in a decrease in LTP and therefore suggesting an excitatory role of A_{2A}Rs, a phenomenon that becomes exacerbated as animals age (de Mendoca

& Ribeiro, 1994; Costenla *et al.*, 2011). In addition, in the hippocampus the A_{2A} receptors are necessary for the LTP facilitation by BDNF (Fontinha *et al.*, 2008). This piece of evidence is particularly interesting due to the important role BDNF plays in the formation of E-LTP (Korte *et al.*, 1995; Patterson *et al.*, 1996).

However, no significant differences in the fEPSP amplitudes were observed upon the application of KW-6002 to the hippocampal slices, accompanied by TBS stimulation. However, it is worthy of note that in experiments outlined here E-LTP appeared reduced although it was not systematically analysed. Also, in the presence of 2 mM D-Glucose the change in fEPSP amplitude was somewhat lower than those seen in experiments accompanied by 10 and 5 mM D-Glucose aCSF, a similar pattern was collectively produced the 10, 5 and 2 mM D-glucose vehicle control experiments. Therefore, it could be argued that as in the case with the vehicle experiments, even in the presence of KW-6002, low levels of extracellular glucose contributed towards the overall electrophysiological output of the hippocampal circuit in question.

On the other hand, application of KW-6002 in the presence of both 5 and 2 mM, showed a reduction in post-tetanic potentiation (PTP), a change in synaptic plasticity that previously has been observed at hippocampal mossy fiber synapses, in the presence of A₁ receptor antagonist DPCPX (Kimberly *et al.*, 2003). While the involvement of the A₁R cannot be entirely excluded under these experimental conditions, due to the established A₁ – A_{2A} receptor interactions, it is also plausible that the glial cell ability to release ATP is another contributing factor. For example, a lower level of ATP release would lead to a lower concentration of adenosine in the synaptic cleft and a subsequent activation of A₁Rs, resulting in a lower PTP.

3.15.4 Effects of the A_{2B} receptor antagonist PSB603 on LTP induced in CA1 in the presence of 10 mM extracellular glucose

Determining the definite role of the A_{2B} receptor in the context of hippocampal LTP and metabolism remains elusive, primarily due to the low presence of this receptor in the brain, compared to the A₁R or A_{2A}R. Nevertheless, increasing evidence points towards the necessity of the A_{2B}R under certain pathological states. For example, its low binding affinity to adenosine suggests that A_{2B}R is activated when adenosine levels are higher than normal due to inflammation, trauma, ischemia or hypoxia (Fredholm *et al.*, 2001).

It has been shown that A_{2B} receptors control astrocytic and neuronal glycogen metabolism, and glucose utilization in hippocampal slices (Magistretti *et al.*, 1986; Allaman *et al.*, 2003; Lemos *et al.*, 2013). In addition, previous oxygen-glucose deprivation (OGD) research shows that just like in controls, pre-treatment with A_{2B} receptor antagonists to CA1 pyramidal neurons does not result in morphological changes, nor increased apoptosis or activated mTOR levels (Fusco *et al.*, 2018). Therefore, the A_{2B} receptor can be considered as having a protective function within the CA1 of the hippocampus, especially in cases of acute ischemic/hypoxic damage. In conclusion, since our data of PSB603 application do not show any significant deviations from the vehicle data, the experimental conditions involving 10 mM D-glucose were optimal for this context.

3.15.5 Effects of the A₃ receptor antagonist MRS1523 on LTP induced in CA1 in the presence of 10 mM extracellular glucose

Understanding the function of the A₃ receptor in the CNS remains a challenge due to its relatively limited presence in tissue and reduced affinity for adenosine ($K_i = 1 \mu\text{M}$), compared to adenosine receptors A₁ ($K_i = 10 \text{ nM}$) and A_{2A} ($K_i = 0.5 \text{ nM}$). However, considering that baseline adenosine levels can increase dramatically not only under pathological stresses, such as injury, hypoxia or ischemia, but can also rise transiently during synaptic plasticity, it is possible that the A₃ adenosine receptor contributes towards modulation of LTP.

The selective A₃ receptor antagonist MRS1523 has been reported to reduce the effects of ischemic injury *in vitro*. Although the exact role of A₃ receptor antagonists in synaptic activity under hypoxia/ischemia remains conflicting, the existing data suggests that the protective or disruptive outcomes of A₃R activation may depend on the cell type involved, as well as the duration of activation. For example, the application of MRS1523 to an *in vitro* brain slice preparation, before and during a severe oxygen-glucose deprivation (OGD) protocol stimulates a recovery of neurotransmission, whereas application of this antagonist before a brief OGD results in a reduction of the OGD-induced depression of fEPSPs in the CA1 of the hippocampus (Pugliese *et al.*, 2007).

Since it is universally recognized that cerebral stroke and other ischemic insults are likely consequences of chronic and progressive inflammation, which in turn are likely accompanying features of T2D, metabolic syndrome and AD, exploring all possible options for preventing the detrimental effects of cerebral ischemic injury are required (Lindsberg & Grau, 2003).

3.15.6 Effects of the non-selective adenosine receptor antagonist CGS15943 on LTP induced in CA1 in the presence of 10 and 5 mM extracellular glucose

CGS15943 is a compound which in the brain acts as a potent A₁ and A_{2A} receptor antagonist, and its effects on animal behaviour in experimental settings are often compared to those of caffeine (Holtzman, 1991; Weerts & Griffiths, 2003). Evidence suggests that in both humans and animals, chronic consumption of caffeine has been associated with prevention of memory dysfunction, age-related cognitive impairment, and even reduced incidence of Alzheimer's disease (Takahashi *et al.*, 2008; Ritchie *et al.*, 2007; Maia & de Mendonça, 2002; Eskelinen *et al.*, 2009).

Given the significance of LTP as a possible neurophysiological correlate of learning and memory, the use of caffeine would be expected to result in facilitation of LTP. However, this is not the case, since application of caffeine, accompanied by high-frequency stimulation to the Schaffer collaterals, results in a reduction in LTP recorded from the CA1 fibers of the hippocampus (Costenla *et al.*, 2010; Lopes *et al.*, 2019). Similarly, the effect of CGS15943 upon the magnitude of LTP is not facilitatory, regardless of whether the experiment was carried out in the presence of 10 or 5 mM D-glucose.

Therefore, it is of importance to draw attention to the commonly drawn parallels between the increase in LTP magnitude and memory performance. It is also possible that adenosine and its receptors contribute to the formation of learning and memory outside the hippocampus.

3.16 Future Experiments

One of the biggest drawbacks of the current study was the relative low n numbers associated with many aspects of the study, in particular the experiments with low levels of glucose. Future studies will need to address this, the current unusual situation globally preventing completion of the experiments here. In addition, we must draw attention to the challenge that presents itself upon utilizing low glucose-containing aCSF solutions, as in these cases it is less frequent to detect adequate fEPSPs, resulting in the low n counts in our experiments of 5 and 2 mM glucose aCSF. This effect becomes even more apparent if an experiment is started using 10 mM glucose aCSF which is then swapped with an aCSF containing 2 mM of glucose, i.e., more often than not, the fEPSP will diminish over the course of the experiment.

Interestingly, experiments outlined here failed to replicate similar experiments previously undertaken in this lab that showed even narrow changes in extracellular glucose between 2 and 5 mM markedly affecting LTP whereas 10 mM glucose produced lower LTP than 5 mM. It is unclear at present why this was the case. Further work would be required to clarify this as few recordings were made here at lower concentrations of extracellular glucose where our previous studies had suggested the system was most sensitive. In addition, experiments should be repeated looking at the effects of extracellular glucose and adenosine receptor antagonists on basal extracellular field potentials to determine the role of ambient glucose levels and tonic adenosine drive on low frequency synaptic transmission. It would also be beneficial to perform more control experiments before continuing with adenosine receptor antagonists.

In conclusion data presented here suggest little or no effect of extracellular glucose on LTP and offer little support to the notion that ambient extracellular glucose levels impact LTP via a glial-adenosine-dependent mechanism as is observed in hypothalamus.

Chapter 4: An electrophysiological evaluation of novel, $\alpha 7$ nAChR-targeting compounds

4.1 Introduction

Decades worth of research into the vast landscape of disorders associated with cognitive deficits and decline, has yielded a surprisingly limited number of effective and reliable treatments. At present, the approved compounds for Alzheimer's disease management include cholinesterase inhibitors, e.g., donepezil, rivastigmine, and galantamine, and the NMDA glutamatergic receptor blocker memantine, all of which have modest efficacy upon the cognitive impairment seen in AD. Similarly, most drugs used to treat schizophrenia block the dopamine D2 receptor, alleviating symptoms such as delusions and hallucinations, yet failing to improve the deficits in cognitive processes which also involve dopamine-related activity (Casey *et al.*, 2010; Szeto & Lewis, 2016; Patel *et al.*, 2014).

Although most of the reported positive effects of these drugs have been moderate in magnitude overall and are highly unpredictable in terms of outcome across individuals, they have had an enormous impact, generating interest in the concept of cognitive enhancement not only for patients with brain disorders, but also for healthy persons. Nevertheless, the use of substances that enhance components of the memory and learning brain circuits, e.g., dopamine, glutamate, and norepinephrine, and therefore stand to elevate brain function in healthy individuals beyond their baseline functioning remains controversial (Sahakian *et al.*, 2015).

4.2 $\alpha 7$ nACh - the target of interest

Stimulation of alpha 7 nicotinic receptors ($\alpha 7$ nAChRs) elevates cholinergic neurotransmission and the release of glutamate and dopamine, therefore improving cognitive functions in both humans and rodents (Lewis *et al.*, 2017; Potasiewicz *et al.*, 2017; Lendvai *et al.*, 2013; Yang *et al.*, 2017).

Mounting evidence suggests that the $\alpha 7$ nicotinic acetylcholine receptor (nAChR) may play a substantial role in cognitive performance. In the central nervous system (CNS), the $\alpha 7$ nAChRs are highly expressed in hippocampus, cerebral cortex, and thalamus, brain regions involved in cognitive function, and activation of $\alpha 7$ nAChR has been shown to modulate synaptic function and influence the release of a range of neurotransmitters, e.g., glutamate, γ -aminobutyric acid (GABA), ACh, norepinephrine, and dopamine (Livingstone *et al.*, 2009; Huang *et al.*, 2014; Koranda *et al.*, 2014). Preclinical studies in multiple species have shown that boosting $\alpha 7$ nAChR activity improves cognitive deficits in episodic memory (Sahdeo *et al.*, 2014; Weed *et al.*, 2017), working memory (Ng *et al.*, 2007; Castner *et al.*, 2011), as well as attention (Pichat *et al.*, 2007; Rezvani *et al.*, 2009), whereas blocking or genetically deleting the $\alpha 7$ nAChR is associated with impaired cognitive performance (Keller *et al.*, 2005; Young *et al.*, 2007). Furthermore, the expression level of $\alpha 7$ nAChR can be affected by several pathologic conditions, including Alzheimer's disease (AD) and schizophrenia (Freedman *et al.*, 1995; Guan *et al.*, 2000; Wevers *et al.*, 2000; Kadir *et al.*, 2006). Information provided by human genetic studies indicates that both large deletions to the region of 15q13.3 in chromosome 15 and smaller deletions to the gene for the $\alpha 7$ nAChR, *CHRNA7*, frequently produce cognitive impairments (Sharp *et al.*, 2008; Le Pichon *et al.*, 2013). In addition, an unusually high affinity interaction exists between A β and $\alpha 7$ nAChRs, indicating towards a role in the pathophysiology of Alzheimer's disease and therefore fortifying the likely significance of this nicotinic receptor even further (Wang *et al.*, 2000).

As a result, the $\alpha 7$ nAChR has attracted a substantial amount of attention as a target for cognitive deficits seen in Alzheimer's disease and schizophrenia. And taken together, based on receptor localization, genetics implicating its involvement in cognitive disturbances, promising preclinical findings, and encouraging, if somewhat mixed, clinical data involving $\alpha 7$ nACh orthosteric agonists has emerged.

4.2.1 $\alpha 7$ nAChR agonists

At present, most of the developed $\alpha 7$ nAChR modulators are partial agonists, rather than full agonists. Unlike full agonists, such as endogenous acetylcholine (ACh), partial agonists are orthosteric ligands which, upon binding to the receptor, can only elicit a submaximal response, even at concentrations where all available receptors are occupied (Lape *et al.*, 2008).

For example, encenicline (EVP-6124) is a selective $\alpha 7$ nAChR partial agonist developed by Bayer Healthcare and in 2004 licensed to Envivo Pharmaceuticals, which in 2014 became FORUM Pharmaceuticals Inc. The rationale underlying the development of EVP-6124 was to boost cholinergic transmission and thus cognitive enhancement by taking advantage of selective $\alpha 7$ nAChR agonism without causing side-effects associated with overactivation of other nicotinic receptors, such as $\alpha 4\beta 2$ or muscarinic AChRs. For example, an advantage for targeting $\alpha 7$ nAChRs lies in the evidence that unlike the $\beta 2$ nAChRs, they do not appear to be involved in activation of behavioural reward pathways and, hence, may not be associated with development of addiction.

The lack of cognitive benefits for individuals suffering from schizophrenia or AD, can be explained by a number of limitations associated with medication including a lack of target selectivity leading to dose-limiting side-effects. In addition, sustained exposure to an agonist can result in desensitization and loss of function. Another shortcoming associated with orthosteric approaches for targeting $\alpha 7$ nAChRs is an inverted U-shape dose-

response curve which may impede the efficacy of an $\alpha 7$ agonist to a very specific and narrow range of drug exposure (Deardorff *et al.*, 2015).

4.2.2 $\alpha 7$ nAChR positive allosteric modulators (PAMs)

To overcome the limitations of the endogenous ACh site-binding orthosteric agonists, alternative ways of influencing the $\alpha 7$ nAChR activity have been proposed. Positive allosteric modulators (PAMs) of the $\alpha 7$ nAChR bind to a unique binding site on the receptor and potentiate the actions of the endogenous ligand ACh, and thus may pose an improved clinical profile, compared to orthosteric $\alpha 7$ agonists. PAMs show enhanced selectivity over related Cys-loop superfamily of ligand-gated ion channels via binding to a non-conserved region of the $\alpha 7$ nAChR (Dinklo *et al.*, 2011; Williams *et al.*, 2011). In addition, PAMs do not appear to promote receptor desensitization, unlike $\alpha 7$ agonists, desensitization in this case referring to the rapid inactivation of the receptor in the presence of ligand rather than loss of the response to repeated applications. Hence, $\alpha 7$ PAMs may provide efficacy over a wider range of concentrations and sustain efficacy upon repeated dosing events. Various structurally diverse $\alpha 7$ PAMs have been identified, and according to their impact upon receptor desensitization kinetics, at least two distinct types of PAMs have been defined. Type I PAMs, such as BNC375, potentiate the agonist-induced peak current without affecting the desensitization kinetics. Type II PAMs, affect not only the peak current but also delay receptor desensitization (Bertrand *et al.*, 2015).

The aim of the work described here was to test the effects of three nicotinic $\alpha 7$ ligands on long-term potentiation (LTP) of synaptic transmission in the hippocampus *in vitro* to determine the utility of these ligands as potential enhancers of learning and memory. The ligands investigated were:

- a novel $\alpha 7$ nAChR ligand (L-436, MERCK).
- partial agonist (EVP-614, Forum Pharmaceuticals).
- PAM (BNC375, MERCK).

4.3 Results: The Effects of Encenicline (EVP-614) on LTP in the hippocampus *in vitro*

Extracellular recordings of field excitatory postsynaptic potentials (fEPSPs) were recorded in the CA1 region of septo-hippocampal brain sections, obtained from Sprague-Dawley rats (6-8 weeks, 120-250 g), in response to electrical stimulation of the Schaffer collateral pathway. A 10-minute baseline was recorded, followed by a 20-minute application of EVP-6124, or vehicle (aCSF + 0.1% DMSO), applied 15 minutes before and washed 5 minutes after the induction of LTP. Experiments with unstable baselines were abandoned. Five concentrations of EVP-6124 were tested: 1 nM, 1.78 nM, 3.16 nM, 5.62 nM, 10 nM. This narrow concentration range was chosen based on previous studies carried out by this lab with Envivo and subsequently Forum Pharmaceuticals. The range of concentrations used here was based on the fact that the concentration response curve is U-shaped and 1 to 10 nM is within the range where peak effects were observed (Neurosolutions, unpublished observations). LTP in the hippocampal CA1 region was measured as an increase in the amplitude of the fEPSP relative to controls, in adult male rat septo-hippocampal slices induced by a 10xTBS of the Schaffer collaterals linking CA3 to CA1.

LTP in CA1 induced in response to TBS, in the presence of 0.1% DMSO (vehicle control) amounted to a 123.58 ± 4.72 % (mean \pm SEM) increase in the fEPSP compared to pre-TBS baseline levels), measured by analyzing the data gathered at the last 10 minutes of the recording following LTP induction, when said trace is the most stable ($n = 10$). LTP induced in the presence of EVP-6124 at a concentration of 1 nM was associated with an increase in the fEPSP to 122.37 ± 3.27 % (mean \pm SEM) of pre-TBS levels. This effect was not significantly different to that observed in the vehicle control group ($n = 10$; $p > 0.05$; Dunnett's post-hoc test; see Fig. 4.1.). EVP-6124 at a concentration of 1.78 nM was associated with an increase in the fEPSP to 124.56 ± 2.51 % (mean \pm SEM) of control values, again an effect that was not significantly different to LTP induced in the vehicle control group ($n = 9$; $p > 0.05$; Dunnett's post-hoc test; see Fig. 4.2.). LTP induced in the presence of 3.16 nM EVP6124 amounted to an increase in fEPSP to $133.40 + 4.20$ % (mean \pm SEM) of baseline levels. As previously, this rise in fEPSP was not significantly different to that recorded from the vehicle experiments ($n = 10$; $p > 0.05$; Dunnett's post-hoc test; see Fig. 4.3.).

Subsequent utilization of 5.62 nM of EVP-6124 resulted in an increase in fEPSP to 139.76 ± 2.04 % (mean \pm SEM). LTP induced by this concentration of EVP-6124 was significantly enhanced compared to control experiments alone ($n = 11$; $p < 0.01$; Dunnett's post-hoc test; see Fig. 4.4.). Similarly, a significant increase of 144.84 ± 3.51 % (mean \pm SEM) in fEPSP amplitudes was observed in response to 10 nM EVP-6124 ($n = 10$; $p < 0.01$; Dunnett's post-hoc test; see Fig. 4.5.). In summary, the experiments described here show that EVP-6124 enhanced LTP in the hippocampal CA1 region in a concentration-dependent manner (Figs. 4.5.; 4.6.; 4.7.).

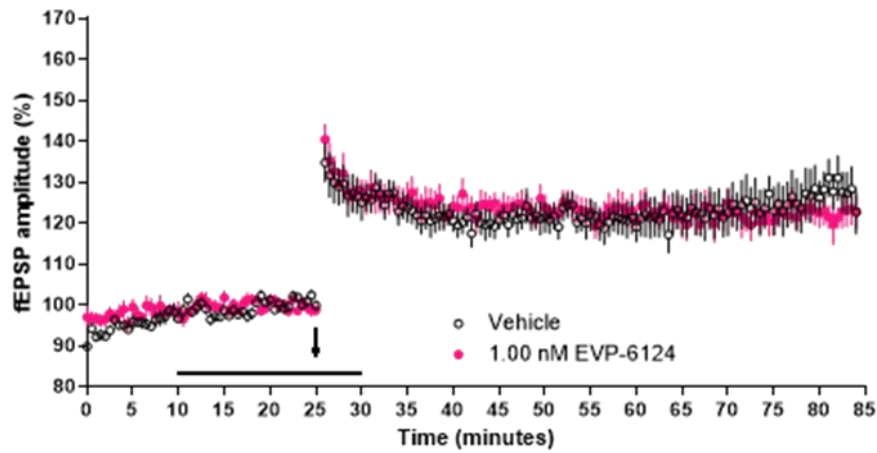


Figure 4.1. The effect of 1 nM EVP-6124 on LTP in the CA1 region of the hippocampus

Time-course plot showing the effect of EVP-6124 on LTP of fEPSPs. Data are expressed as a percentage of the average of fEPSP amplitudes recorded during the 10-minute baseline period immediately before delivery of TBS. Following a 10-minute stable baseline recording period (no compound treatment), vehicle (open circles) or 1.00 nM EVP-6124 (pink circles) was applied for 20 minutes (solid bar). Theta-burst stimulation (10xTBS; indicated by the arrow), induced LTP. Note EVP-6124 at a concentration of 1 nM had little effect on LTP compared to vehicle control. Error bars represent standard error of the mean (SEM). N = 10 for both the vehicle and 1.00 nM EVP-6124 groups.

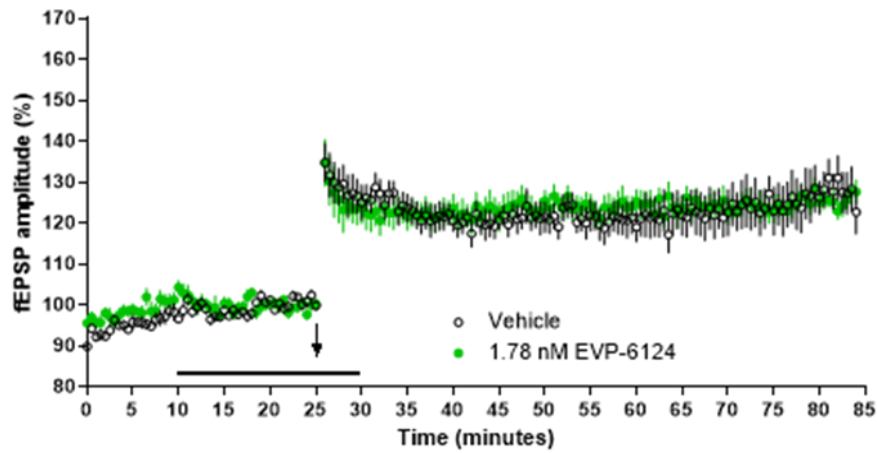
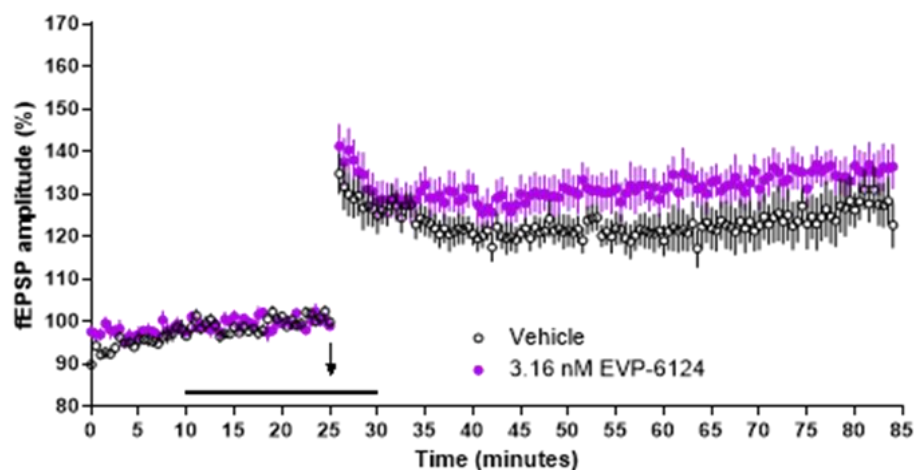


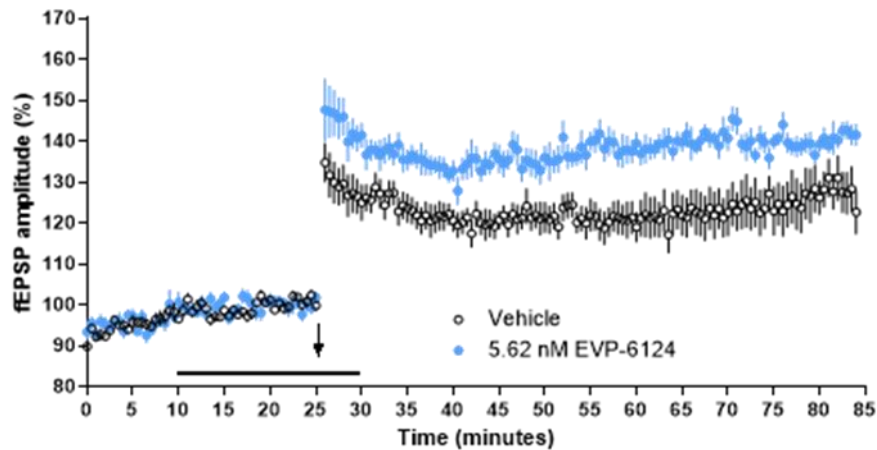
Figure 4.2. The effect of 1.78 nM EVP-6124 on LTP in the CA1 region of the hippocampus.

A combined scatterplot showing the effect of EVP-6124 on LTP of fEPSPs. Average evoked field excitatory postsynaptic potentials (fEPSPs) recorded from septo-hippocampal slices. Data are shown as a percentage increase in the responses for average fEPSP amplitude recorded during the 10-minute period immediately before TBS induction of LTP for each slice. Following a 10-minute baseline period, vehicle (control; open circles) or 1.78 nM EVP-6124 (green circles) was applied for 20 minutes (solid bar). Application of theta-burst stimulation (10xTBS; arrow) induced stable long-term potentiation (LTP). EVP-6124 at 1.78 nM had no effect on LTP relative to the control. Error bars are standard error of the mean (SEM). N (vehicle = 10; 1.78 nM EVP-6124 = 9).



4.3. The Effect of 3.16 nM EVP-6124 on LTP in the CA1 region of the hippocampus

Average evoked field excitatory postsynaptic potentials (fEPSPs) recorded from septo-hippocampal slices. Data are presented as a percent of the responses for average fEPSP amplitude recorded during the 10-minute period immediately before TBS induction of LTP for each slice. Following a 10-minute baseline period, vehicle (open circles) or 3.16 nM EVP-6124 (purple circles) was applied for 20 minutes (solid bar). Theta-burst stimulation (10xTBS; arrow) evoked stable long-term potentiation (LTP). At the concentration of 3.16 nM, EVP-6124 marginally increased LTP relative to control. Error bars are standard error of the mean (SEM). N =10 for both vehicle and 3.16 nM EVP-6124 groups.



4.4. The Effect of 5.62 nM EVP-6124 on LTP in the CA1 region of the hippocampus

Time-course plot showing the effect of EVP-6124 on LTP of fEPSPs. Data is shown as a percent of the responses for average fEPSP amplitude recorded during the 10-minute period immediately before TBS induction of LTP for each slice. Following a 10-minute baseline period (no compound treatment), vehicle (open circles) or 5.62 nM EVP-6124 (blue circles) was applied to the slice for 20 minutes (solid bar). Theta-burst stimulation (TBS; arrow) of the afferent fibers evoked stable long-term potentiation (LTP). At the concentration of 5.62 nM, EVP-6124 significantly increased LTP relative to vehicle. Error bars are standard error of the mean (SEM). N (vehicle) = 10; (5.62 nM EVP-6124) = 11.

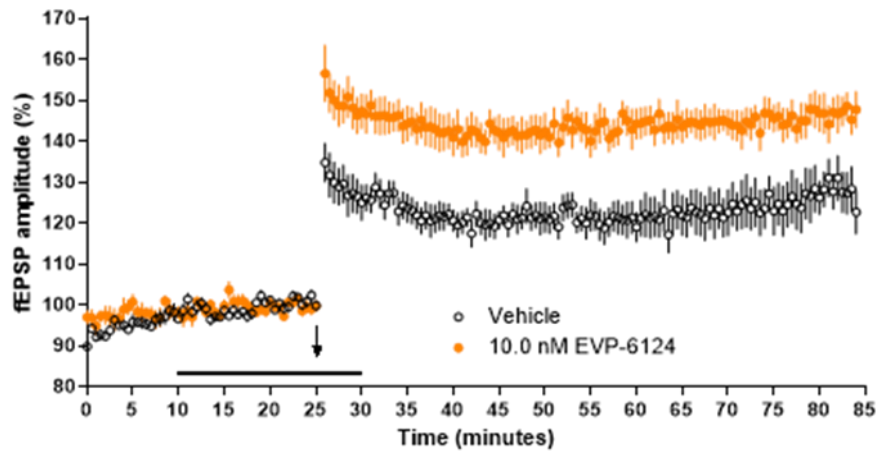


Figure 4.5. The Effect of 10 nM EVP-6124 on LTP in the CA1 region of the hippocampus

Scatterplot showing the effect of EVP-6124 on LTP of fEPSPs. Data are expressed as a percentage of the responses for average fEPSP amplitude recorded during the 10-minute period immediately before TBS induction of LTP for each slice. Following a 10-minute baseline period (no compound treatment), vehicle (open circles) or 10.0 nM EVP-6124 (orange circles) was infused for 20 minutes (solid bar). Theta-burst stimulation (TBS; arrow) of the Schaffer collaterals evoked stable long-term potentiation (LTP). Note the enhanced effect of 10 nM EVP-6124 upon LTP relative to vehicle. Error bars are standard error of the mean (SEM). N = 10 for both vehicle and 10.0 nM EVP-6124 groups.

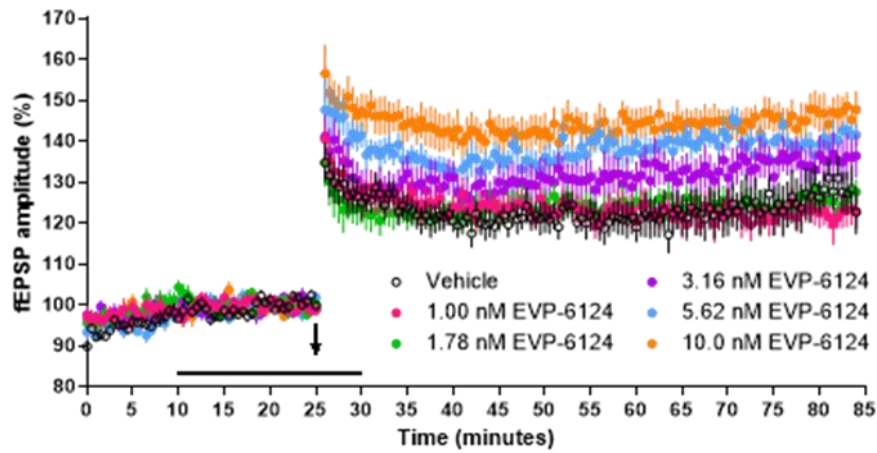


Figure 4.6. The effects of increasing concentrations of EVP-6124 on LTP in the CA1 region of the hippocampus

Composite scatterplot of the experimental data, which are expressed as a percentage of the average of fEPSP amplitudes recorded during the 10-minute period immediately before delivery of TBS. Following a 10-minute baseline period (no compound treatment), vehicle or EVP-6124 at the concentrations indicated was bath applied for 20 minutes (solid bar). Theta-burst stimulation (TBS; arrow) of the afferent fibers evoked stable long-term potentiation (LTP). EVP-6124 enhanced LTP relative to vehicle in a concentration-dependent manner. Error bars are standard error of the mean (SEM). N: 9-11 per group.

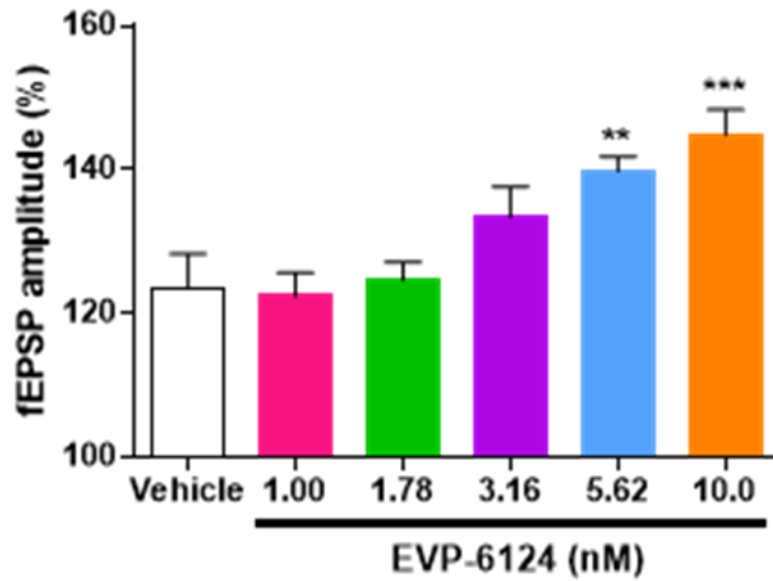


Figure 4.7. EVP-6124 induced a concentration-dependent enhancement of LTP in the CA1 region of the hippocampus

Histograms summarizing the effects of increasing concentrations of EVP-6124 on LTP. The magnitude of LTP was measured as the average of the evoked fEPSPs recorded during the last 10 minutes of a 60 minute period expressed as a percentage of the average baseline fEPSP amplitude recorded in the 10-minute period immediately prior to induction of LTP (mean \pm SEM; $n = 9-11$ per group). Note the concentration-dependent enhancement of LTP with EVP-6124, the effect reaching statistical significance at 5.62 and 10 nM (** $p < 0.01$; *** $p < 0.001$, respectively; Dunnett's post-hoc test, comparing each EVP-6124 treatment group with the vehicle group).

4.4. Results: The Effects of BNC375 and L-436 on LTP in the hippocampus *in vitro*

In the following set of “blinded” experiments, the effects of a known positive allosteric modulator (PAM), BNC375, at a concentration of 10 μ M, were compared with two concentrations (10 and 30 μ M) of a novel Merck α 7 nAChR-targeting compound (L-436), on long term potentiation (LTP) in hippocampal brain slices. These experiments were performed with two different genotypes of mice – wild type (WT) and α 7 nAChR KO (Acr α 7-), both supplied by MERCK, to confirm activity of these compounds at α 7 nAChR.

4.4.1 The effects of α 7 nAChR-targeting compounds in the hippocampi of WT mice

In WT mice, LTP in CA1 induced in response to 10xTBS, in the presence of 0.1% DMSO (vehicle control), amounted to a 117.1 ± 4.0 % (mean \pm SEM) increase in the fEPSP compared to pre-TBS baseline levels, measured at the last 10 minute period (50 to 60mins) minutes following LTP induction (n = 8). In the presence of the α 7 nAChR -targeting compound L-436, at a concentration of 10 μ M, yielded LTP magnitude of 109.5 ± 2.1 % (mean \pm SEM), (n = 6) compared to parallel vehicle control experiments in wild type mice. This change in fEPSP amplitude was not significant.

On the other hand, application of 30 μ M of L-436 led to a marked increase in fEPSP magnitude to 134.1 ± 6.6 % (mean \pm SEM) and the induced LTP at this concentration was significantly enhanced compared to control experiments alone (n = 6; $p < 0.05$; Unpaired Student’s t-test; see Figs. 4.8., 4.9. and Table 4.1.). Likewise, the α 7 nAChR positive allosteric modulator, BNC375 at a concentration of 10 μ M, significantly increased the magnitude of

LTP to 145.0 ± 6.4 %, compared to parallel vehicle control experiments ($n = 6$; $p < 0.01$; Unpaired Student's t-test; see Figs. 4.8., 4.9. and Table 4.1).

4.4.2 The effects of $\alpha 7$ nAChR-targeting compounds in the hippocampi of $\text{Ac}\alpha 7$ - mice

Following treatment with vehicle, the fEPSP amplitude recorded 60 minutes after theta burst stimulation was $129.1 \pm 2.3\%$ of baseline ($n = 10$) in $\text{Ac}\alpha 7$ - mice. It is important to note that these experiments were blinded and no obvious differences between the KO and WT animals were apparent, i.e., there was no difficulty in finding and recording of fEPSPs, nor there was an apparent difference in the stability of the recordings. Treatment with $10 \mu\text{M}$ or $30 \mu\text{M}$ L-436 had no effect on the level of LTP recorded 60 minutes after TBS with mean fEPSP amplitude amounting to $125.5 \pm 2.8\%$ and $125.9 \pm 1.9\%$, respectively of baseline ($n = 7, 9$, *NS*, Student's unpaired t-test, Figures 4.10. and 4.11., Table 4.2.).

Data were plotted normalised to the mean fEPSP amplitude 50-60 mins post TBS of the time-matched vehicle control recordings for each mouse genotype to compare the effects of the compound between genotypes. The magnitude of LTP normalised in this manner amounted to $93.5 \pm 1.8\%$ and 97.2 ± 2.1 % in the presence of $10 \mu\text{M}$ L-436 in WT and $\text{Ac}\alpha 7$ - mice, respectively, hence no significant effect on either genotype. However, the magnitude of LTP in $30 \mu\text{M}$ L-436 amounted to $114.5 \pm 5.7\%$ in WT and $97.5 \pm 1.5\%$ in $\text{Ac}\alpha 7$ - mice, LTP being significantly enhanced in WT but without effect in the KO mice. These data suggest $\alpha 7$ nAChR are a pre-requisite for the action of this compound on LTP. The effects of $10 \mu\text{M}$ L-436 in the $\text{Ac}\alpha 7$ - group was significantly different to the $30 \mu\text{M}$ L-436 WT group, as was the $30 \mu\text{M}$ L-436 – induced effects between both mouse genotypes (** $P < 0.01$, One-way ANOVA with Bonferroni's multiple comparisons test; See Figure 4.12. and Table 4.3.).

4.4.3 The effects of $\alpha 7$ nAChR-targeting compounds in the hippocampi of SD rats

To further clarify and confirm activity of L-436 at $\alpha 7$ nAChR, we undertook additional pharmacological studies in rats utilizing a selective $\alpha 7$ nAChR antagonist, MLA (200 nM). This series of experiments were performed on rat hippocampal brain slices obtained from male SD rats 6-9 weeks old. A 10-minute baseline was recorded, followed by a 20-minute application of vehicle (aCSF + 0.1%DMSO), 0.3, 3 or 10 μ M of L-436. The effect of the antagonist MLA was tested on 10 μ M L-436-induced responses. The compound perfusion started 15 minutes before and ended 5 minutes after the induction of LTP.

Following treatment with vehicle, the fEPSP amplitude recorded after theta burst stimulation was $124.5 \pm 2.6\%$ of baseline ($n = 14$). Treatment with 0.3 μ M L-436 had no effect on the level of LTP recorded 60 minutes after TBS with mean fEPSP amplitude amounting to $128.3 \pm 5.6\%$ of baseline ($n = 6$). Perfusion with 3 μ M L-436 however significantly increased the level of LTP recorded after TBS with mean fEPSP amplitude amounting to $136.3 \pm 5.6\%$ of baseline ($n = 6$, $P < 0.05$, Student's unpaired t-test). Treatment with 10 μ M L-436 also significantly increased the level of LTP recorded 60 minutes after TBS with mean fEPSP amplitude amounting to $149.7 \pm 4.8\%$ of baseline ($n = 9$, $P < 0.01$, Student's unpaired t-test, Figures 4.13., Table 4.4.). Treatment with 200 nM MLA alone had no effect on the level of LTP, with mean fEPSP amplitude amounting to $125.8 \pm 2.7\%$ of baseline ($n = 7$) (Figure 4.14). When MLA was co-administered with 10 μ M L-436 the level of LTP recorded 60 minutes after TBS was not-significantly different from that of the vehicle control with mean fEPSP amplitude amounting to $129.8 \pm 2.8\%$ of baseline ($n = 5$, Figures 4.15. and 4.16., Table 4.4). However, the level of LTP was significantly lower than that observed upon treatment with 10 μ M L-436 $149.7 \pm 4.8\%$ ($n = 9$, $P < 0.05$, Student's unpaired t-test, Figures 4.15. and 4.16., Table 4.4).

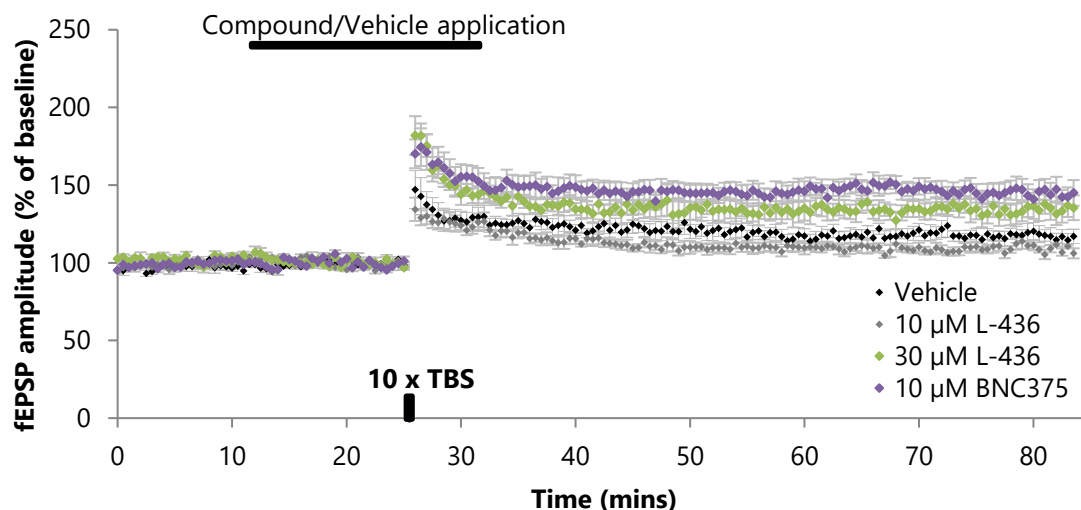


Figure 4.8. The effects of compounds L-436 and BNC375 on LTP in the CA1 region of the hippocampus of WT mice.

Composite scatter plot showing the effects of increasing concentrations (10 and 30 μ M) of L-436 and 10 μ M of BNC375 on LTP of fEPSPs. Data is shown as a percentage of the response for average fEPSP amplitude recorded during the 10-minute period immediately before 10xTBS induction of LTP for each slice. A baseline period (no compound application) of 10 minutes was followed by a 20-minute period of application (solid bar) of either vehicle (black diamonds), 10 μ M L-436 (grey diamonds), 30 μ M L-436 (green diamonds), or 10 μ M BNC375 (purple diamonds) mean normalised fEPSP amplitudes before and after 10xTBS in hippocampal slices prepared from wild type mice. Theta-burst stimulation (10xTBS; black bar) of the Schaffer collaterals evoked stable long-term potentiation (LTP). At the concentration of 30 μ M, L-436 increased LTP relative to vehicle, as did 10 μ M BNC375. Error bars are standard error of the mean (SEM). N = 8;6 for vehicle and for all the compound groups, respectively.

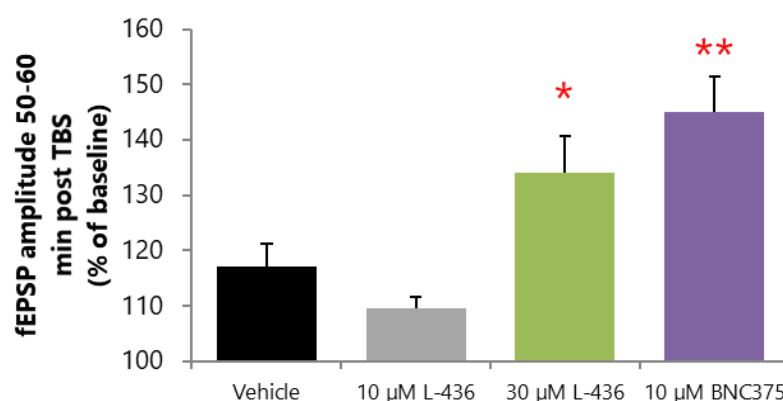


Figure 4.9 The effects of $\alpha 7$ nAChR-targeting compounds on LTP in the CA1 region of the hippocampus.

Summary histograms representing the level of LTP measured 50-60 minutes after a 10xTBS induction paradigm from hippocampal slices prepared from wild type (WT) mice treated with vehicle or test compound. A significant increase in fEPSP amplitudes was associated with either 30 μ M L-436 or 10 μ M BNC375 (*/** $P < 0.05/0.01$ compared to vehicle, unpaired Student's t-test; N: vehicle = 8, 10 μ M L-436 = 6, 30 μ M L-436 = 6, 10 μ M BNC375 = 6).

Table 4.1. Summary table showing the mean magnitude of LTP measured 50-60 minutes after a 10xTBS stimulation in WT mice hippocampal slices treated with vehicle (aCSF + 0.1% DMSO) or test compounds (unpaired Student's t-test, NS, non-significant).

Treatment	Mean	SEM	n	<i>P</i> vs Vehicle
Vehicle	117.1	4.0	8	
10 μ M L-436	109.5	2.1	6	0.57
30 μ M L-436	134.1	6.6	6	0.039
10 μ M BNC375	145.0	6.4	6	0.002

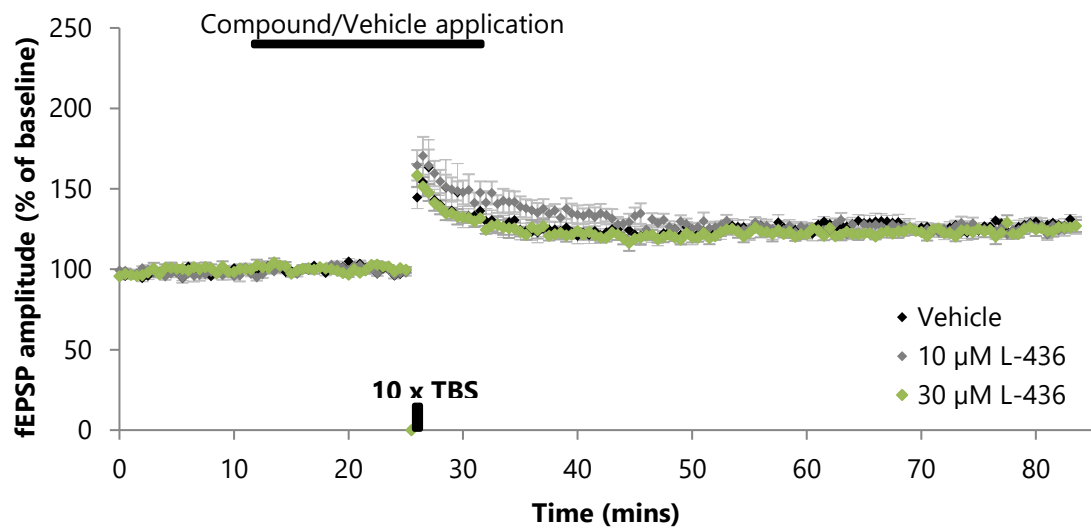


Figure 4.10. The effects of L-436 on LTP in the CA1 region of the hippocampus of *Acra7-* mice.

Composite scatter plot showing the effects of increasing concentrations (10 and 30 μ M) of L-436 on LTP of fEPSPs. Data is shown as a percentage of the response for average fEPSP amplitude recorded during the 10-minute period immediately before 10xTBS induction of LTP for each slice. Hippocampal slices prepared from *Acra7-* mice were subject to a baseline period (no compound application) of 10 minutes, followed by a 20-minute period of application (solid bar) of either vehicle (black diamonds), 10 μ M L-436 (grey diamonds) or 30 μ M L-436 (green diamonds). Theta-burst stimulation (10xTBS) of the Schaffer collaterals evoked stable long-term potentiation (LTP). Error bars are standard error of the mean (SEM). N = 10 (vehicle); 7 (10 μ M L-436); 9 (30 μ M L-436). Note the lack of effect of the compound in KO mice compared to WT shown in Fig 4.8.

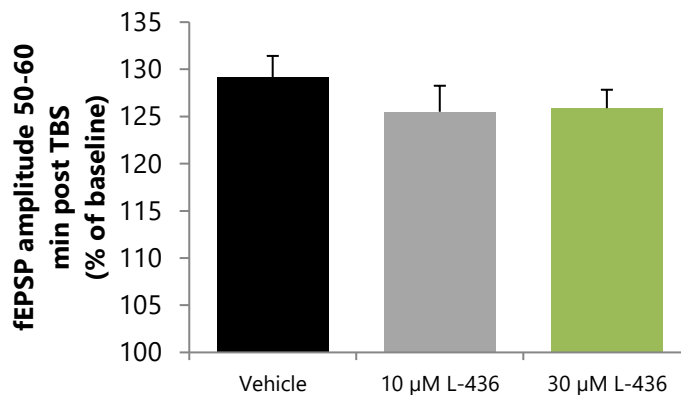


Figure 4.11. Summary of the effect of L-436, a $\alpha 7$ nAChR-targeting compound on LTP in the CA1 region of the hippocampus of *Acra7*- mice.

Summary histograms representing the level of LTP measured 50-60 minutes after a 10xTBS induction paradigm from hippocampal slices prepared from wild type *Acra7*- mice treated with vehicle or test compound. No significant increase in fEPSP amplitudes was associated with application of either concentration of L-436, compared to the vehicle ($P > 0.05$; unpaired Student's t-test, N: vehicle = 10; 10 μ M L-436 = 7; 30 μ M L-436 = 9).

Table 4.2. Summary table showing the mean magnitude of LTP measured 50-60 minutes after a 10xTBS stimulation in *Acra7*- mice hippocampal slices treated with vehicle (aCSF + 0.1% DMSO) or test compounds (unpaired Student's t-test, NS, non-significant).

Treatment	Mean	SEM	n	<i>P</i> vs Vehicle
Vehicle	129.1	2.3	10	
10 μ M L-436	125.5	2.8	7	0.327
30 μ M L-436	125.9	1.9	9	0.301

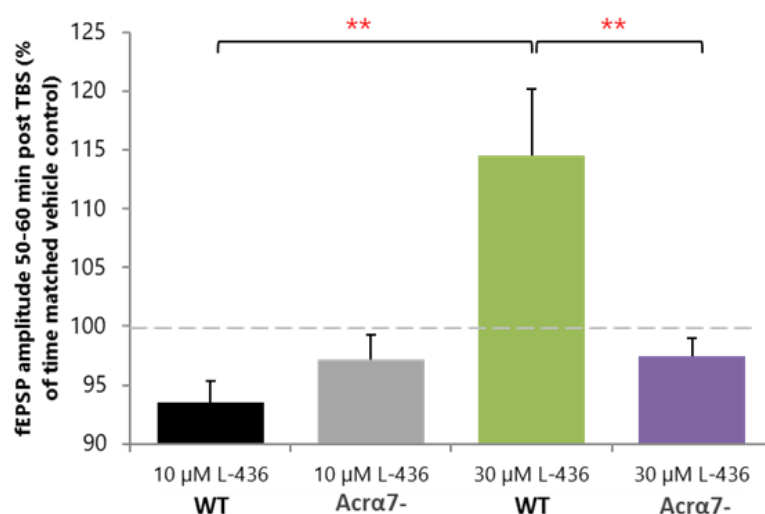


Figure 4.12. Summary bar chart comparing the effect of the nAChR-targeting compound L-436 on LTP in the CA1 region of the hippocampus of WT and *Acra7-* mice.

Summary of histograms representing the level of LTP measured 50-60 minutes after TBS in hippocampal slices treated with L-436 within this study. (** $P < 0.01$, One-way ANOVA with Bonferroni's multiple comparisons test). Data plotted normalised to the mean fEPSP amplitude 50-60 mins post TBS of the time-matched vehicle control recordings for each mouse genotype.

Table 4.3. Comparison of the mean fEPSP amplitudes measured 50-60 minutes after a TBS in hippocampal slices treated with L-436 L, an $\alpha 7$ nAChR-targeting compound within this study, (One-way ANOVA with Bonferroni's multiple comparisons test). Data are normalised to the mean fEPSP amplitude 50-60 mins post TBS of the time-matched vehicle control recordings for each mouse genotype.

Treatment	Mean	SEM	n	<i>P</i> vs 10 μ M L-436 (WT)	<i>P</i> vs 30 μ M L-436 (WT)
10 μ M L-436 (WT)	93.5	1.8	6		0.0005
10 μ M L-436 (KO)	97.2	2.1	7	NS	0.0028
30 μ M L-436 (WT)	114.5	5.7	6	0.0005	
30 μ M L-436 (KO)	97.5	1.5	9	NS	0.0019

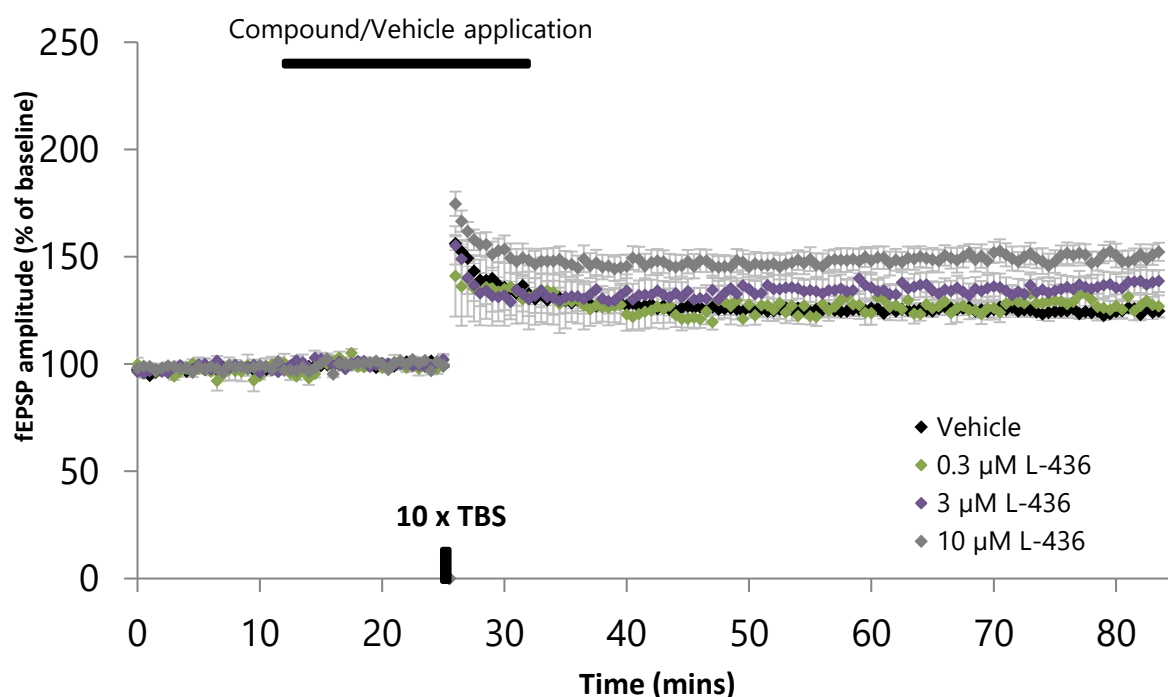


Figure 4.13. The effects of increasing concentrations of L-436 on LTP in the CA1 region of the hippocampus of SD rats.

Composite scatter plot showing the effects of increasing concentrations (0.3, 3 and 10 μM) of L-436 on LTP of fEPSPs. Data is shown as a percentage of the response for average fEPSP amplitude recorded during the 10-minute period immediately before 10xTBS induction of LTP for each slice. A baseline period (no compound application) of 10 minutes was followed by a 20-minute period of application (solid bar) of either vehicle (black diamonds), 0.3 μM L-436 (green diamonds), 3 μM L-436 (purple diamonds), or 10 μM L-436 (grey diamonds). Theta-burst stimulation (10xTBS; black bar) of the Schaffer collaterals evoked stable long-term potentiation (LTP). At the concentrations of 3 and 10 μM , L-436 significantly increased LTP relative to vehicle. Error bars are standard error of the mean (SEM). N = 14 (vehicle); 6 (0.3 μM L-436); 6 (3 μM L-436); 9 (10 μM L-436).

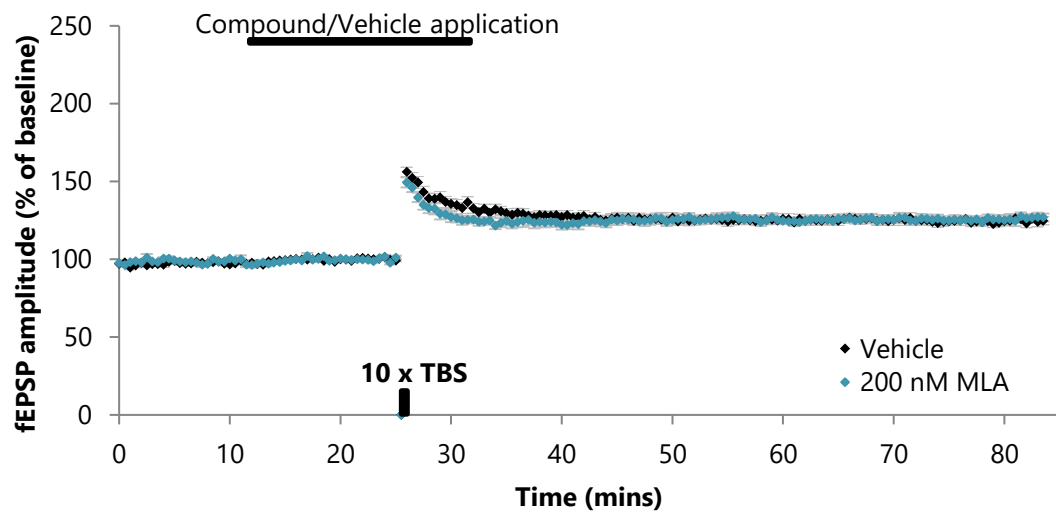


Figure 4.14. The effects of the $\alpha 7$ nAChR antagonist MLA on LTP in the CA1 region of the hippocampus of SD rats.

Composite scatter plot representing mean normalised fEPSP amplitudes before and after 10xTBS in rat hippocampal slices treated for 20 minutes with either vehicle (black diamonds) or MLA (blue diamonds). No significant changes in fEPSP amplitude was observed, compared with the vehicle. Error bars are standard error of the mean (SEM). N = 14 (vehicle); 7 (MLA).

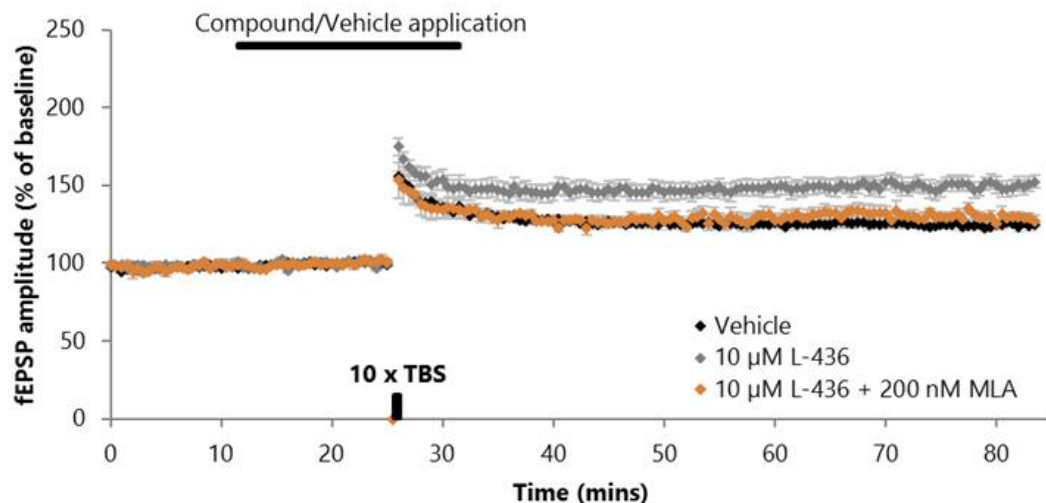


Figure 4.15. The effects of MLA on L-436-induced enhancement of LTP in the hippocampus of SD rats.

Composite scatterplot of mean normalised fEPSP amplitude before and after 10xTBS application in rat hippocampal slices treated for 20 minutes with either vehicle (black diamonds), 10 μ M L-436 (grey diamonds) or 200 nM 10 μ M L-436 + 200 nM MLA (orange diamonds). At the concentration of 10 μ M, L-436 significantly increased LTP relative to vehicle, an effect absent in the presence of the $\alpha 7$ nAChR antagonist MLA. Error bars are standard error of the mean (SEM). N = 14 (vehicle); 9 (10 μ M MLA); 5 (200 nM L-436 + 10 μ M MLA).

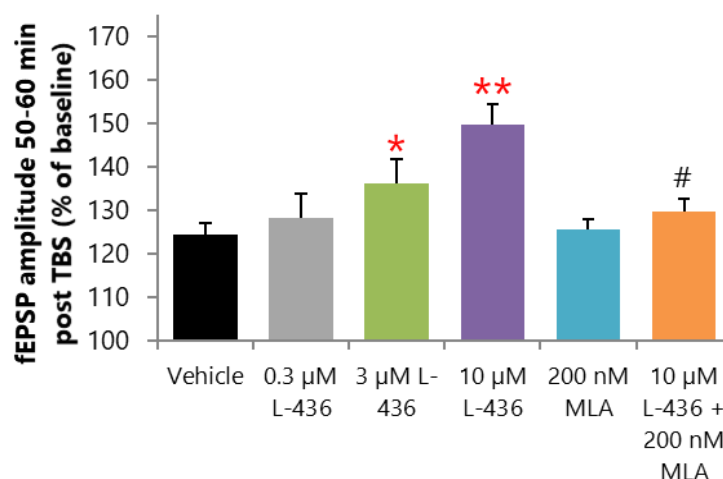


Figure 4.16. Summary bar chart showing the effects of increasing concentrations of the $\alpha 7$ nAChR-targeting compound L-436 on LTP and the effects of the $\alpha 7$ nAChR antagonist MLA on L-436-induced effects.

Summary histograms representing the level of LTP measured 50-60 minutes after a TBS induction paradigm from rat hippocampal slices treated with vehicle or test compound. (*/** P<0.05/0.01 compared to vehicle, # P<0.05 compared to 10 μ M L-436, unpaired Student's t-test). Note the concentration-dependent enhancement of LTP by L-436 and the reversal of this effect in the presence of the $\alpha 7$ nAChR antagonist MLA.

Table 4.4. Summary table showing the effects of increasing concentrations of the $\alpha 7$ nAChR-targeting compound L-436 on LTP and the effects of the $\alpha 7$ nAChR antagonist MLA on L-436-induced effects. Mean fEPSP amplitudes measured 50-60 minutes after TBS in rat hippocampal slices treated with vehicle or test compound, (Statistical comparison; unpaired Student's t-test).

Treatment	Mean	SEM	n	P vs Vehicle	P vs 10 μ M L-436
Vehicle	124.5	2.6	14		
0.3 μ M L-436	128.3	5.6	6	0.334	
3 μ M L-436	136.3	5.6	6	0.026	
10 μ M L-436	149.7	4.8	9	0.0001	
200 nM MLA	125.8	2.4	7	0.480	
10 μ M L-436 + 200 nM MLA	129.8	2.8	5	0.153	0.013

4.5 Conclusions and Discussion

The main aim of the current study was to validate a novel putative PAM of $\alpha 7$ nAChRs, developed by Merck, L-436, and to compare the effectiveness of this compound against known modulators of these receptors: a partial agonist, EVP-6124 and a PAM BNC-375. The principal findings from this study are that L-436 induced a concentration-dependent enhancement of LTP in both mouse and rat hippocampal slices. This effect was lost in mice lacking $\alpha 7$ nAChRs ($\text{Ac}\alpha 7^-$ mice) unlike their wild-type littermates. In rat hippocampal slices, the peak effect of L-436 on LTP, observed around a concentration of 10 μM , was inhibited in the presence of the selective $\alpha 7$ nAChR antagonist MLA. Taken together these data suggest that L-436 enhances LTP via a direct effect on $\alpha 7$ nAChRs, although the exact mechanism of action remains unknown to us due to L-436 being the client's property. However, we can seek to explain the possible mechanism of action of L-436 by likening its effects to those similar to already established partial agonists of $\alpha 7$ nAChRs such as EVP-6124, GTS-21, S 24795 and SSR180711 (Biton *et al.*, 2007; Lagostena *et al.*, 2008; Hunter *et al.*, 1994; Hurst *et al.*, 2013; Bertrand *et al.*, 2015; Townsend *et al.*, 2016). $\alpha 7$ nAChRs have long been known to have a role in LTP (Mansvelder & McGehee, 2000). Previous studies have shown bath application of $\alpha 7$ nAChR agonists facilitated LTP induction (Hunter *et al.*, 1994; Fujii *et al.*, 1999), leading to enhanced and early and late phase LTP in the CA1 region of the hippocampus and involves both enhanced pre-synaptic glutamate release and post-synaptic depolarization (Kroger *et al.*, 2011). Distributed widely throughout the brain $\alpha 7$ nAChRs, located on pre- and post-synaptic terminals and in extra-synaptic locations (see Dani & Bertrand, 2007), modulate the release of a number of neurotransmitters, including glutamate, GABA, dopamine and noradrenaline in an intracellular calcium-dependent manner (Dickinson, Kew & Wonnacott, 2008; Zappettini, *et al.*, 2011; Molas & Dierssen, 2014; Quarta, *et al.*, 2009).

A rise in intracellular calcium is a pre-requisite for the transient early phase of LTP (E-LTP), the long lasting late phase of LTP (L-LTP) requiring

protein synthesis via signalling through MAP kinase and phosphorylation of ERK and cAMP-Responsive Element Binding (CREB) transcription factor, all features of responses to ligand-induced activation of $\alpha 7$ nAChRs (Bitner *et al.*, 2007; Bitner *et al.*, 2010). Other signalling cascades that could contribute to $\alpha 7$ nAChRs-mediated contributions to LTP and synaptic plasticity are the CaMKII pathway and cAMP-PKA pathways (Sharma *et al.*, 2008; Dajas-Bailador *et al.*, 2002; Welsby *et al.*, 2009). The calcium permeability of $\alpha 7$ nAChRs is similar to that of NMDA receptors and is believed to be a key feature of these receptors contributing to driving long-term changes in synaptic plasticity (Seguela *et al.*, 1993; Uteshev, 2012; Fagen *et al.*, 2003; McKay *et al.*, 2007). It is also possible that membrane depolarisation via $\alpha 7$ nAChRs could contribute to relieving the magnesium block of NMDA receptors and co-incident activation of $\alpha 7$ nAChRs and NMDA receptors driving enhanced calcium influx and enhanced LTP. Taken together $\alpha 7$ nAChR-dependent signalling pathways appear ideally equipped to modulate and enhance LTP.

In the hippocampus $\alpha 7$ nAChRs mRNA and $\alpha 7$ nAChRs associated α -bungarotoxin binding sites are found distributed widely in the dentate gyrus, CA1 and CA3 (Sudweeks & Yakel, 2000; Fabian-Fine *et al.*, 2001; Adams *et al.*, 2002). (Adams *et al.*, 2002). $\alpha 7$ nAChRs-mediated currents have been localised to dentate gyrus granule cells, GABAergic interneurons, CA3 and CA1 pyramidal neurones (Ji *et al.*, 2001; Grybko *et al.*, 2011; Gu *et al.*, 2012; John *et al.*, 2015; Jones & Yakel, 1999). Elevations in intracellular calcium associated with $\alpha 7$ nAChRs-mediated currents have been imaged localised at the level of the dendrites of CA1, CA3 pyramidal neurones and dentate granule cell mossy fibre terminals (Fayuk & Yakel, 2005; 2007; Grybko *et al.*, 2011; Cheng & Yakel, 2014). Located on the pre- and post-synaptic terminals of GABAergic interneurons and glutamatergic synapses ((Fabian-Fine *et al.*, 2001), $\alpha 7$ nAChRs are positioned to modulate neurotransmitter release (Jones *et al.* 1999; Dajas-Bailador & Wonnacott, 2004; Dani & Bertrand, 2007), and post-synaptic transmission, respectively, all the ingredients required to drive functional changes in synaptic plasticity as occurs in LTP.

Three $\alpha 7$ nAChR agonists were investigated for their effects on LTP here. EVP-6124 was tested at 5 concentrations: 1.0 nM, 1.78 nM, 3.16 nM, 5.62 nM and 10.0 nM. This study was in fact part of an extensive range of investigations undertaken by this lab to identify mechanism of action of the compound and to provide “proof-of-concept” studies for its ability to enhance cognitive function. Initial studies revealed the compound to be effective at low concentrations in vivo and in vitro and associated with a “bell-shaped” concentration response curve (see also Townsend *et al.*, 2016). EVP-6124 enhanced LTP at low concentrations and enhanced cholinergic currents in vitro (Prickaerts *et al.*, 2012). Prickaerts *et al.*, (2012) showed EVP-6124 enhanced acetylcholine-induced currents mediated via human $\alpha 7$ nAChRs over the range of 0.3 to 1 nM whereas higher concentrations yielded inhibition with an IC_{50} around 3 nM. Data presented here show a remarkable sensitivity to EVP-6124 in LTP assays in rat, the compound showing a concentration-dependent enhancement of LTP over the range 1 to 10 nM, the effect being significant at 5.62 and 10.0 nM. However, compared to data on human $\alpha 7$ nAChRs, the effective concentration to yield significant LTP was in the range reported for the compound to suppress h $\alpha 7$ nAChRs currents. The most likely explanation for this discrepancy is a species difference or a penetration issue in slice preparations, as used here, compared to oocytes used by Prickaerts’s team. Nevertheless, data presented here on LTP show a remarkable sensitivity to EVP-6124. Precisely how this compound works is not entirely clear. It is proposed to act as a potent, partial, selective agonist for $\alpha 7$ nAChRs and co-agonist activity is a feature of its action. Co-agonist activity is where any one receptor has two binding positions and occupancy of both positions is required to activate channel opening. Thus, if a single high affinity molecule, such as EVP-6124 were to occupy a site, the probability of a lower affinity ligand such as acetylcholine simultaneously occupying the second site leading to channel opening is increased. At higher concentrations where EVP-6124 as a partial but high affinity agonist occupies both sites would limit available binding sites for ACh and potentially diminish the response (Prickaerts *et al.*, 2012). This same group proposed that with EVP-6124 acting at sub-nanomolar concentrations in a co-agonist-dependent manner would lead to an improved

side-effect profile than a classic full agonist approach and would increase drug safety margin. It is therefore of interest that EVP-6124 showed initial success in Phase 2 clinical trials for cognitive deficits in schizophrenia (Preskorn *et al.*, 2014). However, in Phase 3, the drug concentration was increased, and the trials halted due to adverse side-effects and lack of efficacy at primary end-points (BusinessWire, 2015). It is therefore tempting to speculate that the “bell-shaped” concentration response observed with this compound may in fact be an undesirable feature extremely sensitive to drug dosage.

BNC375 was another $\alpha 7$ nAChR-targeting ligand profiled extensively in our lab for Merck. BNC375 was proposed to be a $\alpha 7$ nAChR positive allosteric modulator (PAM) of these receptors. $\alpha 7$ nAChR PAMs enhance the effects of ACh by binding to a unique non-conserved region of the $\alpha 7$ nAChR and are generally not associated with receptor desensitization to the same extent that agonists of this receptor are (Dinklo *et al.*, 2011; Williams *et al.*, 2011). Two types of PAM have so far been proposed based upon their effects on receptor desensitization properties. Note receptor desensitization in this context refers to effectively rapid inactivation of conductances in the presence of the ligand rather than a loss of effect upon repeated applications of ligand. Type I PAMS enhance agonist-induced peak currents with little effect on desensitization whereas TYPE II PAMS potentiate peak currents and delay desensitization. PAMs are suggested to be able to generate efficacy over a broader range of concentrations and maintain efficacy with repeat dosing, features that are suggested to promote improved clinical profiles compared to classic orthosteric agonists. In the present study we used BNC375 as a positive control to test and compare the effects of a novel Merck compound L-436, as we had previously extensively profiled BNC375 and identified the compound as a positive allosteric modulator of $\alpha 7$ nAChR. A recent publication, based on data from our lab, has shown BNC375 to be a selective $\alpha 7$ nAChR PAM (Wang *et al.*, 2020). The compound enhances ACh-induced currents with little effect on desensitization kinetics classifying it as a Type I PAM. BNC375 also displayed a wide-range of pro-cognitive effects in rodent and primate pre-clinical models (Wang *et al.*, 2020; note, in this paper data displayed in figures

3, 4 and 5 and associated text were written and generated by Neurosolutions; Harvey *et al.*, 2019).

Similar to BNC375, L-436 also enhanced LTP although when directly compared to BNC375 in the same series of experiments it showed less sensitivity than the latter: 10 μ M BNC375 inducing enhanced LTP to greater extent than L-436 at a concentration of 30 μ M. However, it is also noteworthy that L-436 induced a greater effect in mice compared to rats although in this instance we did not directly compare these effects with BNC375. Nevertheless, L-436 may be a worthy addition to the growing α 7nAChR PAM pipeline for future clinical evaluation.

Regardless of its origin and progression, decline in and retention of cognitive function remains one of the main challenges of the neuroscience research community. In addition to the established public health crisis related to the continued increase in the prevalence in Alzheimer's disease, the sustained rise in obesity, type II diabetes and associated metabolic issues appear to be exacerbating the worldwide struggle with cognitive decline with advancing age.

More than 17 years have elapsed since the FDA approval of memantine as an anti-AD treatment. Although in 2014 a combination treatment of both donepezil and memantine (Namzaric) was also confirmed as a viable medication, this is currently marketed as a "temporary relief" from the symptoms of AD. Thus, the challenge of finding a novel and competent therapy method remains at large.

Consequently, the lack of success of EVP-614 in Phase III clinical trials came as another blow to the already lacklustre output of the AD-targeting drug pipeline. Due to the established involvement of the α 7nAChRs in both normal and pathological brain states, it is reasonable to predict a significant research and clinical focus upon compounds targeting these receptors. Despite promising preclinical findings reported both here and by Prickaerts *et al.*

(2012), and favourable Phase II clinical trial outcomes on both AD and schizophrenia patients, application of encenicline did not yield the desired cognitive improvements in either group in the Phase III trials. The AD trials were suspended due to unexpected and severe gastrointestinal problems in some volunteers. In addition, the schizophrenia trial group failed to meet the co-primary endpoints for improved cognitive function (Forum Pharmaceuticals, 2016).

This failure contrasts with the strong preclinical evidence and some promising clinical findings, and several reasons can be offered to explain for these conflicting outcomes. First, a lack of selectivity leading to dose-limiting side-effects such as serotonin 5-HT₃ receptor antagonism. Second, a loss in function due to desensitization with sustained exposure to the compound. And finally, the inverted U-shaped dose-response curve might indicate that the efficacy of an $\alpha 7$ agonist lies within a specific and narrow range of drug exposure (Deardorff *et al.*, 2015).

However, certain observations obtained from these trials revealed additional factors suggestive for shortcomings in study design could have contributed towards the failure of this compound in the Phase III clinical setting. These include the significance of accounting and justifying for non-adherence to treatment, a lack of plateau in learning effects post repeated testing sessions, and unexpected improvement within the placebo groups (Brannan, 2019). Therefore, it is possible that these Phase III results are less reflective of the true efficacy of encenicline, compared to the previous findings of phase II trial (Keefe *et al.*, 2015).

In order to circumvent the previously reported, albeit rare GI side-effects associated with the conventional oral mode of delivery of EVP-614, alternative routes such as transdermal, transbuccal, or intranasal should be considered. Whilst at present no evidence exists that encenicline alone can be delivered via a transdermal patch, a previous Phase IIb trial involving a transdermal nicotine patch (NRT) in conjunction with encenicline attempted

to tackle smoking withdrawal-associated cognitive deficits and tobacco abstinence. Although a combination of both NRT and encenicline improved odds of abstinence by 3-fold compared to encenicline and placebo patch, overall, this was not a lasting or significant effect (Schuster *et al.*, 2018). Nevertheless, the transdermal route of drug delivery should be regarded as an efficacious option due to its successful use in delivering rivastigmine for Alzheimer's disease treatment (Nieto *et al.*, 2016).

In addition, transbuccal route of drug delivery has been proposed as a reliable method for adhering to a correct dose regimen. More specifically, patients suffering from dementia often experience difficulties in complying with the prescribed dosage, as well as problems related to swallowing tablets. Promising findings have been reported by an *in vivo* animal study utilising an intraoral device (IntelliDrug) to deliver galantamine in pigs, showing that transbuccal delivery can provide long-lasting and controlled blood-levels of the drug (Giannola *et al.*, 2010).

In the recent years, delivery of compounds via intranasal route for the purpose of AD treatment has gained a fair amount of attention, perhaps due to the initially promising outcomes of Phase II/III clinical trials, investigating the cognitive effects of intranasal administration of insulin on patients with AD (Craft *et al.*, 2020). The initial patent application for encenicline included both intranasal and transdermal routes as possible modes of administration (Oliver-Schaffer *et al.*, 2014). In addition, another patent proposal outlining the advantages of rivastigmine application via the intranasal route, suggested the inclusion of encenicline as an additional therapeutic agent (Morgan, 2020).

The promising effects of BNC375 on LTP reported both here and by Wang *et al.*, (2020) indicate that this compound may hold potential as the next candidate for cognition-targeting clinical trials. Although at present there is no additional information regarding the future of BNC375 as a potential cognitive enhancer in humans, in scopolamine-impaired rhesus monkeys BNC375 reversed scopolamine-induced cognitive impairment in a dose-dependent

fashion, i.e., showing increasingly significant improvement at BNC375 dosages of both 1 and 10mg/kg but not at 0.1 mg/kg.

On the other hand, $\alpha 7$ agonists, such as GTS-21, encenicline, and AZD0328, have frequently shown sharp inverted U-shaped dose-effect function in non-human primate cognition assays (Castner *et al.*, 2011; Cannon *et al.*, 2013; Weed *et al.*, 2017). For example, GTS-21 reversed ketamine-induced deficit in rhesus object retrieval detour (ORD) assay only at 0.03 mg/kg but not at 0.1 or 0.01 mg/kg (Cannon *et al.*, 2013). In a rhesus paired associated learning task, encenicline was evaluated at six doses ranging from 0.003 to 1 mg/kg, but a significant reversal of the scopolamine-induced impairment was only noted at 0.01 mg/kg (Weed *et al.*, 2017). These outcomes indicate that $\alpha 7$ PAMs may demonstrate efficacy over a much broader range of exposures as compared to the agonists.

In summary, here we report a significant and concentration-dependant amplified effect of the $\alpha 7$ nAChR partial agonist EVP-614 (encenicline) upon 10xTBS-induced LTP in the rat hippocampal CA3-CA1 synapse. Likewise, the investigation of a novel $\alpha 7$ nAChR-targetting compound L-436 confirmed its intended target due to showing no significant changes in the LTP levels in the same synapse of $\alpha 7$ nAChR KO (Acr $\alpha 7$ -) mice. In their wild-type counterparts, the effects of L-436 were significant, albeit lower than the LTP enhanced by the positive-allosteric modulator (PAM) BNC375, suggesting an adjusted range of compound concentrations in the future. The validity of L-436 as a $\alpha 7$ nAChR-targetting substance was further supported upon showing a significant decrease in LTP via co-administration of MLA, an established $\alpha 7$ antagonist, suggesting the observed effects of L-436 in the absence of MLA were due to activation of $\alpha 7$ nAChRs. Therefore, our data supports the potential of $\alpha 7$ nAChR-targetting compounds for the enhancement of LTP.

Chapter 5: The pursuit of the mechanism of action of SD118, a novel SV2A-targeting compound

5.1 Introduction

Although seizures are the defining clinical manifestation of the epilepsies, individuals suffering from epilepsy are at a high risk of exhibiting a myriad of co-morbidities, such as cognitive deficits (Committee on the Public Health Dimensions of the Epilepsies, 2012). In addition, an estimated 10-22% of patients with Alzheimer's disease suffer from clinically obvious epilepsies; however, it should be noted that in clinical practice, epilepsies in individuals with AD can often go unnoticed as they can present as nonconvulsive status epilepticus or focal impaired awareness seizures and may overlap with other AD symptoms (Jenssen & Schere, 2010; Hommet et al., 2008; Larner et al., 2012; Vossel et al., 2017).

The cognitive difficulties associated with epilepsy have been shown to hinder educational progress throughout life (Berg *et al.*, 2012; Bell *et al.*, 2011), as well as contribute towards cognitive regression in adults to a magnitude which in some individuals would be clinically classified as having a presenile dementia (Thompson & Duncan, 2005). In addition, children who suffer from pharmaco-resistant epileptic seizures are more likely to exhibit lower IQ scores than children with well-managed seizures (Berg *et al.*, 2012). To complicate matters further, many of the frequently prescribed antiepileptic drugs (AEDs), e.g., phenobarbital and topiramate, exhibit some degrees of toxicity leading to cognitive adverse effects in epilepsy patients (Eddy *et al.*, 2011). Therefore, it can be hypothesized that the ideal AED would reduce neuronal irritability without altering neuronal excitability and cognitive functions.

5.2 Racetams and cognition

The use of racetam compounds as cognitive enhancers is not a new concept, albeit the exact mechanism of action of this class of drugs remains elusive. Due to the prevailing interest in repurposing racetams as valid therapeutic options, more insight regarding this aspect is necessary.

Piracetam is one of the more frequently used racetams as an add-on treatment for myoclonus epilepsy (Fedi *et al.*, 2001). However, it has also been used to treat cognitive impairment in ageing or dementia, or traumatic brain injury (Waegemans *et al.*, 2002, El Sayed *et al.*, 2016). Likewise, piracetam and piracetam-like nootropics have been implicated in the reversal of scopolamine-induced amnesia (Gouliakov & Senning, 1994). Since piracetam improves membrane fluidity in aged brain tissue without having any effect on young brains, it is possible that piracetam's mode of action targets the biochemical deficits commonly observed in the ageing brains (Müller *et al.*, 1997). Interestingly, piracetam has been shown to enhance mitochondrial functioning by improving glucose uptake and ATP production (Naftalin *et al.*, 2004). Therefore, this compound and its analogues might hold a beneficial solution to the prevailing negative effects of ageing-associated cognitive decline.

5.3 Levetiracetam: The New Generation AED

Levetiracetam (Keppra®), or (S)-α-ethyl-2-oxo-pyrrolidine acetamide is a water-soluble pyrrolidine derivative, whose chemical structure and mechanism of action differs from other AEDs. It is one of the so-called newer generation AEDs, i.e., developed after the 1990s with the intention of providing superior efficacy and safety, compared to the old generation compounds, such as phenobarbital. Indeed, since its approval for clinical use in 2002, Levetiracetam (LEV) has become a widely prescribed AED, showing effectiveness in both partial and generalized epilepsy syndromes as a sole or

add-on treatment (De Smedt *et al.*, 2007). Furthermore, clinical studies indicate that Levetiracetam not only appears to lack adverse cognitive effects frequently associated with other AEDs, but also enhances memory in epilepsy patients, even in individuals with existing cognitive limitations (Huang *et al.*, 2008; Lippa *et al.*, 2010).

5.3.1 Levetiracetam: Mechanism of action

Experimental evidence points towards the anti-epileptic potential of LEV due to its modulatory properties in various seizure activity animal models of chronic epilepsy (e.g., kindling models, pilocarpine model, genetic absence epilepsy rats from Strasbourg GAERS) with negligible effect in most models of acute seizures (Glien *et al.* 2002; Klitgaard *et al.* 1998; Löscher and Hönack, 1993). These findings are consistent with the experimental observations that LEV only affects GABAergic transmission within epileptic tissue or under conditions that occur during epilepsy, e.g., by inhibiting the proepileptogenic GABA_A run-down in the neocortex, leading to an increase in GABAergic inhibition, whereas it has no effect on GABA_A receptors from controls (Palma *et al.* 2007; Rigo *et al.* 2002).

Taken together, this evidence suggests that the mechanism of LEV may work in a preferential manner in cases of chronic application or under chronic epilepsy-associated conditions. However, most of the experiments to investigate LEV's cellular mechanism of action have been performed with acute application, reporting its acute cellular effects. A further consideration is that LEV is now being proposed as an acute treatment for seizures. An intravenous formulation is available (Ramael *et al.* 2006) that has already been shown to terminate status epilepticus after acute intravenous application (Knake *et al.* 2008). Interestingly, LEV is effective in one model of acute epilepsy (6Hz psychomotor seizure model) (Shannon *et al.* 2005; Barton *et al.* 2001) with the maximal effect occurring 1 h after intraperitoneal injection (Barton *et al.* 2001). These findings suggest that LEV can have an effect in

some acute seizure models. One possible explanation for these dichotomous findings in animal models of acute and chronic epilepsy is that LEV may have different mechanisms of action whether given acutely or chronically and in epileptic and control tissue, a conclusion that should be considered when evaluating the definitive mechanism of this compound.

Despite the promising clinical outcomes, the exact molecular mechanism of action of Levetiracetam was largely unknown until 2004 when Lynch *et al* showed that LEV exclusively binds to the synaptic vesicle protein SV2A.

Synaptic vesicle glycoprotein SV2A belongs to a major facilitator superfamily (MFA) of transporter proteins and is expressed throughout the entire brain. This protein is an essential component of synaptic vesicle membranes, specifically in regulating action potential-dependent neurotransmitter release (Custer *et al.*, 2016). Although the complexities of SV2A roles remain elusive, it participates in maturing primed presynaptic vesicles for Ca^{2+} -induced exocytosis via the regulation of synaptotagmin – a synaptic vesicle calcium sensor protein, which is essential for calcium-mediated exocytosis (Lynch *et al.*, 2004; Chang & Südhof, 2009; Kochubey *et al.*, 2011). It is of importance to note, however, that LEV reduces the release of presynaptic glutamate, especially in neurons with prolonged and high frequency firing (Yang *et al.*, 2007). Furthermore, the anti-epileptic effectiveness of LEV is correlated with its binding affinity to SV2A (Lynch *et al.*, 2004).

In summary, the clinical behaviour of Levetiracetam has highlighted SV2A as a potentially significant component of the presynaptic machinery, contributing towards improved cognitive functioning. While at present the entire mechanism of action of LEV is not known, the promise of this potential target for action has prompted the development of various novel Levetiracetam-derived compounds, such as Brivaracetam and more recently – SD118.

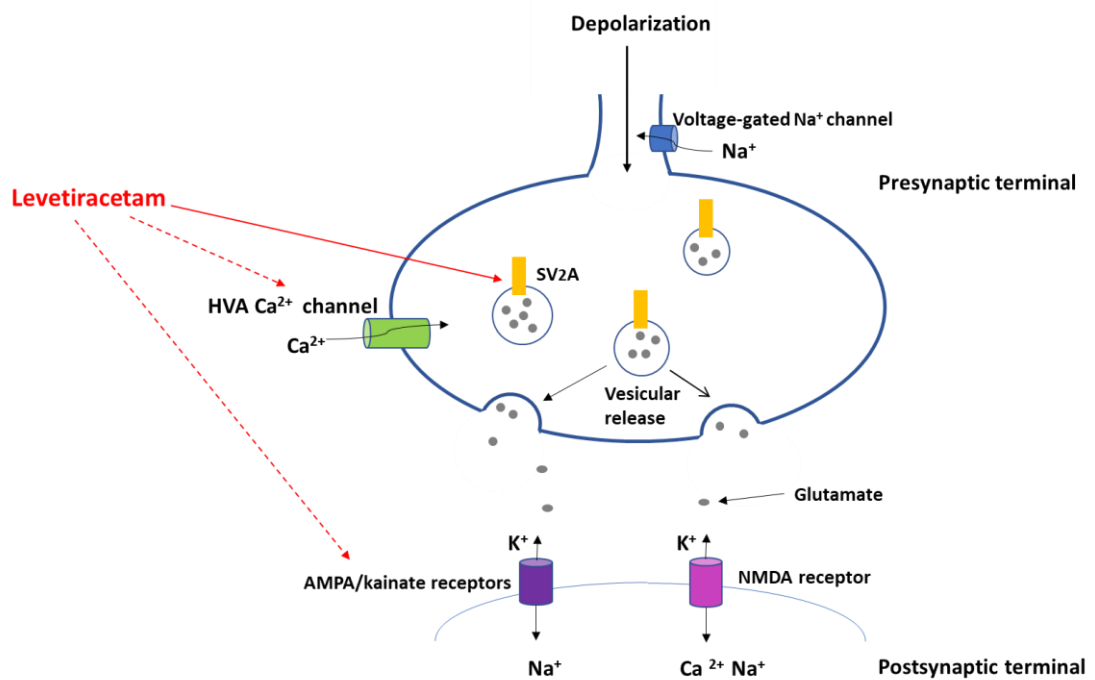


Figure 5.1. A schematic representation of the proposed mechanisms of action of Levetiracetam (LEV) in the excitatory synapse, with SV2A regarded as the main target (solid arrow).

LEV has also been proposed to exert some influence via binding to HVA Ca^{2+} channels and AMPA/kainate receptors (dashed arrows). AMPA, α -amino-3-hydroxy-5-methyl-4-isoxazolepropionic acid; SV2A, synaptic vesicle protein 2A; HVA Ca^{2+} , high-voltage activated calcium ion channels.

5.4 Results

The aim of the following sets of experiments was to investigate the mechanism of action of a novel SV2A-targeting compound SD118, developed by Syndesi Therapeutics™. At present, the specifics regarding the structure and pharmacology of SD118 are not available due to contractual obligations with Syndesi Therapeutics™. However, SD118 is part of a series of compounds designed with Levetiracetam as the “scaffold”. Unlike Levetiracetam, SD118 is highly membrane permeable and shows no anticonvulsant properties despite binding to the same target, SV2A. Whilst showing no anticonvulsant activity SD118 is effective as a cognitive enhancer in rodent models. The aim of the current study was to provide insight into the mechanism of action of SD118.

A series of pilot experiments were undertaken using whole-cell patch clamp recording techniques to record from CA1 pyramidal neurones in adult rat hippocampal slice preparations. Pharmacologically isolated EPSCs and IPSCs were evoked by electrical stimulation of the Schafer-collateral pathway at a range of frequencies (0.1, 1, 5 and 10Hz). SDI-118 (3 μ M) had no effect on EPSCs or IPSCs evoked at 0.1Hz and little effect on EPSCs evoked at 1 Hz with no effect on IPSPs. However, EPSCs evoked at 5 and 10 Hz were enhanced in the presence of SDI-118 unlike IPSCs which were unaffected. Furthermore, EPSCs evoked at low frequency stimulation (0.1Hz) in cells also stimulated at 5 or 10Hz were also enhanced in SDI-118 (Spanswick, unpublished observations). Based on this pilot data we designed a protocol to investigate the effects of SDI-118 on high (1-20Hz) and low (0.1Hz) frequency stimulation evoked, pharmacologically isolated EPSCs. Vehicle control experiments (0.01% DMSO) had no effect on EPSCs evoked using the protocols outline below with cycles of high frequency trains and low frequency stimulation recorded for upto 3 hours (Spanswick, unpublished observations).

5.4.1 Effects of SD118 on Paired-pulse Ratio

Paired-pulse facilitation (PPF) experiments were performed on rat hippocampal slices, prepared using methods outlined in Chapter 2. The rationale behind selecting PPF as an experimental paradigm lies within the classical explanation for its mechanism of action. According to the residual calcium hypothesis, upon the initial action potential Ca^{2+} ions enter the presynaptic terminal, where they subsequently bind to synaptotagmin, leading to NT release. However, a small amount of calcium ions will remain in the active presynaptic zone, i.e., “passive ions”. Should a second action potential be delivered to the presynaptic terminal within milliseconds of the first one, a second influx of Ca^{2+} will follow, adding to the residual Ca^{2+} load. This increase in Ca^{2+} presence at the presynaptic terminal will lead to an elevated number of synaptic vehicles ready for release. In addition, mossy fiber to CA3 PPR increases with increases in extracellular Ca^{2+} concentration. But in Schaffer to CA1 PPR decreases with increases in extracellular Ca^{2+} (Blatow *et al.*, 2003).

Low frequency stimulation (0.1Hz) interspersed with PPF stimuli were applied to rat hippocampal slices initially using conventional fEPSP recordings. In one set of experiments the stimulating electrode was placed in the MF pathway and the recording electrode located within the CA3 area. In another group of experiments, the stimulating electrodes were located in CA3 to activate fEPSPs in CA1. Low frequency stimulation was applied until a stable baseline was reached and a PPF paradigm was applied to investigate the interaction. The pairs of stimuli were delivered every 20 seconds, with 50, 100 and 250 msec interstimulus intervals (ISIs).

As an example, the typical paired pulse ratio (50 msec inter-stimulus interval) in control experiments amounted to values of 1.41 and 1.4 ($n = 2$). Subsequently, following exposure to SD118 (3 μM) the paired pulse ratios amounted to 1.37. Similarly, the exposure to the 100msec ISIs yielded values of 1.27 and 1.25 for controls ($n = 2$), and upon application of SD118 (3 μM):

1.25 and 1.26 ($n = 2$). Likewise, the PPR for the wash-out period was 1.26. Although at present, no significant effect on paired-pulse ratio of SD118 was observed, the volume of data generated from these experiments calls for thorough analysis and adjustments in the experimental protocol, as well as an overall stability (lack of drift) of the experiment (see Figs 5.2, 5.3 and 5.4.).

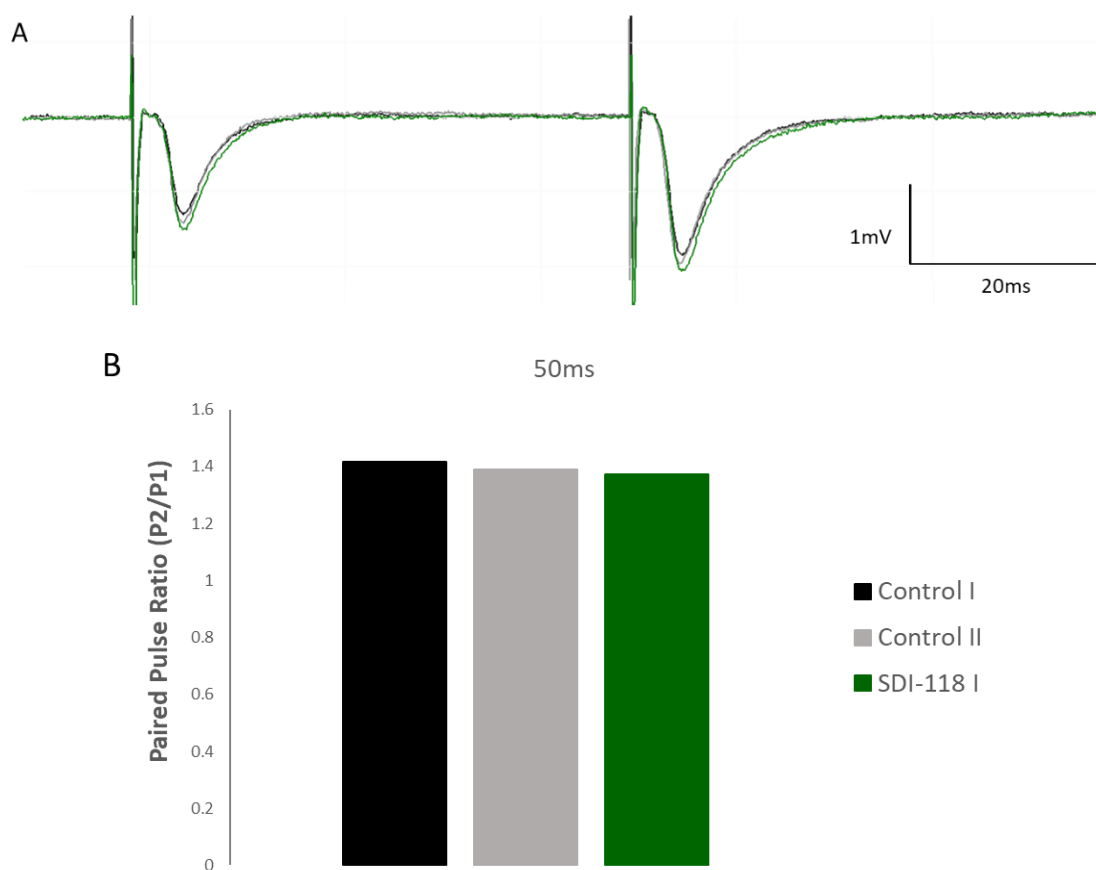


Figure 5.2 An example of a typical paired-pulse experiment subject to 50-msec ISIs.

A. A composite illustration of the events in the presence of control, SD118 or wash conditions, subject to 50msec interstimulus intervals. B. A composite image of bar charts showing the paired pulse ratios of control and Syndesi compound, subject to 50msec stimuli.

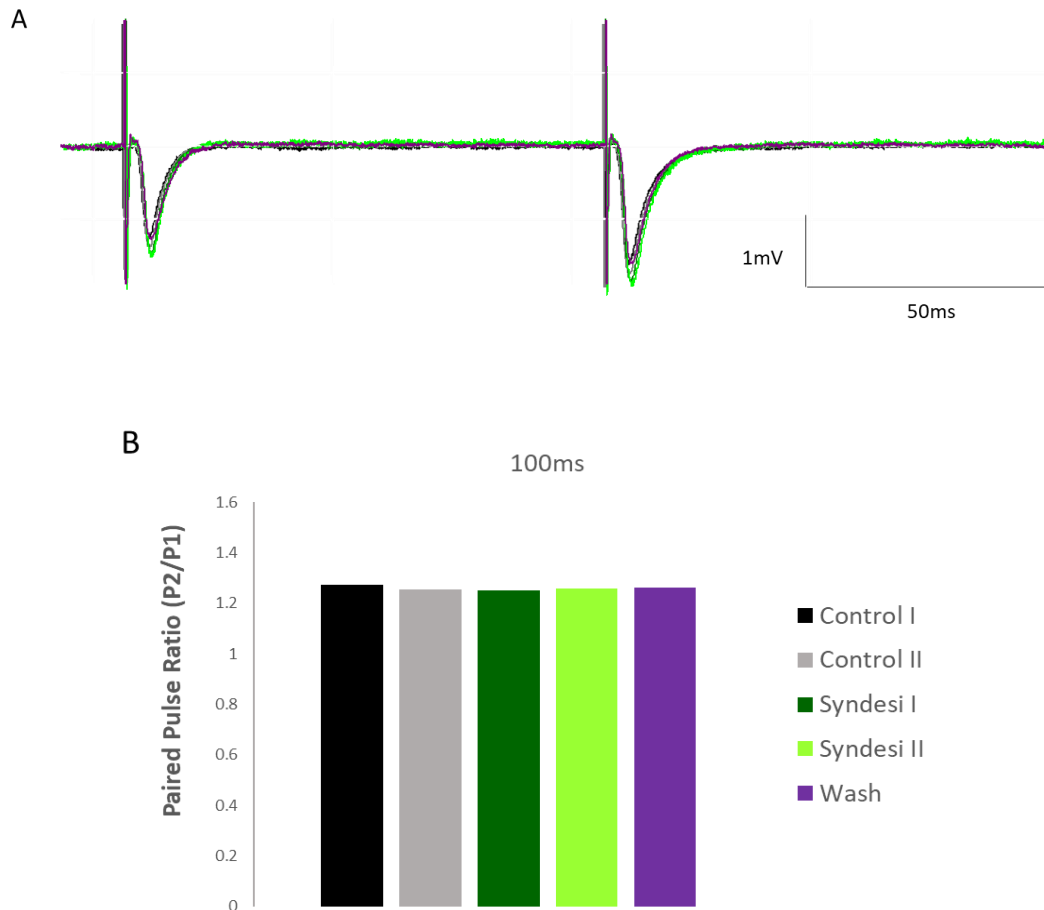


Figure 5.3 An example of a typical paired-pulse experiment subject to 100 msec ISIs.

A. A composite illustration of the events in the presence of control, SD118 or wash conditions, subject to 100msec interstimulus intervals. B. A composite image of bar charts showing the paired pulse ratios of control and Syndesi compound (SD118), subject to 100msec stimuli.

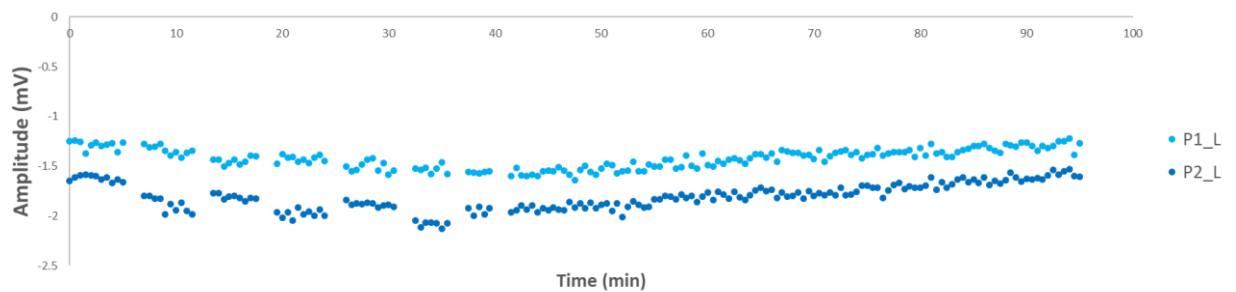


Figure 5.4 An example of a control paired-pulse experiment, showing stability in amplitude (mV) throughout the course of the experiment at the CA3-CA1 synapse.

5.4.2 Frequency-dependent effects of SD118 on excitatory synaptic transmission

Preliminary findings using a paired-pulse protocol revealed little effect of SD118 on paired-pulse ratio. Previous studies with Levetiracetam indicated that the anticonvulsant had an activity-dependent effect on both excitatory and inhibitory synaptic transmission with higher frequencies of stimulation (20-80Hz) leading to a suppression of both excitatory and inhibitory synaptic transmission (Meehan *et al.*, 2012; 2011; Yang *et al.*, 2007; Yang & Rothman, 2009). Here we designed a protocol to determine if the mechanism of action of SD118 was similarly frequency-dependent. The protocol was specifically designed to determine if the compound had a frequency-dependence to its mechanism and what the impact of modulation of synaptic transmission at high frequencies had on low frequency stimulation. Thus, the protocols comprised of a period of low-frequency stimulation (0.1Hz) followed by 3 bursts of high frequency stimulation (1, 2, 5, 10 and 20Hz; interburst interval 30 seconds) followed again by low frequency stimulation before the next cycle of high frequency burst stimulations. These cycles were repeated for control and subsequently in the presence of SD118. Precise stimulation protocols are provided in each subsection.

5.4.2.1 Frequency-dependent effects of SD118 on excitatory synaptic transmission: 1Hz.

Whole-cell patch clamp recordings were obtained from 6 neurones located in the CA1 region of the hippocampus. Upon establishing whole-cell access, neurones were exposed to aCSF containing D-AP5 (20 μ M), gabazine (10 μ M) and CGP55485 (400 nM) to block NMDA, GABA_A and GABA_B receptors, respectively, and to isolate non-NMDA, AMPA receptor-mediated EPSCs. This cocktail of antagonists was also designed to limit activity-dependent synaptic plasticity mediated by NMDA receptors. Neurones were

clamped at a holding potential of -70 to -75mV in the voltage-clamp configuration and EPSCs evoked by stimulation of the Schaffer-collateral pathway at a frequency of 0.1 Hz, followed by 3 bursts of stimuli at 1 Hz (see Fig 5.5 for details). The last 12 events evoked prior to high frequency stimulation were pooled for control and following exposure to SD118 and analysed to quantify the effects of SD118 on low-frequency synaptic transmission. Data from each EPSC evoked in individual trial of bursts were analysed for control and in the presence of SD118.

EPSCs evoked at low frequency stimulation (0.1Hz) amounted to 107.5 ± 14.8 pA (mean \pm SEM; $n = 6$) and 95.2 ± 22.7 pA in the presence of SD118 (3 μ M). This small reduction in peak amplitude, to 90.2 ± 17.4 % of control was not statistically significant ($p = 0.6$; paired student t-test). Although this effect was not significant, inspection of data on a cell-by-cell basis revealed changes in EPSCs in all cells with 3 neurones (data from 3 slices from 3 animals) characterised by an increase in EPSC amplitude in SD118 (e.g see Fig 5.5) and 3 by a decrease. Figure 5.6 summarises the effects of SD118 on EPSCs evoked at low frequency in combination with bursts of stimuli at 1Hz.

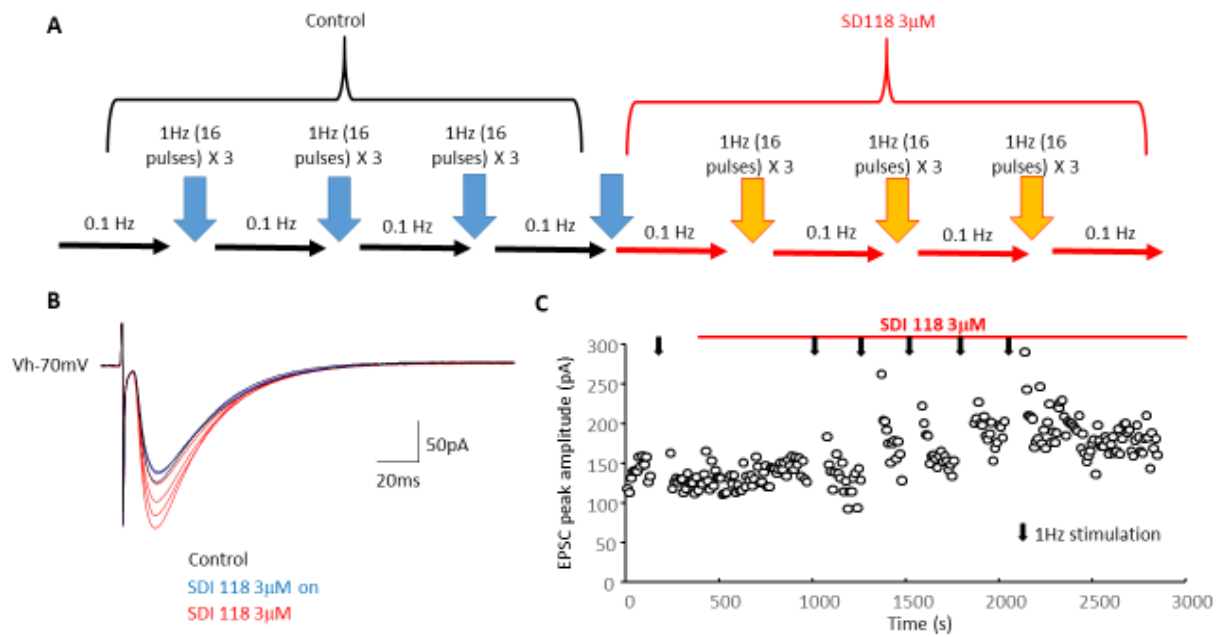


Figure 5.5. A summary of the frequency-dependent effects of SD118, novel putative cognition-enhancing compound on excitatory synaptic transmission

A. A schematic of the stimulation protocol used in this aspect of the study (0.1 Hz combined with 1 Hz stimulation protocols). B. Samples of a continuous record showing superimposed EPSCs evoked at 0.1 Hz in control, during and after exposure of slices to SD118 (each record is the average of 12 consecutively evoked EPSCs). C. Time-course plot of the effects of SD118 on EPSC evoked at 0.1 Hz. Note the increase in amplitude of EPSCs in SD118.

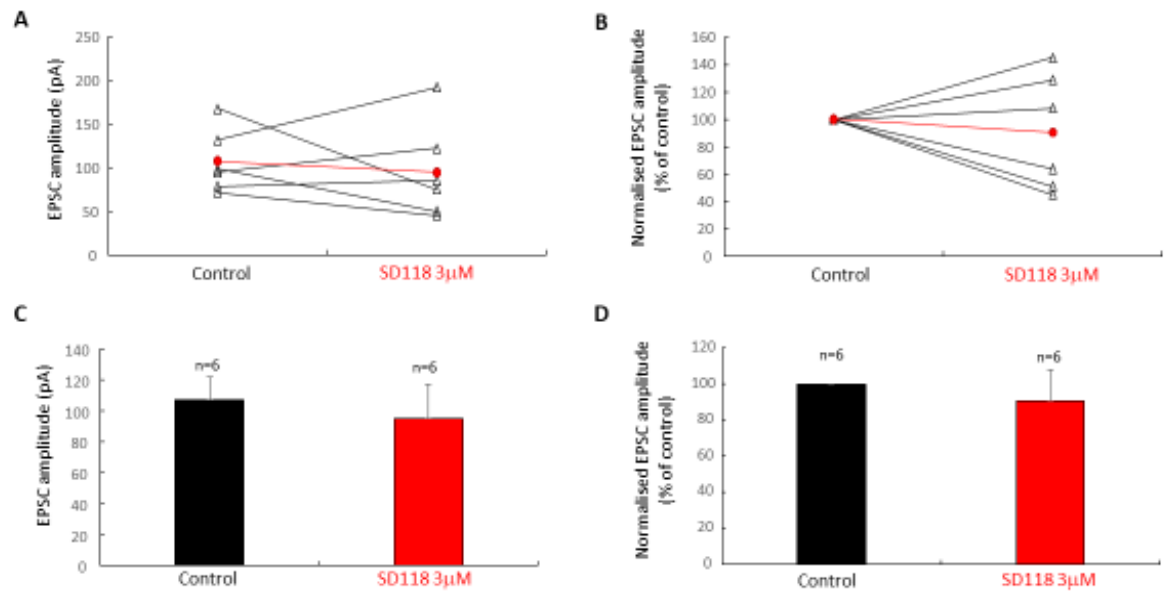


Figure 5.6. Summary data of the effects of SD118 on EPSCs evoked at low frequency (with 1 Hz high frequency).

A shows changes in amplitude of EPSCs evoked in each cell with data normalised to control shown in B. The red line indicates the mean of all cells. C shows a bar chart summarising mean peak amplitude of EPSCs in SD118 compared to control with the same data normalised to control shown in D. Error bars indicate SEM. Note the lack of effect of SD118.

Analysis of EPSCs evoked by 1 Hz stimulation revealed EPSCs in control amounting to 110.6 ± 26.7 pA (mean \pm SEM; n=6 cells, from 6 slices, 4 animals) for trial one of the three 1 Hz trains, and reduced to 81.9 ± 19.3 pA in SD118, amounting to a $77.8 \pm 10.4\%$ non-significant reduction in the amplitude of EPSCs. In trial 2 the mean peak amplitude of EPSCs evoked at 1 Hz was 110.3 ± 31.5 pA, increasing to 122.6 ± 45.6 pA ($100.5 \pm 12.9\%$ of control). Trial 3 EPSCs evoked at 1 Hz had mean peak amplitude of 102.1 ± 27.1 pA for control and increased to 150.8 ± 72.0 pA in SD118 corresponding to a $119.4 \pm 25.6\%$ increase when normalised to control (100%). When data from all trials were pooled, the mean peak EPSC amplitude was little changed in the presence of SD118 amounting to $98.9 \pm 12.6\%$ of control. None of these effects of SD118 on EPSCs evoked at 1 Hz were statistically significant. Inspection of responses observed in individual cells revealed peak EPSC amplitude was reduced in 4 cells in the presence of SD118 and increased in two. Figures 5.7 and 5.8 show examples of the effects of SD118 on EPSCs evoked at 1 Hz (3 trials). Figure 5.9 shows the pooled data for the effects of SD118 on EPSCs evoked at 1 Hz.

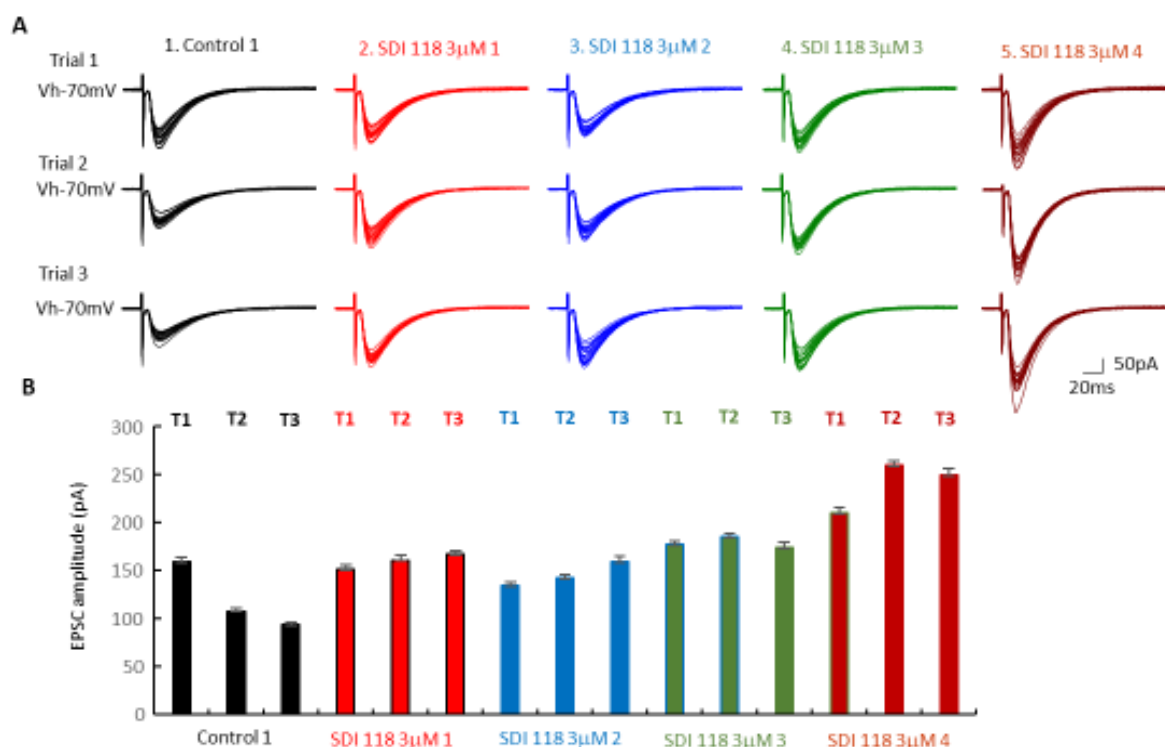


Figure 5.7. EPSCs during application of SD118

A. Samples of a continuous record showing superimposed EPSCs evoked at 1Hz in control (3 individual trials) and during exposure of slices to SD118 (each record is the average of 16 consecutively evoked EPSCs). B. Time-course bar chart plots showing the effects of SD118 on EPSC evoked at 1Hz. SD118, 1, 2, 3 and 4 indicate the mean peak amplitude of EPSCs with progressive exposure to SD118. Note the increase in amplitude of EPSCs in SD118.

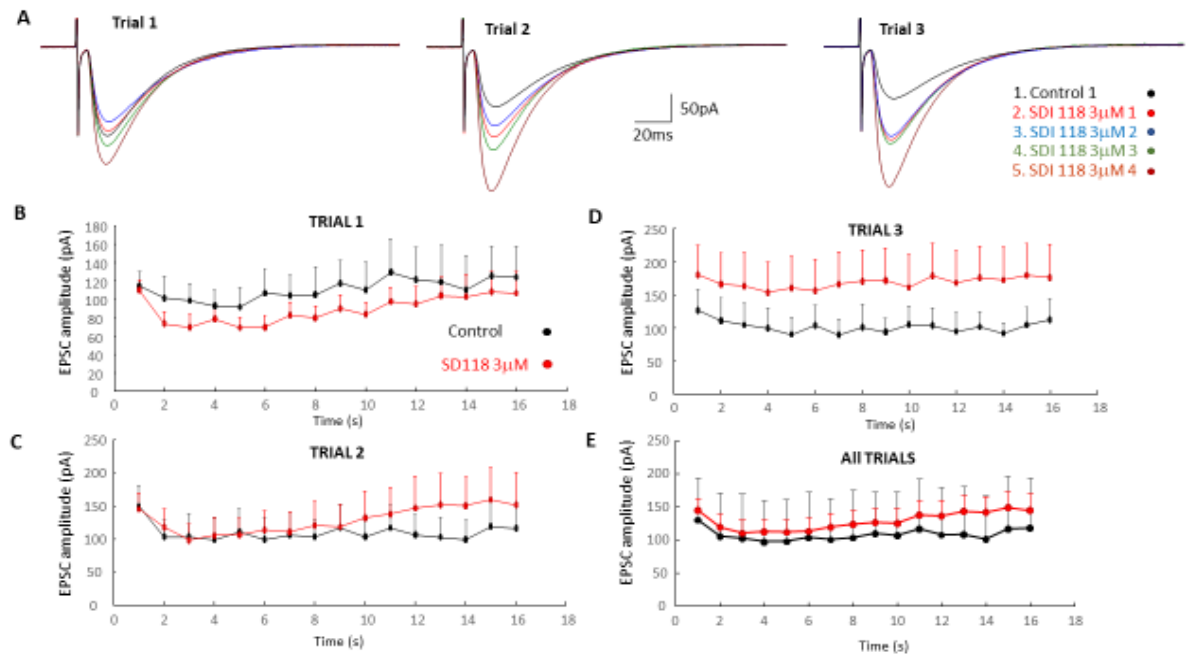


Figure 5.8. EPSCs throughout SD118 trials

A. Samples of a continuous record showing superimposed EPSCs evoked at 1Hz in control (3 individual trials) and during exposure of slices to SD118 (each record is the average of 16 consecutively evoked EPSCs). B-D. Time-course plots of the effects of SD118 on EPSCs evoked at 1Hz for trials, 1, 2 and 3, respectively. E. Shows the time-course plots for all trials combined. Error bars represent SEM.

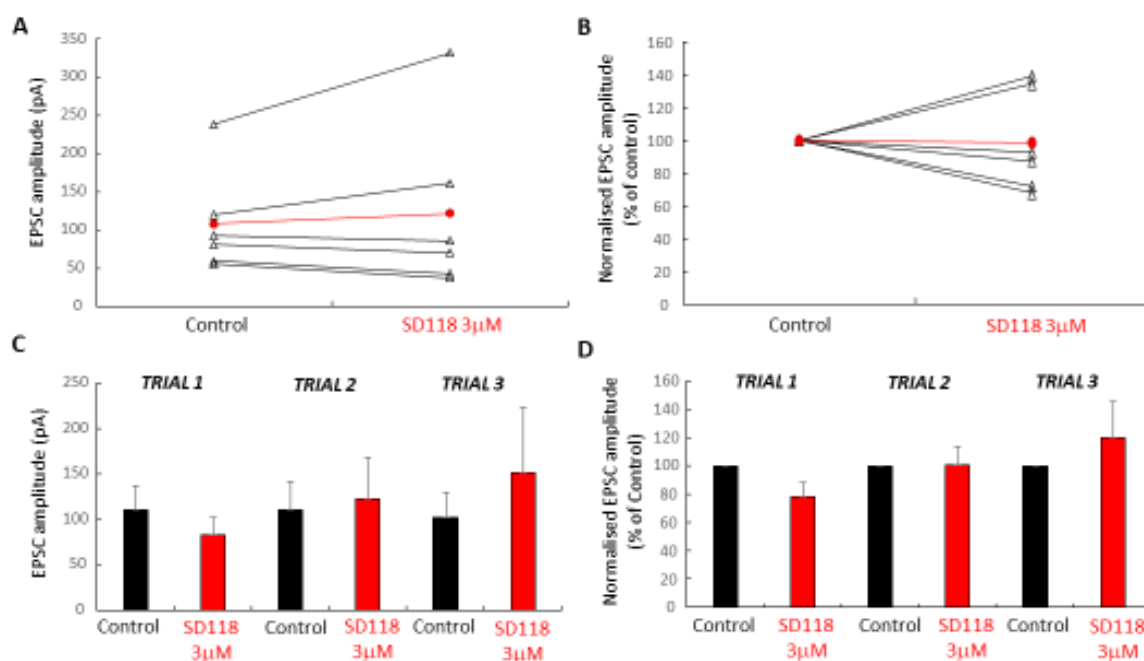


Figure 5.9. Summary data of the effects of SD118 on EPSCs evoked at 1 Hz

A shows changes in amplitude of EPSCs evoked in each cell with data normalised to control shown in B. The red line indicates the mean of all cells. C shows a bar chart summarising changes in mean EPSC amplitude in SD118 (data for all cells; $n = 6$) compared to control for each of the 3 trials with the same data normalised to control shown in D. There was no significant effect of SD118.

5.4.2.2 Frequency-dependent effects of SD118 on excitatory synaptic transmission: 2Hz

Whole-cell patch clamp recordings were obtained from a further 3 neurones (recorded from 3 slices from 3 animals), located in the CA1 region of the hippocampus. Neurones were clamped at a holding potential of -70 to -75mV in the voltage-clamp configuration and EPSCs evoked by stimulation of the Schaffer-collateral pathway at a frequency of 0.1 Hz, followed by 3 bursts of 2 Hz (see Fig 5.10 for details). The last 12 events evoked prior to high frequency stimulation were pooled for control and following exposure to SD118 and analysed to quantify the effects of SD118 on low-frequency synaptic transmission. Data from each EPSC evoked in individual 2Hz trials or bursts were analysed for control and in the presence of SD118.

EPSCs evoked at low frequency stimulation (0.1Hz) had a mean peak amplitude of 69.3 ± 14.3 pA (mean \pm SEM; $n = 3$) and in the presence of SD118 (3 μ M) increased to 75.7 ± 11.7 pA. This increase in peak amplitude, to 111.3 ± 15.6 % of control, was not statistically significant. Although this effect was not significant, inspection of data on a cell-by-cell basis revealed changes in EPSCs in two of the three neurones displayed an increase in EPSC amplitude in SD118 (see Fig 5.11). Figure 5.11 summarises the effects of SD118 on EPSCs evoked at low frequency in combination with bursts of stimuli at 2 Hz.

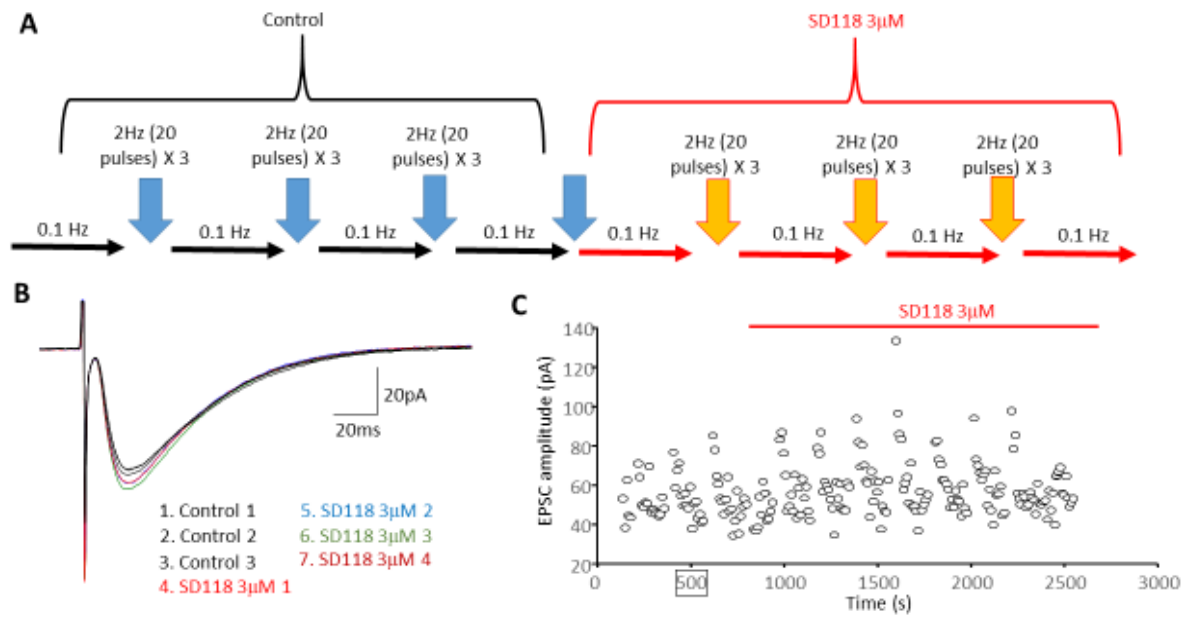


Figure 5.10. The effects of SD118 on EPSCs evoked at low frequency (with 2 Hz high frequency)

A. A schematic of the stimulation protocol used in this aspect of the study (0.1 Hz combined with 2 Hz stimulation protocols). B. Samples of a continuous record showing superimposed EPSCs evoked at 0.1 Hz in control, during application and in the presence of SD118 (each record is the average of 12 consecutively evoked EPSCs). C. Time-course plot of the effects of SD118 on EPSC evoked at 0.1 Hz.

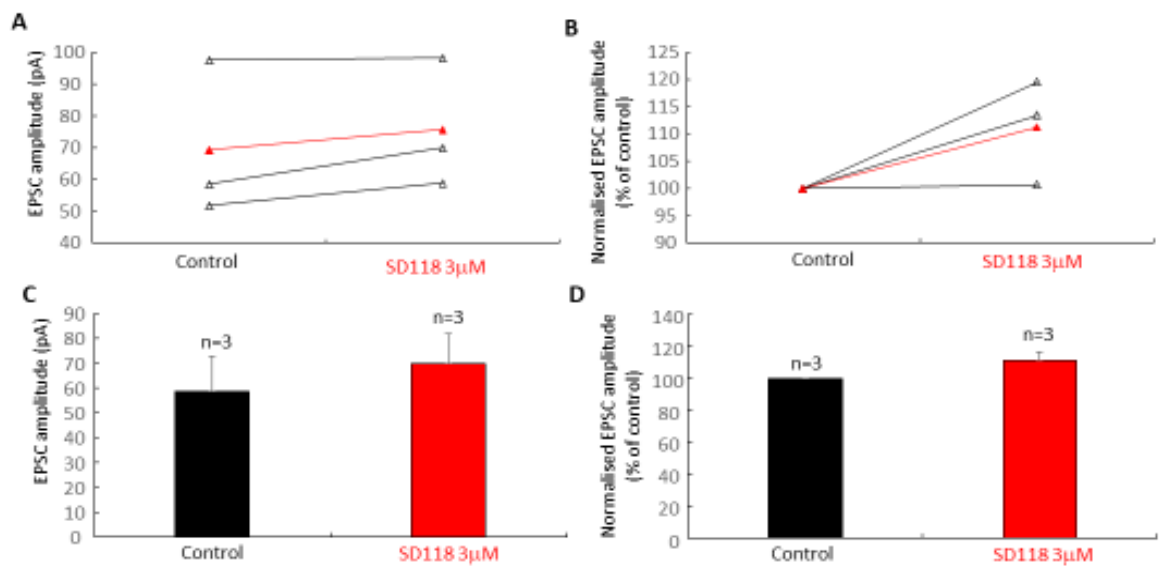


Figure 5.11. Summary data of the effects of SD118 on EPSCs evoked at low frequency (with 2 Hz high frequency)

A shows changes in amplitude of EPSCs evoked in each cell in the absence and presence of SD118 with data normalised to control shown in B. The red line indicates the mean of all cells. C shows a bar chart summarising changes in the mean peak amplitude of EPSCs in SD118 compared to control with the same data normalised to control shown in D (n = 3; error bars indicate SEM).

Analysis of EPSCs evoked by 2 Hz stimulation revealed EPSCs in control of peak amplitude 67.7 ± 19.0 pA (mean \pm sem; $n = 3$) for trial one of three 2 Hz trains, and increased to 73.7 ± 22.6 pA in SD118, amounting to a 108.2 ± 9.8 % increase in the amplitude of EPSCs. In trial 2 the mean peak amplitude of EPSCs evoked at 2 Hz was 74.8 ± 16.9 pA, increasing to 81.8 ± 21.5 pA, amounting to 108.5 ± 8.0 % of control values. Trial 3 EPSCs evoked at 2 Hz had mean peak amplitude of 75.7 ± 17.0 pA for control and increased to 81.2 ± 19.4 pA in SD118 corresponding to a 7.8 ± 8.6 % increase relative to control. When data from all trials were pooled, the mean peak EPSC amplitude was little changed in the presence of SD118 amounting to $108.2 \pm 8.7\%$ of control (100%). None of these effects of SD118 on EPSCs evoked at 2 Hz were statistically significant. Inspection of responses observed in individual cells revealed peak EPSC amplitude increased in 2 cells in the presence of SD118 and was reduced in one. Figures 5.12 shows an example of the effects of SD118 on EPSCs evoked at 2 Hz (3 trials). Figure 5.13 shows the pooled data for the effects of SD118 on EPSCs evoked at 2 Hz.

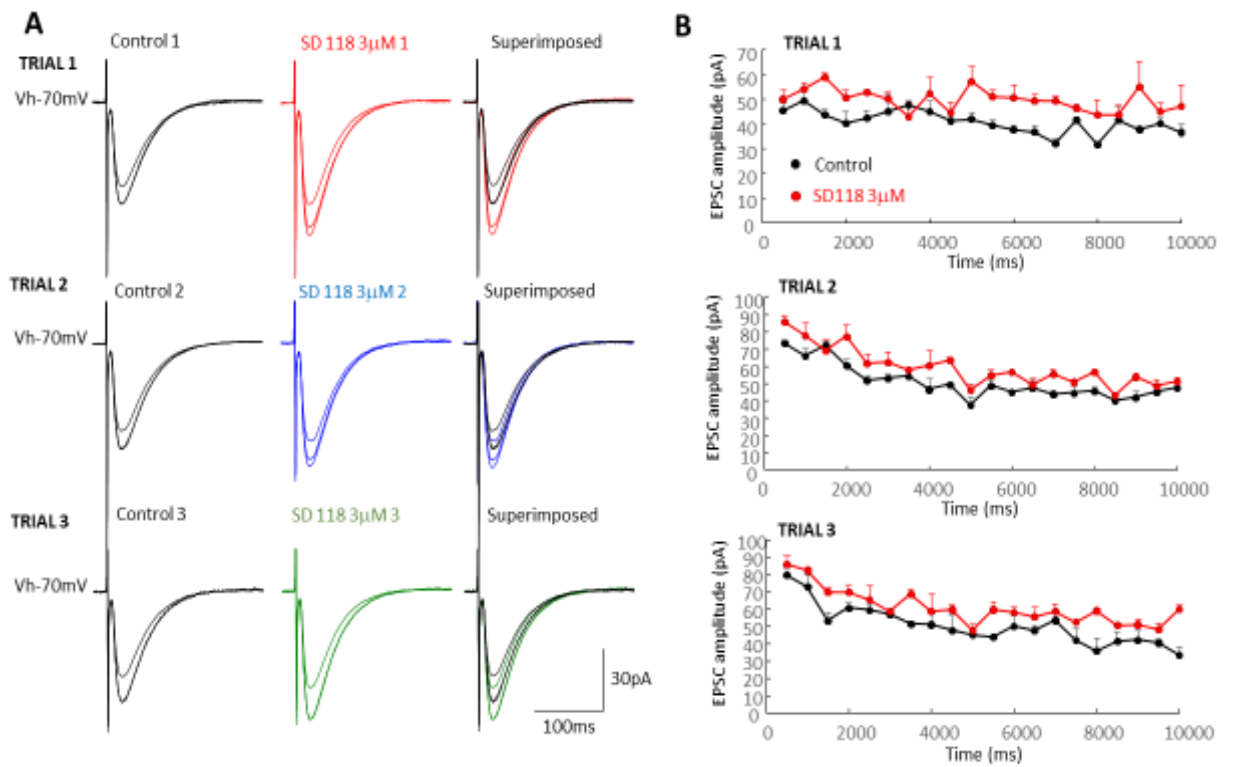


Figure 5.12. EPSCs during stimulation trials

A. Samples of a continuous record showing superimposed EPSCs evoked at 2Hz in control (3 individual trials) and during exposure of slices to SD118 (each record is the average of 20 consecutively evoked EPSCs). B-D. Time-course plots of the effects of SD118 on EPSCs evoked at 2Hz for trials, 1, 2 and 3, respectively for the cell shown in A. Error bars represent SEM.

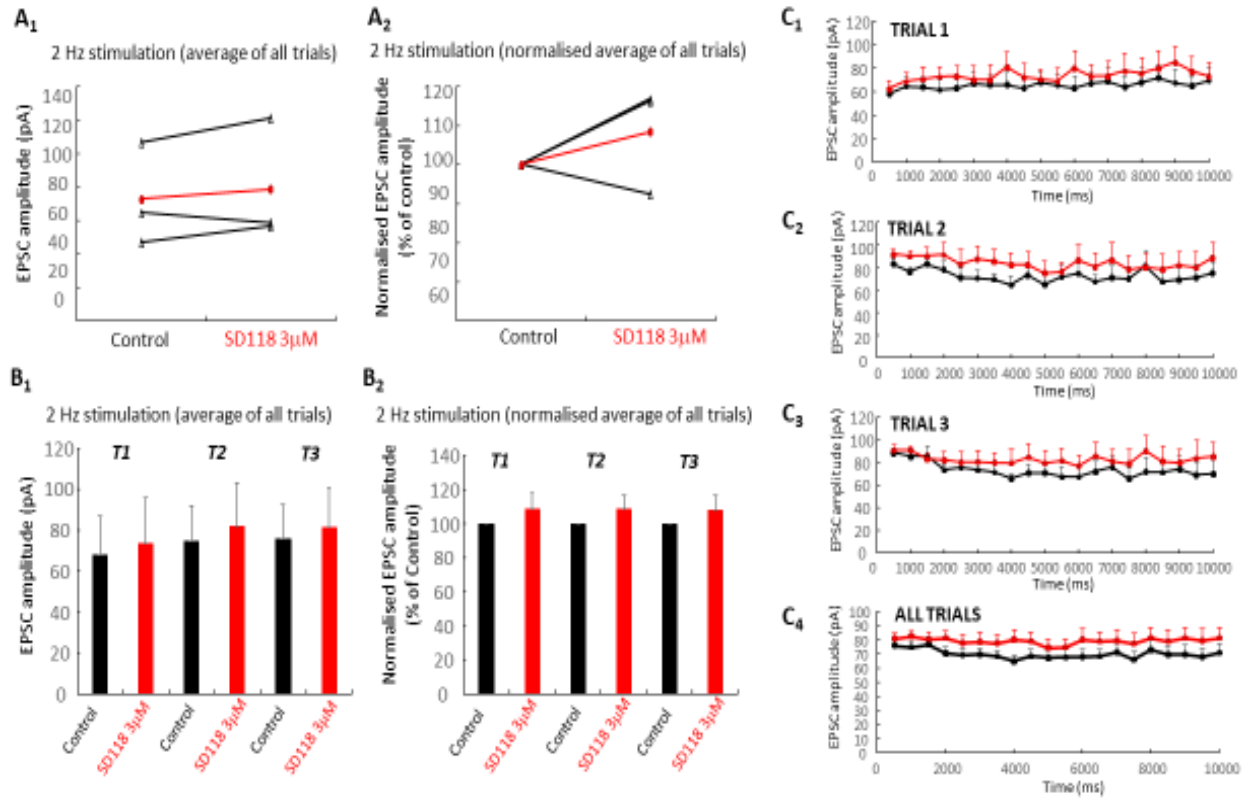


Figure 5.13. Summary data of the effects of SD118 on EPSCs evoked at 2 Hz

A shows changes in amplitude of EPSCs evoked in each cell with data normalised to control shown in A2. The red line indicates the mean of all cells. B shows a bar chart summarising mean peak amplitude of EPSCs amplitude in SD118 compared to control for each of the 3 trials for all cells with the same data normalised to control shown in B2. C shows time-course plots of data for all cells and trials 1 to 3 and the average of all trials pooled and displayed in C4. Error bars represent sem.

5.4.2.3 Frequency-dependent effects of SD118 on excitatory synaptic transmission: 5Hz

Whole-cell patch clamp recordings were obtained from 5 neurones (recorded from 5 slices from 4 animals) located in the CA1 region of the hippocampus. Neurones were clamped at a holding potential of -70 to -75mV in the voltage-clamp configuration and EPSCs evoked by stimulation of the Schaffer-collateral pathway at a frequency of 0.1 Hz, followed by 3 bursts of 5 Hz (see Fig 5.14 for details). The last 12 events evoked prior to high frequency stimulation were pooled for control and following exposure to SD118 and analysed to quantify the effects of SD118 on low-frequency synaptic transmission. Data from each EPSC evoked in individual trials of bursts were analysed for control and in the presence of SD118.

EPSCs evoked at low frequency stimulation (0.1Hz) had a mean peak amplitude of 92.6 ± 25.0 pA (mean \pm SEM; $n = 5$) and in the presence of SD118 (3 μ M) increased to 107.3 ± 30.2 pA. This increase in peak amplitude, to 115.5 ± 11.5 % of control (100%), was not statistically significant. Inspection of data on a cell-by-cell basis revealed changes in EPSCs in four of the five neurones with an increase in EPSC amplitude observed in SD118 in 3 cells (see Figure 5.14 and 5.15), a decrease in amplitude in 1 cell and no change in 1 cell. In 2 cells in which an increase in EPSC amplitude was observed in SD118, these effects were reversed following washout of the compound (e.g. see Figure 5.15). Figure 5.16 summarises the effects of SD118 on EPSCs evoked at low frequency (0.1 Hz) in combination with bursts of stimuli at 5 Hz.

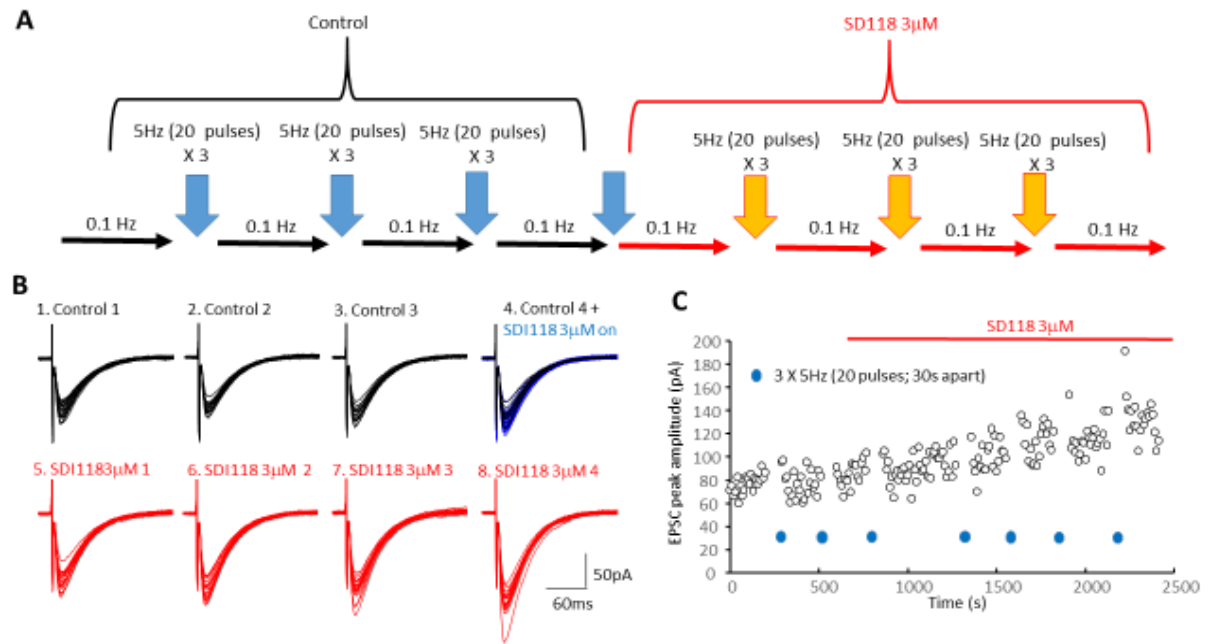


Figure 5.14. Summary of the effects of SD118 on EPSCs evoked at low frequency (with 5 Hz high frequency)

A. A schematic of the stimulation protocol used in this aspect of the study (0.1 Hz combined with 5 Hz stimulation protocols). B. Samples of a continuous record showing superimposed EPSCs evoked at 0.1Hz in control, during application and in the presence of SD118 (each record is the average of 12 consecutively evoked EPSCs). C. Time-course plot of the effects of SD118 on EPSC evoked at 0.1Hz.

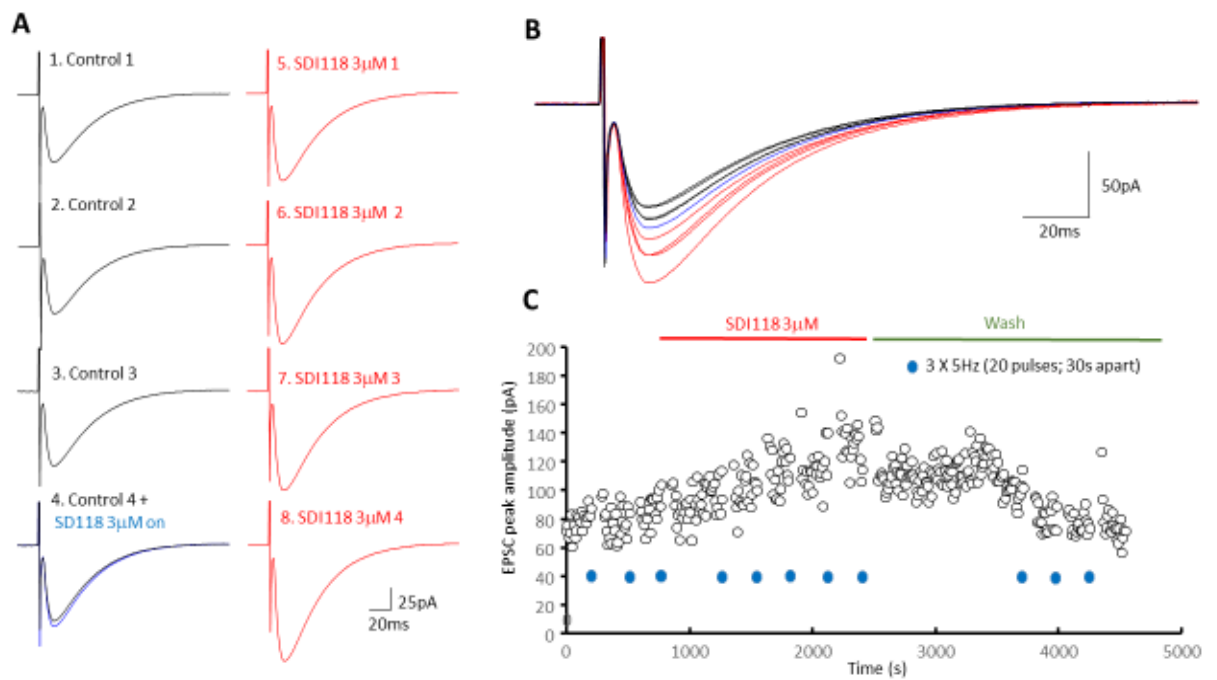


Figure 5.15. EPSCs during stimulation trials A. Samples of a continuous record showing superimposed EPSCs evoked at 0.1 Hz in control, during application and in the presence of SD118 (each record is the average of 12 consecutively evoked EPSCs shown superimposed in B). C. Same neurone as A and B showing a time-course plot of the effects of SD118 on EPSC evoked at 0.1 Hz. Note the increase in EPSC amplitude in SD118 and the reversal of this effect following washout of the compound.

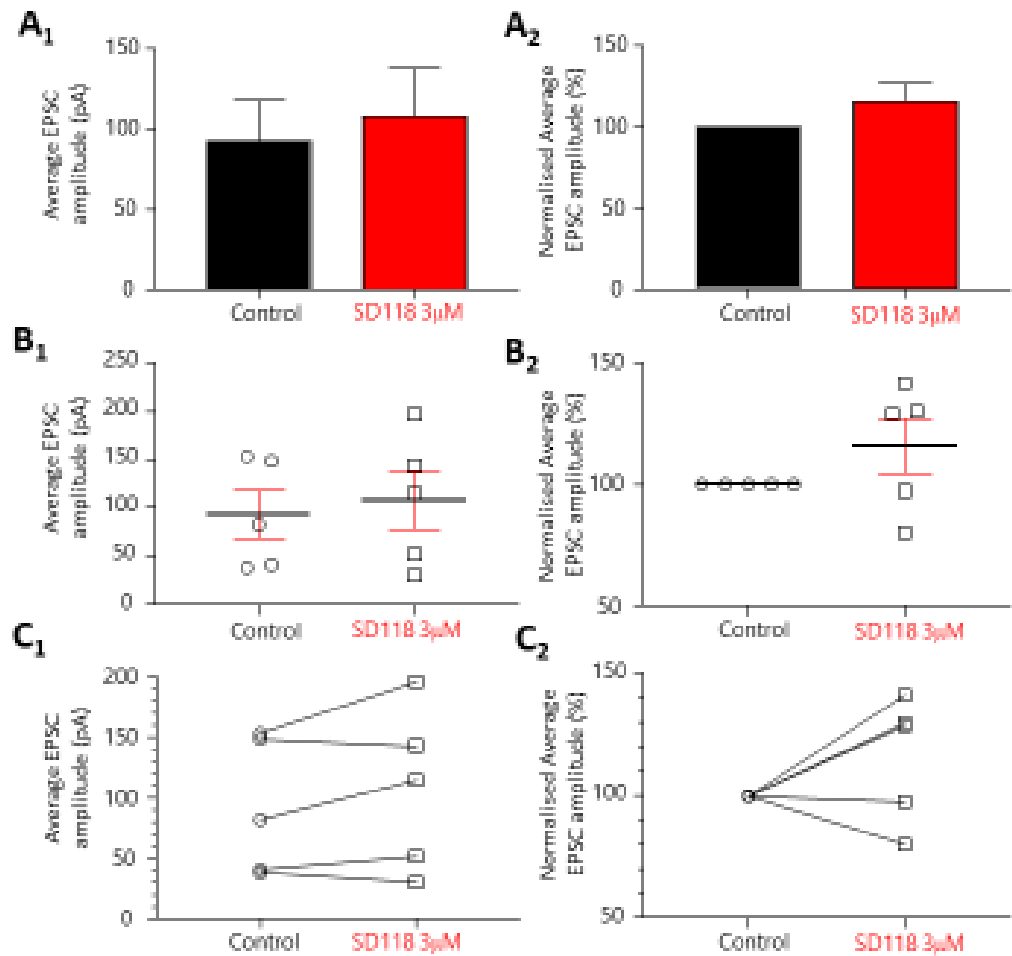


Figure 5.16. The effects of SD118 on EPSCs evoked at low frequency (with 5 Hz high frequency)

A shows a bar chart summarising changes in mean EPSC amplitude in SD118 compared to control with the same data normalised to control shown in A2. B Plot of the peak amplitude of EPSCs for each cell in the presence and absence of SD118 and the same data normalised to the controls shown in B2. C shows changes in amplitude of EPSCs evoked in each cell in the presence of SD118 with data normalised to control shown in C2.

Analysis of EPSCs evoked by 5 Hz stimulation revealed EPSCs in control amounting to 131.2 ± 31.3 pA (mean \pm SEM; $n = 5$) for trial one of the three 5 Hz trains and 134.2 ± 34.5 pA in SD118, amounting to a non-significant change in the amplitude of EPSCs. In trial 2 the mean peak amplitude of EPSCs evoked at 5 Hz was 123.8 ± 27.9 pA, increasing to 135.9 ± 33.5 pA, amounting to an increase in amplitude to 107.3 ± 5.6 % of control (100%), although again this was not significant. Trial 3 EPSCs evoked at 5 Hz had mean peak amplitude of 127.6 ± 30.9 pA for control and increased to 131.7 ± 31.6 pA in SD118 corresponding to a 103.8 ± 6.7 % of control (100%). As with other trials this small increase in EPSC amplitude in SD118 was not statistically significant. When data from all trials were pooled the mean peak amplitude of EPSCs was 127.6 ± 16.1 pA for control and 131.7 ± 17.8 pA for SD118, the latter corresponding to 103.7 ± 3.4 % of control (100%). Thus, SD118 had no significant effect on EPSCs evoked at a frequency of 5 Hz. Inspection of responses observed in individual cells revealed peak EPSC amplitude in 3 cells increased in the presence of SD118 and decreased in two. Figures 5.17 shows an example of the effects of SD118 on EPSCs evoked at 5 Hz (3 trials). Figure 5.18 and 5.19 shows the pooled data for the effects of SD118 on EPSCs evoked at 5 Hz for each trial (Figure 5.18) and with all data for all trials pooled (Figure 5.19).

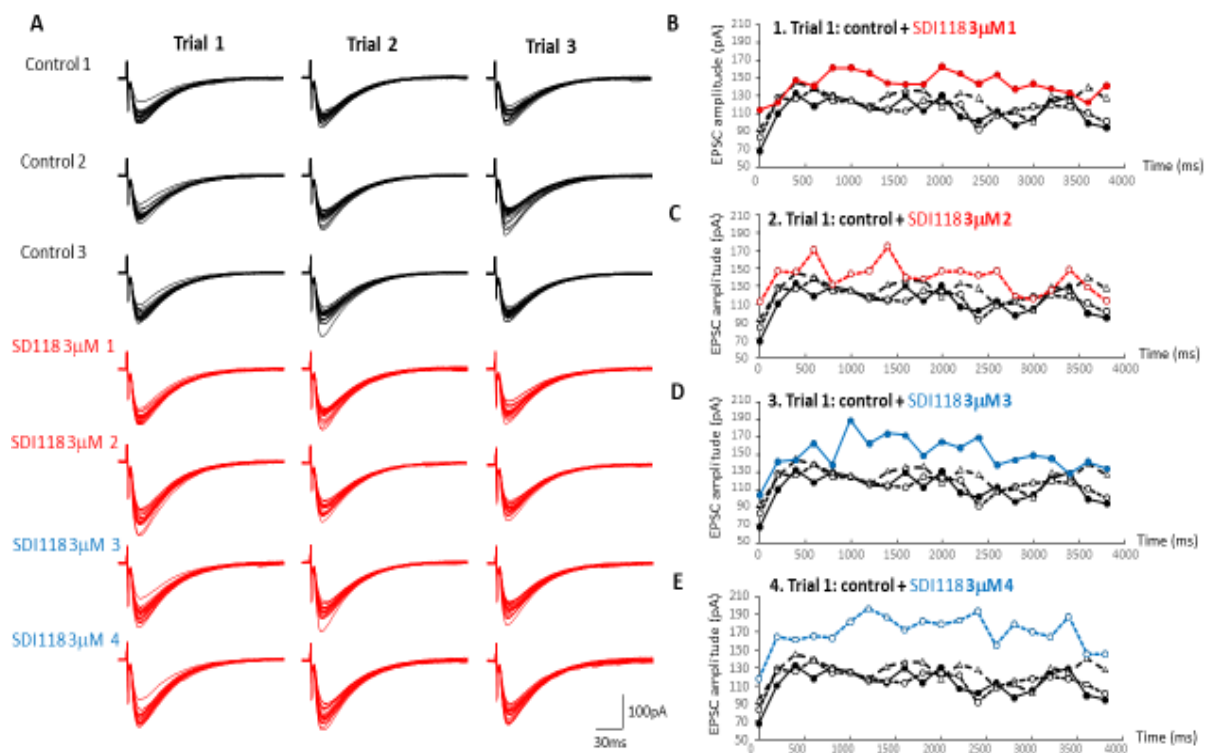


Figure 5.17. A summary of the frequency-dependent effects of SD118 on excitatory synaptic transmission at 5 Hz trials

A. Samples of a continuous record showing superimposed EPSCs evoked at 5 Hz in control (3 individual trials) and during exposure of slices to SD118 (each record shows 20 consecutively evoked EPSCs). B-E. Time-course plots of the effects of SD118 on EPSCs evoked at 5 Hz for trials, 1, 2 and 3, respectively for the cell shown in A. Note S118 3 μ M labelled 1 to 4 represents progressively repeating cycles of low and high frequency stimulation.

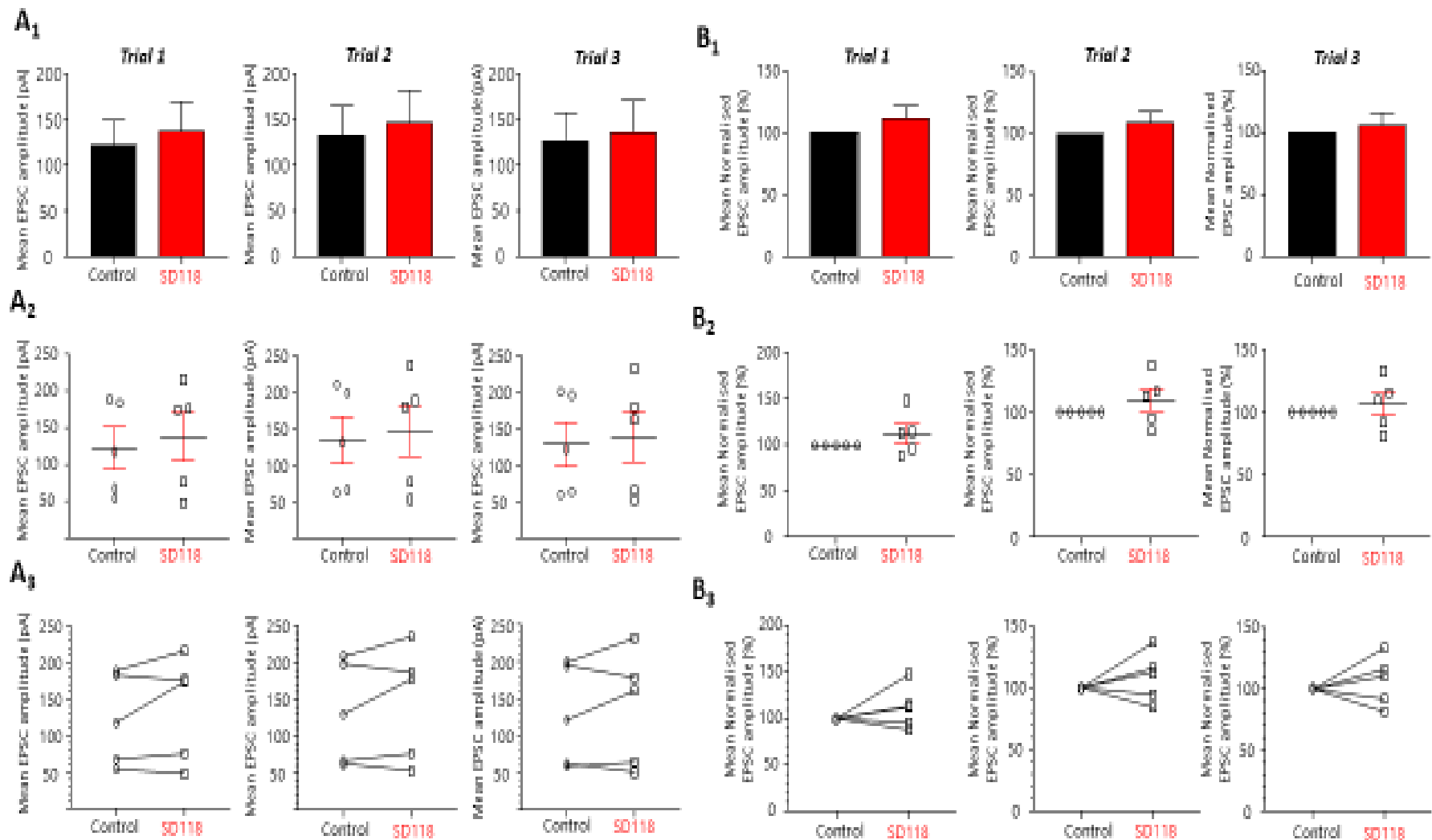


Figure 5.18. Summary data of the effects of SD118 on EPSCs evoked at 5 Hz. A1 shows bar charts of mean peak EPSC amplitude for control and in the presence of SD118 for each trial of 5Hz stimulation with data normalised to control shown in B1. Middle traces (A2) show peak amplitude of EPSCs for each cell in control and in SD118 with data normalised to controls shown in B2. C1 shows changes in peak amplitude of EPSCs for all cells in SD118 from control. SD118 had no significant effect on EPSCs evoked at 5 Hz.

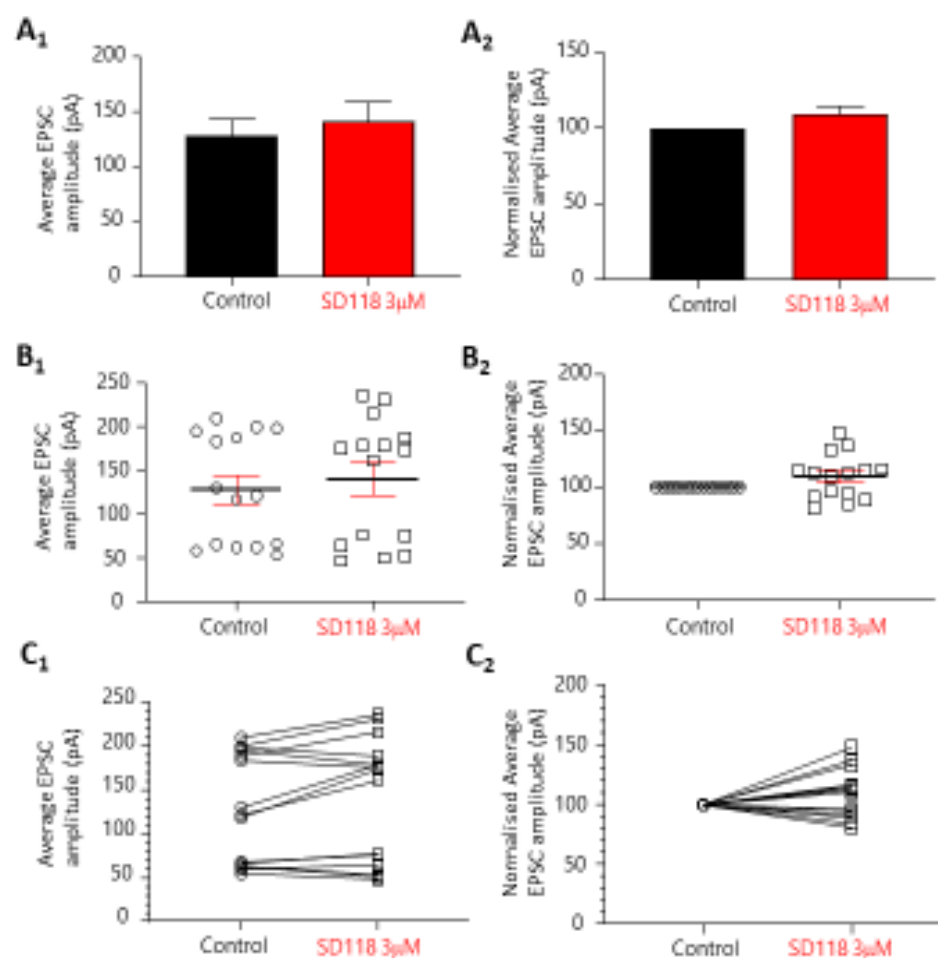


Figure 5.19. Summary data of the effects of SD118 on EPSC amplitudes evoked at 5 Hz

A shows bar charts representing mean peak amplitude of EPSCs for control and in the presence of SD118. Absolute values are shown in 1 and data normalised to control in 2 for all trials in all cells. B shows peak amplitude of EPSCs for each cell in control and in SD118 with data normalised to control in 2. C shows mean changes in peak amplitude of EPSCs in SD118 from control with data normalised in B. SD118 had no significant effect on EPSCs evoked at 5 Hz.

5.4.2.4 Frequency-dependent effects of SD118 on excitatory synaptic transmission: 10Hz

Whole-cell patch clamp recordings were obtained from a further 6 (recorded from 6 slices from 4 animals) neurones located in the CA1 region of the hippocampus. Neurones were clamped at a holding potential of -70 to -75mV in the voltage-clamp configuration and EPSCs evoked by stimulation of the Schaffer-collateral pathway at a frequency of 0.1 Hz, followed by 3 bursts or trains of 10 Hz (see Fig 5.20 for details). The last 12 events evoked prior to high frequency stimulation were pooled for control and following exposure to SD118 and analysed to quantify the effects of SD118 on low-frequency synaptic transmission. Data from each EPSC evoked in individual trials or 10 Hz bursts were analysed for control and in the presence of SD118.

EPSCs evoked at low frequency stimulation (0.1Hz) had a mean peak amplitude of 117.2 ± 52.4 pA (mean \pm SEM; $n = 6$) and, despite the variation, in the presence of SD118 (3 μ M) significantly increased to 152.0 ± 72.3 pA ($p = 0.014$; paired Student's t -test). This increase in peak amplitude, to 130.4 ± 6.0 % of control (100%), was even more significant when normalised to control ($p = 0.004$; paired Student's t -test). Inspection of data on a cell-by-cell basis revealed EPSCs in all 6 cells increased in peak amplitude in SD118 (3 μ M). In 2 cells in which an increase in EPSC amplitude was observed in SD118, these effects were reversed following washout of the compound (e.g., see Figure 5.20). Figure 5.21 summarises the effects of SD118 on EPSCs evoked at low frequency (0.1 Hz) in combination with bursts of stimuli at 10 Hz.

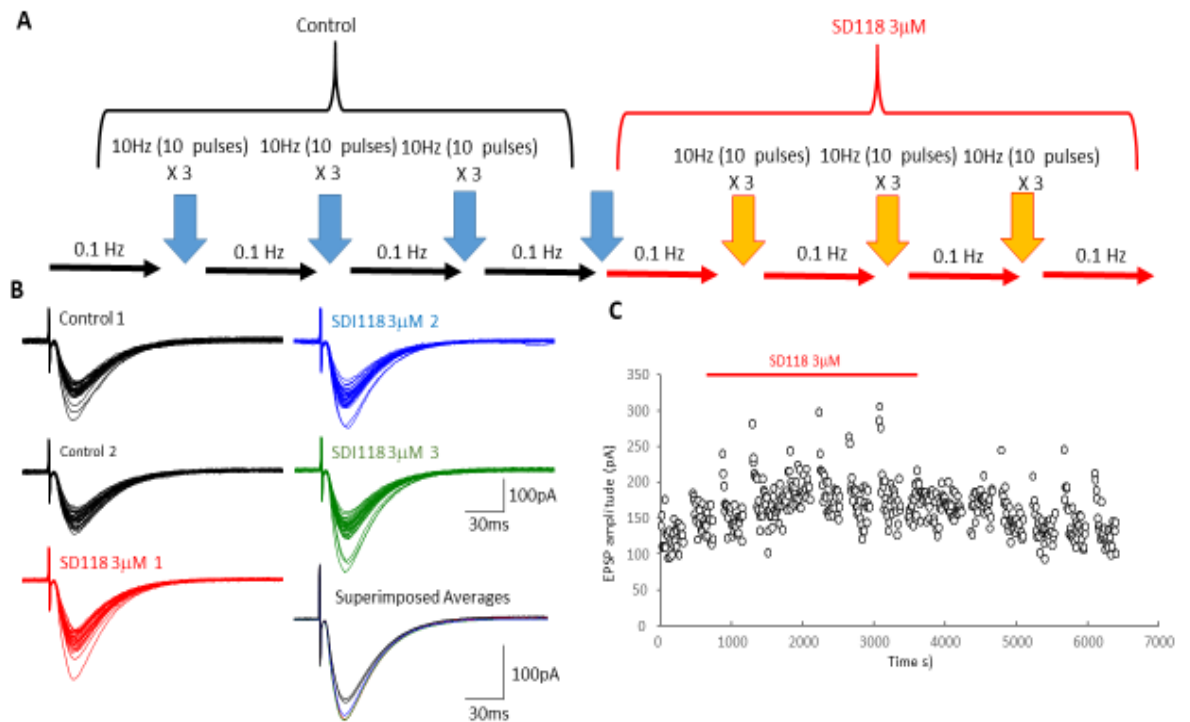


Figure 5.20. Summary data of the effects of SD118 on EPSCs evoked at low frequency (with 10 Hz high frequency) A. A schematic of the stimulation protocol used in this aspect of the study (0.1 Hz combined with 10 Hz stimulation protocols). B. Samples of a continuous record showing superimposed EPSCs evoked at 0.1Hz in control and in the presence of SD118 (each record shows 10 consecutively evoked EPSCs). C. Time-course plot of the effects of SD118 on EPSC evoked at 0.1Hz.

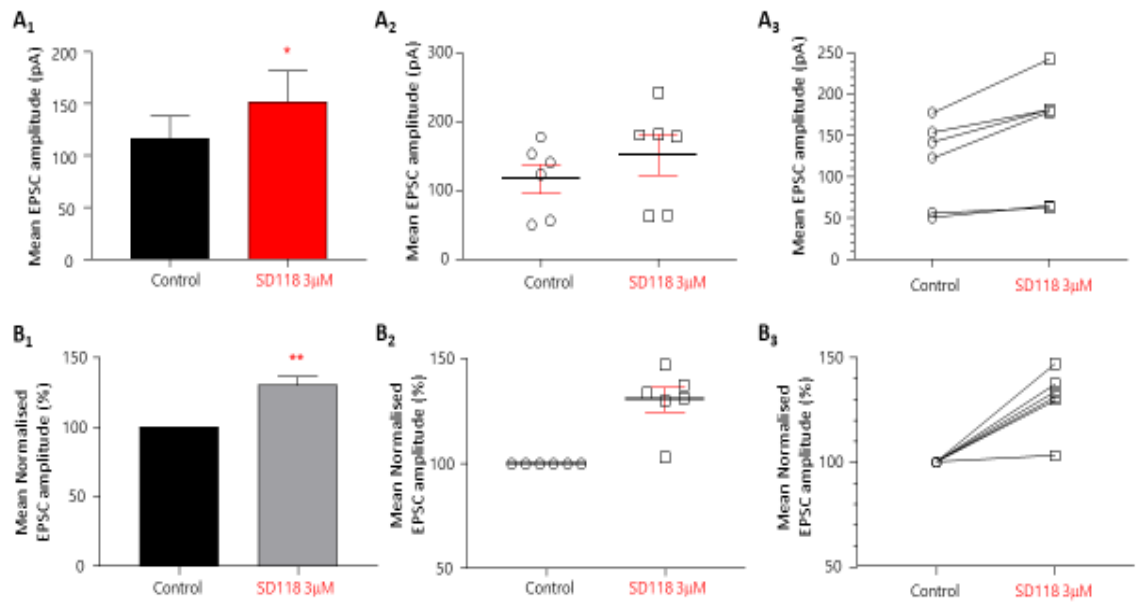


Figure 5.21. Summary data of the effects of SD118 on EPSCs evoked at 0.1 Hz (with 10 Hz high frequency stimulation)

A1 shows a bar chart summarising changes in EPSC amplitude in SD118 compared to control with the same data normalised to control shown in B1. A2 shows amplitude of EPSCs for each cell in presence and absence of SD118 and changes in amplitude relative to control shown in A3 with the corresponding data normalised shown in B2 and B3, respectively. Note the significant increase in EPSC amplitude in SD118 ($p = 0.014$ in A1 and $P = 0.004$ in B1).

Analysis of EPSCs evoked by 10 Hz stimulation revealed EPSCs in control amounting to 158.2 ± 22.8 pA (mean \pm SEM; $n = 6$) for trial one of the three 10 Hz trains and significantly increased to 192.6 ± 30.5 pA in SD118 ($p = 0.0022$; paired Student's t -test). This increase in peak amplitude of EPSCs in SD118 equates to 120.3 ± 6.1 % of control (100%; $p = 0.021$). In trial 2 the mean peak amplitude of EPSCs evoked at 10 Hz was 167.7 ± 24.6 pA, significantly increasing in SD118 to 194.6 ± 31.7 pA ($p = 0.015$), amounting to an increase in amplitude to 114.6 ± 2.1 % of control (100%), again representing a significant increase in EPSC amplitude in SD118 ($p = 0.001$). Trial 3 EPSCs evoked at 10 Hz had mean peak amplitude of 178.1 ± 27.8 pA for control and increased to 190.5 ± 31.1 pA in SD118 corresponding to a mean peak normalised EPSc amplitude of 106.3 ± 4.6 % of control (100%). This

effect was not statistically significant. When data from all trials were pooled the mean peak amplitude of EPSCs was 168.0 ± 13.8 pA for control and significantly increased to 192.6 ± 16.9 pA for SD118 ($p = 0.00013$), the latter corresponding to a magnitude of 113.7 ± 2.8 % of control (100%; $p = 0.00015$). Thus, SD118 significantly enhanced EPSCs evoked at a frequency of 10 Hz. Inspection of responses observed in individual cells revealed peak EPSC amplitude in 5 of 6 cells increased in the presence of SD118. Figures 5.22 shows an example of the effects of SD118 on EPSCs evoked at 10 Hz (3 trials). Figure 5.23 and 5.24 shows the pooled data for the effects of SD118 on EPSCs evoked at 10 Hz for each trial (Figure 5.23) and with all data for all trials pooled (Figure 5.24).

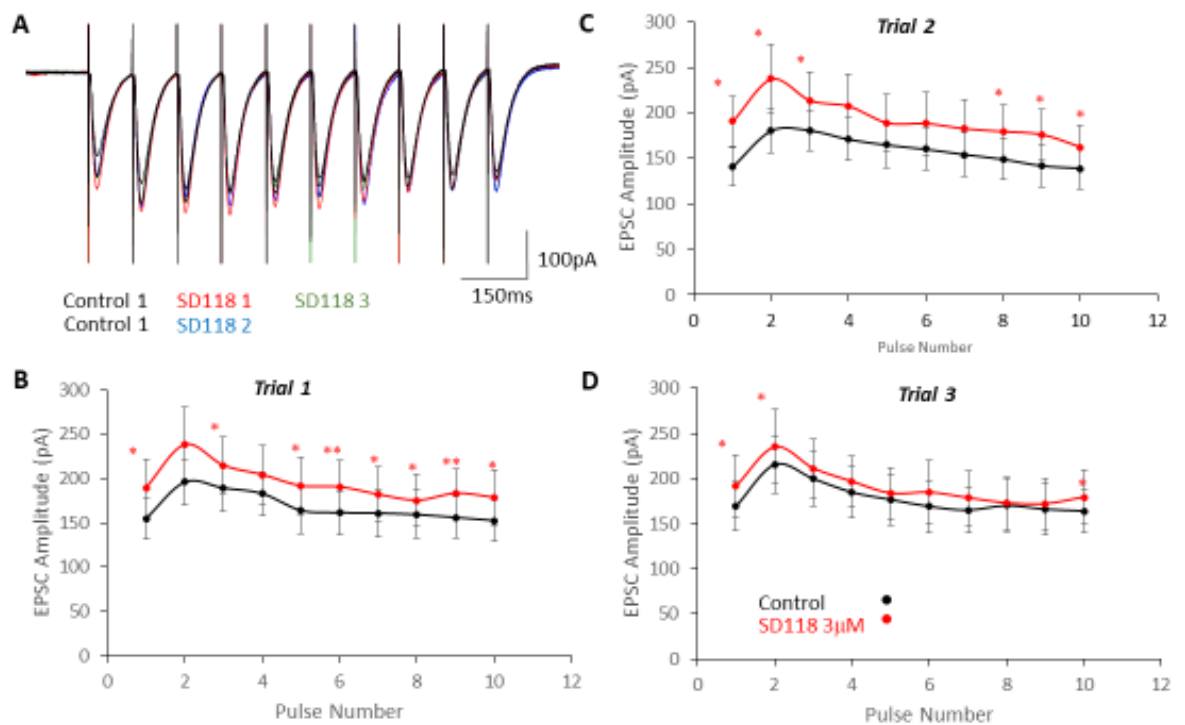


Figure 5.22. An example of the effects of SD118 on EPSCs evoked at 10 Hz (3 trials)

A. Samples of a continuous record showing superimposed trains of EPSCs evoked at 10Hz in control and during exposure of slices to SD118 (each record is the average of 3 trains of EPSCs). B-D. Time-course plots of the effects of SD118 on EPSCs evoked at 10Hz for trials, 1, 2 and 3. Note S118 3 μ M labelled 1 to 4 represent repeat cycles of low and high frequency stimulation. Error bars represent sem. Asterisks indicate significance at points along the train of EPSCs (paired Student's t-test).

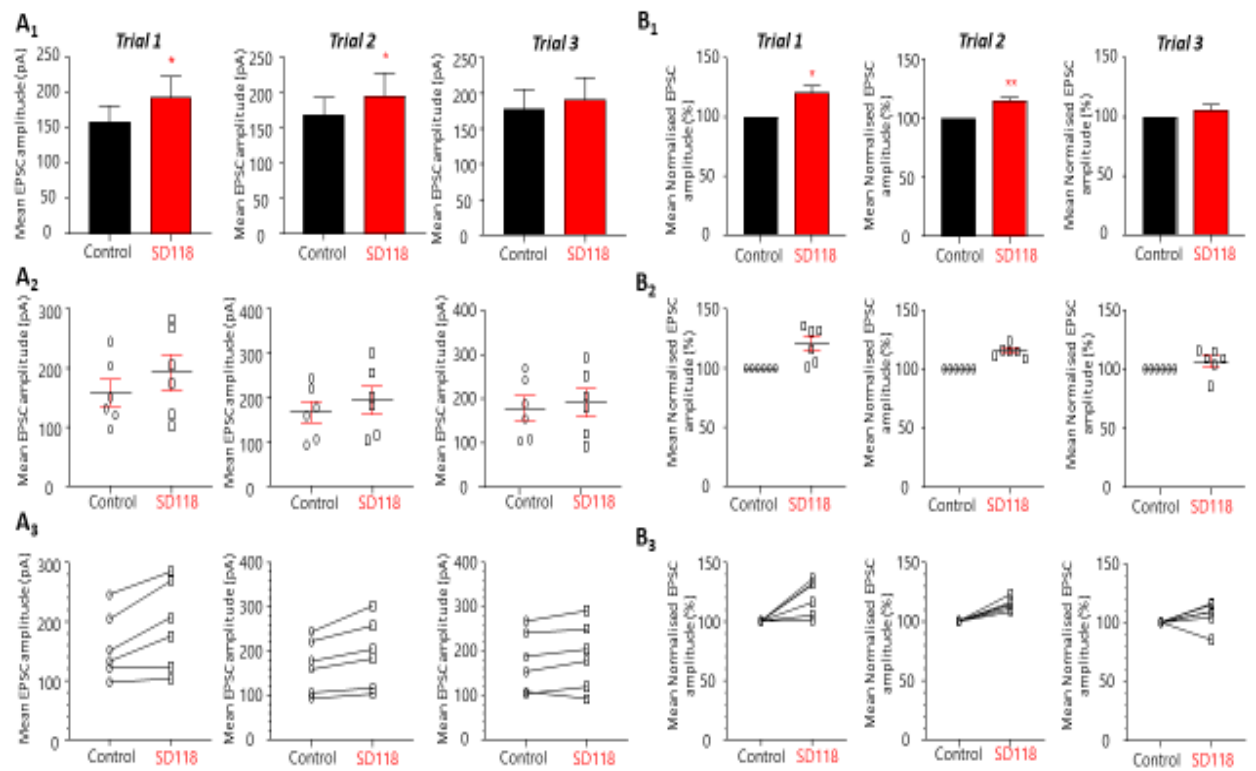


Figure 5.23. Summary data of the effects of SD118 on EPSCs evoked at 10 Hz.

A shows bar charts representing mean peak amplitude for each individual trial in control and presence of SD118. A2 shows mean peak amplitude of EPSCs for each cell in control and in SD118 for each trial. A3 shows mean changes in peak amplitude of EPSCs in SD118 from control levels. Panels shown in B represents the corresponding data from A panels normalised to control. SD118 significantly increased EPSC amplitude associated with trials 1 and 2 but had no significant effect on trial 3.

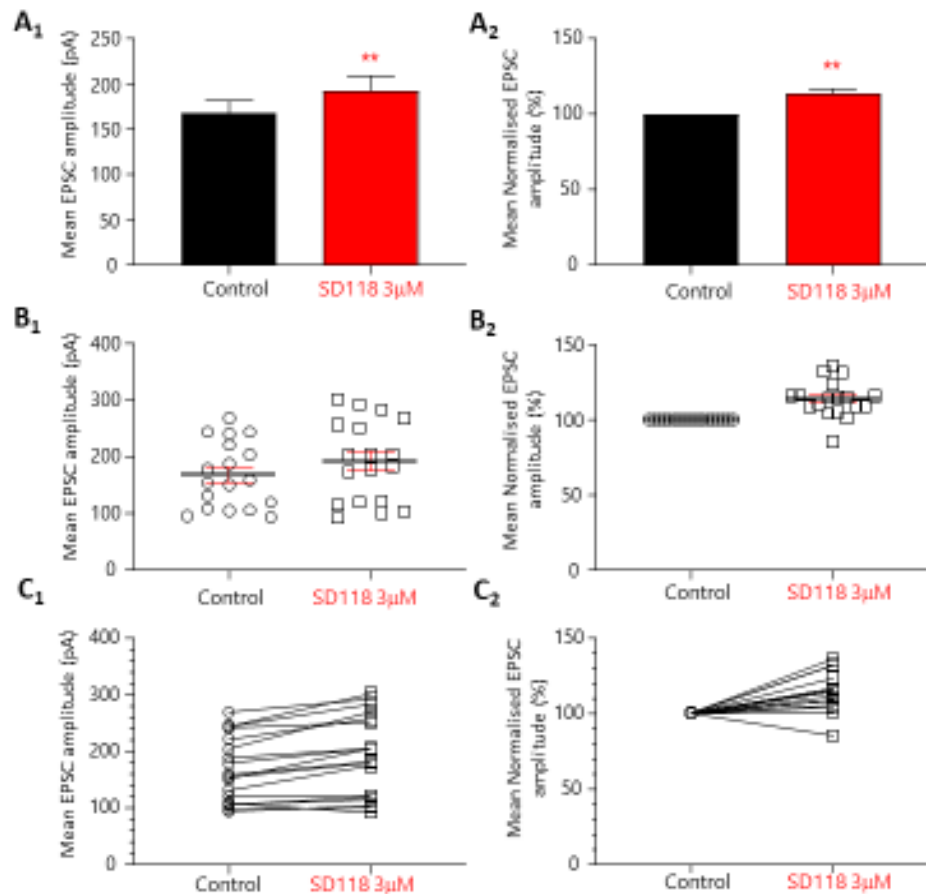


Figure 5.24. Summary data of the effects of SD118 on EPSCs evoked at 10 Hz with data pooled from all trials.

A shows bar charts representing mean peak amplitude of EPSCs for control and in the presence of SD118. Absolute values are shown in 1 and data normalised to control in 2 for all trials in all cells. B shows peak amplitude of EPSCs for each cell in control and in SD118 with data normalised to control in 2. C shows changes in mean peak amplitude of EPSCs in SD118 from control with data normalised in 2. SD118 significantly increased EPSCs peak amplitude evoked at 10 Hz.

5.4.2.5 Frequency-dependent effects of SD118 on excitatory synaptic transmission: 20Hz

Whole-cell patch clamp recordings were obtained from a further 6 neurones (recorded from 6 slices from 5 animals) located in the CA1 region of the hippocampus. Neurones were clamped at a holding potential of -70 to -75mV in the voltage-clamp configuration and EPSCs evoked by stimulation of the Schaffer-collateral pathway at a frequency of 0.1 Hz, followed by 3 bursts of 20 Hz (see Fig 5.25 for details). The last 12 events evoked prior to high frequency stimulation were pooled for control and following exposure to SD118 and analysed to quantify the effects of SD118 on low-frequency synaptic transmission. Data from each EPSC evoked in individual trial of bursts were analysed for control and in the presence of SD118.

EPSCs evoked at low frequency stimulation (0.1Hz) had a mean peak amplitude of 87.4 ± 20.9 pA (mean \pm SEM; $n = 6$) and significantly increased in the presence of SD118 (3 μ M) to 119.5 ± 30.9 pA ($p = 0.003$; paired Student's t -test). When normalised to controls, this increase in peak amplitude, to 134.6 ± 9.5 % of control (100%), was also significant ($p = 0.015$; paired Student's t -test). Inspection of data on a cell-by-cell basis revealed EPSCs in all 6 cells increased in peak amplitude in SD118 (3 μ M), markedly in 5 of these. In 2 cells in which an increase in EPSC amplitude was observed in SD118, these effects were reversed following washout of the compound (e.g., see Figures 5.25, 5.26 and 5.27). Figure 5.28 summarises the effects of SD118 on EPSCs evoked at low frequency (0.1 Hz) in series with bursts of stimuli at 20 Hz.

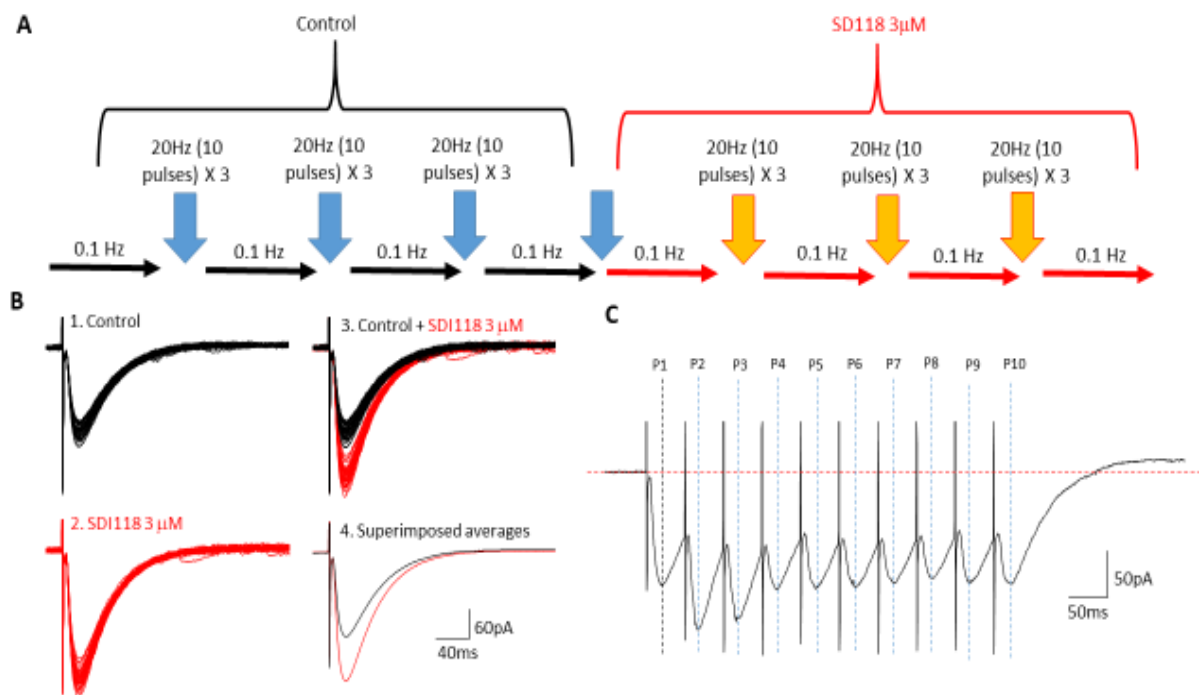


Figure 5.25. A summary of the frequency-dependent effects of SD118 on excitatory synaptic transmission

A. A schematic of the stimulation protocol used in this aspect of the study (0.1 Hz combined with 20 Hz stimulation protocols). B. Samples of a continuous record showing superimposed EPSCs evoked at 0.1Hz in control (1) and in the presence of SD118 (2) shown superimposed in 3 (each record shows 12 consecutively evoked EPSCs). B4 shows superimposed averages of the data shown in 1 to 3). C. Diagram outlining how peak amplitude of EPSCs was determined in 20 Hz trains, these trains showing possible facilitation of individual EPSCs. All peak amplitude measurements were made relative to baseline before the onset of the train of stimuli.

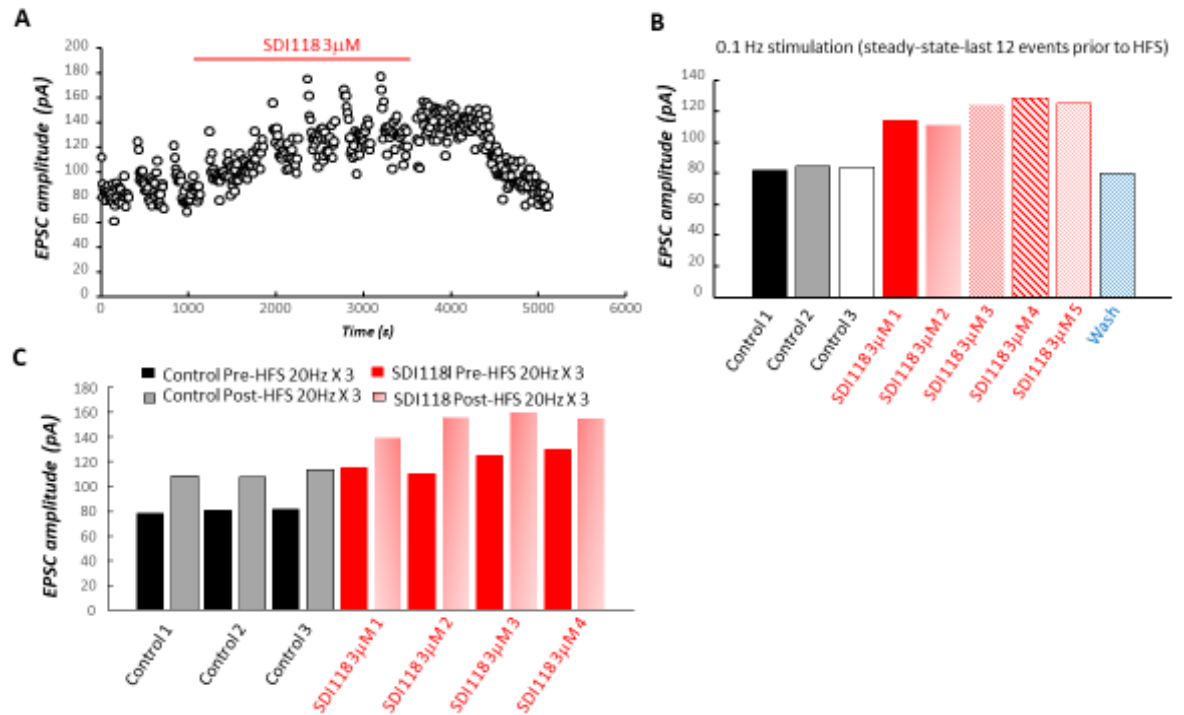


Figure 5.26. The reversal of the SD118 effect

A. Time-course plot showing the effects of SD118 on EPSCs evoked at 0.1Hz. Note the increase in peak amplitude of EPSCs in the presence of SD118, effects that were reversed on washout of the compound. B. Bar chart summarising data shown in A with mean peak amplitude of EPSCs shown at progressive time-points for control, through application of SD118 and following wash. C. Bar chart summarising data shown in A highlighting change in EPSC amplitude before and following high frequency stimulation (20Hz X 3). Note the increase in peak amplitude of EPSCs evoked at low frequency immediately following the 3-train high-frequency bursts.

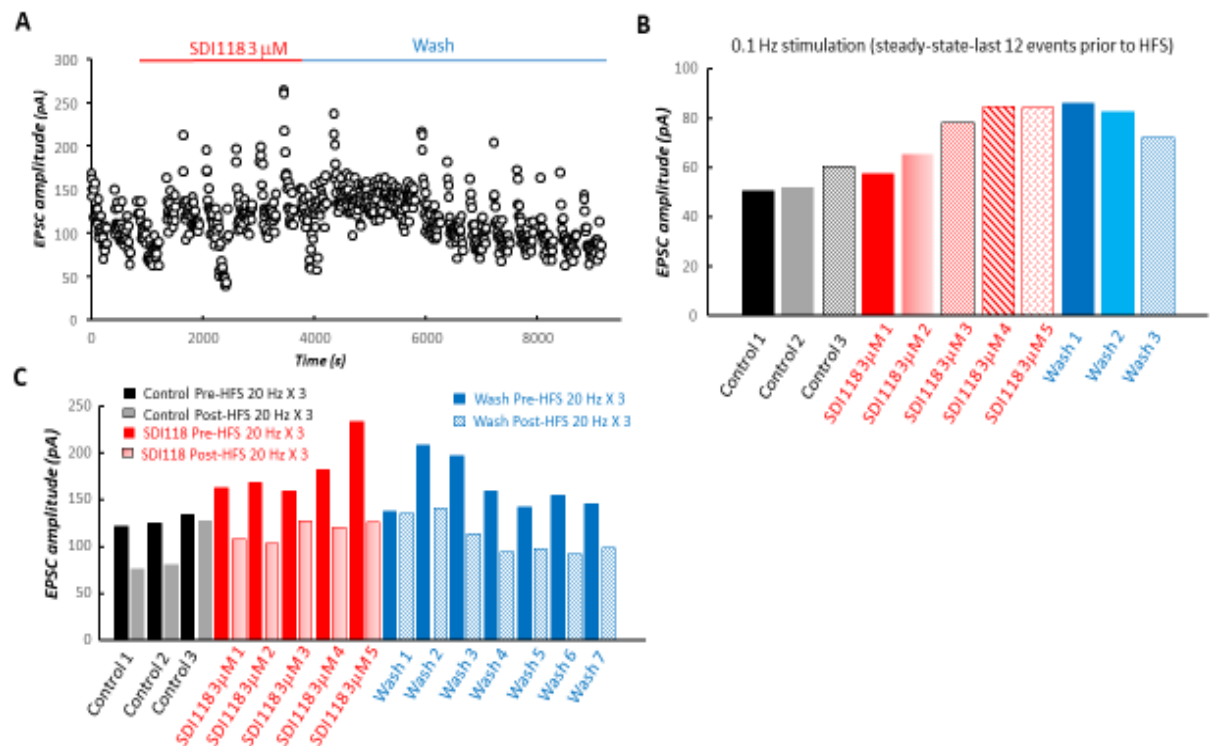


Figure 5.27. The reversal of the SD118 effect on EPSC amplitudes

A. Time-course plot showing the effects of SD118 on EPSCs evoked at 0.1Hz. Note the increase in peak amplitude of EPSCs in the presence of SD118, effects that were reversed on washout of the compound. B. Bar chart summarising data shown in A with mean peak amplitude of EPSCs shown at progressive time-points for control, through application of SD118 and following wash. C. Bar chart summarising data shown in A highlighting change in EPSC amplitude before and following high frequency stimulation (20Hz X 3).

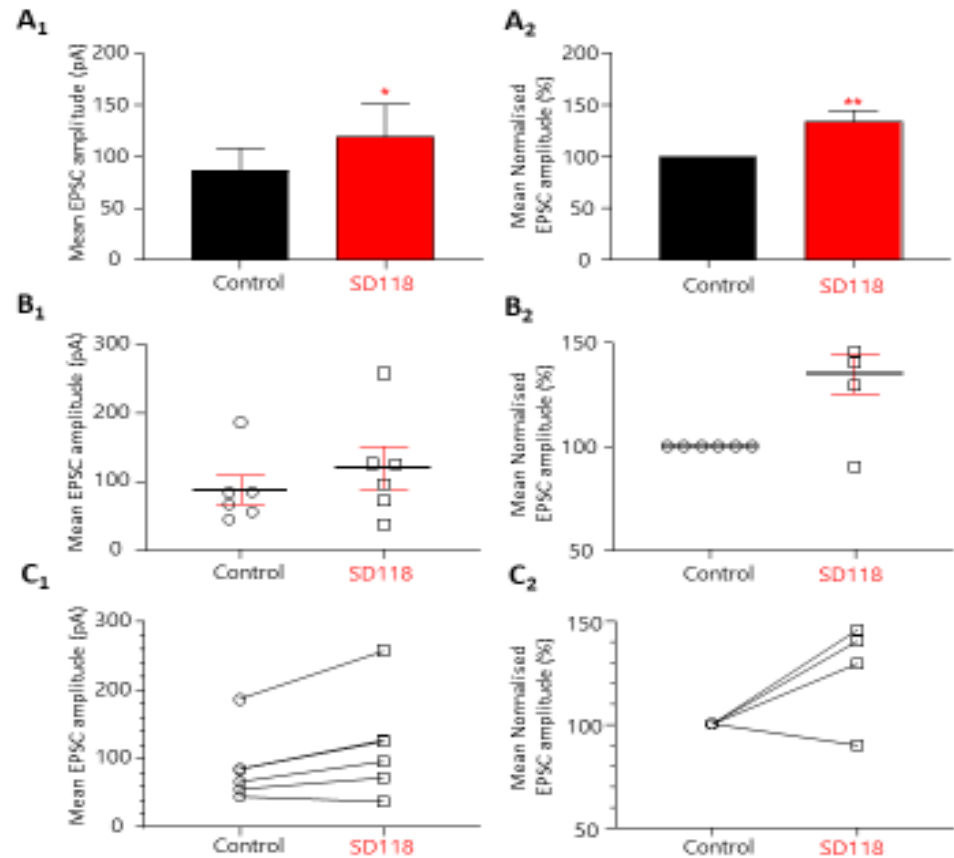


Figure 5.28. Summary data of the effects of SD118 on EPSCs evoked at 0.1 Hz (with 20 Hz high frequency trains)

A1 shows a bar chart summarising changes in EPSC amplitude in SD118 compared to control with the same data normalised to control shown in A2. B1 shows amplitude of EPSCs for each cell in the presence and absence of SD118 and changes in amplitude relative to control with data normalised to control shown in B2. C1 shows data for individual cells and changes in mean peak EPSC amplitude induced by SD118 relative to controls for each cell. C2 shows the same data as shown in 1 normalised to control baseline levels. Note the significant increase in EPSC amplitude in SD118.

Analysis of EPSCs evoked by 20 Hz stimulation yielded EPSCs in control amounting to 141.7 ± 29.0 pA (mean \pm SEM; $n = 6$) for trial 1 of the three 20 Hz trains and increased to 151.0 ± 23.5 pA in SD118 (not significant). This increase in peak amplitude of EPSCs in SD118 equates to 110.9 ± 5.6 % of control (100%; ns). In trial 2 the mean peak amplitude of EPSCs evoked at 20 Hz was 145.0 ± 35.1 pA, significantly increasing to 177.3 ± 46.7 pA ($p = 0.043$) in SD118, amounting to an increase in amplitude to 120.2 ± 3.8 % of control (100%), again representing a significant increase in EPSC amplitude in SD118 ($p = 0.003$; paired student t-test). Trial 3 EPSCs evoked at 20 Hz had mean peak amplitude of 117.0 ± 18.1 pA for control and increased to 171.0 ± 41.5 pA in SD118 corresponding to an increase in peak EPSC amplitude to 116.8 ± 14.4 % of control (100%). This effect was not statistically significant. When data from all trials were pooled the mean peak amplitude of EPSCs was 138.1 ± 17.7 pA for control and significantly increased to 166.4 ± 21.1 pA for SD118 ($p = 0.01016$), the latter corresponding to a magnitude of 115.8 ± 3.7 % of control (100%; $p = 0.0008$). Thus, SD118 significantly enhanced EPSCs evoked at a frequency of 20 Hz. Inspection of responses observed in individual cells revealed peak EPSC amplitude in 4 of 6 cells increased in the presence of SD118, decreased in one cell and had no effect in one cell. Figures 5.29 shows an example of the effects of SD118 on EPSCs evoked at 20 Hz (3 trials). Figure 5.30 and 5.31 shows the pooled data for the effects of SD118 on EPSCs evoked at 20 Hz for each trial (Figure 5.30) and with all data for all trials pooled (Figure 5.31).

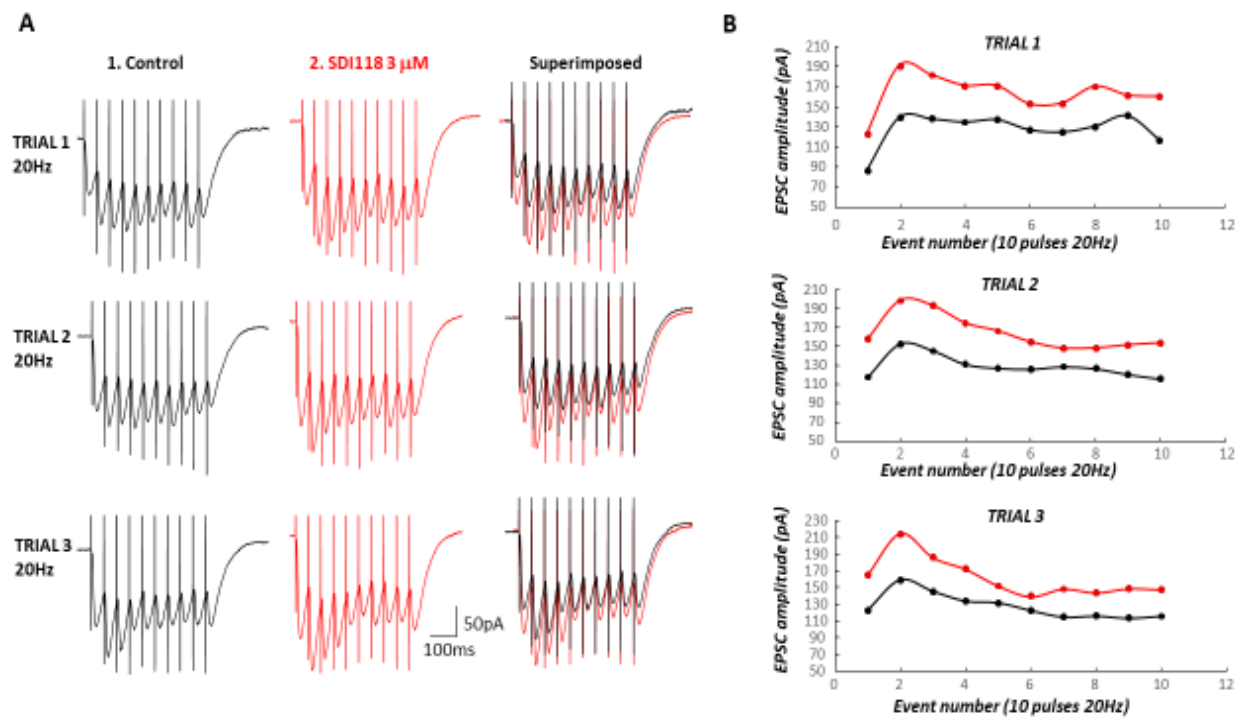


Figure 5.29. An example of the effects of SD118 on EPSCs evoked at 20 Hz (3 trials)

A. Samples of a continuous record showing trains of EPSCs evoked at 20Hz in control (3 individual trials), during exposure of slices to SD118 and shown superimposed in the far-right panels. B. Time-course plots of the effects of SD118 on EPSCs evoked at 20Hz for trials, 1, 2 and 3, respectively for the cell shown in A. Note the increase in amplitude of EPSCs in the presence of SD118.

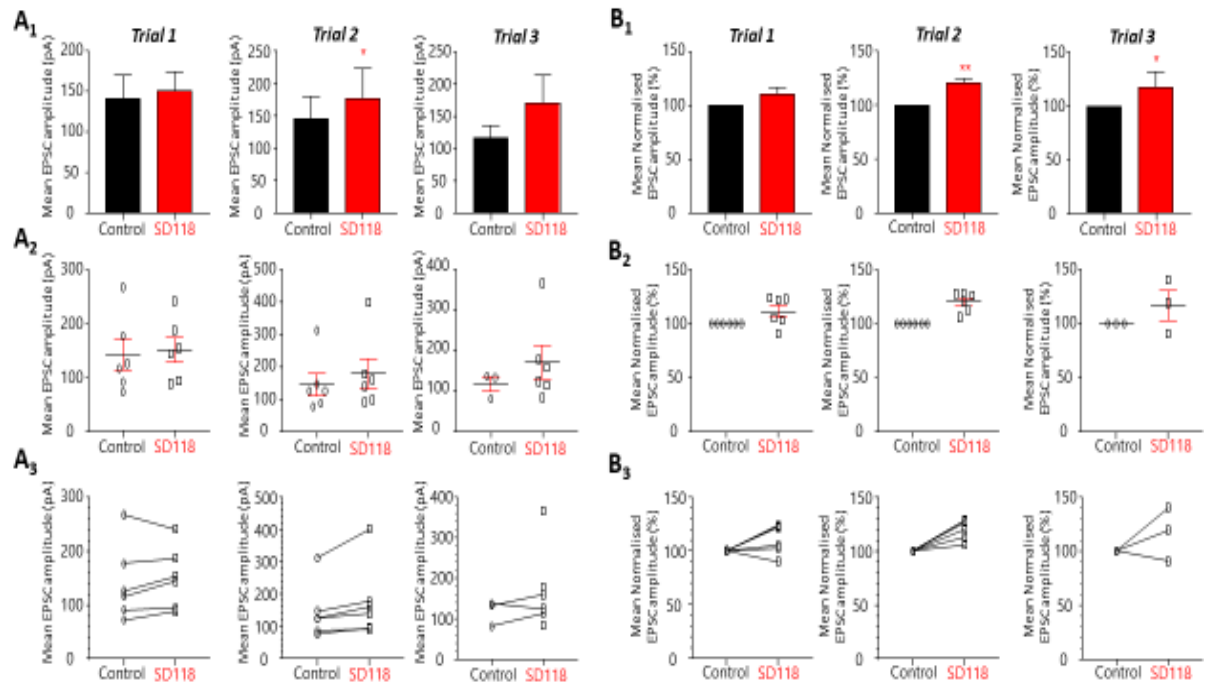


Figure 5.30. Summary data of the effects of SD118 on EPSCs evoked at 20 Hz. A1 shows bar charts representing mean EPSC amplitude in control and in the presence of SD118 for each individual trial. Corresponding data normalised to controls is shown in B1. Note the increase in mean peak amplitude of EPSCs in trials/trains 2 and 3, the latter when data was normalised to controls. A2 shows changes in amplitude of EPSCs evoked in each individual cell with data normalised to control shown in B2. C1 shows changes in mean peak amplitude of EPSCs for each cell in SD118 from control and C2 shows the same data normalised to control.

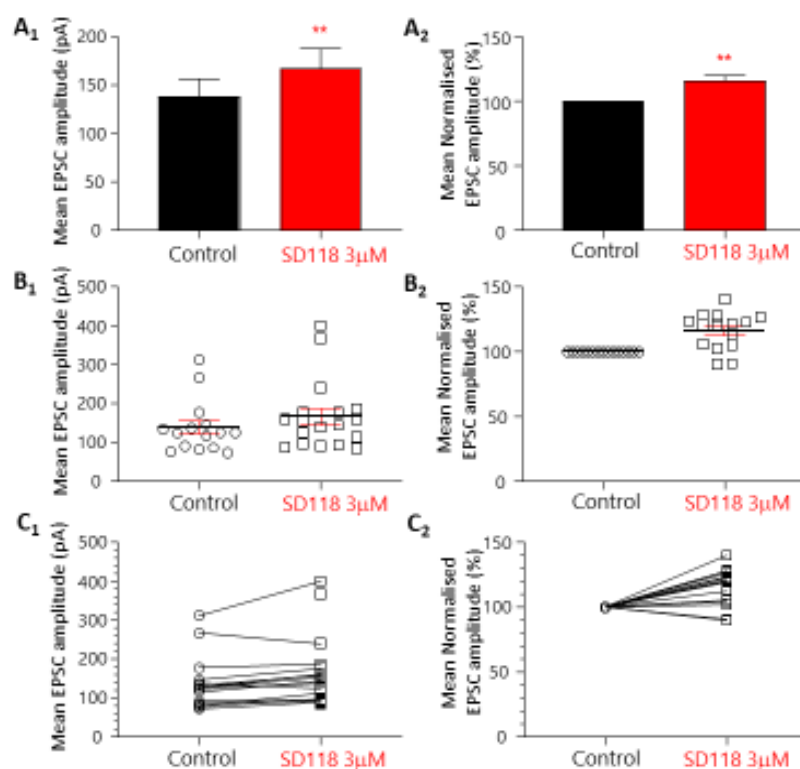


Figure 5.30. Summary data of the effects of SD118 on EPSCs evoked at 20 Hz with data pooled from all cells and all trials.

A shows bar charts representing mean peak amplitude of EPSCs for control and in the presence of SD118. Absolute values are shown in 1 and data normalised to control in 2 for all trials in all cells. B shows peak amplitude of EPSCs for each cell in control and in SD118 with data normalised to control shown in 2. C shows changes in mean peak amplitude of EPSCs in SD118 from control with data shown normalised to control in 2. SD118 significantly increased EPSCs peak amplitude evoked at 20 Hz.

5.5. Discussion

The aim of the current study was to provide insight into the mechanism of action of the novel cognitive enhancing drug SD118, a compound developed by Syndesi using Levetiracetam as the scaffold structure. Like Levetiracetam, SD118 targets the synaptic vesicle protein SV2A, confirmed by binding studies showing SD118 binding to this protein and displacing Levetiracetam (Syndesi, personal communication). The principal findings from the current study described here were that SD118 had no effect

on excitatory synaptic transmission evoked at low frequency alone (0.1 to 2 Hz) in the hippocampus. However, using whole-cell patch clamp recording techniques in hippocampal brain slices here we demonstrate a frequency-dependent effect of SD118. The stimulation protocol we employed was designed to investigate the effects of SD118 on a range of frequencies of stimulation and also to investigate the effects of high frequency stimulation on subsequent low frequency synaptic transmission in the presence of SD118. SD118 had little or no effect on pharmacologically isolated AMPA receptor-mediated EPSCs evoked at 0.1 Hz with 1 and 2 Hz. Although SD118 had no statistically significant effect on EPSCs evoked at 5 Hz and subsequently 0.1Hz there was a trend towards enhanced synaptic transmission. At higher frequencies, 10 and 20Hz, SD118 induced an increase in excitatory synaptic transmission both for EPSCs evoked at 10 Hz and 20 Hz and increased EPSC amplitude at low frequency (0.1 Hz) in the same neurones challenged with 10Hz and 20Hz trains of stimuli. Figure 5.3.1 shows a summary comparison of the effects of SD118 on EPSCs evoked over a range of frequencies and low frequency stimulation monitored in the same cells. Thus, the principal mechanism of action of SD118 is to enhance excitatory synaptic transmission in a frequency-dependent manner.

Previous research with Levetiracetam has shown this compound to suppress both excitatory and inhibitory synaptic transmission. This effect is only apparent at higher frequencies of stimulation (20-80Hz; Meehan *et al.*, 2012; 2011; Yang *et al.*, 2007; Yang & Rothman, 2009). This frequency-dependence is thought to reflect synaptic vesicle fusion and recycling facilitating Levetiracetam access to synaptic vesicles and subsequently to bind to SV2A (Meehan *et al.*, 2011). Although multiple functions of SV2A have been suggested, its only clearly defined function is its interaction with synaptotagmin, SV2 modulating both the levels of expression of this protein and its trafficking in the synapse (Nowak *et al.*, 2010; Yao *et al.*, 2010; Zhang *et al.*, 2015; Kaempf *et al.*, 2015).

That SV2A is a principal target of Levetiracetam and related compounds is also unquestionable: Levetiracetam binds SV2A (Lynch *et al.*, 2004); the anticonvulsant effect of Levetiracetam and related compounds directly correlates with their affinity for SV2A (Kaminski *et al.*, 2009); SV2A hypomorphic mice (SV2A^{+/-}) are less sensitive to the anticonvulsant effects of this compound (Kaminski *et al.*, 2012); over-expression of SV2A in cultured neurones gives rise to abnormal synaptic transmission that is reversed by Levetiracetam (Nowack *et al.*, 2011); SV2A acts as a “chaperone” for synaptotagmin and may play a role in both endo and exocytosis .

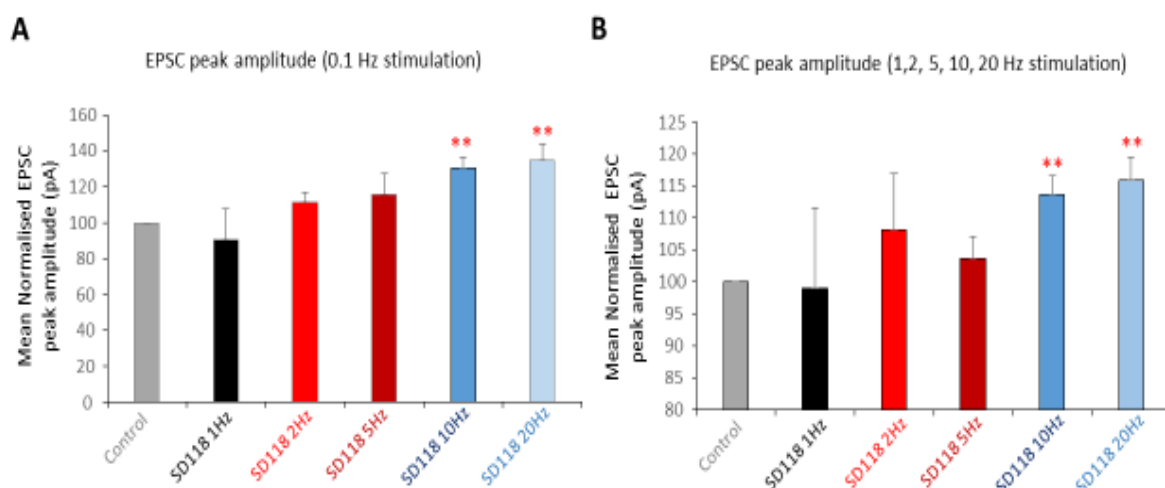


Figure 5.3.1. A. Summary overview data of the effects of SD118 on EPSCs evoked at a frequency of 0.1 Hz (in series with high frequency trains of stimuli at 1, 2, 5, 10 and 20Hz)

Note the frequency-dependent effect of SD118, EPSCs evoked at low frequency being enhanced when combined with higher frequency stimulation, the effect being significant when associated with 10 and 20 Hz trains of stimuli. B. Summary overview of the effects of SD118 on EPSCs evoked at increasing frequencies. Note SD118 enhanced EPSCs with increasing frequency of stimulation, the effect being significant for 10 and 20 Hz trains.

The effects of SD118 described here had a distinct similarity to effects described for Levetiracetam, specifically, the frequency-dependence of the effect. However, the outcomes are completely opposite, Levetiracetam suppressing EPSCs whereas SD118 enhanced EPSCs. From a functional perspective this fits with observations *in vivo* where Levetiracetam is anticonvulsant whereas SD118 has no anticonvulsant activity but enhances cognition (Syndesi, personal communication). SV2A has been shown to be needed to maintain pools of vesicles available for calcium-dependent exocytosis, the readily-releasable pool of vesicles being shown reduced in adrenal chromaffin cells of SV2A knockout animals (Xu & Bajjalieh, 2001). This study also suggested that SV2 modulates the formation of protein complexes needed for synaptic vesicle fusion and release of transmitters. Thus, SV2 appears critical in defining the pathway of vesicles to a fusion-competent state and in doing so modulates the size of the secretory vesicle readily-

releasable pool. As Levetiracetam suppresses excitatory synaptic transmission it is tempting to suggest that this compound acts as an inhibitor or antagonist leading to a loss of function of SV2A, whereas SD118 interacts with SV2A leading to a gain of function, acting as an agonist/activator of the protein.

Several observations over the course of this study suggest SD118 acts to increase the readily-releasable pool of vesicles at the synapse. Firstly, the observation that EPSCs were enhanced in a stimulus frequency-dependent manner. Secondly, although not systematically analysed here it was notable that following high frequency stimulation, EPSCs subsequently evoked at low frequency were initially significantly enhanced in SD118 compared to control. This effect was transient, EPSCs recovering relatively rapidly with progressive low frequency stimulation. It is tempting to speculate that during high frequency stimulation the readily-releasable pool is enhanced in the presence of SD118 underpinning an increase in transmitter release upon subsequent low frequency stimulation. In this scenario, whilst SD118 may act as a “positive activator/modulator” of SV2A function and levetiracetam as a “negative inhibitor/modulator” of SV2A function, there are other possible explanations. One possibility is that both compounds bind in the same manner to suppress the function of SV2A but with differential affinities. For example, if SD118 binds SV2A relatively weakly and/or in a use and activity-dependent manner and “unbinds” during inactivity at the synapse, periods of high frequency stimulation in SD118 may delay the preparation of the release competent readily releasable pool of vesicles. Following cessation of the high frequency stimulation and unbinding of SD118, the release competent readily releasable pool is increased giving rise to enhanced transmitter release upon subsequent stimulation. Supporting this notion is the fact that the effects of SD118 were relatively rapidly reversed upon washout of the compound suggesting the compound “unbinds” rapidly.

Since the concepts discussed above are somewhat speculative, further research is required to clarify the mechanism of action of SD118. One interesting feature of the frequency-dependent action of Levetiracetam is its time to take effect. A 3-hour incubation with the compound at high concentrations is required for the activity-dependent suppression of EPSCs whereas the effect on inhibitory synaptic transmission is faster (around 30 mins) and requires lower concentrations. Precisely why this is the case is unclear but may reflect poor membrane permeability of this compound or higher levels of activity at inhibitory synapses promoting its uptake into vesicles (see Meehan *et al.*, 2012). SD118, unlike levetiracetam is highly membrane permeable and thus most likely reaches its target rapidly, this being reflected in the relatively rapid onset effects of the compound on EPSCs once stimulation commences. However, further studies testing the effects of SD118 on IPSCs and studies with prolonged incubation periods would be of interest to further clarify the role of this compound in modulating synaptic vesicle trafficking and expression levels of trafficking proteins. Other studies using manipulations to alter presynaptic activity along with further electrophysiological experiments investigating higher frequencies of stimulation and manoeuvres to manipulate readily releasable transmitter pools will help clarify the mechanism of action of SD118.

In summary, here we show SD118 enhances excitatory synaptic transmission in a frequency-dependent manner. This effect of SD118 may be key to its cognitive-function enhancing effect *in vivo*.

Chapter 6: General Discussion

The pursuit of neuroprotection and cognitive enhancement remains an uphill battle despite the wealth of information regarding the pathological states associated with cognitive dysfunction and decline. Work described in this document investigates several aspects beneficial for potentially successful drug development, for the purpose of battling cognitive deterioration. First, the validity of a novel, $\alpha 7$ nAChRs-targeting ligands were assessed. Second, the role of extracellular glucose in the context of LTP was explored, pointing towards the significance of appropriate metabolic homeostasis and LTP. Finally, facets of the prospective mechanism of action of SD118, a novel cognition-enhancing compound, were elucidated.

6.1 The effects of $\alpha 7$ nAChR-targeting ligands on LTP in the hippocampus *in vitro*

Collective evidence from both preclinical and clinical sources indicates that $\alpha 7$ nicotinic acetylcholine receptors have a likely role in processes and mechanisms encompassed in the mental action of cognition. The main objective of this set of experiments was to authenticate L-436, a novel PAM of $\alpha 7$ nAChRs, developed by Merck & Co., Inc., and to evaluate the effectiveness of this compound against established modulators of these receptors: a partial agonist and a PAM, EVP-6124 and BNC-375, respectively.

The primary findings from this study are that in both mouse and rat hippocampal slices, L-436 induced a concentration-dependent enhancement of LTP. This effect was not found in mice lacking $\alpha 7$ nAChRs ($A\alpha 7^{-/-}$ mice), compared with their wild-type littermates. In rat hippocampal slices, the maximum effect of L-456 on LTP, achieved at a concentration level of 10 μ M, was inhibited in the presence of the selective $\alpha 7$ nAChR antagonist MLA. In summary, these data propose that L-436 increases LTP via a direct action on $\alpha 7$ nAChRs. Hence, the effects of L-436 are comparable to those of partial

agonists of $\alpha 7$ nAChRs, such as EVP-6124, GTS-21, S 24795 and SSR180711 (Biton *et al.*, 2007; Lagostena *et al.*, 2008; Hunter *et al.*, 1994; Hurst *et al.*, 2013; Bertrand *et al.*, 2015; Townsend *et al.*, 2016).

6.2 The role of extracellular glucose in LTP in the hippocampus *in vitro*

The findings of this study indicate that the extracellular glucose level has little to no influence upon LTP in the hippocampus. In addition, these results are not in agreement with historic data from Neurosolutions LTD and other groups (unpublished material and Professor Andy Randall, personal communication) which showed that the magnitude of LTP was substantially affected depending on the extracellular glucose concentration.

6.3 Mechanism of action of SD118: a novel cognitive enhancer

The aim of this study was to provide insight into the mechanism of action of the novel cognitive enhancing drug SD118, a compound developed by Syndesi using Levetiracetam as the scaffold structure. Like Levetiracetam, SD118 targets the synaptic vesicle protein SV2A but unlike Levetiracetam, SD118 has no anticonvulsant activity. Using whole-cell patch clamp recording techniques in hippocampal slices SD118 was shown to enhance excitatory glutamatergic synaptic transmission in the hippocampus in a frequency-dependent manner. Excitatory synaptic responses were little affected at low frequencies of stimulation (0.1 to 2 Hz) but were potentiated at higher frequencies (10 and 20 Hz). Thus, SD118 has a similar frequency-dependent effect on excitatory synaptic transmission to Levetiracetam but the outcomes are total opposites, Levetiracetam having been shown to suppress excitatory synaptic transmission, presumably contributing to its anticonvulsant activity, whereas SD118 enhances synaptic transmission, a feature that could contribute to its cognitive enhancing properties. As both compounds target the synaptic

vesicle protein SV2A further research is required to understand how these compounds interact with this protein to bring about opposing electrophysiological and behavioural outcomes.

6.4 Conclusions and future work

Key findings of the studies reported here offer a deeper insight into the role of $\alpha 7$ nAChRs, via data obtained by utilising the field electrophysiological technique, a widely accepted model for learning and memory, thus reinforcing the significance of these receptors in LTP, as well as validating this subset of nicotinic receptors as adequate drug targets. Likewise, the role of adenosine presence and LTP has been discussed, raising important questions regarding the validity of the classic field electrophysiology experimental paradigm in the context of this research hypothesis. Finally, a novel compound with promising clinical potential and intriguing mechanism of action has been assessed. Therefore, the collective wealth of information discussed in thesis contains valuable evidence in favour of the pursuit of cognitive enhancers as potential AD treatment options.

Based on the data discussed here, the future role of $\alpha 7$ nAChR-targeting ligands could be of some significance and potential benefit as cognitive enhancers. Indeed, the pre-clinical performance of BNC375 foreshadows substantial promise for the ongoing Phase I clinical trials of this compound. In addition, it would be beneficial to explore alternative drug delivery routes for the delivery of EVP-6124, to bypass the GI tract and thus eliminate the previously reported side-effects.

For a continued exploration of the relationship between LTP and extracellular glucose, several potentially beneficial additions to the experimental design can be suggested. For example, in addition to the wild-type animals involved in this study, other animal models could be considered, e.g., aged animals, animals subject to a model of the high-carbohydrate, high-

fat “Western diet”, or to streptozotocin-induced diabetes. Monitoring of the average glucose levels of both plasma and cerebrospinal fluid as well as glucose tolerance tests could also be included, thereby setting the scene on whether systemic changes in metabolism are accompanied by changes in LTP in these animal models.

The promising effects of SD118 *in vitro* is an exciting new development which has led to a fast-tracking of this compound into Phase I trials. Future experiments should focus on determining how this compound interacts with and affects the function of SV2A to enhance synaptic transmission and cognition.

Chapter 7: Bibliography

Abraham, W. C., Jones, O. D. & Glanzman, D. L. (2019) Is plasticity of synapses the mechanism of long-term memory storage? *NPJ Sci Learn*, 4 9.

Abraham, W. C., Logan, B., Greenwood, J. M. & Dragunow, M. (2002) Induction and experience-dependent consolidation of stable long-term potentiation lasting months in the hippocampus. *J Neurosci*, 22 (21): 9626-9634.

Actavis & Adamas Pharmaceuticals, (2015) FDA approves new drug to treat dementia. *J Gerontol Nurs*, 41 (3): 5.

Adams, C. E., Broide, R. S., Chen, Y., Winzer-Serhan, U. H., Henderson, T. A., Leslie, F. M. & Freedman, R. (2002) Development of the $\alpha 7$ nicotinic cholinergic receptor in rat hippocampal formation. *Brain Res Dev Brain Res*, 139 (2): 175-187.

Akter, K., Lanza, E. A., Martin, S. A., Myronyuk, N., Rua, M. & Raffa, R. B. (2011) Diabetes mellitus and Alzheimer's disease: shared pathology and treatment? *Br J Clin Pharmacol*, 71 (3): 365-376.

Alcolea-Palafox, M., Posada-Moreno, P., Ortuño-Soriano, I., Pacheco-del-Cerro, J. L., Martinez-Rincon, C., Rodríguez-Martínez, D. & Pacheco-Cuevas, L. (2014) Research Strategies Developed for the Treatment of Alzheimer's Disease. Reversible and Pseudo-Irreversible Inhibitors of Acetylcholinesterase: Structure-Activity Relationships and Drug Design.

Alexander, G. C. & Karlawish, J. (2021) The Problem of Aducanumab for the Treatment of Alzheimer Disease. *Ann Intern Med*,

Almeida, T., Rodrigues, R. J., de Mendonça, A., Ribeiro, J. A. & Cunha, R. A. (2003) Purinergic P2 receptors trigger adenosine release leading to adenosine A2A receptor activation and facilitation of long-term potentiation in rat hippocampal slices. *Neuroscience*, 122 (1): 111-121.

Altman, J. & Bayer, S. <https://braindevelopmentmaps.org/>. [online] Available from: (Accessed 20.06.2021).

Andersen, P. (2007) *The hippocampus book*. Oxford ; New York: Oxford University Press.

Apostolova, L. G., Risacher, S. L., Duran, T., Stage, E. C., Goukasian, N., West, J. D., Do, T. M., Grotts, J., Wilhalme, H., Nho, K., Phillips, M., Elashoff, D. & Saykin, A. J. (2018) Associations of the Top 20 Alzheimer Disease Risk Variants With Brain Amyloidosis. *JAMA Neurol*, 75 (3): 328-341.

Araque, A. & Navarrete, M. (2010) Glial cells in neuronal network function. *Philos Trans R Soc Lond B Biol Sci*, 365 (1551): 2375-2381.

Bachurin, S. O., Bovina, E. V. & Ustyugov, A. A. (2017) Drugs in Clinical Trials for Alzheimer's Disease: The Major Trends. *Med Res Rev*, 37 (5): 1186-1225.

- Barrientos, R. M., Sprunger, D. B., Campeau, S., Watkins, L. R., Rudy, J. W. & Maier, S. F. (2004) BDNF mRNA expression in rat hippocampus following contextual learning is blocked by intrahippocampal IL-1 β administration. *J Neuroimmunol*, 155 (1-2): 119-126.
- Barton, M. E., Klein, B. D., Wolf, H. H. & White, H. S. (2001a) Pharmacological characterization of the 6 Hz psychomotor seizure model of partial epilepsy. *Epilepsy Res*, 47 (3): 217-227.
- Barton, M. E., Klein, B. D., Wolf, H. H. & White, H. S. (2001b) Pharmacological characterization of the 6 Hz psychomotor seizure model of partial epilepsy. *Epilepsy Res*, 47 (3): 217-227.
- Beach, T. G. (2013) Alzheimer's disease and the "Valley Of Death": not enough guidance from human brain tissue? *J Alzheimers Dis*, 33 Suppl 1 S219-233.
- Beggiato, S., Antonelli, T., Tomasini, M. C., Borelli, A. C., Agnati, L. F., Tanganelli, S., Fuxe, K. & Ferraro, L. (2014) Adenosine A2A-D2 receptor-receptor interactions in putative heteromers in the regulation of the striato-pallidal gaba pathway: possible relevance for parkinson's disease and its treatment. *Curr Protein Pept Sci*, 15 (7): 673-680.
- Beilharz, J. E., Maniam, J. & Morris, M. J. (2014) Short exposure to a diet rich in both fat and sugar or sugar alone impairs place, but not object recognition memory in rats. *Brain Behav Immun*, 37 134-141.
- Belanger, M., Allaman, I. & Magistretti, P. J. (2011) Brain energy metabolism: focus on astrocyte-neuron metabolic cooperation. *Cell Metab*, 14 (6): 724-738.
- Bell, B., Lin, J. J., Seidenberg, M. & Hermann, B. (2011) The neurobiology of cognitive disorders in temporal lobe epilepsy. *Nat Rev Neurol*, 7 (3): 154-164.
- Benke, T. A., Luthi, A., Isaac, J. T. & Collingridge, G. L. (1998) Modulation of AMPA receptor unitary conductance by synaptic activity. *Nature*, 393 (6687): 793-797.
- Berg, A. T., Zelko, F. A., Levy, S. R. & Testa, F. M. (2012) Age at onset of epilepsy, pharmacoresistance, and cognitive outcomes: a prospective cohort study. *Neurology*, 79 (13): 1384-1391.
- Berg, D. K. & Conroy, W. G. (2002) Nicotinic α 7 receptors: synaptic options and downstream signaling in neurons. *J Neurobiol*, 53 (4): 512-523.
- Berthele, A., Boxall, S. J., Urban, A., Anneser, J. M., Zieglgänsberger, W., Urban, L. & Tölle, T. R. (1999) Distribution and developmental changes in metabotropic glutamate receptor messenger RNA expression in the rat lumbar spinal cord. *Brain Res Dev Brain Res*, 112 (1): 39-53.
- Bertrand, D., Lee, C. H., Flood, D., Marger, F. & Donnelly-Roberts, D. (2015) Therapeutic Potential of α 7 Nicotinic Acetylcholine Receptors. *Pharmacol Rev*, 67 (4): 1025-1073.
- Bertrand, D. & Wallace, T. L. (2020) A Review of the Cholinergic System and Therapeutic Approaches to Treat Brain Disorders. *Curr Top Behav Neurosci*, 45 1-28.

- Billingsley, M. L. & Kincaid, R. L. (1997) Regulated phosphorylation and dephosphorylation of tau protein: effects on microtubule interaction, intracellular trafficking and neurodegeneration. *Biochem J*, 323 (Pt 3) 577-591.
- Bitner, R. S., Bunnelle, W. H., Anderson, D. J., Briggs, C. A., Buccafusco, J., Curzon, P., Decker, M. W., Frost, J. M., Gronlien, J. H., Gubbins, E., Li, J., Malysz, J., Markosyan, S., Marsh, K., Meyer, M. D., Nikkel, A. L., Radek, R. J., Robb, H. M., Timmermann, D., Sullivan, J. P. & Gopalakrishnan, M. (2007) Broad-spectrum efficacy across cognitive domains by alpha7 nicotinic acetylcholine receptor agonism correlates with activation of ERK1/2 and CREB phosphorylation pathways. *J Neurosci*, 27 (39): 10578-10587.
- Bitner, R. S., Bunnelle, W. H., Decker, M. W., Drescher, K. U., Kohlhaas, K. L., Markosyan, S., Marsh, K. C., Nikkel, A. L., Browman, K., Radek, R., Anderson, D. J., Buccafusco, J. & Gopalakrishnan, M. (2010) In vivo pharmacological characterization of a novel selective alpha7 neuronal nicotinic acetylcholine receptor agonist ABT-107: preclinical considerations in Alzheimer's disease. *J Pharmacol Exp Ther*, 334 (3): 875-886.
- Biton, B., Bergis, O. E., Galli, F., Nedelec, A., Lochead, A. W., Jegham, S., Godet, D., Lanneau, C., Santamaria, R., Chesney, F., Leonardon, J., Granger, P., Debono, M. W., Bohme, G. A., Sgard, F., Besnard, F., Graham, D., Coste, A., Oblin, A., Curet, O., Vige, X., Voltz, C., Rouquier, L., Souilhac, J., Santucci, V., Gueudet, C., Francon, D., Steinberg, R., Griebel, G., Oury-Donat, F., George, P., Avenet, P. & Scatton, B. (2007) SSR180711, a novel selective alpha7 nicotinic receptor partial agonist: (1) binding and functional profile. *Neuropsychopharmacology*, 32 (1): 1-16.
- Bland, B. H. (1986) The physiology and pharmacology of hippocampal formation theta rhythms. *Prog Neurobiol*, 26 (1): 1-54.
- Blatow, M., Caputi, A., Burnashev, N., Monyer, H. & Rozov, A. (2003) Ca²⁺ buffer saturation underlies paired pulse facilitation in calbindin-D28k-containing terminals. *Neuron*, 38 (1): 79-88.
- Bliss, T. V. & Lomo, T. (1973a) Long-lasting potentiation of synaptic transmission in the dentate area of the anaesthetized rabbit following stimulation of the perforant path. *J Physiol*, 232 (2): 331-356.
- Bliss, T. V. & Lomo, T. (1973b) Long-lasting potentiation of synaptic transmission in the dentate area of the anaesthetized rabbit following stimulation of the perforant path. *J Physiol*, 232 (2): 331-356.
- Blázquez, E., Velázquez, E., Hurtado-Carneiro, V. & Ruiz-Albusac, J. M. (2014) Insulin in the brain: its pathophysiological implications for States related with central insulin resistance, type 2 diabetes and Alzheimer's disease. *Front Endocrinol (Lausanne)*, 5 161.
- Bodhinathan, K., Kumar, A. & Foster, T. C. (2010) Redox sensitive calcium stores underlie enhanced after hyperpolarization of aged neurons: role for ryanodine receptor mediated calcium signaling. *J Neurophysiol*, 104 (5): 2586-2593.
- Boissonneault, V., Plante, I., Rivest, S. & Provost, P. (2009) MicroRNA-298 and microRNA-328 regulate expression of mouse beta-amyloid precursor protein-converting enzyme 1. *J Biol Chem*, 284 (4): 1971-1981.

- Borea, P. A., Varani, K., Vincenzi, F., Baraldi, P. G., Tabrizi, M. A., Merighi, S. & Gessi, S. (2015) The A3 adenosine receptor: history and perspectives. *Pharmacol Rev*, 67 (1): 74-102.
- Bourtchouladze, R., Lidge, R., Catapano, R., Stanley, J., Gossweiler, S., Romashko, D., Scott, R. & Tully, T. (2003) A mouse model of Rubinstein-Taybi syndrome: defective long-term memory is ameliorated by inhibitors of phosphodiesterase 4. *Proc Natl Acad Sci U S A*, 100 (18): 10518-10522.
- Bourtchouladze, R., Frenguelli, B., Blendy, J., Cioffi, D., Schutz, G. & Silva, A. J. (1994) Deficient long-term memory in mice with a targeted mutation of the cAMP-responsive element-binding protein. *Cell*, 79 (1): 59-68.
- Bramham, C. R., Alme, M. N., Bittins, M., Kuipers, S. D., Nair, R. R., Pai, B., Panja, D., Schubert, M., Soule, J., Tiron, A. & Wibrand, K. (2010) The Arc of synaptic memory. *Exp Brain Res*, 200 (2): 125-140.
- Brannan, S. (2019) 32.2 TWO GLOBAL PHASE III TRIALS OF ENCENICLINE FOR COGNITIVE IMPAIRMENT IN CHRONIC SCHIZOPHRENIA PATIENTS: RED FLAGS AND LESSONS LEARNED. In: *Schizophr Bull.* © The Author(s) 2019. Published by Oxford University Press on behalf of the Maryland Psychiatric Research Center. All rights reserved. For permissions, please email: journals.permissions@oup.com.: S141-142.
- Cannon, C. E., Puri, V., Vivian, J. A., Egbertson, M. S., Eddins, D. & Uslander, J. M. (2013) The nicotinic $\alpha 7$ receptor agonist GTS-21 improves cognitive performance in ketamine impaired rhesus monkeys. *Neuropharmacology*, 64 191-196.
- Capron, B., Sindic, C., Godaux, E. & Ris, L. (2006) The characteristics of LTP induced in hippocampal slices are dependent on slice-recovery conditions. *Learn Mem*, 13 (3): 271-277.
- Casey, D. A., Antimisiaris, D. & O'Brien, J. (2010) Drugs for Alzheimer's disease: are they effective? *P t*, 35 (4): 208-211.
- Castner, S. A., Smagin, G. N., Piser, T. M., Wang, Y., Smith, J. S., Christian, E. P., Mrzljak, L. & Williams, G. V. (2011a) Immediate and sustained improvements in working memory after selective stimulation of $\alpha 7$ nicotinic acetylcholine receptors. *Biol Psychiatry*, 69 (1): 12-18.
- Castner, S. A., Smagin, G. N., Piser, T. M., Wang, Y., Smith, J. S., Christian, E. P., Mrzljak, L. & Williams, G. V. (2011b) Immediate and sustained improvements in working memory after selective stimulation of $\alpha 7$ nicotinic acetylcholine receptors. *Biol Psychiatry*, 69 (1): 12-18.
- Cavuş, I. & Teyler, T. (1996) Two forms of long-term potentiation in area CA1 activate different signal transduction cascades. *J Neurophysiol*, 76 (5): 3038-3047.
- Chang, W. P. & Südhof, T. C. (2009) SV2 renders primed synaptic vesicles competent for Ca^{2+} -induced exocytosis. *J Neurosci*, 29 (4): 883-897.

- Cheng, Q. & Yakel, J. L. (2014) Presynaptic $\alpha 7$ nicotinic acetylcholine receptors enhance hippocampal mossy fiber glutamatergic transmission via PKA activation. *J Neurosci*, 34 (1): 124-133.
- Clarke, P. B. (1992) The fall and rise of neuronal alpha-bungarotoxin binding proteins. *Trends Pharmacol Sci*, 13 (11): 407-413.
- Claxton, A., Baker, L. D., Hanson, A., Trittschuh, E. H., Cholerton, B., Morgan, A., Callaghan, M., Arbuckle, M., Behl, C. & Craft, S. (2015) Long-acting intranasal insulin detemir improves cognition for adults with mild cognitive impairment or early-stage Alzheimer's disease dementia. *J Alzheimers Dis*, 44 (3): 897-906.
- Collingridge, G. L., Kehl, S. J. & McLennan, H. (1983) Excitatory amino acids in synaptic transmission in the Schaffer collateral-commissural pathway of the rat hippocampus. *J Physiol*, 334 33-46.
- Corkin, S., Amaral, D. G., González, R. G., Johnson, K. A. & Hyman, B. T. (1997) H. M.'s medial temporal lobe lesion: findings from magnetic resonance imaging. *J Neurosci*, 17 (10): 3964-3979.
- Costenla, A. R., Cunha, R. A. & de Mendonça, A. (2010) Caffeine, adenosine receptors, and synaptic plasticity. *J Alzheimers Dis*, 20 Suppl 1 S25-34.
- Court, J. A., Lloyd, S., Johnson, M., Griffiths, M., Birdsall, N. J., Piggott, M. A., Oakley, A. E., Ince, P. G., Perry, E. K. & Perry, R. H. (1997) Nicotinic and muscarinic cholinergic receptor binding in the human hippocampal formation during development and aging. *Brain Res Dev Brain Res*, 101 (1-2): 93-105.
- Craft, S. (2009) The role of metabolic disorders in Alzheimer disease and vascular dementia: two roads converged. *Arch Neurol*, 66 (3): 300-305.
- Craft, S., Baker, L. D., Montine, T. J., Minoshima, S., Watson, G. S., Claxton, A., Arbuckle, M., Callaghan, M., Tsai, E., Plymate, S. R., Green, P. S., Leverenz, J., Cross, D. & Gerton, B. (2012) Intranasal insulin therapy for Alzheimer disease and amnesic mild cognitive impairment: a pilot clinical trial. *Arch Neurol*, 69 (1): 29-38.
- Craft, S., Claxton, A., Baker, L. D., Hanson, A. J., Cholerton, B., Trittschuh, E. H., Dahl, D., Caulder, E., Neth, B., Montine, T. J., Jung, Y., Maldjian, J., Whitlow, C. & Friedman, S. (2017) Effects of Regular and Long-Acting Insulin on Cognition and Alzheimer's Disease Biomarkers: A Pilot Clinical Trial. *J Alzheimers Dis*, 57 (4): 1325-1334.
- Craft, S., Raman, R., Chow, T. W., Rafii, M. S., Sun, C. K., Rissman, R. A., Donohue, M. C., Brewer, J. B., Jenkins, C., Harless, K., Gessert, D. & Aisen, P. S. (2020) Safety, Efficacy, and Feasibility of Intranasal Insulin for the Treatment of Mild Cognitive Impairment and Alzheimer Disease Dementia: A Randomized Clinical Trial. *JAMA Neurol*, 77 (9): 1099-1109.
- Cummings, J., Feldman, H. H. & Scheltens, P. (2019) The "rights" of precision drug development for Alzheimer's disease. *Alzheimers Res Ther*, 11 (1): 76.

- Custer, K. L., Austin, N. S., Sullivan, J. M. & Bajjalieh, S. M. (2006) Synaptic vesicle protein 2 enhances release probability at quiescent synapses. *J Neurosci*, 26 (4): 1303-1313.
- Dajas-Bailador, F. A., Soliakov, L. & Wonnacott, S. (2002) Nicotine activates the extracellular signal-regulated kinase 1/2 via the $\alpha 7$ nicotinic acetylcholine receptor and protein kinase A, in SH-SY5Y cells and hippocampal neurones. *J Neurochem*, 80 (3): 520-530.
- Dani, J. A. & Bertrand, D. (2007) Nicotinic acetylcholine receptors and nicotinic cholinergic mechanisms of the central nervous system. *Annu Rev Pharmacol Toxicol*, 47 699-729.
- Dash, P. K., Orsi, S. A. & Moore, A. N. (2006) Spatial memory formation and memory-enhancing effect of glucose involves activation of the tuberous sclerosis complex-Mammalian target of rapamycin pathway. *J Neurosci*, 26 (31): 8048-8056.
- Davidson, T. L., Chan, K., Jarrard, L. E., Kanoski, S. E., Clegg, D. J. & Benoit, S. C. (2009) Contributions of the hippocampus and medial prefrontal cortex to energy and body weight regulation. *Hippocampus*, 19 (3): 235-252.
- Davies, K. D., Goebel-Goody, S. M., Coultrap, S. J. & Browning, M. D. (2008) Long term synaptic depression that is associated with GluR1 dephosphorylation but not α -amino-3-hydroxy-5-methyl-4-isoxazolepropionic acid (AMPA) receptor internalization. *J Biol Chem*, 283 (48): 33138-33146.
- Davies, P. & Maloney, A. J. (1976) Selective loss of central cholinergic neurons in Alzheimer's disease. In: *Lancet*. England: 1403.
- Davies, S. N., Lester, R. A., Reymann, K. G., Collingridge, G. L. (1989) Temporally distinct pre- and post-synaptic mechanisms maintain long-term potentiation. *Nature*. 1989 6;338(6215):500-3
- de Mendonça, A. & Ribeiro, J. A. (1994) Endogenous adenosine modulates long-term potentiation in the hippocampus. *Neuroscience*, 62 (2): 385-390.
- de Mendonça, A. & Ribeiro, J. A. (2001) Adenosine and synaptic plasticity. *Drug Development Research*, 52 (1-2): 283-290.
- De Smedt, T., Raedt, R., Vonck, K. & Boon, P. (2007) Levetiracetam: the profile of a novel anticonvulsant drug-part I: preclinical data. *CNS Drug Rev*, 13 (1): 43-56.
- Deardorff, W. J., Shobassy, A. & Grossberg, G. T. (2015) Safety and clinical effects of EVP-6124 in subjects with Alzheimer's disease currently or previously receiving an acetylcholinesterase inhibitor medication. *Expert Rev Neurother*, 15 (1): 7-17.
- Decourt, B., Boumelhem, F., Pope, E. D., 3rd, Shi, J., Mari, Z. & Sabbagh, M. N. (2021) Critical Appraisal of Amyloid Lowering Agents in AD. *Curr Neurol Neurosci Rep*, 21 (8): 39.
- Dickerson, B. C., Stoub, T. R., Shah, R. C., Sperling, R. A., Killiany, R. J., Albert, M. S., Hyman, B. T., Blacker, D. & Detolledo-Morrell, L. (2011) Alzheimer-signature MRI

biomarker predicts AD dementia in cognitively normal adults. *Neurology*, 76 (16): 1395-1402.

Dickinson, J. A., Kew, J. N. & Wonnacott, S. (2008) Presynaptic alpha 7- and beta 2-containing nicotinic acetylcholine receptors modulate excitatory amino acid release from rat prefrontal cortex nerve terminals via distinct cellular mechanisms. *Mol Pharmacol*, 74 (2): 348-359.

Dienel, G. A., Cruz, N. F., Mori, K., Holden, J. E. & Sokoloff, L. (1991) Direct measurement of the lambda of the lumped constant of the deoxyglucose method in rat brain: determination of lambda and lumped constant from tissue glucose concentration or equilibrium brain/plasma distribution ratio for methylglucose. *J Cereb Blood Flow Metab*, 11 (1): 25-34.

Dinklo, T., Shaban, H., Thuring, J. W., Lavreysen, H., Stevens, K. E., Zheng, L., Mackie, C., Grantham, C., Vandenberg, I., Meulders, G., Peeters, L., Verachtert, H., De Prins, E. & Lesage, A. S. (2011) Characterization of 2-[[4-fluoro-3-(trifluoromethyl)phenyl]amino]-4-(4-pyridinyl)-5-thiazolemethanol (JNJ-1930942), a novel positive allosteric modulator of the {alpha}7 nicotinic acetylcholine receptor. *J Pharmacol Exp Ther*, 336 (2): 560-574.

Double, K. L., Halliday, G. M., Kril, J. J., Harasty, J. A., Cullen, K., Brooks, W. S., Creasey, H. & Broe, G. A. (1996) Topography of brain atrophy during normal aging and Alzheimer's disease. *Neurobiol Aging*, 17 (4): 513-521.

Drisdell, R. C. & Green, W. N. (2000) Neuronal alpha-bungarotoxin receptors are alpha7 subunit homomers. *J Neurosci*, 20 (1): 133-139.

Dunwiddie, T. V., Diao, L., Kim, H. O., Jiang, J. L. & Jacobson, K. A. (1997) Activation of hippocampal adenosine A3 receptors produces a desensitization of A1 receptor-mediated responses in rat hippocampus. *J Neurosci*, 17 (2): 607-614.

Dunwiddie, T. V. & Masino, S. A. (2001) The role and regulation of adenosine in the central nervous system. *Annu Rev Neurosci*, 24 31-55.

Eddy, C. M., Rickards, H. E. & Cavanna, A. E. (2011) The cognitive impact of antiepileptic drugs. *Ther Adv Neurol Disord*, 4 (6): 385-407.

Ehlers, M. D. (2000) Reinsertion or degradation of AMPA receptors determined by activity-dependent endocytic sorting. *Neuron*, 28 (2): 511-525.

Ehlers, M. D. (2003) Activity level controls postsynaptic composition and signaling via the ubiquitin-proteasome system. *Nat Neurosci*, 6 (3): 231-242.

Eichenbaum, H. (1997) Declarative memory: insights from cognitive neurobiology. *Annu Rev Psychol*, 48 547-572.

El Sayed, I., Zaki, A., Fayed, A. M., Shehata, G. M. & Abdelmonem, S. (2018) A meta-analysis of the effect of different neuroprotective drugs in management of patients with traumatic brain injury. *Neurosurg Rev*, 41 (2): 427-438.

- Eskelinen, M. H., Ngandu, T., Tuomilehto, J., Soininen, H. & Kivipelto, M. (2009) Midlife coffee and tea drinking and the risk of late-life dementia: a population-based CAIDE study. *J Alzheimers Dis*, 16 (1): 85-91.
- Eslinger, P. J. & Damasio, A. R. (1986) Preserved motor learning in Alzheimer's disease: implications for anatomy and behavior. *J Neurosci*, 6 (10): 3006-3009.
- Fabian-Fine, R., Skehel, P., Errington, M. L., Davies, H. A., Sher, E., Stewart, M. G. & Fine, A. (2001) Ultrastructural distribution of the $\alpha 7$ nicotinic acetylcholine receptor subunit in rat hippocampus. *J Neurosci*, 21 (20): 7993-8003.
- Fagen, Z. M., Mansvelder, H. D., Keath, J. R. & McGehee, D. S. (2003) Short- and long-term modulation of synaptic inputs to brain reward areas by nicotine. *Ann N Y Acad Sci*, 1003 185-195.
- Fayuk, D. & Yakel, J. L. (2005) Ca^{2+} permeability of nicotinic acetylcholine receptors in rat hippocampal CA1 interneurons. *J Physiol*, 566 (Pt 3): 759-768.
- Fayuk, D. & Yakel, J. L. (2007) Dendritic Ca^{2+} signalling due to activation of $\alpha 7$ -containing nicotinic acetylcholine receptors in rat hippocampal neurons. *J Physiol*, 582 (Pt 2): 597-611.
- Fedi, M., Reutens, D., Dubeau, F., Andermann, E., D'Agostino, D. & Andermann, F. (2001) Long-term efficacy and safety of piracetam in the treatment of progressive myoclonus epilepsy. *Arch Neurol*, 58 (5): 781-786.
- Ferré, S., Quiroz, C., Woods, A. S., Cunha, R., Popoli, P., Ciruela, F., Lluís, C., Franco, R., Azdad, K. & Schiffmann, S. N. (2008) An update on adenosine A2A-dopamine D2 receptor interactions: implications for the function of G protein-coupled receptors. *Curr Pharm Des*, 14 (15): 1468-1474.
- Fogel, D. B. (2018) Factors associated with clinical trials that fail and opportunities for improving the likelihood of success: A review. *Contemp Clin Trials Commun*, 11 156-164.
- Folch, J., Busquets, O., Ettcheto, M., Sánchez-López, E., Castro-Torres, R. D., Verdager, E., García, M. L., Olloquequi, J., Casadesús, G., Beas-Zarate, C., Pelegri, C., Vilaplana, J., Auladell, C. & Camins, A. (2018) Memantine for the Treatment of Dementia: A Review on its Current and Future Applications. *J Alzheimers Dis*, 62 (3): 1223-1240.
- Foster, T. C., Sharrow, K. M., Masse, J. R., Norris, C. M. & Kumar, A. (2001) Calcineurin links Ca^{2+} dysregulation with brain aging. *J Neurosci*, 21 (11): 4066-4073.
- Foster T.C., Kumar A. (2007) Susceptibility to induction of long-term depression is associated with impaired memory in aged Fischer 344 rats. *Neurobiol Learn Mem*, 87(4):522-35.
- Fredholm, B. B., AP, I. J., Jacobson, K. A., Linden, J. & Müller, C. E. (2011) International Union of Basic and Clinical Pharmacology. LXXXI. Nomenclature and classification of adenosine receptors--an update. *Pharmacol Rev*, 63 (1): 1-34.

- Freedman, R., Hall, M., Adler, L. E. & Leonard, S. (1995) Evidence in postmortem brain tissue for decreased numbers of hippocampal nicotinic receptors in schizophrenia. *Biol Psychiatry*, 38 (1): 22-33.
- Frey, U., Huang, Y. Y. & Kandel, E. R. (1993) Effects of cAMP simulate a late stage of LTP in hippocampal CA1 neurons. *Science*, 260 (5114): 1661-1664.
- Fujii, S., Ji, Z., Morita, N. & Sumikawa, K. (1999) Acute and chronic nicotine exposure differentially facilitate the induction of LTP. *Brain Res*, 846 (1): 137-143.
- Gandhi, G. K., Cruz, N. F., Ball, K. K., Dienel, G. A. (2009) Astrocytes are poised for lactate trafficking and release from activated brain and for supply of glucose to neurons. *J Neurochem*, 111(2):522-36.
- Gant, J. C., Sama, M. M., Landfield, P. W. & Thibault, O. (2006) Early and simultaneous emergence of multiple hippocampal biomarkers of aging is mediated by Ca²⁺-induced Ca²⁺ release. *J Neurosci*, 26 (13): 3482-3490.
- Gao, J., Cohen, I. S., Mathias, R. T. & Baldo, G. J. (1998) The inhibitory effect of beta-stimulation on the Na/K pump current in guinea pig ventricular myocytes is mediated by a cAMP-dependent PKA pathway. *Pflugers Arch*, 435 (4): 479-484.
- Gemma, C. & Bickford, P. C. (2007) Interleukin-1beta and caspase-1: players in the regulation of age-related cognitive dysfunction. *Rev Neurosci*, 18 (2): 137-148.
- Gemma, C., Stellwagen, H., Fister, M., Coultrap, S. J., Mesches, M. H., Browning, M. D. & Bickford, P. C. (2004) Rosiglitazone improves contextual fear conditioning in aged rats. *Neuroreport*, 15 (14): 2255-2259.
- Gessi, S., Merighi, S., Fazzi, D., Stefanelli, A., Varani, K. & Borea, P. A. (2011) Adenosine receptor targeting in health and disease. *Expert Opin Investig Drugs*, 20 (12): 1591-1609.
- Giannakopoulos, P., Herrmann, F. R., Bussi re, T., Bouras, C., K vari, E., Perl, D. P., Morrison, J. H., Gold, G. & Hof, P. R. (2003) Tangle and neuron numbers, but not amyloid load, predict cognitive status in Alzheimer's disease. *Neurology*, 60 (9): 1495-1500.
- Giannola, L. I., Paderni, C., De Caro, V., Florena, A. M., Wolff, A. & Campisi, G. (2010) New perspectives in the delivery of galantamine for elderly patients using the IntelliDrug intraoral device: in vivo animal studies. *Curr Pharm Des*, 16 (6): 653-659.
- Glien, M., Brandt, C., Potschka, H. & L scher, W. (2002) Effects of the novel antiepileptic drug levetiracetam on spontaneous recurrent seizures in the rat pilocarpine model of temporal lobe epilepsy. *Epilepsia*, 43 (4): 350-357.
- Gold, P. E. (1986) Glucose modulation of memory storage processing. *Behav Neural Biol*, 45 (3): 342-349.
- Gouliaev, A. H. & Senning, A. (1994) Piracetam and other structurally related nootropics. *Brain Res Brain Res Rev*, 19 (2): 180-222.

- Greenwood, C. E., Kaplan, R. J., Hebblethwaite, S. & Jenkins, D. J. (2003) Carbohydrate-induced memory impairment in adults with type 2 diabetes. *Diabetes Care*, 26 (7): 1961-1966.
- Grieb, P., Forster, R. E., Strome, D., Goodwin, C. W. & Pape, P. C. (1985) O₂ exchange between blood and brain tissues studied with 18O₂ indicator-dilution technique. *J Appl Physiol* (1985), 58 (6): 1929-1941.
- Grover, L. M. (1998) Evidence for postsynaptic induction and expression of NMDA receptor independent LTP. *J Neurophysiol*, 79 (3): 1167-1182.
- Grover, L. M. & Teyler, T. J. (1992) N-methyl-D-aspartate receptor-independent long-term potentiation in area CA1 of rat hippocampus: input-specific induction and preclusion in a non-tetanized pathway. *Neuroscience*, 49 (1): 7-11.
- Gruetter, R., Ugurbil, K. & Seaquist, E. R. (1998) Steady-state cerebral glucose concentrations and transport in the human brain. *J Neurochem*, 70 (1): 397-408.
- Grybko, M. J., Hahm, E. T., Perrine, W., Parnes, J. A., Chick, W. S., Sharma, G., Finger, T. E. & Vijayaraghavan, S. (2011) A transgenic mouse model reveals fast nicotinic transmission in hippocampal pyramidal neurons. *Eur J Neurosci*, 33 (10): 1786-1798.
- Gu, Z., Lamb, P. W. & Yakel, J. L. (2012) Cholinergic coordination of presynaptic and postsynaptic activity induces timing-dependent hippocampal synaptic plasticity. *J Neurosci*, 32 (36): 12337-12348.
- Guan, Z. Z., Zhang, X., Ravid, R. & Nordberg, A. (2000) Decreased protein levels of nicotinic receptor subunits in the hippocampus and temporal cortex of patients with Alzheimer's disease. *J Neurochem*, 74 (1): 237-243.
- Gundlfinger, A., Bischofberger, J., Jochenning, F. W., Torvinen, M., Schmitz, D. & Breustedt, J. (2007) Adenosine modulates transmission at the hippocampal mossy fibre synapse via direct inhibition of presynaptic calcium channels. *J Physiol*, 582 (Pt 1): 263-277.
- Haas, H. L. & Greene, R. W. (1984) Adenosine enhances afterhyperpolarization and accommodation in hippocampal pyramidal cells. *Pflugers Arch*, 402 (3): 244-247.
- Haass, C., Koo, E. H., Mellon, A., Hung, A. Y. & Selkoe, D. J. (1992) Targeting of cell-surface beta-amyloid precursor protein to lysosomes: alternative processing into amyloid-bearing fragments. *Nature*, 357 (6378): 500-503.
- Hall, J. & Frenguelli, B. G. (2018) The combination of ribose and adenine promotes adenosine release and attenuates the intensity and frequency of epileptiform activity in hippocampal slices: Evidence for the rapid depletion of cellular ATP during electrographic seizures. *J Neurochem*, 147 (2): 178-189.
- Hansson, O., Lehmann, S., Otto, M., Zetterberg, H. & Lewczuk, P. (2019) Advantages and disadvantages of the use of the CSF Amyloid β (A β) 42/40 ratio in the diagnosis of Alzheimer's Disease. *Alzheimers Res Ther*, 11 (1): 34.

- Hapca, S., Burton, J. K., Cvorc, V., Reynish, E. & Donnan, P. T. (2019) Are antidementia drugs associated with reduced mortality after a hospital emergency admission in the population with dementia aged 65 years and older? *Alzheimers Dement (N Y)*, 5 431-440.
- Harris, E. W. & Cotman, C. W. (1986) Long-term potentiation of guinea pig mossy fiber responses is not blocked by N-methyl D-aspartate antagonists. *Neurosci Lett*, 70 (1): 132-137.
- Harris, J.J., Jolivet, R., Attwell, D. (2012) Synaptic energy use and supply. *Neuron*, 6;75(5):762-77.
- Harvey, A. J., Avery, T. D., Schaeffer, L., Joseph, C., Huff, B. C., Singh, R., Morice, C., Giethlen, B., Grishin, A. A., Coles, C. J., Kolesik, P., Wagner, S., Andriambeloson, E., Huyard, B., Poiraud, E., Paul, D. & O'Connor, S. M. (2019) Discovery of BNC375, a Potent, Selective, and Orally Available Type I Positive Allosteric Modulator of $\alpha 7$ nAChRs. *ACS Med Chem Lett*, 10 (5): 754-760.
- Henneberger, C., Papouin, T., Oliet, S. H. & Rusakov, D. A. (2010) Long-term potentiation depends on release of D-serine from astrocytes. *Nature*, 463 (7278): 232-236.
- Hoffmeister, P. G., Donat, C. K., Schuhmann, M. U., Voigt, C., Walter, B., Nieber, K., Meixensberger, J., Bauer, R. & Brust, P. (2011) Traumatic brain injury elicits similar alterations in $\alpha 7$ nicotinic receptor density in two different experimental models. *Neuromolecular Med*, 13 (1): 44-53.
- Hollmann, M. & Heinemann, S. (1994) Cloned glutamate receptors. *Annu Rev Neurosci*, 17 31-108.
- Holtzman, S. G. (1991) CGS 15943, a nonxanthine adenosine receptor antagonist: effects on locomotor activity of nontolerant and caffeine-tolerant rats. *Life Sci*, 49 (21): 1563-1570.
- Hommet, C., Mondon, K., Camus, V., De Toffol, B. & Constans, T. (2008) Epilepsy and dementia in the elderly. *Dement Geriatr Cogn Disord*, 25 (4): 293-300.
- Hovelsø, N., Sotty, F., Montezinho, L. P., Pinheiro, P. S., Herrik, K. F. & Mørk, A. (2012) Therapeutic potential of metabotropic glutamate receptor modulators. *Curr Neuroparmacol*, 10 (1): 12-48.
- Howarth, C., Gleeson, P. & Attwell, D. (2012) Updated energy budgets for neural computation in the neocortex and cerebellum. *J Cereb Blood Flow Metab*, 32 (7): 1222-1232.
- Hu, F. B., van Dam, R. M. & Liu, S. (2001) Diet and risk of Type II diabetes: the role of types of fat and carbohydrate. *Diabetologia*, 44 (7): 805-817.
- Hu, M., Liu, Q. S., Chang, K. T. & Berg, D. K. (2002) Nicotinic regulation of CREB activation in hippocampal neurons by glutamatergic and nonglutamatergic pathways. *Mol Cell Neurosci*, 21 (4): 616-625.
- Hu, Y. & Wilson, G. S. (1997) Rapid changes in local extracellular rat brain glucose observed with an in vivo glucose sensor. *J Neurochem*, 68 (4): 1745-1752.

- Huang, C. W., Pai, M. C. & Tsai, J. J. (2008) Comparative cognitive effects of levetiracetam and topiramate in intractable epilepsy. *Psychiatry Clin Neurosci*, 62 (5): 548-553.
- Huang, L. K., Chao, S. P. & Hu, C. J. (2020) Clinical trials of new drugs for Alzheimer disease. *J Biomed Sci*, 27 (1): 18.
- Huang, M., Felix, A. R., Kwon, S., Lowe, D., Wallace, T., Santarelli, L. & Meltzer, H. Y. (2014) The alpha-7 nicotinic receptor partial agonist/5-HT₃ antagonist RG3487 enhances cortical and hippocampal dopamine and acetylcholine release. *Psychopharmacology (Berl)*, 231 (10): 2199-2210.
- Hunter, B. E., de Fiebre, C. M., Papke, R. L., Kem, W. R. & Meyer, E. M. (1994) A novel nicotinic agonist facilitates induction of long-term potentiation in the rat hippocampus. *Neurosci Lett*, 168 (1-2): 130-134.
- Hurst, R., Rollema, H. & Bertrand, D. (2013) Nicotinic acetylcholine receptors: from basic science to therapeutics. *Pharmacol Ther*, 137 (1): 22-54.
- J., A., K.E, M. & L., W. (2018) *Methods for Pathological Classification of Alzheimer's Disease*. New York, NY: Humana Press.
- Jenssen, S. & Schere, D. (2010) Treatment and management of epilepsy in the elderly demented patient. *Am J Alzheimers Dis Other Demen*, 25 (1): 18-26.
- Ji, D., Lape, R. & Dani, J. A. (2001) Timing and location of nicotinic activity enhances or depresses hippocampal synaptic plasticity. *Neuron*, 31 (1): 131-141.
- John, D., Shelukhina, I., Yanagawa, Y., Deuchars, J. & Henderson, Z. (2015) Functional alpha7 nicotinic receptors are expressed on immature granule cells of the postnatal dentate gyrus. *Brain Res*, 1601 15-30.
- Jones, S., Sudweeks, S. & Yakel, J. L. (1999) Nicotinic receptors in the brain: correlating physiology with function. *Trends Neurosci*, 22 (12): 555-561.
- Jones, S. & Yakel, J. L. (1999) Inhibitory interneurons in hippocampus. *Cell Biochem Biophys*, 31 (2): 207-218.
- Kadir, A., Almkvist, O., Wall, A., Långström, B. & Nordberg, A. (2006) PET imaging of cortical 11C-nicotine binding correlates with the cognitive function of attention in Alzheimer's disease. *Psychopharmacology (Berl)*, 188 (4): 509-520.
- Kaempfer, N., Kochlamazashvili, G., Puchkov, D., Maritzen, T., Bajjalieh, S. M., Kononenko, N. L. & Haucke, V. (2015) Overlapping functions of stonin 2 and SV2 in sorting of the calcium sensor synaptotagmin 1 to synaptic vesicles. *Proc Natl Acad Sci U S A*, 112 (23): 7297-7302.
- Kamal, A., Biessels, G. J., Duis, S. E. & Gispen, W. H. (2000) Learning and hippocampal synaptic plasticity in streptozotocin-diabetic rats: interaction of diabetes and ageing. *Diabetologia*, 43 (4): 500-506.

- Kamal, A., Ramakers, G. M., Gispen, W. H. & Biessels, G. J. (2013) Hyperinsulinemia in rats causes impairment of spatial memory and learning with defects in hippocampal synaptic plasticity by involvement of postsynaptic mechanisms. *Exp Brain Res*, 226 (1): 45-51.
- Kaminski, R. M., Gillard, M. & Klitgaard, H. (2012) Targeting SV2A for Discovery of Antiepileptic Drugs. In: Noebels, J. L., Avoli, M., Rogawski, M. A., Olsen, R. W. & Delgado-Escueta, A. V., eds. *Jasper's Basic Mechanisms of the Epilepsies*. Bethesda (MD): National Center for Biotechnology Information (US) Copyright © 2012, Michael A Rogawski, Antonio V Delgado-Escueta, Jeffrey L Noebels, Massimo Avoli and Richard W Olsen.
- Kaminski, R. M., Gillard, M., Leclercq, K., Hanon, E., Lorent, G., Dasselès, D., Matagne, A. & Klitgaard, H. (2009) Proepileptic phenotype of SV2A-deficient mice is associated with reduced anticonvulsant efficacy of levetiracetam. *Epilepsia*, 50 (7): 1729-1740.
- Keefe, R. S., Meltzer, H. A., Dgetluck, N., Gawryl, M., Koenig, G., Moebius, H. J., Lombardo, I. & Hilt, D. C. (2015) Randomized, Double-Blind, Placebo-Controlled Study of Encenicline, an $\alpha 7$ Nicotinic Acetylcholine Receptor Agonist, as a Treatment for Cognitive Impairment in Schizophrenia. *Neuropsychopharmacology*, 40 (13): 3053-3060.
- Kellar, D., Lockhart, S. N., Aisen, P., Raman, R., Rissman, R. A., Brewer, J. & Craft, S. (2021) Intranasal Insulin Reduces White Matter Hyperintensity Progression in Association with Improvements in Cognition and CSF Biomarker Profiles in Mild Cognitive Impairment and Alzheimer's Disease. *J Prev Alzheimers Dis*, 8 (3): 240-248.
- Kelleher, R. J., 3rd, Govindarajan, A. & Tonegawa, S. (2004) Translational regulatory mechanisms in persistent forms of synaptic plasticity. *Neuron*, 44 (1): 59-73.
- Keller, J. J., Keller, A. B., Bowers, B. J. & Wehner, J. M. (2005) Performance of $\alpha 7$ nicotinic receptor null mutants is impaired in appetitive learning measured in a signaled nose poke task. *Behav Brain Res*, 162 (1): 143-152.
- Kida, S. (2012) A Functional Role for CREB as a Positive Regulator of Memory Formation and LTP. *Exp Neurobiol*, 21 (4): 136-140.
- Kiliaan, A. J., Arnoldussen, I. A. & Gustafson, D. R. (2014) Adipokines: a link between obesity and dementia? *Lancet Neurol*, 13 (9): 913-923.
- King, A. E., Ackley, M. A., Cass, C. E., Young, J. D. & Baldwin, S. A. (2006) Nucleoside transporters: from scavengers to novel therapeutic targets. *Trends Pharmacol Sci*, 27 (8): 416-425.
- Klinger, M., Kuhn, M., Just, H., Stefan, E., Palmer, T., Freissmuth, M. & Nanoff, C. (2002) Removal of the carboxy terminus of the A2A-adenosine receptor blunts constitutive activity: differential effect on cAMP accumulation and MAP kinase stimulation. *Naunyn Schmiedeberg's Arch Pharmacol*, 366 (4): 287-298.
- Klitgaard, H., Matagne, A., Gobert, J. & Wülfert, E. (1998) Evidence for a unique profile of levetiracetam in rodent models of seizures and epilepsy. *Eur J Pharmacol*, 353 (2-3): 191-206.

- Knake, S., Gruener, J., Hattemer, K., Klein, K. M., Bauer, S., Oertel, W. H., Hamer, H. M. & Rosenow, F. (2008) Intravenous levetiracetam in the treatment of benzodiazepine refractory status epilepticus. *J Neurol Neurosurg Psychiatry*, 79 (5): 588-589.
- Knowles, R. B., Wyart, C., Buldyrev, S. V., Cruz, L., Urbanc, B., Hasselmo, M. E., Stanley, H. E. & Hyman, B. T. (1999) Plaque-induced neurite abnormalities: implications for disruption of neural networks in Alzheimer's disease. *Proc Natl Acad Sci U S A*, 96 (9): 5274-5279.
- Kochubey, O., Lou, X. & Schneggenburger, R. (2011) Regulation of transmitter release by Ca(2+) and synaptotagmin: insights from a large CNS synapse. *Trends Neurosci*, 34 (5): 237-246.
- Kopf, S. R. & Baratti, C. M. (1996) Memory modulation by post-training glucose or insulin remains evident at long retention intervals. *Neurobiol Learn Mem*, 65 (2): 189-191.
- Koranda, J. L., Cone, J. J., McGehee, D. S., Roitman, M. F., Beeler, J. A. & Zhuang, X. (2014) Nicotinic receptors regulate the dynamic range of dopamine release in vivo. *J Neurophysiol*, 111 (1): 103-111.
- Kroker, K. S., Rast, G. & Rosenbrock, H. (2011) Differential effects of subtype-specific nicotinic acetylcholine receptor agonists on early and late hippocampal LTP. *Eur J Pharmacol*, 671 (1-3): 26-32.
- Kumar, A., Thinschmidt, J. S., Foster, T. C. (2019) Subunit contribution to NMDA receptor hypofunction and redox sensitivity of hippocampal synaptic transmission during aging. *Aging*, 11(14):5140-5157.
- Lagostena, L., Trocme-Thibierge, C., Morain, P. & Cherubini, E. (2008) The partial alpha7 nicotine acetylcholine receptor agonist S 24795 enhances long-term potentiation at CA3-CA1 synapses in the adult mouse hippocampus. *Neuropharmacology*, 54 (4): 676-685.
- Landfield, P. W., Pitler, T. A. (1984) Prolonged Ca²⁺-dependent afterhyperpolarizations in hippocampal neurons of aged rats. *Science*, 226 (4678):1089-92.
- Lape, R., Colquhoun, D. & Sivilotti, L. G. (2008) On the nature of partial agonism in the nicotinic receptor superfamily. *Nature*, 454 (7205): 722-727.
- Larner, A. J. (2010) Epileptic seizures in AD patients. *Neuromolecular Med*, 12 (1): 71-77.
- Le Pichon, J. B., Yu, S., Kibiryeve, N., Graf, W. D. & Bittel, D. C. (2013) Genome-wide gene expression in a patient with 15q13.3 homozygous microdeletion syndrome. *Eur J Hum Genet*, 21 (10): 1093-1099.
- Lendvai, B., Kassai, F., Szájlí, A. & Némethy, Z. (2013) $\alpha 7$ nicotinic acetylcholine receptors and their role in cognition. *Brain Res Bull*, 93 86-96.
- Lewis, A. S., van Schalkwyk, G. I. & Bloch, M. H. (2017) Alpha-7 nicotinic agonists for cognitive deficits in neuropsychiatric disorders: A translational meta-analysis of rodent and human studies. *Prog Neuropsychopharmacol Biol Psychiatry*, 75 45-53.

- Lewis, D. K., Bake, S., Thomas, K., Jezierski, M. K. & Sohrabji, F. (2010) A high cholesterol diet elevates hippocampal cytokine expression in an age and estrogen-dependent manner in female rats. *J Neuroimmunol*, 223 (1-2): 31-38.
- Li, J. J., Dolios, G., Wang, R. & Liao, F. F. (2014a) Soluble beta-amyloid peptides, but not insoluble fibrils, have specific effect on neuronal microRNA expression. *PLoS One*, 9 (3): e90770.
- Lindsberg, P. J. & Grau, A. J. (2003) Inflammation and infections as risk factors for ischemic stroke. *Stroke*, 34 (10): 2518-2532.
- Lippa, C. F., Rosso, A., Hepler, M., Jenssen, S., Pillai, J. & Irwin, D. (2010) Levetiracetam: a practical option for seizure management in elderly patients with cognitive impairment. *Am J Alzheimers Dis Other Dement*, 25 (2): 149-154.
- Lisman, J., Schulman, H. & Cline, H. (2002a) The molecular basis of CaMKII function in synaptic and behavioural memory. *Nat Rev Neurosci*, 3 (3): 175-190.
- Livingstone, P. D., Srinivasan, J., Kew, J. N., Dawson, L. A., Gotti, C., Moretti, M., Shoaib, M. & Wonnacott, S. (2009) $\alpha 7$ and non- $\alpha 7$ nicotinic acetylcholine receptors modulate dopamine release in vitro and in vivo in the rat prefrontal cortex. *Eur J Neurosci*, 29 (3): 539-550.
- Lopes, J. P., Pliássova, A. & Cunha, R. A. (2019) The physiological effects of caffeine on synaptic transmission and plasticity in the mouse hippocampus selectively depend on adenosine A(1) and A(2A) receptors. *Biochem Pharmacol*, 166 313-321.
- Lynch, B. A., Lambeng, N., Nocka, K., Kensel-Hammes, P., Bajjalieh, S. M., Matagne, A. & Fuks, B. (2004) The synaptic vesicle protein SV2A is the binding site for the antiepileptic drug levetiracetam. *Proc Natl Acad Sci U S A*, 101 (26): 9861-9866.
- Lynch, G., Muller, D., Seubert, P. & Larson, J. (1988) Long-term potentiation: persisting problems and recent results. *Brain Res Bull*, 21 (3): 363-372.
- Löscher, W. & Hönack, D. (1993) Profile of ucb L059, a novel anticonvulsant drug, in models of partial and generalized epilepsy in mice and rats. *Eur J Pharmacol*, 232 (2-3): 147-158.
- Löwel, S. & Singer, W. (1992) Selection of intrinsic horizontal connections in the visual cortex by correlated neuronal activity. *Science*, 255 (5041): 209-212.
- MacLeod, R., Hillert, E. K., Cameron, R. T. & Baillie, G. S. (2015) The role and therapeutic targeting of α -, β - and γ -secretase in Alzheimer's disease. *Future Sci OA*, 1 (3): Fso11.
- Magaki, S., Gardner, T., Khanlou, N., Yong, W. H., Salamon, N. & Vinters, H. V. (2015) Brain biopsy in neurologic decline of unknown etiology. *Hum Pathol*, 46 (4): 499-506.
- Maggi, L., Sher, E. & Cherubini, E. (2001) Regulation of GABA release by nicotinic acetylcholine receptors in the neonatal rat hippocampus. *J Physiol*, 536 (Pt 1): 89-100.

- Maia, L. & de Mendonça, A. (2002) Does caffeine intake protect from Alzheimer's disease? *Eur J Neurol*, 9 (4): 377-382.
- Malenka, R. C. & Bear, M. F. (2004) LTP and LTD: an embarrassment of riches. *Neuron*, 44 (1): 5-21.
- Malenka, R. C., Kauer, J. A., Zucker, R. S. & Nicoll, R. A. (1988) Postsynaptic calcium is sufficient for potentiation of hippocampal synaptic transmission. *Science*, 242 (4875): 81-84.
- Malenka, R. C. & Nicoll, R. A. (1999) Long-term potentiation--a decade of progress? *Science*, 285 (5435): 1870-1874.
- Manahan-Vaughan, D. & Braunewell, K. H. (2005) The metabotropic glutamate receptor, mGluR5, is a key determinant of good and bad spatial learning performance and hippocampal synaptic plasticity. *Cereb Cortex*, 15 (11): 1703-1713.
- Mansvelder, H. D. & McGehee, D. S. (2000) Long-term potentiation of excitatory inputs to brain reward areas by nicotine. *Neuron*, 27 (2): 349-357.
- Marks, M. J. & Collins, A. C. (1982) Characterization of nicotine binding in mouse brain and comparison with the binding of alpha-bungarotoxin and quinuclidinyl benzilate. *Mol Pharmacol*, 22 (3): 554-564.
- Martin, L. J., Blackstone, C. D., Huganir, R. L. & Price, D. L. (1992) Cellular localization of a metabotropic glutamate receptor in rat brain. *Neuron*, 9 (2): 259-270.
- Martyn, J. A., Kaneki, M. & Yasuhara, S. (2008) Obesity-induced insulin resistance and hyperglycemia: etiologic factors and molecular mechanisms. *Anesthesiology*, 109 (1): 137-148.
- Matsuzaki, M., Honkura, N., Ellis-Davies, G. C. & Kasai, H. (2004) Structural basis of long-term potentiation in single dendritic spines. *Nature*, 429 (6993): 761-766.
- Mayer, M. L. & Armstrong, N. (2004) Structure and function of glutamate receptor ion channels. *Annu Rev Physiol*, 66 161-181.
- McFadden, K. L., Cornier, M. A. & Tregellas, J. R. (2014) The role of alpha-7 nicotinic receptors in food intake behaviors. *Front Psychol*, 5 553.
- McKay, B. E., Placzek, A. N. & Dani, J. A. (2007) Regulation of synaptic transmission and plasticity by neuronal nicotinic acetylcholine receptors. *Biochem Pharmacol*, 74 (8): 1120-1133.
- McNay, E. C. & Gold, P. E. (2001) Age-related differences in hippocampal extracellular fluid glucose concentration during behavioral testing and following systemic glucose administration. *J Gerontol A Biol Sci Med Sci*, 56 (2): B66-71.
- Melnikova, I. (2007) Therapies for Alzheimer's disease. *Nat Rev Drug Discov*, 6 (5): 341-342.

Molas, S. & Dierssen, M. (2014) The role of nicotinic receptors in shaping and functioning of the glutamatergic system: a window into cognitive pathology. *Neurosci Biobehav Rev*, 46 Pt 2 315-325.

Morgan, S.L., Teyler, T.J. (1999) VDCCs and NMDARs underlie two forms of LTP in CA1 hippocampus in vivo. *J Neurophysiol*, 82(2):736-40.

Morgan, T.M. (2020) Intranasal Compositions For Treatment of Neurological And Neurodegenerative Diseases And Disorders, US Patent US20210145789A1, Available from: GooglePatents [01/08/2021].

Moriguchi, S., Oomura, Y., Shioda, N., Han, F., Hori, N., Aou, S. & Fukunaga, K. (2011) Ca²⁺/calmodulin-dependent protein kinase II and protein kinase C activities mediate extracellular glucose-regulated hippocampal synaptic efficacy. *Mol Cell Neurosci*, 46 (1): 101-107.

Morris, M. C., Evans, D. A., Bienias, J. L., Tangney, C. C. & Wilson, R. S. (2004) Dietary fat intake and 6-year cognitive change in an older biracial community population. *Neurology*, 62 (9): 1573-1579.

Morris, R. G., Anderson, E., Lynch, G. S. & Baudry, M. (1986) Selective impairment of learning and blockade of long-term potentiation by an N-methyl-D-aspartate receptor antagonist, AP5. *Nature*, 319 (6056): 774-776.

Mulkey, R. M. & Malenka, R. C. (1992) Mechanisms underlying induction of homosynaptic long-term depression in area CA1 of the hippocampus. *Neuron*, 9 (5): 967-975.

Murchison, D. & Griffith, W. H. (1999) Age-related alterations in caffeine-sensitive calcium stores and mitochondrial buffering in rat basal forebrain. *Cell Calcium*, 25 (6): 439-452.

Murray, C. A. & Lynch, M. A. (1998) Evidence that increased hippocampal expression of the cytokine interleukin-1 beta is a common trigger for age- and stress-induced impairments in long-term potentiation. *J Neurosci*, 18 (8): 2974-2981.

Muñoz-Jiménez, M., Zaarkti, A., García-Arnés, J. A. & García-Casares, N. (2020) Antidiabetic Drugs in Alzheimer's Disease and Mild Cognitive Impairment: A Systematic Review. In: *Dement Geriatr Cogn Disord*. Switzerland: © 2020 S. Karger AG, Basel.: 423-434.

Müller, M., Kuiperij, H. B., Claassen, J. A., Küsters, B. & Verbeek, M. M. (2014) MicroRNAs in Alzheimer's disease: differential expression in hippocampus and cell-free cerebrospinal fluid. *Neurobiol Aging*, 35 (1): 152-158.

Müller, W. E., Koch, S., Scheuer, K., Rostock, A. & Bartsch, R. (1997) Effects of piracetam on membrane fluidity in the aged mouse, rat, and human brain. *Biochem Pharmacol*, 53 (2): 135-140.

Naftalin, R. J., Cunningham, P. & Afzal-Ahmed, I. (2004) Piracetam and TRH analogues antagonise inhibition by barbiturates, diazepam, melatonin and galanin of human erythrocyte D-glucose transport. *Br J Pharmacol*, 142 (3): 594-608.

Nelson, P. T., Alafuzoff, I., Bigio, E. H., Bouras, C., Braak, H., Cairns, N. J., Castellani, R. J., Crain, B. J., Davies, P., Del Tredici, K., Duyckaerts, C., Frosch, M. P., Haroutunian, V., Hof, P. R., Hulette, C. M., Hyman, B. T., Iwatsubo, T., Jellinger, K. A., Jicha, G. A., Kövari, E., Kukull, W. A., Leverenz, J. B., Love, S., Mackenzie, I. R., Mann, D. M., Masliah, E., McKee, A. C., Montine, T. J., Morris, J. C., Schneider, J. A., Sonnen, J. A., Thal, D. R., Trojanowski, J. Q., Troncoso, J. C., Wisniewski, T., Woltjer, R. L. & Beach, T. G. (2012) Correlation of Alzheimer disease neuropathologic changes with cognitive status: a review of the literature. *J Neuropathol Exp Neurol*, 71 (5): 362-381.

Ng, H. J., Whittemore, E. R., Tran, M. B., Hogenkamp, D. J., Broide, R. S., Johnstone, T. B., Zheng, L., Stevens, K. E. & Gee, K. W. (2007) Nootropic $\alpha 7$ nicotinic receptor allosteric modulator derived from GABAA receptor modulators. *Proc Natl Acad Sci U S A*, 104 (19): 8059-8064.

Nieto, R. A., Deardorff, W. J. & Grossberg, G. T. (2016) Efficacy of rivastigmine tartrate, transdermal system, in Alzheimer's disease. *Expert Opin Pharmacother*, 17 (6): 861-870.

Nishanth, G. & Schlüter, D. (2019) Blood-Brain Barrier in Cerebral Malaria: Pathogenesis and Therapeutic Intervention. *Trends Parasitol*, 35 (7): 516-528.

Nisticò, R., Cavallucci, V., Piccinin, S., Macrì, S., Pignatelli, M., Mehdaawy, B., Blandini, F., Laviola, G., Lauro, D., Mercuri, N. B. & D'Amelio, M. (2012) Insulin receptor β -subunit haploinsufficiency impairs hippocampal late-phase LTP and recognition memory. *Neuromolecular Med*, 14 (4): 262-269.

Norris, C. M., Blalock, E. M., Chen, K. C., Porter, N. M., Landfield, P. W. (2002) Calcineurin enhances L-type Ca^{2+} channel activity in hippocampal neurons: increased effect with age in culture. *Neuroscience*, 110(2):213-25.

Norris, C. M., Korol, D. L. & Foster, T. C. (1996) Increased susceptibility to induction of long-term depression and long-term potentiation reversal during aging. *J Neurosci*, 16 (17): 5382-5392.

Nowack, A., Malarkey, E. B., Yao, J., Bleckert, A., Hill, J. & Bajjalieh, S. M. (2011) Levetiracetam reverses synaptic deficits produced by overexpression of SV2A. *PLoS One*, 6 (12): e29560.

Nowack, A., Yao, J., Custer, K. L. & Bajjalieh, S. M. (2010) SV2 regulates neurotransmitter release via multiple mechanisms. *Am J Physiol Cell Physiol*, 299 (5): C960-967.

Okada, H., Ouchi, Y., Ogawa, M., Futatsubashi, M., Saito, Y., Yoshikawa, E., Terada, T., Oboshi, Y., Tsukada, H., Ueki, T., Watanabe, M., Yamashita, T. & Magata, Y. (2013) Alterations in $\alpha 4 \beta 2$ nicotinic receptors in cognitive decline in Alzheimer's aetiopathology. *Brain*, 136 (Pt 10): 3004-3017.

Oliver-Schaffer (2016) A crystalline form of (r) -7-chloro-n- (quinuclidin-3-yl) benzo [b] thiophene-2-carboxamide hydrochloride monohydrate.

Ota, Y., Zanetti, A. T. & Hallock, R. M. (2013) The role of astrocytes in the regulation of synaptic plasticity and memory formation. *Neural Plast*, 2013 185463.

- Palmer, T. M., Benovic, J. L. & Stiles, G. L. (1996) Molecular basis for subtype-specific desensitization of inhibitory adenosine receptors. Analysis of a chimeric A1-A3 adenosine receptor. *J Biol Chem*, 271 (25): 15272-15278.
- Park, P., Volianskis, A., Sanderson, T. M., Bortolotto, Z. A., Jane, D. E., Zhuo, M., Kaang, B. K. & Collingridge, G. L. (2014) NMDA receptor-dependent long-term potentiation comprises a family of temporally overlapping forms of synaptic plasticity that are induced by different patterns of stimulation. *Philos Trans R Soc Lond B Biol Sci*, 369 (1633): 20130131.
- Parnet, P., Kelley, K. W., Bluthé, R. M. & Dantzer, R. (2002) Expression and regulation of interleukin-1 receptors in the brain. Role in cytokines-induced sickness behavior. *J Neuroimmunol*, 125 (1-2): 5-14.
- Parsons, C. G. (2019) CNS repurposing - Potential new uses for old drugs: Examples of screens for Alzheimer's disease, Parkinson's disease and spasticity. *Neuropharmacology*, 147 4-10.
- Pasinetti, G. M. & Eberstein, J. A. (2008) Metabolic syndrome and the role of dietary lifestyles in Alzheimer's disease. *J Neurochem*, 106 (4): 1503-1514.
- Patel, S., Grizzell, J. A., Holmes, R., Zeitlin, R., Solomon, R., Sutton, T. L., Rohani, A., Charry, L. C., Iarkov, A., Mori, T. & Echeverria Moran, V. (2014) Cotinine halts the advance of Alzheimer's disease-like pathology and associated depressive-like behavior in Tg6799 mice. *Front Aging Neurosci*, 6 162.
- Pellerin, L. & Magistretti, P. J. (1994) Glutamate uptake into astrocytes stimulates aerobic glycolysis: a mechanism coupling neuronal activity to glucose utilization. *Proc. Natl. Acad. Sci.*, 91: 10625-10629
- Pichat, P., Bergis, O. E., Terranova, J. P., Urani, A., Duarte, C., Santucci, V., Gueudet, C., Voltz, C., Steinberg, R., Stemmelin, J., Oury-Donat, F., Avenet, P., Griebel, G. & Scatton, B. (2007) SSR180711, a novel selective alpha7 nicotinic receptor partial agonist: (II) efficacy in experimental models predictive of activity against cognitive symptoms of schizophrenia. *Neuropsychopharmacology*, 32 (1): 17-34.
- Pistell, P. J., Morrison, C. D., Gupta, S., Knight, A. G., Keller, J. N., Ingram, D. K. & Bruce-Keller, A. J. (2010) Cognitive impairment following high fat diet consumption is associated with brain inflammation. *J Neuroimmunol*, 219 (1-2): 25-32.
- Potasiewicz, A., Nikiforuk, A., Hołuj, M. & Popik, P. (2017) Stimulation of nicotinic acetylcholine alpha7 receptors rescue schizophrenia-like cognitive impairments in rats. *J Psychopharmacol*, 31 (2): 260-271.
- Potier, B., Poindessous-Jazat, F., Dutar, P. & Billard, J. M. (2000a) NMDA receptor activation in the aged rat hippocampus. *Exp Gerontol*, 35 (9-10): 1185-1199.
- Potter, W. B., O'Riordan, K. J., Barnett, D., Osting, S. M., Wagoner, M., Burger, C. & Roopra, A. (2010) Metabolic regulation of neuronal plasticity by the energy sensor AMPK. *PLoS One*, 5 (2): e8996.

- Prasad, K., de Vries, E. F. J., Elsinga, P. H., Dierckx, R. & van Waarde, A. (2021) Allosteric Interactions between Adenosine A(2A) and Dopamine D(2) Receptors in Heteromeric Complexes: Biochemical and Pharmacological Characteristics, and Opportunities for PET Imaging. *Int J Mol Sci*, 22 (4):
- Prickaerts, J., van Goethem, N. P., Chesworth, R., Shapiro, G., Boess, F. G., Methfessel, C., Reneerkens, O. A., Flood, D. G., Hilt, D., Gawryl, M., Bertrand, S., Bertrand, D. & König, G. (2012) EVP-6124, a novel and selective $\alpha 7$ nicotinic acetylcholine receptor partial agonist, improves memory performance by potentiating the acetylcholine response of $\alpha 7$ nicotinic acetylcholine receptors. *Neuropharmacology*, 62 (2): 1099-1110.
- Quarta, D., Naylor, C. G., Barik, J., Fernandes, C., Wonnacott, S. & Stolerman, I. P. (2009) Drug discrimination and neurochemical studies in alpha7 null mutant mice: tests for the role of nicotinic alpha7 receptors in dopamine release. *Psychopharmacology (Berl)*, 203 (2): 399-410.
- Radeliffe, K. A. & Dani, J. A. (1998) Nicotinic stimulation produces multiple forms of increased glutamatergic synaptic transmission. *J Neurosci*, 18 (18): 7075-7083.
- Ramael, S., Daoust, A., Otoul, C., Toubanc, N., Troenaru, M., Lu, Z. S. & Stockis, A. (2006) Levetiracetam intravenous infusion: a randomized, placebo-controlled safety and pharmacokinetic study. *Epilepsia*, 47 (7): 1128-1135.
- Rangwala, F., Drisdell, R. C., Rakhilin, S., Ko, E., Atluri, P., Harkins, A. B., Fox, A. P., Salman, S. S. & Green, W. N. (1997) Neuronal alpha-bungarotoxin receptors differ structurally from other nicotinic acetylcholine receptors. *J Neurosci*, 17 (21): 8201-8212.
- Rebola, N., Lujan, R., Cunha, R. A. & Mulle, C. (2008) Adenosine A2A receptors are essential for long-term potentiation of NMDA-EPSCs at hippocampal mossy fiber synapses. *Neuron*, 57 (1): 121-134.
- Ris, L. & Godaux, E. (2007) Synapse specificity of long-term potentiation breaks down with aging. *Learn Mem*, 14 (3): 185-189.
- Ritchie, K., Carrière, I., de Mendonca, A., Portet, F., Dartigues, J. F., Rouaud, O., Barberger-Gateau, P. & Ancelin, M. L. (2007) The neuroprotective effects of caffeine: a prospective population study (the Three City Study). *Neurology*, 69 (6): 536-545.
- Roberson, E. D., English, J. D. & Sweatt, J. D. (1996) A biochemist's view of long-term potentiation. *Learn Mem*, 3 (1): 1-24.
- Romano, C., Sesma, M. A., McDonald, C. T., O'Malley, K., Van den Pol, A. N. & Olney, J. W. (1995) Distribution of metabotropic glutamate receptor mGluR5 immunoreactivity in rat brain. *J Comp Neurol*, 355 (3): 455-469.
- Ronne-Engström, E., Carlson, H., Liu, Y., Ungerstedt, U. & Hillered, L. (1995) Influence of perfusate glucose concentration on dialysate lactate, pyruvate, aspartate, and glutamate levels under basal and hypoxic conditions: a microdialysis study in rat brain. *J Neurochem*, 65 (1): 257-262.

- Rosenberg, D., Kartvelishvily, E., Shleper, M., Klinker, C. M., Bowser, M. T. & Wolosker, H. (2010) Neuronal release of D-serine: a physiological pathway controlling extracellular D-serine concentration. *Faseb j*, 24 (8): 2951-2961.
- Ryan, C. M., Freed, M. I., Rood, J. A., Cobitz, A. R., Waterhouse, B. R. & Strachan, M. W. (2006) Improving metabolic control leads to better working memory in adults with type 2 diabetes. *Diabetes Care*, 29 (2): 345-351.
- Sacktor, T. C. (2008) PKMzeta, LTP maintenance, and the dynamic molecular biology of memory storage. *Prog Brain Res*, 169 27-40.
- Sahakian, B. J., Bruhl, A. B., Cook, J., Killikelly, C., Savulich, G., Piercy, T., Hafizi, S., Perez, J., Fernandez-Egea, E., Suckling, J. & Jones, P. B. (2015) The impact of neuroscience on society: cognitive enhancement in neuropsychiatric disorders and in healthy people. *Philos Trans R Soc Lond B Biol Sci*, 370 (1677): 20140214.
- Sahdeo, S., Wallace, T., Hirakawa, R., Knoflach, F., Bertrand, D., Maag, H., Misner, D., Tombaugh, G. C., Santarelli, L., Brameld, K., Milla, M. E. & Button, D. C. (2014) Characterization of RO5126946, a Novel $\alpha 7$ nicotinic acetylcholine receptor-positive allosteric modulator. *J Pharmacol Exp Ther*, 350 (2): 455-468.
- Sawynok, J. (2016) Adenosine receptor targets for pain. *Neuroscience*, 338 1-18.
- Schiöth, H. B., Craft, S., Brooks, S. J., Frey, W. H., 2nd & Benedict, C. (2012) Brain insulin signaling and Alzheimer's disease: current evidence and future directions. *Mol Neurobiol*, 46 (1): 4-10.
- Schott, J. M., Reiniger, L., Thom, M., Holton, J. L., Grieve, J., Brandner, S., Warren, J. D. & Revesz, T. (2010) Brain biopsy in dementia: clinical indications and diagnostic approach. *Acta Neuropathol*, 120 (3): 327-341.
- Schuijer, F., Orzi, F., Suda, S., Lucignani, G., Kennedy, C. & Sokoloff, L. (1990) Influence of plasma glucose concentration on lumped constant of the deoxyglucose method: effects of hyperglycemia in the rat. *J Cereb Blood Flow Metab*, 10 (6): 765-773.
- Schuster, R. M., Pachas, G. N., Stoeckel, L., Cather, C., Nadal, M., Mischoulon, D., Schoenfeld, D. A., Zhang, H., Ulysse, C., Dodds, E. B., Sobolewski, S., Hudziak, V., Hanly, A., Fava, M. & Evins, A. E. (2018) Phase IIb Trial of an $\alpha 7$ Nicotinic Receptor Partial Agonist With and Without Nicotine Patch for Withdrawal-Associated Cognitive Deficits and Tobacco Abstinence. *J Clin Psychopharmacol*, 38 (4): 307-316.
- Scoville, W. B. & Milner, B. (1957) Loss of recent memory after bilateral hippocampal lesions. *J Neurol Neurosurg Psychiatry*, 20 (1): 11-21.
- Sebastião, A. M., Cunha, R. A., de Mendonça, A. & Ribeiro, J. A. (2000) Modification of adenosine modulation of synaptic transmission in the hippocampus of aged rats. *Br J Pharmacol*, 131 (8): 1629-1634.
- Sebastião, A. M. & Ribeiro, J. A. (2009) Triggering neurotrophic factor actions through adenosine A2A receptor activation: implications for neuroprotection. *Br J Pharmacol*, 158 (1): 15-22.

- Sejnowski, T. J. (1999) The book of Hebb. *Neuron*, 24 (4): 773-776.
- Selkoe, D. J. & Hardy, J. (2016) The amyloid hypothesis of Alzheimer's disease at 25 years. *EMBO Mol Med*, 8 (6): 595-608.
- Shankar, G. M., Li, S., Mehta, T. H., Garcia-Munoz, A., Shepardson, N. E., Smith, I., Brett, F. M., Farrell, M. A., Rowan, M. J., Lemere, C. A., Regan, C. M., Walsh, D. M., Sabatini, B. L. & Selkoe, D. J. (2008) Amyloid-beta protein dimers isolated directly from Alzheimer's brains impair synaptic plasticity and memory. *Nat Med*, 14 (8): 837-842.
- Shannon, H. E., Eberle, E. L. & Peters, S. C. (2005) Comparison of the effects of anticonvulsant drugs with diverse mechanisms of action in the formalin test in rats. *Neuropharmacology*, 48 (7): 1012-1020.
- Sharma, G., Grybko, M. & Vijayaraghavan, S. (2008) Action potential-independent and nicotinic receptor-mediated concerted release of multiple quanta at hippocampal CA3-mossy fiber synapses. *J Neurosci*, 28 (10): 2563-2575.
- Sharp, A. J., Mefford, H. C., Li, K., Baker, C., Skinner, C., Stevenson, R. E., Schroer, R. J., Novara, F., De Gregori, M., Ciccone, R., Broomer, A., Casuga, I., Wang, Y., Xiao, C., Barbacioru, C., Gimelli, G., Bernardina, B. D., Torniero, C., Giorda, R., Regan, R., Murday, V., Mansour, S., Fichera, M., Castiglia, L., Failla, P., Ventura, M., Jiang, Z., Cooper, G. M., Knight, S. J., Romano, C., Zuffardi, O., Chen, C., Schwartz, C. E. & Eichler, E. E. (2008) A recurrent 15q13.3 microdeletion syndrome associated with mental retardation and seizures. *Nat Genet*, 40 (3): 322-328.
- Shen, J. X. & Yakel, J. L. (2012) Functional $\alpha 7$ nicotinic ACh receptors on astrocytes in rat hippocampal CA1 slices. *J Mol Neurosci*, 48 (1): 14-21.
- Shigemoto, R., Nomura, S., Ohishi, H., Sugihara, H., Nakanishi, S. & Mizuno, N. (1993) Immunohistochemical localization of a metabotropic glutamate receptor, mGluR5, in the rat brain. *Neurosci Lett*, 163 (1): 53-57.
- Silver, I. A. & Erecińska, M. (1994) Extracellular glucose concentration in mammalian brain: continuous monitoring of changes during increased neuronal activity and upon limitation in oxygen supply in normo-, hypo-, and hyperglycemic animals. *J Neurosci*, 14 (8): 5068-5076.
- Simpson, I. A., Carruthers, A. & Vannucci, S. J. (2007) Supply and demand in cerebral energy metabolism: the role of nutrient transporters. *J Cereb Blood Flow Metab*, 27 (11): 1766-1791.
- Slanzi, A., Iannoto, G., Rossi, B., Zenaro, E. & Constantin, G. (2020) In vitro Models of Neurodegenerative Diseases. *Front Cell Dev Biol*, 8 328.
- Sonawane, S. K., Chidambaram, H., Boral, D., Gorantla, N. V., Balmik, A. A., Dangi, A., Ramasamy, S., Marelli, U. K. & Chinnathambi, S. (2020) EGCG impedes human Tau aggregation and interacts with Tau. *Sci Rep*, 10 (1): 12579.
- Song, I. & Huganir, R. L. (2002) Regulation of AMPA receptors during synaptic plasticity. *Trends Neurosci*, 25 (11): 578-588.

- Squire, L. R. (2004) Memory systems of the brain: a brief history and current perspective. *Neurobiol Learn Mem*, 82 (3): 171-177.
- Stampfer, M. J. (2006) Cardiovascular disease and Alzheimer's disease: common links. *J Intern Med*, 260 (3): 211-223.
- Stenberg, D., Litonius, E., Halldner, L., Johansson, B., Fredholm, B. B. & Porkka-Heiskanen, T. (2003) Sleep and its homeostatic regulation in mice lacking the adenosine A1 receptor. *J Sleep Res*, 12 (4): 283-290.
- Stranahan, A. M., Norman, E. D., Lee, K., Cutler, R. G., Telljohann, R. S., Egan, J. M. & Mattson, M. P. (2008) Diet-induced insulin resistance impairs hippocampal synaptic plasticity and cognition in middle-aged rats. *Hippocampus*, 18 (11): 1085-1088.
- Sudweeks, S. N. & Yakel, J. L. (2000) Functional and molecular characterization of neuronal nicotinic ACh receptors in rat CA1 hippocampal neurons. *J Physiol*, 527 Pt 3 (Pt 3): 515-528.
- Suzuki, A., Stern, S. A., Bozdagi, O., Huntley, G. W., Walker, R. H., Magistretti, P. J., Alberini, C. M. (2011) Astrocyte-neuron lactate transport is required for long-term memory formation. *Cell*, 144: 810-823.
- Szeto, J. Y. & Lewis, S. J. (2016) Current Treatment Options for Alzheimer's Disease and Parkinson's Disease Dementia. *Curr Neuroparmacol*, 14 (4): 326-338.
- Séguéla, P., Wadiche, J., Dineley-Miller, K., Dani, J. A. & Patrick, J. W. (1993) Molecular cloning, functional properties, and distribution of rat brain alpha 7: a nicotinic cation channel highly permeable to calcium. *J Neurosci*, 13 (2): 596-604.
- T.M, M. Intranasal compositions for treatment of neurological and neurodegenerative diseases and disorders.
- Takahashi, R. N., Pamplona, F. A. & Prediger, R. D. (2008) Adenosine receptor antagonists for cognitive dysfunction: a review of animal studies. *Front Biosci*, 13 2614-2632.
- Takebe, T., Imai, R. & Ono, S. (2018) The Current Status of Drug Discovery and Development as Originated in United States Academia: The Influence of Industrial and Academic Collaboration on Drug Discovery and Development. *Clin Transl Sci*, 11 (6): 597-606.
- Tekkök, S. B., Godfraind, J. M. & Krnjević, K. (2002) Moderate hypoglycemia aggravates effects of hypoxia in hippocampal slices from diabetic rats. *Neuroscience*, 113 (1): 11-21.
- Thompson, P. J. & Duncan, J. S. (2005) Cognitive decline in severe intractable epilepsy. *Epilepsia*, 46 (11): 1780-1787.
- Tomek, S. E., Lacrosse, A. L., Nemirovsky, N. E. & Olive, M. F. (2013) NMDA Receptor Modulators in the Treatment of Drug Addiction. *Pharmaceuticals (Basel)*, 6 (2): 251-268.

- Toni, N., Buchs, P. A., Nikonenko, I., Bron, C. R. & Muller, D. (1999) LTP promotes formation of multiple spine synapses between a single axon terminal and a dendrite. *Nature*, 402 (6760): 421-425.
- Toni, N., Buchs, P. A., Nikonenko, I., Povilaitite, P., Parisi, L. & Muller, D. (2001) Remodeling of synaptic membranes after induction of long-term potentiation. *J Neurosci*, 21 (16): 6245-6251.
- Tonkikh, A., Janus, C., El-Beheiry, H., Pennefather, P. S., Samoilova, M., McDonald, P., Ouanounou, A. & Carlen, P. L. (2006) Calcium chelation improves spatial learning and synaptic plasticity in aged rats. *Exp Neurol*, 197 (2): 291-300.
- Tonkikh, A. A. & Carlen, P. L. (2009) Impaired presynaptic cytosolic and mitochondrial calcium dynamics in aged compared to young adult hippocampal CA1 synapses ameliorated by calcium chelation. *Neuroscience*, 159 (4): 1300-1308.
- Townsend, M., Whyment, A., Walczak, J. S., Jeggo, R., van den Top, M., Flood, D. G., Leventhal, L., Patzke, H. & Koenig, G. (2016) $\alpha 7$ -nAChR agonist enhances neural plasticity in the hippocampus via a GABAergic circuit. *J Neurophysiol*, 116 (6): 2663-2675.
- Urbanc, B., Cruz, L., Le, R., Sanders, J., Ashe, K. H., Duff, K., Stanley, H. E., Irizarry, M. C. & Hyman, B. T. (2002) Neurotoxic effects of thioflavin S-positive amyloid deposits in transgenic mice and Alzheimer's disease. *Proc Natl Acad Sci U S A*, 99 (22): 13990-13995.
- Uteshev, V. V. (2012) $\alpha 7$ nicotinic ACh receptors as a ligand-gated source of Ca^{2+} ions: the search for a Ca^{2+} optimum. *Adv Exp Med Biol*, 740 603-638.
- van den Top, M., Zhao, F. Y., Viriyapong, R., Michael, N. J., Munder, A. C., Pryor, J. T., Renaud, L. P. & Spanswick, D. (2017) The impact of ageing, fasting and high-fat diet on central and peripheral glucose tolerance and glucose-sensing neural networks in the arcuate nucleus. *J Neuroendocrinol*, 29 (10):
- van der Heide, L. P., Kamal, A., Artola, A., Gispen, W. H. & Ramakers, G. M. (2005) Insulin modulates hippocampal activity-dependent synaptic plasticity in a N-methyl-D-aspartate receptor and phosphatidylinositol-3-kinase-dependent manner. *J Neurochem*, 94 (4): 1158-1166.
- Varani, K., Vincenzi, F., Merighi, S., Gessi, S. & Borea, P. A. (2017) Biochemical and Pharmacological Role of A(1) Adenosine Receptors and Their Modulation as Novel Therapeutic Strategy. *Adv Exp Med Biol*, 1051 193-232.
- Vehmas, A. K., Kawas, C. H., Stewart, W. F. & Troncoso, J. C. (2003) Immune reactive cells in senile plaques and cognitive decline in Alzheimer's disease. *Neurobiol Aging*, 24 (2): 321-331.
- Verkhratsky, A. & Kirchhoff, F. (2007) NMDA Receptors in glia. *Neuroscientist*, 13 (1): 28-37.
- Vossel, K. A., Tartaglia, M. C., Nygaard, H. B., Zeman, A. Z. & Miller, B. L. (2017) Epileptic activity in Alzheimer's disease: causes and clinical relevance. *Lancet Neurol*, 16 (4): 311-322.

Waegemans, T., Wilsher, C. R., Danniau, A., Ferris, S. H., Kurz, A. & Winblad, B. (2002) Clinical efficacy of piracetam in cognitive impairment: a meta-analysis. *Dement Geriatr Cogn Disord*, 13 (4): 217-224.

Wang, H. Y., Lee, D. H., D'Andrea, M. R., Peterson, P. A., Shank, R. P. & Reitz, A. B. (2000) beta-Amyloid(1-42) binds to $\alpha 7$ nicotinic acetylcholine receptor with high affinity. Implications for Alzheimer's disease pathology. *J Biol Chem*, 275 (8): 5626-5632.

Wang, X., Daley, C., Gakhar, V., Lange, H. S., Vardigan, J. D., Pearson, M., Zhou, X., Warren, L., Miller, C. O., Belden, M., Harvey, A. J., Grishin, A. A., Coles, C. J., O'Connor, S. M., Thomson, F., Duffy, J. L., Bell, I. M. & Uslaner, J. M. (2020) Pharmacological Characterization of the Novel and Selective $\alpha 7$ Nicotinic Acetylcholine Receptor-Positive Allosteric Modulator BNC375. *J Pharmacol Exp Ther*, 373 (2): 311-324.

Wechsler, R. T. (2004) *Blueprints notes & cases : neuroscience*. Malden, Mass. ; Oxford: Blackwell Pub.

Weed, M. R., Polino, J., Signor, L., Bookbinder, M., Keavy, D., Benitex, Y., Morgan, D. G., King, D., Macor, J. E., Zaczek, R., Olson, R. & Bristow, L. J. (2017a) Nicotinic $\alpha 7$ receptor agonists EVP-6124 and BMS-933043, attenuate scopolamine-induced deficits in visuo-spatial paired associates learning. *PLoS One*, 12 (12): e0187609.

Weed, M. R., Polino, J., Signor, L., Bookbinder, M., Keavy, D., Benitex, Y., Morgan, D. G., King, D., Macor, J. E., Zaczek, R., Olson, R. & Bristow, L. J. (2017b) Nicotinic $\alpha 7$ receptor agonists EVP-6124 and BMS-933043, attenuate scopolamine-induced deficits in visuo-spatial paired associates learning. *PLoS One*, 12 (12): e0187609.

Weerts, E. M. & Griffiths, R. R. (2003) The adenosine receptor antagonist CGS15943 reinstates cocaine-seeking behavior and maintains self-administration in baboons. *Psychopharmacology (Berl)*, 168 (1-2): 155-163.

Welsby, P. J., Rowan, M. J. & Anwyl, R. (2009) Intracellular mechanisms underlying the nicotinic enhancement of LTP in the rat dentate gyrus. *Eur J Neurosci*, 29 (1): 65-75.

Wevers, A., Burghaus, L., Moser, N., Witter, B., Steinlein, O. K., Schütz, U., Achnitz, B., Krempel, U., Nowacki, S., Pilz, K., Stoodt, J., Lindstrom, J., De Vos, R. A., Jansen Steur, E. N. & Schröder, H. (2000) Expression of nicotinic acetylcholine receptors in Alzheimer's disease: postmortem investigations and experimental approaches. *Behav Brain Res*, 113 (1-2): 207-215.

Williams, D. K., Wang, J. & Papke, R. L. (2011) Investigation of the molecular mechanism of the $\alpha 7$ nicotinic acetylcholine receptor positive allosteric modulator PNU-120596 provides evidence for two distinct desensitized states. *Mol Pharmacol*, 80 (6): 1013-1032.

Wilson, J. E. (2003) Isozymes of mammalian hexokinase: structure, subcellular localization and metabolic function. *J Exp Biol*, 206 (Pt 12): 2049-2057.

Xiong, J., Verkhratsky, A. & Toescu, E. C. (2002) Changes in mitochondrial status associated with altered Ca^{2+} homeostasis in aged cerebellar granule neurons in brain slices. *J Neurosci*, 22 (24): 10761-10771.

- Xu, T. & Bajjalieh, S. M. (2001) SV2 modulates the size of the readily releasable pool of secretory vesicles. *Nat Cell Biol*, 3 (8): 691-698.
- Yamamoto, M., Guo, D. H., Hernandez, C. M. & Stranahan, A. M. (2019) Endothelial Adora2a Activation Promotes Blood-Brain Barrier Breakdown and Cognitive Impairment in Mice with Diet-Induced Insulin Resistance. *J Neurosci*, 39 (21): 4179-4192.
- Yang, T., Xiao, T., Sun, Q. & Wang, K. (2017) The current agonists and positive allosteric modulators of $\alpha 7$ nAChR for CNS indications in clinical trials. *Acta Pharm Sin B*, 7 (6): 611-622.
- Yang, X. F., Weisenfeld, A. & Rothman, S. M. (2007) Prolonged exposure to levetiracetam reveals a presynaptic effect on neurotransmission. *Epilepsia*, 48 (10): 1861-1869.
- Yao, J., Nowack, A., Kensel-Hammes, P., Gardner, R. G. & Bajjalieh, S. M. (2010) Cotrafficking of SV2 and synaptotagmin at the synapse. *J Neurosci*, 30 (16): 5569-5578.
- Yoshiyama, Y., Lee, V. M. & Trojanowski, J. Q. (2013) Therapeutic strategies for tau mediated neurodegeneration. *J Neurol Neurosurg Psychiatry*, 84 (7): 784-795.
- Young, J. W., Crawford, N., Kelly, J. S., Kerr, L. E., Marston, H. M., Spratt, C., Finlayson, K. & Sharkey, J. (2007) Impaired attention is central to the cognitive deficits observed in alpha 7 deficient mice. *Eur Neuropsychopharmacol*, 17 (2): 145-155.
- Zappettini, S., Grilli, M., Lagomarsino, F., Cavallero, A., Fedele, E. & Marchi, M. (2011) Presynaptic nicotinic $\alpha 7$ and non- $\alpha 7$ receptors stimulate endogenous GABA release from rat hippocampal synaptosomes through two mechanisms of action. *PLoS One*, 6 (2): e16911.
- Zappettini, S., Grilli, M., Salamone, A., Fedele, E. & Marchi, M. (2010) Pre-synaptic nicotinic receptors evoke endogenous glutamate and aspartate release from hippocampal synaptosomes by way of distinct coupling mechanisms. *Br J Pharmacol*, 161 (5): 1161-1171.
- Zhang, N., Gordon, S. L., Fritsch, M. J., Esoof, N., Campbell, D. G., Gourlay, R., Velupillai, S., Macartney, T., Pegg, M., van Aalten, D. M., Cousin, M. A. & Alessi, D. R. (2015) Phosphorylation of synaptic vesicle protein 2A at Thr84 by casein kinase 1 family kinases controls the specific retrieval of synaptotagmin-1. *J Neurosci*, 35 (6): 2492-2507.
- Zielke, H. R., Zielke, C. L. & Baab, P. J. (2009) Direct measurement of oxidative metabolism in the living brain by microdialysis: a review. *J Neurochem*, 109 Suppl 1 (Suppl 1): 24-29.
- Zorec, R., Araque, A., Carmignoto, G., Haydon, P. G., Verkhratsky, A. & Parpura, V. (2012) Astroglial excitability and gliotransmission: an appraisal of Ca^{2+} as a signalling route. *ASN Neuro*, 4 (2):
- zur Nedden, S., Doney, A. S. & Frenguelli, B. G. (2014) Modulation of intracellular ATP determines adenosine release and functional outcome in response to metabolic stress in rat hippocampal slices and cerebellar granule cells. *J Neurochem*, 128 (1): 111-124.

zur Nedden, S., Hawley, S., Pentland, N., Hardie, D. G., Doney, A. S. & Frenguelli, B. G. (2011) Intracellular ATP influences synaptic plasticity in area CA1 of rat hippocampus via metabolism to adenosine and activity-dependent activation of adenosine A1 receptors. *J Neurosci*, 31 (16): 6221-6234.

Library Declaration and Deposit Agreement

1. STUDENT DETAILS

Please complete the following:

Full name: Signe Springe

University ID number: u1592047

2. THESIS DEPOSIT

2.1 Under your registration at the University, you are required to deposit your thesis with the University in BOTH hard copy and in digital format. The digital copy should normally be saved as a single pdf file.

2.2 The hard copy will be housed in the University Library. The digital copy will be deposited in the University's Institutional Repository (WRAP). Unless otherwise indicated (see 2.6 below), this will be made immediately openly accessible on the Internet and will be supplied to the British Library to be made available online via its Electronic Theses Online Service (EThOS) service.

[At present, theses submitted for a Master's degree by Research (MA, MSc, LLM, MS or MMedSci) are not being deposited in WRAP and not being made available via EThOS. This may change in future.]

2.3 In exceptional circumstances, the Chair of the Board of Graduate Studies may grant permission for an embargo to be placed on public access to the thesis **in excess of two years**. This must be applied for when submitting the thesis for examination (further information is available in the *Guide to Examinations for Higher Degrees by Research*.)

2.4 If you are depositing a thesis for a Master's degree by Research, the options below only relate to the hard copy thesis.

2.5 If your thesis contains material protected by third party copyright, you should consult with your department, and if appropriate, deposit an abridged hard and/or digital copy thesis.

2.6 Please tick one of the following options for the availability of your thesis (guidance is available in the *Guide to Examinations for Higher Degrees by Research*):

☐ Both the hard and digital copy thesis can be made publicly available immediately

☐ The hard copy thesis can be made publicly available immediately and the digital copy thesis can be made publicly available after a period of two years (*should you subsequently wish to reduce the embargo period please inform the Library*)

☒ Both the hard and digital copy thesis can be made publicly available after a period of two years (*should you subsequently wish to reduce the embargo period please inform the Library*)

☐ Both the hard copy and digital copy thesis can be made publicly available after _____ (insert time period in excess of two years). **This option requires the prior approval of the Chair of the Board of Graduate Studies (see 2.3 above)**

2.7 The University encourages users of the Library to utilise theses as much as possible, and unless indicated below users will be able to photocopy your thesis.

☐ I **do not** wish for my thesis to be photocopied

3. GRANTING OF NON-EXCLUSIVE RIGHTS

Whether I deposit my Work personally or through an assistant or other agent, I agree to the following:

- Rights granted to the University of Warwick and the British Library and the user of the thesis through this agreement are non-exclusive. I retain all rights in the thesis in its present version or future versions. I agree that the institutional repository administrators and the British Library or their agents may, without changing content, digitise and migrate the thesis to any medium or format for the purpose of future preservation and accessibility.

4. DECLARATIONS

I DECLARE THAT:

- I am the author and owner of the copyright in the thesis and/or I have

the authority of the authors and owners of the copyright in the thesis to make this agreement. Reproduction of any part of this thesis for teaching or in academic or other forms of publication is subject to the normal limitations on the use of copyrighted materials and to the proper and full acknowledgement of its source.

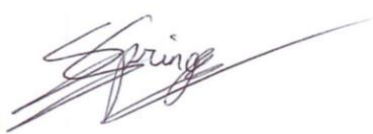
- The digital version of the thesis I am supplying is either the same version as the final, hard-bound copy submitted in completion of my degree once any minor corrections have been completed, or is an abridged version (see 2.5 above).
- I have exercised reasonable care to ensure that the thesis is original, and does not to the best of my knowledge break any UK law or other Intellectual Property Right, or contain any confidential material.
- I understand that, through the medium of the Internet, files will be available to automated agents, and may be searched and copied by, for example, text mining and plagiarism detection software.
- At such time that my thesis will be made publically available digitally (see 2.6 above), I grant the University of Warwick and the British Library a licence to make available on the Internet the thesis in digitised format through the Institutional Repository and through the British Library via the EThOS service.
- If my thesis does include any substantial subsidiary material owned by third-party copyright holders, I have sought and obtained permission to include it in any version of my thesis available in digital format and that this permission encompasses the rights that I have granted to the University of Warwick and to the British Library.

5. LEGAL INFRINGEMENTS

I understand that neither the University of Warwick nor the British Library have any obligation to take legal action on behalf of myself, or other rights holders, in the event of infringement of intellectual property rights, breach of contract or of any other right, in the thesis.

Please sign this agreement and ensure it is bound into the final hard bound copy of your thesis, which should be submitted to the Library.

Student's signature:



Date: 04/09/2021